

# **MERCURY**

Optimized Software for (Single Site) Hybrid Simulation  
From Pseudo Dynamics to Real Time Hybrid Simulation

## **Theory Manual**

Ver. 1

**Dae-Hung Kang**

**Gary Haussmann**

**Victor E. Saouma**

## **Fast Hybrid Testing Laboratory**

<http://fht.colorado.edu>

Department of Civil Environmental and Architectural Engineering  
University of Colorado, Boulder  
Boulder, Colorado 80309-0428



## Contents

<b>1 ELEMENT FORMULATION</b>	<b>9</b>
1.1 Truss Element . . . . .	9
1.1.1 Formulation . . . . .	9
1.1.2 Coordinate system for 2D truss element . . . . .	10
1.1.3 State determination . . . . .	11
1.2 Beam-Column Element . . . . .	11
1.2.1 Stiffness-based 2D beam-column element . . . . .	11
1.2.1.1 Formulation . . . . .	11
1.2.1.2 Coordinate system for stiffness-based 2D beam-column element . . . . .	13
1.2.1.3 State determination . . . . .	13
1.2.1.4 Nonlinear analysis using stiffness-based formulation . . . . .	17
1.2.2 Flexibility-based 2D beam-column element . . . . .	21
1.2.2.1 Formulation . . . . .	22
1.2.2.2 Coordinate system for flexibility-based 2D beam-column element . . . . .	24
1.2.2.3 State determination . . . . .	25
1.2.2.3.1 With element iterations . . . . .	25
1.2.2.3.2 Without element iterations . . . . .	32
1.2.2.4 Nonlinear analysis using flexibility-based method . . . . .	34
1.2.2.4.1 With element iterations . . . . .	34
1.2.2.4.2 Without element iterations . . . . .	40
1.3 Layer/Fiber Section . . . . .	45
1.4 Zero-Length 2D Element Formulation . . . . .	47
1.4.1 Formulation . . . . .	48
1.4.2 Coordinate system in zero-length 2D element . . . . .	50
1.4.3 Element state determination . . . . .	50
1.5 Zero-Length Section Element Formulation . . . . .	52
1.5.1 Formulation . . . . .	53
1.5.2 Coordinate system in zero-length 2D section element . . . . .	54
1.5.3 Element state determination . . . . .	54
1.6 Element Force . . . . .	56
1.7 Summary . . . . .	58
<b>2 CONSTITUTIVE MODELS</b>	<b>59</b>
2.1 Steel Models . . . . .	59
2.1.1 “Exact” Models . . . . .	60
2.1.1.1 Isotropic hardening model . . . . .	60
2.1.1.2 Combined isotropic and kinematic hardening model . . . . .	63
2.1.1.3 Determination for isotropic and kinematic hardening parameters . . . . .	66
2.1.2 Heuristic Models . . . . .	66
2.1.2.1 Simplified Bilinear model with isotropic hardening . . . . .	66
2.1.2.1.1 Stress-strain relation . . . . .	66
2.1.2.1.2 Determination for simplified bilinear model . . . . .	66
2.1.2.2 Giuffre-Menegotto-Pinto Model Modified by Filippou et al. . . . . .	66
2.1.2.2.1 Stress-strain relationship . . . . .	66
2.1.2.2.2 Determination for modified Giuffre-Menegotto-Pinto Model . . . . .	72
2.2 Concrete Models . . . . .	72
2.2.1 Heuristic Models . . . . .	72
2.2.1.1 Modified Kent And Park Model . . . . .	72

2.2.1.1.1	Stress-strain relation . . . . .	72
2.2.1.1.2	Data preparation for modified Kent and Park model . . . . .	81
2.2.1.1.3	Determination for modified Kent and Park model . . . . .	82
2.2.2	“Exact” Models . . . . .	82
2.2.2.1	Anisotropic damage model with effective damage and stiffness recovery . . . . .	82
2.2.2.1.1	Constitutive model . . . . .	82
2.2.2.1.2	Uniaxial multi-fiber formulation . . . . .	85
2.2.2.1.3	Determination for anisotropic damage model . . . . .	86
2.2.2.1.3.1	Tension loading: . . . . .	86
2.2.2.1.3.2	Compressive loading: . . . . .	87
2.2.2.2	Anisotropic damage model with permanent strains . . . . .	90
2.2.2.2.1	Uniaxial numerical scheme . . . . .	93
2.3	Bond-Slip . . . . .	94
2.4	Lumped Plasticity Model . . . . .	96
2.5	Constitutive models for zero length and zero length section elements . . . . .	96
2.5.1	Zero Length Element . . . . .	96
2.5.2	Zero length section element . . . . .	98
2.5.3	Summary . . . . .	99
2.6	Summary . . . . .	99
<b>3</b>	<b>Structural Modeling</b>	<b>101</b>
3.1	Truss, Material Nonlinearity, Static and Dynamic . . . . .	101
3.2	Uniaxial Concrete Nonlinear Element, Cyclic Displacement . . . . .	105
3.3	Uniaxial Steel Nonlinear Element, Cyclic Displacement . . . . .	108
3.4	Steel Beam-columns, Fiber Section, Static, Transient (HHT and Shing) . . . . .	112
3.5	Zero-length and Beam Column, Nonlinear Steel Element, load control . . . . .	116
3.6	Zero-length Section, and Beam Column, Fiber, Nonlinear Steel Element, load control . . . . .	117
3.7	Beam-column, Fiber Section, Nonlinear Material, multi-d.o.f.s displacement control, Pushover Analysis	120
3.8	Reinforced Concrete Beam-Column, Fiber Section, Transient Analysis . . . . .	123
3.9	Ex29: Full Reinforced Concrete Frame, HHT, Shing . . . . .	130
3.9.0.1	Frame discretization and properties . . . . .	130
<b>4</b>	<b>NONLINEAR PUSHOVER ANALYSIS</b>	<b>141</b>
4.1	pushover . . . . .	141
4.2	Shakedown . . . . .	141
4.3	Control Method . . . . .	141
4.4	Classical Pushover . . . . .	141
4.5	Improved Pushover Analysis Procedure . . . . .	141
4.5.1	Load Control . . . . .	143
4.5.2	Displacement Control . . . . .	143
<b>5</b>	<b>DYNAMIC ANALYSIS</b>	<b>147</b>
5.1	Preliminaries . . . . .	147
5.1.1	Variational Formulation . . . . .	147
5.1.2	Mass Representation . . . . .	148
5.1.2.1	Lumped mass . . . . .	148
5.1.2.2	Consistent mass . . . . .	148
5.1.3	Damping Representation . . . . .	149
5.1.4	Euler Methods . . . . .	150
5.2	Time Integration Methods . . . . .	150
5.2.1	Newmark $\beta$ method . . . . .	151
5.2.1.1	Newmark $\beta$ implicit method . . . . .	152
5.2.2	Hilber-Hughes-Taylor Method . . . . .	153
5.2.2.1	General Formulation . . . . .	153
5.3	Free Vibration . . . . .	156
<b>6</b>	<b>Notation</b>	<b>159</b>

## List of Figures

1.1	Internal forces and corresponding displacements, 2D truss element . . . . .	10
1.2	Internal forces and corresponding displacements, stiffness-based 2D element . . . . .	13
1.3	State determination for stiffness-based method . . . . .	15
1.4	State determination procedure for stiffness-based method . . . . .	16
1.5	Flow chart of nonlinear analysis using stiffness-based method (1) . . . . .	18
1.6	Flow chart of nonlinear analysis using stiffness-based method (2) . . . . .	19
1.7	Flow chart of nonlinear analysis using stiffness-based method (3) . . . . .	20
1.8	2D beam-column element without rigid body modes . . . . .	22
1.9	Sign convention on section forces . . . . .	23
1.10	Internal forces and corresponding displacement,flexibility-based 2D element . . . . .	24
1.11	The relationship between rigid body modes and no rigid body modes . . . . .	25
1.12	State determination procedure for flexibility-based method with Newton-Raphson iteration in the element . . . . .	26
1.13	State determination procedure for flexibility-based method without Newton-Raphson iteration in the element . . . . .	27
1.14	State determination for flexibility-based method with element iteration (?) . . . . .	28
1.15	Element and section state determinations . . . . .	29
1.16	State determination for flexibility-based method without element iteration . . . . .	33
1.17	Flow chart of nonlinear analysis, flexibility-based w/ element iteration(1) . . . . .	35
1.18	Flow chart of nonlinear analysis, flexibility-based w/ element iteration(2) . . . . .	36
1.19	Flow chart of nonlinear analysis, flexibility-based w/ element iteration(3) . . . . .	37
1.20	Flow chart of nonlinear analysis, flexibility-based w/o element iteration(1) . . . . .	41
1.21	Flow chart of nonlinear analysis, flexibility-based w/o element iteration(2) . . . . .	42
1.22	Flow chart of nonlinear analysis, flexibility-based w/o element iteration(3) . . . . .	43
1.23	Stress and strain distribution of nonlinear material . . . . .	46
1.24	Layer/fiber section . . . . .	47
1.25	Layer/fiber section state determination . . . . .	48
1.26	Zero-length 2D element(1) . . . . .	49
1.27	Zero-length 2D element(2) . . . . .	50
1.28	Flow chart of zero-length 2D element for element state determination . . . . .	51
1.29	Zero-length 2D section element(1) . . . . .	53
1.30	Zero-length 2D section element(2) . . . . .	54
1.31	Flow chart of zero-length 2D section element for element state determination . . . . .	55
1.32	Forces of an element . . . . .	56
1.33	Nodal equivalent forces of an element . . . . .	57
1.34	Example with element distributed forces and nodal displacement . . . . .	58
2.1	Uniaxial stress-strain curve for steel . . . . .	59
2.2	Idealized stress-strain response hardening material . . . . .	60
2.3	The tangent modulus for isotropic hardening model . . . . .	61
2.4	The evolution of elastic domain in isotropic hardening model . . . . .	61
2.5	Isotropic and kinematic hardening plasticity . . . . .	63
2.6	The evolution of elastic domain in isotropic and kinematic hardening model . . . . .	65
2.7	Determination for isotropic and kinematic hardening model . . . . .	67
2.8	Bilinear model . . . . .	68
2.9	Determination for simplified bilinear model . . . . .	69
2.10	Menegotto-Pinto steel model . . . . .	70
2.11	Definition of curvature parameter $R$ in Menegotto-Pinto steel model . . . . .	70
2.12	Determination (1) for modified Giuffre-Menegotto-Pinto Model . . . . .	72
2.13	Determination (2) for modified Giuffre-Menegotto-Pinto Model . . . . .	73
2.14	Determination (3) for modified Giuffre-Menegotto-Pinto Model . . . . .	74

2.15	Determination (4) for modified Giuffre-Menegotto-Pinto Model . . . . .	75
2.16	Concrete material model in compression . . . . .	76
2.17	Concrete material model under cyclic loading in compression . . . . .	78
2.18	Concrete material model under cyclic loading in tension . . . . .	80
2.19	Determination (1) for modified Kent and Park model . . . . .	83
2.20	Determination (2) for modified Kent and Park model . . . . .	84
2.21	Cracks induced by compression, tension, tension and compression . . . . .	85
2.22	Strain-stress curve for anisotropic damage model without permanent strain . . . . .	89
2.23	Determination (1) for the anisotropic damage model . . . . .	90
2.24	Determination (2) for the anisotropic damage model . . . . .	91
2.25	Determination (3) for the anisotropic damage model . . . . .	92
2.26	Strain-stress curve for anisotropic damage model with permanent strain . . . . .	94
2.27	Longitudinal bar bond stress, steel stress, and strain profiles, (?) . . . . .	95
2.28	Stress slip curve . . . . .	96
2.29	Hysteretic model with strength and stiffness deterioration, (?) . . . . .	97
2.30	Compatibility of NA between beam-column and zero length fiber section . . . . .	99
2.31	Zero length element and section . . . . .	99
3.1	Ex10: Truss, ModGMP material, load control, HHT . . . . .	101
3.2	Cyclic wave without dimension . . . . .	106
3.3	Examples 11- 12 . . . . .	106
3.4	Examples 16- 19 . . . . .	108
3.5	Examples 20- 22 . . . . .	112
3.6	Examples 23 . . . . .	116
3.7	Examples 24 . . . . .	118
3.8	Examples 25- 26 . . . . .	120
3.9	Beam-column elements for Ex27 and Ex28 . . . . .	123
3.10	Bar slip zero-length fiber section element (?) . . . . .	124
3.11	Numerical model for real-time hybrid simulation . . . . .	131
3.12	Shake table test of reinforce concrete frame, ? . . . . .	132
3.13	Section properties of Ex29 . . . . .	132
3.14	Seismic excitation for Ex29 . . . . .	132
4.1	Pushover analysis . . . . .	142
4.2	Determination of pushover displacements magnitudes . . . . .	142
4.3	Pushover Analysis of a Frame . . . . .	142
4.4	Implementation for displacement control . . . . .	145
5.1	Rayleigh damping . . . . .	149
5.2	Geometric interpretation of Euler's method . . . . .	151
5.3	Flow chart (1) using the Newmark $\beta$ implicit method . . . . .	154
5.4	Flow chart (2) using the Newmark $\beta$ implicit method . . . . .	155
5.5	Flow chart using the HHT implicit method . . . . .	157

## List of Tables

3.1	Features of Example Problems . . . . .	102
3.2	Material properties of concrete for Ex27 (unit: kips, in) . . . . .	124
3.3	Material properties of concrete for Ex28 (unit: kips, in) . . . . .	124
3.4	Material properties of reinforcement for Ex27 and Ex28 (unit: kips, in) . . . . .	124
3.5	Property of shear spring in zero-length element for Ex27 and Ex28 (unit: kips, in) . . . . .	124
3.6	Concrete material properties of concrete for Ex29 (unit:kips, in) . . . . .	130
3.7	Material properties of reinforcement for Ex29 (unit: kips, in) . . . . .	131
3.8	Property of shear spring for Ex29 (unit: kips, in) . . . . .	131
3.9	Properties of rigid elements (unit: kips, in) . . . . .	132
3.10	Mass properties in first floor column nodes (unit: <i>kips · sec<sup>2</sup>/in</i> ) . . . . .	133
3.11	Mass properties in column nodes except first floor columns (unit: <i>kips · sec<sup>2</sup>/in</i> ) . . . . .	133
3.12	Mass properties in beam nodes (unit: <i>kips · sec<sup>2</sup>/in</i> ) . . . . .	133
5.1	Properties of the Newmark $\beta$ method . . . . .	152



# Chapter 1

## ELEMENT FORMULATION

This chapter will describe the formulation of the elements in Mercury. It will start with the simplest one, truss and then proceed with beam-column of increasing levels of complexity. Finally zero length element and section element will be addressed.

### 1.1 Truss Element

The truss element has only one degree of freedom associated with each node in local reference whether in 2D or 3D.

#### 1.1.1 Formulation

As with all finite elements, stiffness matrix derivation hinges on three requirements.

**Compatibility** of:

**Displacement** Section displacements are determined from the element nodal displacements through the shape function. Since the truss element has only one d.o.f per node, the generalized relationship between section displacement vector  $\mathbf{d}_s(x)$  and element nodal displacement vector  $\bar{\mathbf{d}}_e$  is expressed through the displacement interpolation functions (shape functions),  $\mathbf{N}_d(x)$  as

$$\begin{aligned}\mathbf{d}_s(x) &= \left\{ u(x) \right\} \\ &= \underbrace{\left[ -\frac{x}{L} + 1 \quad \frac{x}{L} \right]}_{\mathbf{N}_d(x)} \cdot \underbrace{\left\{ \begin{array}{c} \bar{u}_{x1} \\ \bar{u}_{x2} \end{array} \right\}}_{\bar{\mathbf{d}}_e}\end{aligned}$$

**Deformation** of displacements: Under the assumption that displacements are small, the section deformation vector  $\boldsymbol{\varepsilon}_s(x)$  is related to the element nodal displacement vector by

$$\begin{aligned}\boldsymbol{\varepsilon}_s(x) &= \left\{ \varepsilon_x(x) \right\} \\ &= \underbrace{\left[ -\frac{1}{L} \quad \frac{1}{L} \right]}_{\mathbf{B}_d(x)} \cdot \bar{\mathbf{d}}_e\end{aligned}\tag{1.1}$$

where  $\mathbf{B}_d(x)$  is the matrix which relates displacement to strain through the derivatives of  $\mathbf{N}_d(x)$ .

**Constitutive law** is expressed as

$$\underbrace{\left\{ N_x(x) \right\}}_{\boldsymbol{\sigma}_s(x)} = \mathbf{k}_s(x) \cdot \boldsymbol{\varepsilon}_s(x)\tag{1.2}$$

where  $\boldsymbol{\sigma}_s(x)$  is the section<sup>1</sup> force vector, and  $\mathbf{k}_s(x)$  is the section stiffness matrix.

For linear elastic analysis  $\mathbf{k}_s(x)$  is simply a scalar equal to

$$\mathbf{k}_s(x) = [ E(x) \cdot A(x) ]$$

where,  $E(x)$  and  $A(x)$  are elastic modulus and cross sectional area.

**Equilibrium** (weak form) through the principle of virtual work (displacement) which is expressed as

$$\underbrace{\delta \bar{\mathbf{d}}_e^T \cdot \bar{\mathbf{f}}_e}_{\text{External}} = \underbrace{\int_0^{L_e} \delta \boldsymbol{\varepsilon}_s(x)^T \boldsymbol{\sigma}_s(x) dx}_{\text{Internal}}\tag{1.3}$$

---

<sup>1</sup>The notion of section is not essential to understand the formulation of the truss element stiffness matrix. It is nevertheless introduced to be consistent with the subsequent formulation of beam-column (Sec. 1.2)

Substitution of Eq. 1.1 and 1.2 into Eq. 1.3 and since the latter must hold for any arbitrary  $\delta\bar{\mathbf{d}}_e$  leads to

$$\begin{aligned}\delta\bar{\mathbf{d}}_e^T \cdot \bar{\mathbf{f}}_e &= \int_0^{L_e} \delta\bar{\mathbf{d}}_e^T \cdot \mathbf{B}_d(x)^T \cdot \mathbf{k}_s(x) \cdot \boldsymbol{\varepsilon}_s(x) \, dx \\ \bar{\mathbf{f}}_e &= \int_0^{L_e} \mathbf{B}_d(x)^T \cdot \mathbf{k}_s(x) \cdot \boldsymbol{\varepsilon}_s(x) \, dx \\ &= \underbrace{\int_0^{L_e} \mathbf{B}_d(x)^T \cdot \mathbf{k}_s(x) \cdot \mathbf{B}_d(x) \, dx}_{\bar{\mathbf{k}}_e} \cdot \bar{\mathbf{d}}_e \\ \bar{\mathbf{f}}_e &= \bar{\mathbf{k}}_e \cdot \bar{\mathbf{d}}_e\end{aligned}$$

The element stiffness matrix in local reference is thus given by

$$\bar{\mathbf{k}}_e = \int_0^{L_e} \mathbf{B}_d(x)^T \cdot \mathbf{k}_s(x) \cdot \mathbf{B}_d(x) \, dx$$

### 1.1.2 Coordinate system for 2D truss element

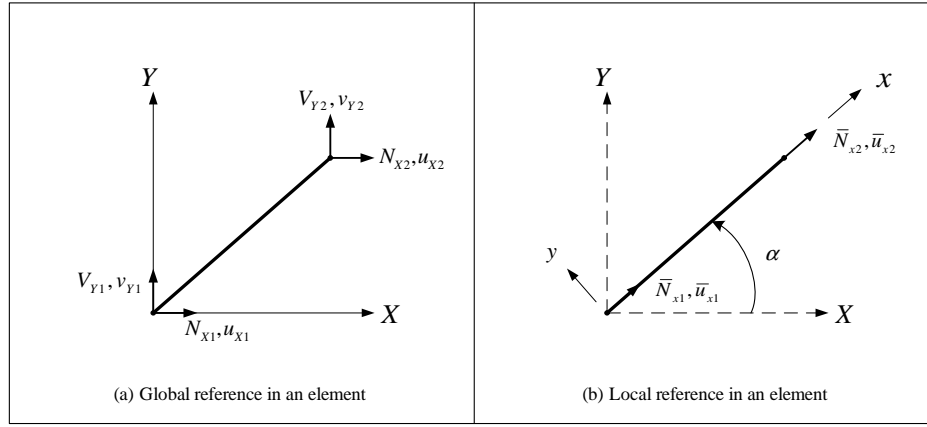


Figure 1.1: Internal forces and corresponding displacements in global and local coordinate system for the 2D truss element

The element nodal forces and displacements are expressed with respect to the global reference, Fig. 1.1(a) as:

$$\begin{aligned}\mathbf{F}_e &= [N_{X1}, V_{Y1}, N_{X2}, V_{Y2}]^T \\ \boldsymbol{\delta}_e &= [u_{X1}, v_{Y1}, u_{X2}, v_{Y2}]^T\end{aligned}$$

Furthermore, the element nodal forces and displacements can also be expressed with respect to the local reference, Fig. 1.1(b)

$$\begin{aligned}\bar{\mathbf{f}}_e &= [\bar{N}_{x1}, \bar{N}_{x2}]^T \\ \bar{\mathbf{d}}_e &= [\bar{u}_{x1}, \bar{u}_{x2}]^T\end{aligned}$$

The rotation matrix which transform global reference, Fig. 1.1(a), to local reference, Fig. 1.1(b), is given by  $\boldsymbol{\Gamma}_e$  such that

$$\begin{aligned}\bar{\mathbf{f}}_e &= \boldsymbol{\Gamma}_e \cdot \mathbf{F}_e \\ \bar{\mathbf{d}}_e &= \boldsymbol{\Gamma}_e \cdot \boldsymbol{\delta}_e \\ \mathbf{K}_e &= \boldsymbol{\Gamma}_e^T \cdot \bar{\mathbf{k}}_e \cdot \boldsymbol{\Gamma}_e\end{aligned}$$

where,  $\mathbf{K}_e$  is the element stiffness matrix in global reference and the rotation matrix is

$$\boldsymbol{\Gamma}_e = \left[ \begin{array}{c|cccc} & N_{X1} & V_{Y1} & N_{X2} & V_{Y2} \\ \hline \overline{N}_{x1} & \cos \alpha & \sin \alpha & 0 & 0 \\ \overline{N}_{x2} & 0 & 0 & \cos \alpha & \sin \alpha \end{array} \right]$$

### 1.1.3 State determination

In a nonlinear structural analysis, state determination for 2D truss element is identical to the stiffness-based 2D beam-column element. It will be discussed in Sec. 1.2.1.3 and 1.2.1.4.

## 1.2 Beam-Column Element

The formulation of nonlinear frame structure using elements with layer/fiber sections can be achieved using the stiffness-based (displacement) method or the flexibility-based (force) method. Both formulations will be presented, with the assumption that deformations are small and plane sections remain plane during the loading history. The stiffness-based method assumes displacement interpolation functions along the element, while the flexibility-based one has force interpolation functions along the element. As will be shown later, a smaller number of flexibility based elements (albeit with a greater number of integration points) than stiffness based ones is often needed to achieve the same level of accuracy.

However, the element formulation in the flexibility-based method is more complex than that of the stiffness-based one as we need to perform an additional loop of iterations at the element level in order to obtain  $\varepsilon$  from material constitutive models which are usually expressed as  $\sigma = \sigma(\varepsilon)$  (?). On the other hand, stiffness based elements are much simpler to formulate.

Both formulations are described next.

### 1.2.1 Stiffness-based 2D beam-column element

We next formulate the stiffness matrix of the beam-column elements (also known as “frame” element) by considering the “classical” stiffness-based formulation first. The formulation is based on linear polynomial interpolation for the axial displacements, and cubic for the transverse ones.

#### 1.2.1.1 Formulation

As for the truss element we consider each of the three requirements which must be met.

##### Compatibility of

**Displacement** Section displacements are determined from the element nodal displacements through the shape functions. The generalized relationship between section displacement vector  $\mathbf{d}_s(x)$  and the element nodal displacement vector  $\bar{\mathbf{d}}_e$  can be expressed as

$$\begin{aligned} \mathbf{d}_s(x) &= \begin{Bmatrix} u(x) \\ v(x) \end{Bmatrix} \\ &= \mathbf{N}_d(x) \cdot \underbrace{\begin{bmatrix} \bar{u}_{x1}, & \bar{v}_{y1}, & \bar{\theta}_{z1}, & \bar{u}_{x2}, & \bar{v}_{y2}, & \bar{\theta}_{z2} \end{bmatrix}^T}_{\bar{\mathbf{d}}_e} \end{aligned}$$

where  $\mathbf{N}_d(x)$  is the matrix of displacement interpolation functions which can be expressed as

$$\mathbf{N}_d(x) = \begin{bmatrix} \psi_1(x) & 0 & 0 & \psi_2(x) & 0 & 0 \\ 0 & \phi_1(x) & \phi_2(x) & 0 & \phi_3(x) & \phi_4(x) \end{bmatrix}$$

where  $\psi_1$ ,  $\psi_2$ ,  $\phi_1$ ,  $\phi_2$ ,  $\phi_3$  and  $\phi_4$  are the interpolation functions for axial and transverse displacements respectively and are given by

$$\begin{aligned} \psi_1(x) &= -\frac{x}{L_e} + 1 & \psi_2(x) &= \frac{x}{L_e} \\ \phi_1(x) &= 2\frac{x^3}{L_e^3} - 3\frac{x^2}{L_e^2} + 1 & \phi_2(x) &= \frac{x^3}{L_e^2} - 2\frac{x^2}{L_e} + x \\ \phi_3(x) &= -2\frac{x^3}{L_e^3} + 3\frac{x^2}{L_e^2} & \phi_4(x) &= \frac{x^3}{L_e^2} - \frac{x^2}{L_e} \end{aligned}$$

We note the uncoupling between axial and transverse displacements since geometric nonlinearity is ignored.

**Deformation** Under the assumptions of small displacements and plane sections remaining plane (Euler Bernouilli as opposed to Timoshenko), the section deformation vector  $\boldsymbol{\varepsilon}_s(x)$  (axial strain  $\varepsilon_x(x)$  and curvature  $\phi_z(x)$ ) is related to the element nodal displacement vector

$$\begin{aligned}\boldsymbol{\varepsilon}_s(x) &= \begin{Bmatrix} \varepsilon_x(x) \\ \phi_z(x) \end{Bmatrix} \\ &= \mathbf{B}_d(x) \cdot \bar{\mathbf{d}}_e\end{aligned}\quad (1.4)$$

where  $\mathbf{B}_d(x)$  is the matrix obtained from the appropriate derivatives of the displacement interpolation functions.

$$\mathbf{B}_d(x) = \begin{bmatrix} \psi'_1(x) & 0 & 0 & \psi'_2(x) & 0 & 0 \\ 0 & \phi''_1(x) & \phi''_2(x) & 0 & \phi''_3(x) & \phi''_4(x) \end{bmatrix}$$

with

$$\begin{aligned}\psi'_1(x) &= -\frac{1}{L_e} & \psi'_2(x) &= \frac{1}{L_e} \\ \phi''_1(x) &= \frac{12x}{L_e^3} - \frac{6}{L_e^2} & \phi''_2(x) &= \frac{6x}{L_e^2} - \frac{4}{L_e} \\ \phi''_3(x) &= -\frac{12x}{L_e^3} + \frac{6}{L_e^2} & \phi''_4(x) &= \frac{6x}{L_e^2} - \frac{2}{L_e}\end{aligned}$$

### Constitutive law

Section constitutive law relates axial strain and curvature to axial force and moment

$$\underbrace{\begin{Bmatrix} N_x(x) \\ M_z(x) \end{Bmatrix}}_{\boldsymbol{\sigma}_s(x)} = \mathbf{k}_s(x) \boldsymbol{\varepsilon}_s(x) \quad (1.5)$$

where  $\boldsymbol{\sigma}_s(x)$  is the section force vector, and  $\mathbf{k}_s(x)$  is the section stiffness matrix.

If  $\mathbf{k}_s(x)$  is not derived from layer/fiber discretization of the cross section, and for linear elastic case  $\mathbf{k}_s(x)$  is simply equal to

$$\mathbf{k}_s(x) = \begin{bmatrix} E(x) \cdot A(x) & 0 \\ 0 & E(x) \cdot I_z(x) \end{bmatrix} \quad (1.6)$$

where,  $E(x)$ ,  $A(x)$ , and  $I_z(x)$  are elastic modulus, cross sectional area, and section moment of inertia.

**Equilibrium** will be satisfied only in the weak sense through the principle of virtual displacement expressed as

$$\underbrace{\delta \bar{\mathbf{d}}_e^T \cdot \bar{\mathbf{f}}_e}_{\text{External}} = \underbrace{\int_0^{L_e} \delta \boldsymbol{\varepsilon}_s(x)^T \cdot \boldsymbol{\sigma}_s(x) dx}_{\text{Internal}} \quad (1.7)$$

Substituting Eq. 1.4 and Eq. 1.5 into Eq. 1.7 and since the latter must hold for any arbitrary  $\delta \bar{\mathbf{d}}_e$ , the principle of virtual work leads to

$$\begin{aligned}\delta \bar{\mathbf{d}}_e^T \cdot \bar{\mathbf{f}}_e &= \int_0^{L_e} \delta \bar{\mathbf{d}}_e^T \cdot \mathbf{B}_d(x)^T \cdot \mathbf{k}_s(x) \cdot \boldsymbol{\varepsilon}_s(x) dx \\ \bar{\mathbf{f}}_e &= \int_0^{L_e} \mathbf{B}_d(x)^T \cdot \mathbf{k}_s(x) \cdot \boldsymbol{\varepsilon}_s(x) dx \\ &= \underbrace{\int_0^{L_e} \mathbf{B}_d(x)^T \cdot \mathbf{k}_s(x) \cdot \mathbf{B}_d(x) dx}_{\bar{\mathbf{k}}_e} \cdot \bar{\mathbf{d}}_e \\ \bar{\mathbf{f}}_e &= \bar{\mathbf{k}}_e \cdot \bar{\mathbf{d}}_e\end{aligned}$$

The element stiffness matrix in local reference is thus given by

$$\bar{\mathbf{k}}_e = \int_0^{L_e} \mathbf{B}_d(x)^T \cdot \mathbf{k}_s(x) \cdot \mathbf{B}_d(x) dx \quad (1.8)$$

### 1.2.1.2 Coordinate system for stiffness-based 2D beam-column with Bernoulli beam theory

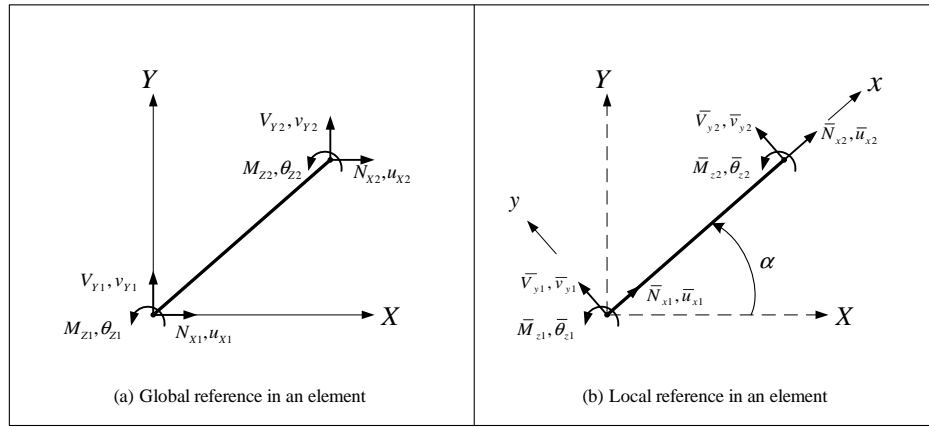


Figure 1.2: Internal forces and corresponding displacements in global and local coordinate system for the stiffness-based 2D beam-column element

The element nodal forces and displacements are expressed with respect to the global reference, Fig. 1.2(a) as

$$\mathbf{F}_e = [N_{X1}, V_{Y1}, M_{Z1}, N_{X2}, V_{Y2}, M_{Z2}]^T$$

$$\boldsymbol{\delta}_e = [u_{X1}, v_{Y1}, \theta_{Z1}, u_{X2}, v_{Y2}, \theta_{Z2}]^T$$

Again, the element nodal forces and displacements of the element can be expressed with respect to the local reference as shown in Fig. 1.2(b)

$$\bar{\mathbf{f}}_e = [\bar{N}_{x1}, \bar{V}_{y1}, \bar{M}_{z1}, \bar{N}_{x2}, \bar{V}_{y2}, \bar{M}_{z2}]^T$$

$$\bar{\boldsymbol{\delta}}_e = [\bar{u}_{x1}, \bar{v}_{y1}, \bar{\theta}_{z1}, \bar{u}_{x2}, \bar{v}_{y2}, \bar{\theta}_{z2}]^T$$

As for the truss element, the rotation matrix which transforms from global reference, (Fig. 1.2(a)) to local reference (Fig. 1.2(b)) is given by  $\boldsymbol{\Gamma}_e$  such that

$$\begin{aligned} \bar{\mathbf{f}}_e &= \boldsymbol{\Gamma}_e \cdot \mathbf{F}_e \\ \bar{\boldsymbol{\delta}}_e &= \boldsymbol{\Gamma}_e \cdot \boldsymbol{\delta}_e \\ \mathbf{K}_e &= \boldsymbol{\Gamma}_e^T \cdot \bar{\mathbf{k}}_e \cdot \boldsymbol{\Gamma}_e \end{aligned} \quad (1.9)$$

where,  $\mathbf{K}_e$  is the element stiffness matrix in global reference.

The rotation matrix is then given by

$$\boldsymbol{\Gamma}_e = \left[ \begin{array}{c|cccccc} & N_{X1} & V_{Y1} & M_{Z1} & N_{X2} & V_{Y2} & M_{Z2} \\ \hline \bar{N}_{x1} & \cos \alpha & \sin \alpha & 0 & 0 & 0 & 0 \\ \bar{V}_{y1} & -\sin \alpha & \cos \alpha & 0 & 0 & 0 & 0 \\ \bar{M}_{z1} & 0 & 0 & 1 & 0 & 0 & 0 \\ \bar{N}_{x2} & 0 & 0 & 0 & \cos \alpha & \sin \alpha & 0 \\ \bar{V}_{y2} & 0 & 0 & 0 & -\sin \alpha & \cos \alpha & 0 \\ \bar{M}_{z2} & 0 & 0 & 0 & 0 & 0 & 1 \end{array} \right]$$

### 1.2.1.3 State determination

It is important to note that we do operate at three different levels in the structural analysis: a) structure level, b) element level, and c) section level. Fig. 1.3 shows the interaction of those three levels, and accompanying state

determinations.

In an incremental nonlinear analysis, to each increment of force corresponds an increment of displacement from which the total displacement is then determined. Those nodal displacements are in turn used to determine internal section forces.

State determination is the process of determining internal forces and tangent stiffness matrix corresponding to element nodal displacements. It is composed of three parts, Fig. 1.3:

**1. Structure** state determination, Fig. 1.3(a). The element tangent stiffness matrices and internal element force vector of all the elements are assembled to form the (augmented) tangent stiffness matrix  $\mathbf{K}_S^{tan}$  and internal nodal force vector  $\mathbf{P}_S^{int}$  ( $\mathbf{P}_S^{int} = \mathbf{P}_t^{int} + \mathbf{P}_u^{int}$ ) of the structure. Subscript  $t$  and  $u$  refer to free and constrained degrees of freedom respectively (that is along the natural and essential boundaries).

**2. Element** state determination, Fig. 1.3(b). The element tangent stiffness matrices and internal element nodal forces of each element are determined from the internal section forces for each element which are in turn computed from section deformations

**3. Section** state determination, Fig. 1.3(c), where internal section forces are computed from section deformations which are in turn determined from element nodal displacements.

Once the structure state determination is complete, the internal nodal force vector ( $\mathbf{P}_{t,n}^{int}$ ) is compared with the total applied external nodal force vector ( $\mathbf{P}_{t,n}^{ext}$ ) and the difference ( $\mathbf{P}_{t,n}^R$ ), is the residual nodal force vector which is then reapplied to the structure in an iterative solution process until convergence (equilibrium) is satisfied.

The state determination procedure is straightforward for a stiffness-based 2D beam-column element. The section deformation vectors  $\boldsymbol{\varepsilon}_{s,e}(x)$  are determined from the element nodal displacement vector  $\bar{\mathbf{d}}_e$  as shown in Eq. 1.4. The corresponding section tangent stiffness matrices  $\mathbf{k}_{s,e}^{tan}(x)$  and the internal section force vectors  $\boldsymbol{\sigma}_{s,e}^{int}(x)$  are determined from the section constitutive law, Eq. 1.5. The element tangent stiffness matrices  $\bar{\mathbf{k}}_e^{tan}$  are obtained from Eq. 1.8, while the internal element nodal force vectors  $\bar{\mathbf{f}}_e^{int}$  are determined from the principle of virtual work

$$\bar{\mathbf{f}}_e^{int} = \int_0^{L_e} \mathbf{B}_{d,e}(x)^T \cdot \boldsymbol{\sigma}_{s,e}^{int}(x) dx \quad (1.10)$$

It is important to note that this method leads to an erroneous element response in the nonlinear case. This problem is again illustrated by Fig. 1.3 which shows the evolution of the structure, element and section states during one incremental external force vector at free degrees of freedom  $\Delta\mathbf{P}_{t,n}$  that requires several iterations  $k$ , (?). Subscript  $n$  refers to external force step, superscript  $k$  the  $k^{th}$  iteration within the external force step  $n$ .

The Newton-Raphson iteration method operates in the global coordinate (structural level) system. At each Newton-Raphson iteration, Fig. 1.4, the incremental nodal displacement vector at the structure level is determined from the nodal incremental force vector, and then the total element nodal displacement vectors (②) are determined next.

At the  $k^{th}$  Newton-Raphson iteration, the element nodal displacement vectors in local reference  $\bar{\mathbf{d}}_{e,n}$  (③) of the nodal displacement vector  $\mathbf{u}_{S,n}^k$  ( $\mathbf{u}_{S,n}^k = \mathbf{u}_{t,n}^k + \mathbf{u}_{u,n}^k$ ) of degrees of freedom at the structure level are determined for each element.

Using Eq. 1.5 the section deformation vectors  $\boldsymbol{\varepsilon}_{s,e,n}^k(x)$  (④) for each section are computed. This is the first approximation of the element state determination, since  $\mathbf{B}_{d,e}(x)$  is exact only in the linear elastic case of a prismatic member.

Assuming that the section constitutive law is explicitly known, the section tangent stiffness matrices  $\mathbf{k}_{s,e,n}^{tan,k}(x)$  and the internal section force vectors  $\boldsymbol{\sigma}_{s,e,n}^{int,k}(x)$  are readily determined from  $\boldsymbol{\varepsilon}_{s,e,n}^k(x)$  (⑤). Then, using Eq. 1.8 and Eq. 1.10 the element stiffness matrices  $\bar{\mathbf{k}}_{e,n}^k$  in local reference and the internal element nodal force vectors in local reference  $\bar{\mathbf{f}}_{e,n}^{int,k}$  are determined next (⑥).

Finally, through assembly of the global stiffness matrix, the structures' tangent stiffness matrix and vector of nodal internal forces are determined (⑦), before the residual is computed (⑧) for convergence assessment.

Since  $\mathbf{B}_{d,e}(x)$  is only approximate<sup>2</sup> (since we are approximating the displacement field), the integrals for the element tangent stiffness matrix in local reference and the internal element nodal force vector in local reference will also yield approximate results. The approximation of  $\mathbf{B}_{d,e}(x)$  leads to stiffer solution, Fig. 1.3 (a) and (b). Note that the curve labeled "Exact solution" is only exact within the assumptions of the section constitutive law and the kinematic approximations that deformations are small and plane sections remain plane.

To overcome numerical errors that arise from the approximation of  $\mathbf{B}_{d,e}(x)$ , analysts resort to fine mesh discretization of the structure, especially, in frame regions that undergo highly nonlinear behaviors, such as the member ends. Even so, numerical convergence problems persist. This is precisely why the flexibility based element (as will be shown later) yields better results.

<sup>2</sup>We shall see later that the corresponding term in the flexibility based element is not approximate.

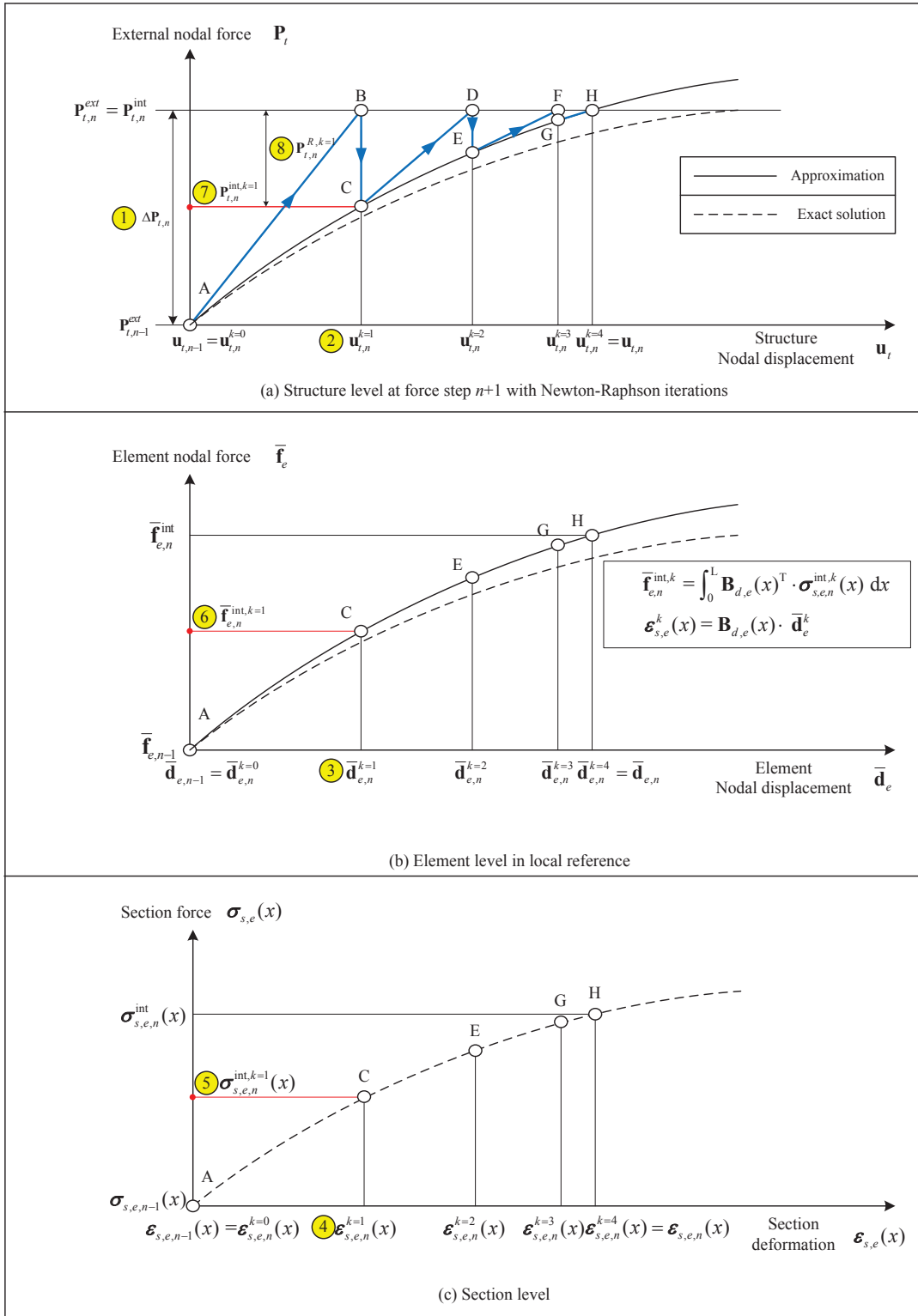
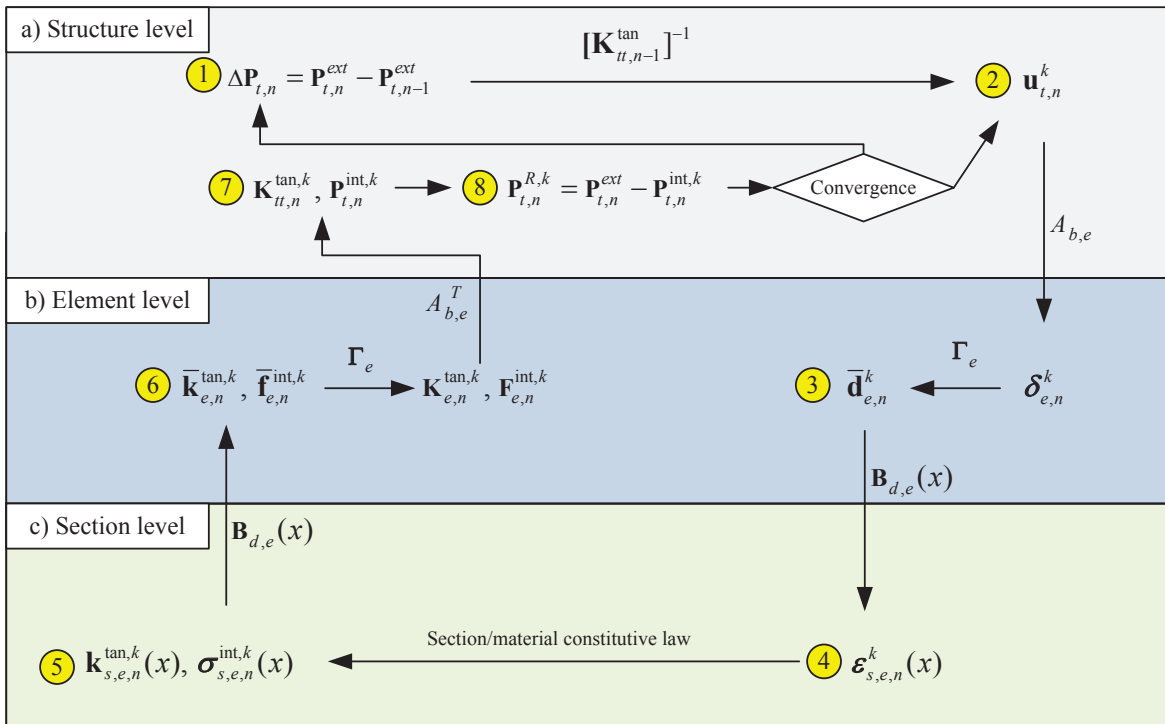
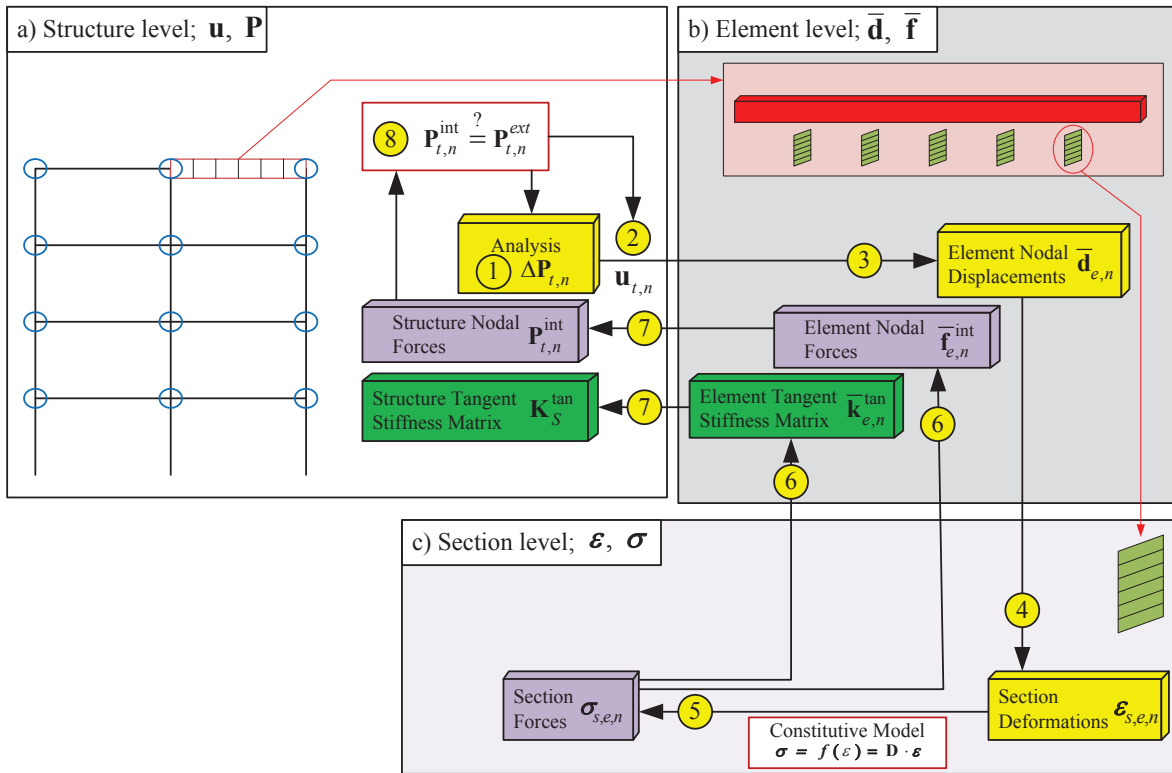


Figure 1.3: State determination for stiffness-based method



where,  $\mathbf{A}_{b,e}$  and  $\mathbf{A}_{b,e}^T$  are the displacement extracting operator and the force assembling operator.

Figure 1.4: State determination procedure for stiffness-based method

#### 1.2.1.4 Nonlinear analysis using stiffness-based formulation

With reference to Fig. 1.4 to 1.7, we will examine one single step of the Newton-Raphson method for the nonlinear analysis with section constitutive law. Force and displacement control, mentioned here, are discussed in Sec. 4.4 and 4.5. Layer or fiber section procedure in Fig. 1.7 will be described in Sec. 1.3.

Again step numbers refer to those in Fig. 1.3.

- ① Compute the incremental nodal force vector  $\Delta \mathbf{P}_{t,n}^{ext}$ .

$$\Delta \mathbf{P}_{t,n}^{ext} = \mathbf{P}_{t,n}^{ext} - \mathbf{P}_{t,n-1}^{ext}$$

- ② Expressing the augmented stiffness matrix  $\mathbf{K}_S$  as

$$\begin{Bmatrix} \mathbf{P}_t \\ \mathbf{P}_u \end{Bmatrix} = \begin{bmatrix} \mathbf{K}_{tt} & \mathbf{K}_{tu} \\ \mathbf{K}_{ut} & \mathbf{K}_{uu} \end{bmatrix} \begin{Bmatrix} \mathbf{u}_t \\ \mathbf{u}_u \end{Bmatrix} \quad (1.11)$$

where subscript  $t$  and  $u$  are associated with free end constrained degrees of freedom respectively, compute the incremental nodal displacement vector  $\delta \mathbf{u}_{t,n}$  and corresponding total nodal displacement vector  $\mathbf{u}_{t,n}$  in the structure level. Initially, iteration starts from Eq. 1.12 with  $k = 1$ .

If  $k = 1$ ,

$$\begin{aligned} \delta \mathbf{u}_{u,n}^k &= \mathbf{u}_{u,n} - \mathbf{u}_{u,n-1}, \quad \mathbf{u}_{u,n} = \mathbf{u}_{u,n-1} + \delta \mathbf{u}_{u,n}^k \\ \delta \mathbf{u}_{t,n}^k &= [\mathbf{K}_{tt,n}^{tan,k-1}]^{-1} \cdot [\Delta \mathbf{P}_{t,n}^{ext} - \mathbf{K}_{tu,n}^{tan,k-1} \delta \mathbf{u}_{u,n}^k] \\ \mathbf{u}_{t,n}^k &= \mathbf{u}_{t,n}^{k-1} + \delta \mathbf{u}_{t,n}^k \end{aligned} \quad (1.12)$$

If  $k \neq 1$ ,

$$\begin{aligned} \mathbf{P}_{t,n}^{R,k} &= \mathbf{P}_{t,n}^{ext} - \mathbf{P}_{t,n}^{int,k} \\ \delta \mathbf{u}_{t,n}^{k+1} &= [\mathbf{K}_{tt,n}^{tan,k}]^{-1} \cdot \mathbf{P}_{t,n}^{R,k} \\ \mathbf{u}_{t,n}^{k+1} &= \mathbf{u}_{t,n-1} + \Delta \mathbf{u}_{t,n}^{k+1} = \mathbf{u}_{t,n}^k + \delta \mathbf{u}_{t,n}^{k+1} \end{aligned} \quad (1.13)$$

where, superscript  $k$  is the iteration counter,  $\mathbf{P}_t^R$  the residual nodal force vector in structural level,  $\Delta \mathbf{u}_{t,n}^{k+1}$  the total incremental displacement vector from the last converged step, and  $\delta \mathbf{u}_n^{k+1}$  the last incremental displacement vector.

- ③ Loop over all the elements and determine their state.

- Determine the element nodal displacement vector in global reference.

If  $k = 1$ ,

$$\delta \boldsymbol{\delta}_{e,n}^k = \mathcal{A}_{b,e} \cdot \delta \mathbf{u}_{t,n}^k + \mathcal{A}_{b,e} \cdot \delta \mathbf{u}_{u,n}^k$$

If  $k \neq 1$ ,

$$\delta \boldsymbol{\delta}_{e,n}^k = \mathcal{A}_{b,e} \cdot \delta \mathbf{u}_{t,n}^k$$

where,  $\mathcal{A}_{b,e}$  is a displacement extracting operator.

$$\boldsymbol{\delta}_{e,n}^k = \boldsymbol{\delta}_{e,n}^{k-1} + \delta \boldsymbol{\delta}_{e,n}^k$$

and,  $\boldsymbol{\delta}_{e,n}^0$  corresponds to  $\boldsymbol{\delta}_{e,n-1}$ .

- Determine the element nodal displacement vector in local reference

$$\begin{aligned} \delta \bar{\mathbf{d}}_{e,n}^k &= \boldsymbol{\Gamma}_e \cdot \boldsymbol{\delta}_{e,n}^k \\ \bar{\mathbf{d}}_{e,n}^k &= \bar{\mathbf{d}}_{e,n}^{k-1} + \delta \bar{\mathbf{d}}_{e,n}^k \end{aligned}$$

and,  $\bar{\mathbf{d}}_{e,n}^0$  corresponds to  $\bar{\mathbf{d}}_{e,n-1}$ .

- ④ Start the section state determination by looping over the element's sections. The total number of section may vary from element to element. Therefore, the total number of sections in an element is  $nIp_e$  and it depends on the number of integration points in the Gauss Legendre quadrature rule.

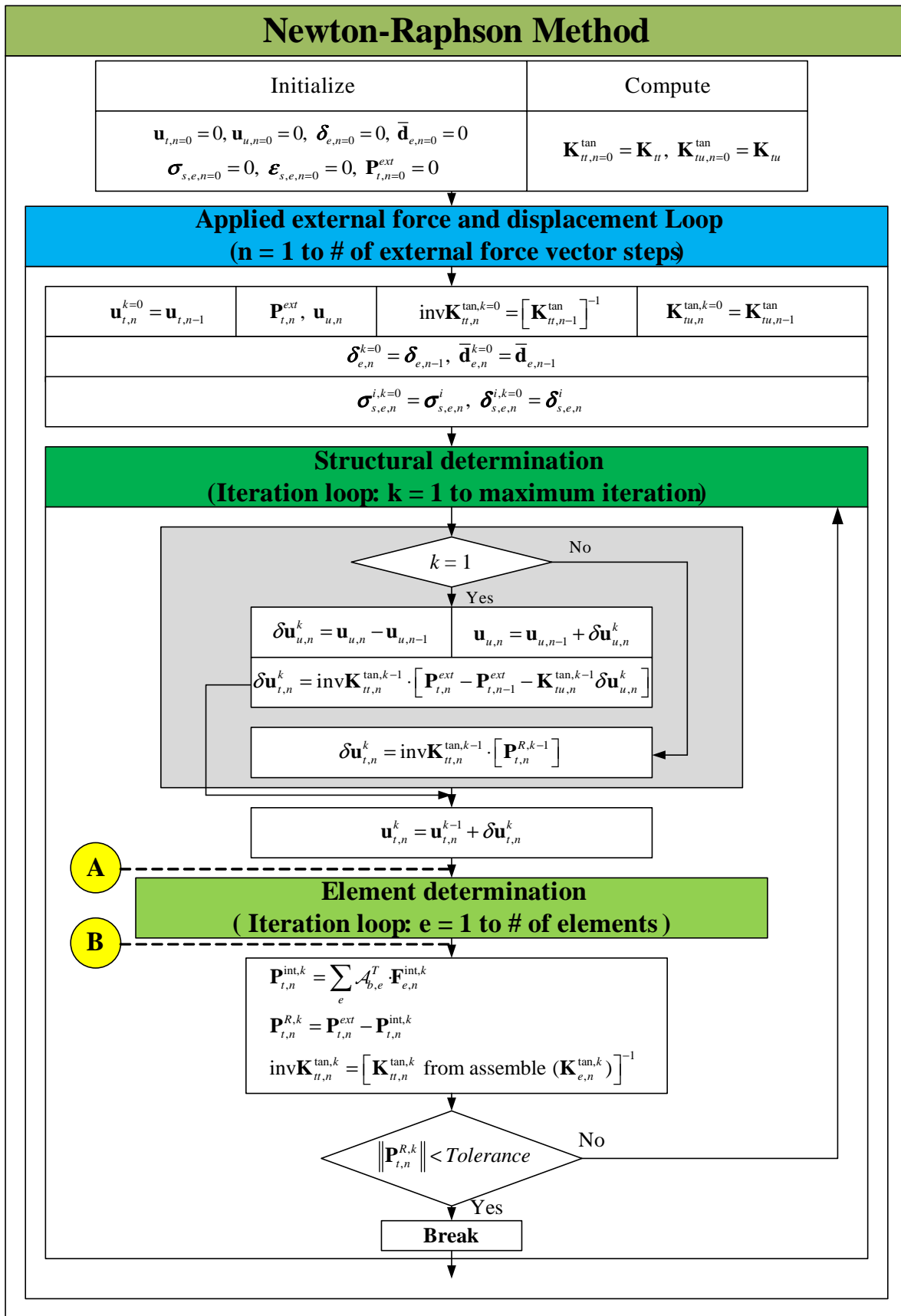


Figure 1.5: Flow chart of nonlinear analysis using stiffness-based method (1)

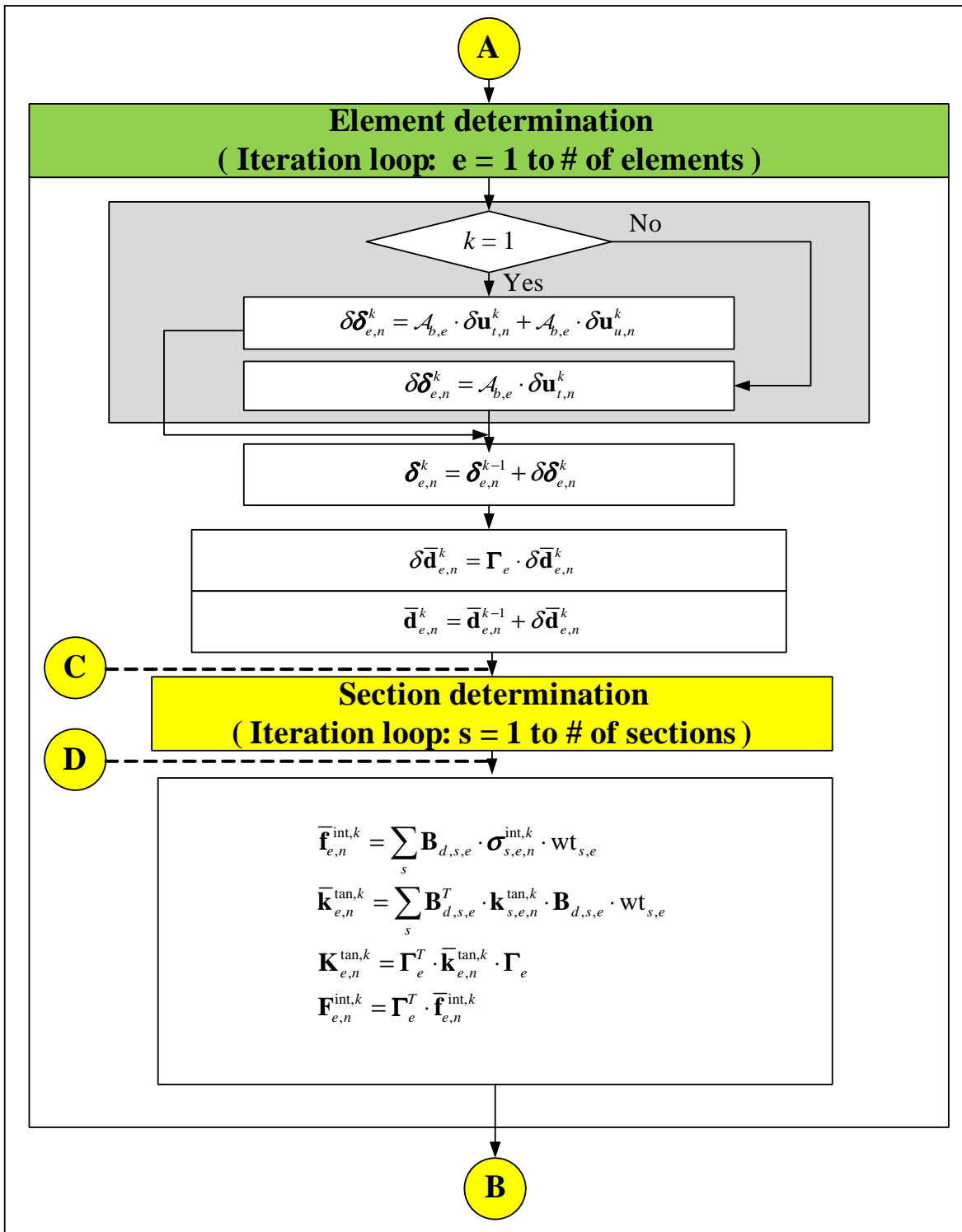


Figure 1.6: Flow chart of nonlinear analysis using stiffness-based method (2)

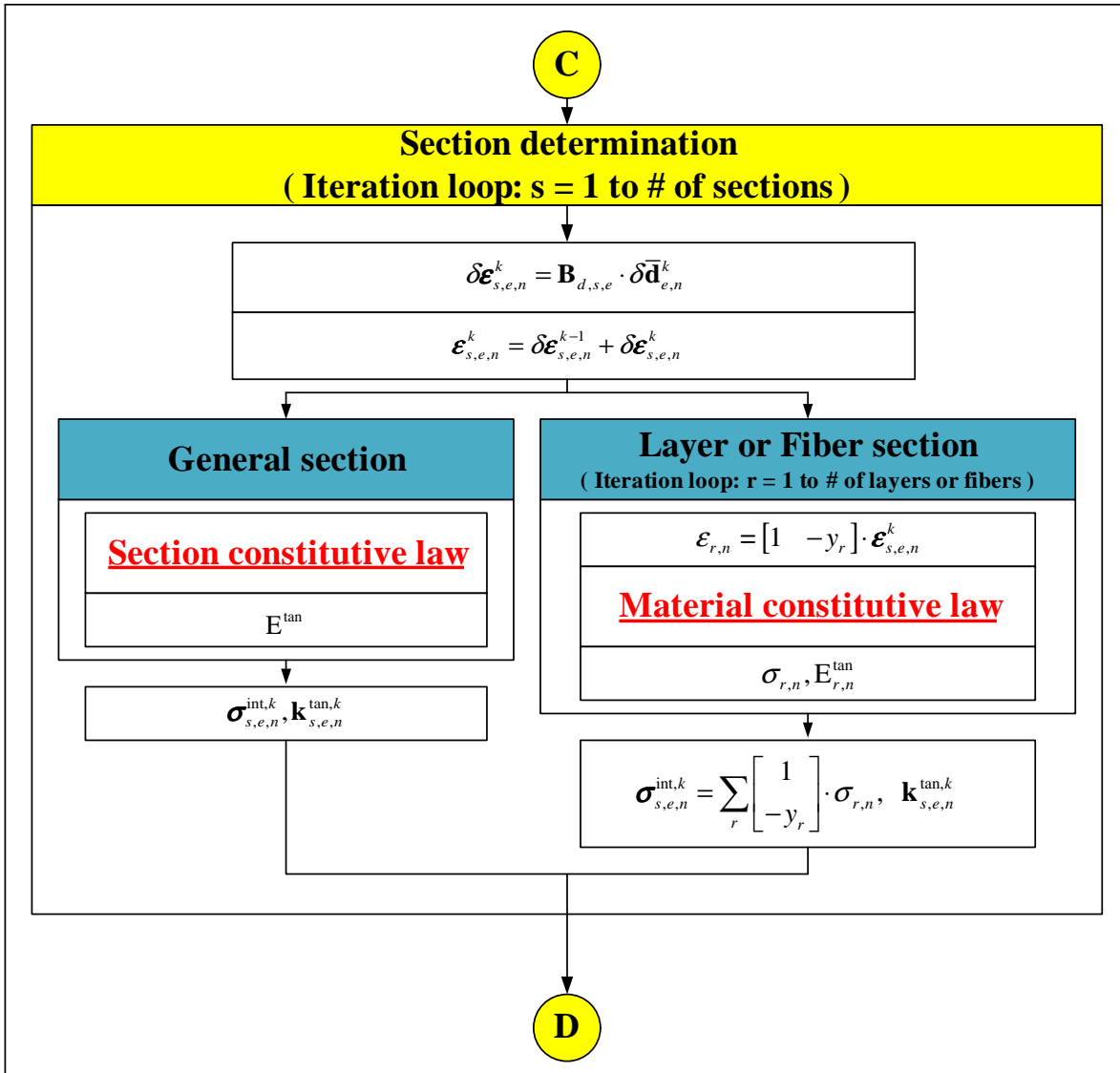


Figure 1.7: Flow chart of nonlinear analysis using stiffness-based method (3)

For the section state determination, we first need to distinguish between general section and fiber section as described later in Sec. 1.3. Presently, we only consider general section. The state determination of each section is computed within loop  $s$  which refers to the  $s^{th}$  section.

$$\delta\boldsymbol{\epsilon}_{s,e,n}^k = \mathbf{B}_{d,s,e} \cdot \delta\bar{\mathbf{d}}_{e,n}^k$$

where,  $\mathbf{B}_{d,s,e}$  is the matrix derived (derivatives) from the displacement interpolation functions at  $s^{th}$  section of  $e^{th}$  element.

$$\boldsymbol{\epsilon}_{s,e,n}^k = \boldsymbol{\epsilon}_{s,e,n}^{k-1} + \delta\boldsymbol{\epsilon}_{s,e,n}^k$$

and,  $\boldsymbol{\epsilon}_{s,e,n}^0$  corresponds to  $\boldsymbol{\epsilon}_{s,e,n-1}$ .

- ⑤ Determine the section tangent stiffness matrix and the internal section force vector. If the section constitutive law is explicitly known, then  $\mathbf{k}_{s,e,n}^{tan,k}$  and  $\boldsymbol{\sigma}_{s,e,n}^{int,k}$  are determined from  $\boldsymbol{\epsilon}_{s,e,n}^k$ . For linear elastic section, we need not to recompute  $\mathbf{k}_{s,e,n}^{tan,k}$  as it is identical to the initial section stiffness matrix  $\mathbf{k}_{s,e}$ .

Thus, for elastic sections:

$$\begin{aligned}\mathbf{k}_{s,e,n}^{tan,k} &= \mathbf{k}_{s,e} \\ \boldsymbol{\sigma}_{s,e,n}^{int,k} &= \mathbf{k}_{s,e,n}^{tan,k} \cdot \boldsymbol{\epsilon}_{s,e,n}^k\end{aligned}$$

where,  $\mathbf{k}_{s,e,n}^{tan,k}$  is the section tangent stiffness matrix at  $k^{th}$  iteration.

- ⑥ Determine first the internal element nodal force vector and the element tangent stiffness matrix, then from Eq. 1.10 and Eq. 1.8, determine  $\bar{\mathbf{f}}_{e,n}^{int,k}$  and  $\bar{\mathbf{k}}_{e,n}^{tan,k}$ .

$$\bar{\mathbf{f}}_{e,n}^{int,k} = \sum_s \mathbf{B}_{d,s,e}^T \cdot \boldsymbol{\sigma}_{s,e,n}^{int,k} \text{wt}_{s,e}$$

where,  $\text{wt}_{s,e}$  is the weight coefficient associated with the Jacobian at the  $s^{th}$  section of the  $e^{th}$  element.

$$\bar{\mathbf{k}}_{e,n}^{tan,k} = \sum_s \mathbf{B}_{d,s,e}^T \cdot \mathbf{k}_{s,e,n}^{tan,k} \cdot \mathbf{B}_{d,s,e} \cdot \text{wt}_{s,e}$$

where,  $\bar{\mathbf{k}}_{e,n}^{tan,k}$  is the element tangent stiffness matrix in local reference.

Finally, from Eq. 1.9, determine  $\mathbf{F}_{e,n}^{int,k}$  and  $\mathbf{K}_{e,n}^{tan,k}$ .

$$\begin{aligned}\mathbf{F}_{e,n}^{int,k} &= \boldsymbol{\Gamma}_e^T \cdot \bar{\mathbf{f}}_{e,n}^{int,k} \\ \mathbf{K}_{e,n}^{tan,k} &= \boldsymbol{\Gamma}_e^T \cdot \bar{\mathbf{k}}_{e,n}^{tan,k} \cdot \boldsymbol{\Gamma}_e\end{aligned}$$

- ⑦ Determine the internal nodal force vector and the augmented tangent stiffness matrix.

$$\begin{aligned}\mathbf{P}_{t,n}^{int,k} &= \sum_e \mathcal{A}_{b,e}^T \cdot \mathbf{F}_{e,n}^{int,k} \\ \mathbf{K}_{S,n}^{tan,k} &= \sum_e \mathcal{A}_{b,e}^T \cdot \mathbf{K}_{e,n}^{tan,k} \cdot \mathcal{A}_{b,e}\end{aligned}$$

where,  $\mathcal{A}_{b,e}^T$  is a force assembling operator, and  $\mathbf{K}_{S,n}^{tan,k}$  encompasses the four submatrices,  $\mathbf{K}_{tt,n}^{tan,k}$ ,  $\mathbf{K}_{tu,n}^{tan,k}$ ,  $\mathbf{K}_{ut,n}^{tan,k}$ , and  $\mathbf{K}_{uu,n}^{tan,k}$  as shown Eq. 1.11.

- ⑧ Compute the residual nodal force vector at the structural level from Eq. 1.13 and check for convergence:

- If  $\mathbf{P}_{t,n}^{R,k}$  is within the specified tolerance, go to next force increment.
- If  $\mathbf{P}_{t,n}^{R,k}$  is not within the specified tolerance,  $k$  is updated to  $k+1$  and the next Newton-Raphson iteration starts. Eq. 1.13 in ② through ⑧ are repeated until convergence occurs at the structure level.

## 1.2.2 Flexibility-based 2D beam-column element

Flexibility-based 2D beam-column elements are “nonconformist” finite elements since they yield the element flexibility matrix rather than the classical stiffness matrix, and are based on the equations of equilibrium rather than on assumed displacement field. Nevertheless, they do offer some important advantages which will be highlighted later.

### 1.2.2.1 Formulation

In this section we will derive the element flexibility matrix  $\tilde{\mathbf{c}}_e$  without rigid body modes and then invert it to obtain the corresponding element stiffness matrix  $\tilde{\mathbf{k}}_e$  (again without rigid body modes). The retained degrees of freedom are the axial force at node 2, and the two end moments.

This is particularly interesting in those instances where stiffness-based method formulations are approximate and flexibility-based method formulations are exact such as a section varying along the element and elements with material nonlinearity.

Whereas we have used the principle of virtual work (displacement) for the derivation of the stiffness based element, we shall now use the principle of complementary virtual work (force) through the usual three steps.

**Equilibrium** will now be strongly enforced (whereas it was satisfied in the weak sense previously), Fig. 1.8

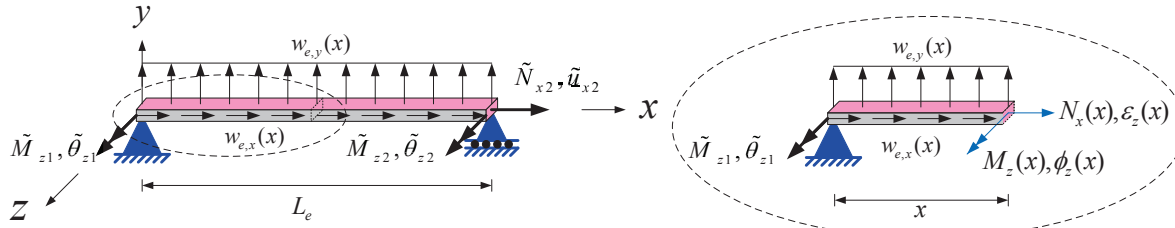


Figure 1.8: 2D beam-column element without rigid body modes

$$\underbrace{\mathbf{w}_e(x)}_{\text{External}} + \underbrace{\mathcal{L}_f \cdot \boldsymbol{\sigma}_s(x)}_{\text{Internal}} = \mathbf{0} \quad (1.14)$$

$$\left\{ \begin{array}{l} w_x^{(e)}(x) \\ w_y^{(e)}(x) \end{array} \right\} + \begin{bmatrix} \frac{d}{dx} & 0 \\ 0 & \frac{d^2}{dx^2} \end{bmatrix} \left\{ \begin{array}{l} N_x(x) \\ M_z(x) \end{array} \right\} = \mathbf{0}$$

where,  $\mathbf{w}_e(x)$  is the external element traction vector and  $\mathcal{L}_f$  is the force differential operator which enforces equilibrium.

By analogy, in the stiffness formulation, the compatibility was “strongly” enforced, and it has led to the interpolation functions for displacements (also known as shape functions in that particular case).

In here, we will be expressing the equilibrium of sectional stresses in terms of the nodal forces through equilibrium. We first assume that there are no external element traction<sup>3</sup>, that is  $\mathbf{w}_e(x) = \mathbf{0}$ . Whereas we previously used displacement interpolation functions, we now need force interpolation functions,  $\mathbf{N}_f(x)$  in order to exactly satisfy equilibrium (Eq. 1.14) along the element

$$\begin{bmatrix} \frac{d}{dx} & 0 \\ 0 & \frac{d^2}{dx^2} \end{bmatrix} \left\{ \begin{array}{l} N_x(x) \\ M_z(x) \end{array} \right\} = \mathbf{0}$$

will yield

$$\begin{aligned} \frac{dN_x(x)}{dx} &= 0 \\ \frac{d^2M_z(x)}{dx^2} &= 0 \end{aligned}$$

Integrating these equations, we obtain

$$\begin{aligned} N_x(x) &= c_3 \\ M_z(x) &= c_1x + c_2 \end{aligned} \quad (1.15)$$

Applying the natural boundary condition from Fig. 1.8 with the sign convention (on section force) shown in Fig. 1.9,

<sup>3</sup>This restriction will be later removed.

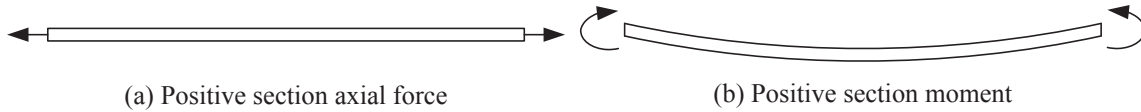


Figure 1.9: Sign convention on section forces

$$N_x(L) = N_{x2}$$

$$M_z(0) = -M_{z1}$$

$$M_z(L) = M_{z2}$$

we obtain

$$\begin{aligned} c_1 &= \frac{M_{z1} + M_{z2}}{L_e} \\ c_2 &= -M_{z1} \\ c_3 &= N_{x2} \end{aligned} \tag{1.16}$$

Substituting Eq. 1.16 into Eq. 1.15,

$$\begin{aligned} N_x(x) &= N_{x2} \\ M_z(x) &= \left( \frac{x}{L_e} - 1 \right) M_{z1} + \frac{x}{L_e} M_{z2} \end{aligned}$$

or

$$\underbrace{\begin{Bmatrix} N_x(x) \\ M_z(x) \end{Bmatrix}}_{\boldsymbol{\sigma}_s(x)} = \underbrace{\begin{bmatrix} 0 & 0 & 1 \\ \frac{x}{L_e} - 1 & \frac{x}{L_e} & 0 \end{bmatrix}}_{\mathbf{N}_f(x)} \underbrace{\begin{Bmatrix} M_{z1} \\ M_{z2} \\ N_{x2} \end{Bmatrix}}_{\tilde{\mathbf{f}}_e} \tag{1.17}$$

where,  $\tilde{\mathbf{f}}_e$  is the element nodal force vector without rigid body modes.

Finally, from Eq. 1.17, we extract the matrix of force interpolation functions.

$$\mathbf{N}_f(x) = \begin{bmatrix} 0 & 0 & 1 \\ \frac{x}{L_e} - 1 & \frac{x}{L_e} & 0 \end{bmatrix}$$

It should be noted that these shape functions enforce equilibrium at any section along the element.

**Constitutive law :** Whereas we have previously expressed section forces in terms of section deformations (Eq. 1.5), we now need to express section deformations in terms of section forces

$$\boldsymbol{\varepsilon}_s(x) = \mathbf{c}_s(x) \cdot \boldsymbol{\sigma}_s(x) \tag{1.18}$$

where,  $\mathbf{c}_s(x)$  is the section flexibility matrix. If  $\mathbf{c}_s(x)$  is not derived from fiber section (which will be discussed in Sec. 1.3), then for linear elastic analysis  $\mathbf{c}_s(x)$  is simply

$$\mathbf{c}_s(x) = \begin{bmatrix} \frac{1}{E(x) \cdot A(x)} & 0 \\ 0 & \frac{1}{E(x) \cdot I_z(x)} \end{bmatrix}$$

which is simply the inverse of Eq. 1.6. We note that shear deformations (but not shear forces) are absent in this classical Euler-Bernoulli formulation, whereas they are included in the so-called Timoshenko formulation.

**Compatibility** of displacements:

This requirement will be enforced only in a weak form through the principle of complementary virtual work (as

opposed to the principle of virtual work for the stiffness-based method in Eq. 1.7).

$$\underbrace{\delta \tilde{\mathbf{f}}_e^T \tilde{\mathbf{d}}_e}_{\text{External}} = \underbrace{\int_0^{L_e} \delta \boldsymbol{\sigma}_s(x)^T \cdot \boldsymbol{\epsilon}_s(x) dx}_{\text{Internal}} \quad (1.19)$$

where  $\tilde{\mathbf{d}}_e$  is the element nodal displacement vector without rigid body modes.

Substituting Eq. 1.17 and Eq. 1.18 into Eq. 1.19 and since the latter must hold for any arbitrary  $\delta \tilde{\mathbf{f}}_e$ , we obtain

$$\begin{aligned} \delta \tilde{\mathbf{f}}_e^T \tilde{\mathbf{d}}_e &= \int_0^{L_e} \delta \tilde{\mathbf{f}}_e^T \cdot \mathbf{N}_f(x)^T \cdot \mathbf{c}_s(x) \cdot \boldsymbol{\sigma}_s(x) dx \\ \tilde{\mathbf{d}}_e &= \int_0^{L_e} \mathbf{N}_f(x)^T \cdot \mathbf{c}_s(x) \cdot \boldsymbol{\sigma}_s(x) dx = \underbrace{\int_0^{L_e} \mathbf{N}_f(x)^T \cdot \mathbf{c}_s(x) \cdot \mathbf{N}_f(x) dx}_{\tilde{\mathbf{c}}_e} \cdot \tilde{\mathbf{f}}_e \\ \tilde{\mathbf{d}}_e &= \tilde{\mathbf{c}}_e \cdot \tilde{\mathbf{f}}_e \end{aligned}$$

The element flexibility matrix without rigid body modes in local reference is thus given by

$$\tilde{\mathbf{c}}_e = \int_0^{L_e} \mathbf{N}_f(x)^T \cdot \mathbf{c}_s(x) \cdot \mathbf{N}_f(x) dx \quad (1.20)$$

which is the counterpart of Eq. 1.8, and the corresponding element stiffness matrix without rigid body modes in local reference is simply

$$\tilde{\mathbf{k}}_e = [\tilde{\mathbf{c}}_e]^{-1}$$

### 1.2.2.2 Coordinate system for flexibility-based 2D beam-column element with Bernoulli beam theory

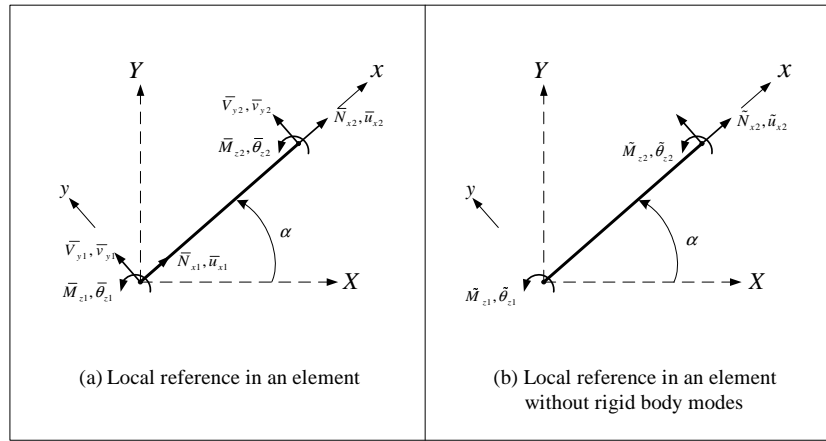


Figure 1.10: Internal forces and corresponding displacements in local coordinate system with or without rigid body modes for the flexibility-based 2D beam-column element

Contrarily to the reference system of the stiffness-based method in Fig. 1.2, we need to consider forces and displacements in local reference with and without rigid body modes as shown in Fig. 1.10.

Element nodal force vector without rigid body modes in local reference are (arbitrarily) selected as

$$\tilde{\mathbf{f}}_e = [\tilde{M}_{z1}, \tilde{M}_{z2}, \tilde{N}_{x2}]^T$$

and the corresponding element nodal displacement vector without rigid body modes in local reference are given by

$$\tilde{\mathbf{d}}_e = [\tilde{\theta}_{z1}, \tilde{\theta}_{z2}, \tilde{u}_{x2}]^T$$

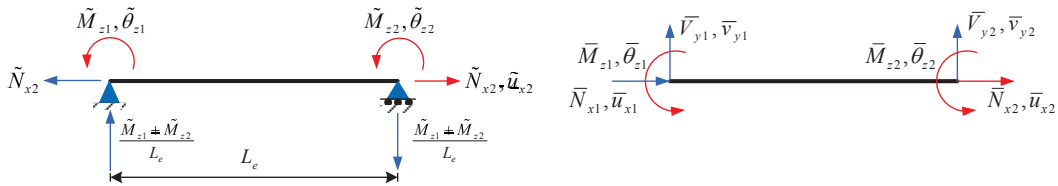


Figure 1.11: The relationship between rigid body modes and no rigid body modes

The relationship between rigid body modes and no rigid body modes is obtained through equilibrium, Fig. 1.11.

$$\left\{ \begin{array}{c} \bar{N}_{x1} \\ \bar{V}_{y1} \\ \bar{M}_{z1} \\ \bar{N}_{x2} \\ \bar{V}_{y2} \\ \bar{M}_{z2} \end{array} \right\} = \underbrace{\begin{bmatrix} 0 & 0 & -1 \\ \frac{1}{L_e} & \frac{1}{L_e} & 0 \\ 1 & 0 & 0 \\ 0 & 0 & 1 \\ -\frac{1}{L_e} & -\frac{1}{L_e} & 0 \\ 0 & 1 & 0 \end{bmatrix}}_{\tilde{\mathbf{r}}_e^T} \left\{ \begin{array}{c} \tilde{M}_{z1} \\ \tilde{M}_{z2} \\ \tilde{N}_{x2} \end{array} \right\} \quad (1.21)$$

$$\begin{aligned} \bar{\mathbf{f}}_e &= \tilde{\mathbf{r}}_e^T \cdot \tilde{\mathbf{f}}_e \\ \bar{\mathbf{d}}_e &= \tilde{\mathbf{r}}_e^T \cdot \tilde{\mathbf{d}}_e \\ \mathbf{K}_e &= \tilde{\mathbf{r}}_e^T \cdot \tilde{\mathbf{k}}_e \cdot \tilde{\mathbf{r}}_e \end{aligned} \quad (1.22)$$

which is the counterpart of Eq. 1.9.

Finally, the derivation of the stiffness matrix from the flexibility one and the equations of equilibrium parallels the one which yielded Eq. ??

$$[\mathbf{K}] = \left[ \begin{array}{c|c} [\mathbf{d}]^{-1} & [\mathbf{d}]^{-1} [\mathcal{B}]^T \\ \hline [\mathcal{B}] [\mathbf{d}]^{-1} & [\mathcal{B}] [\mathbf{d}]^{-1} [\mathcal{B}]^T \end{array} \right] \quad (1.23)$$

### 1.2.2.3 State determination

In their early and pioneering publication ? did not provide a clear and consistent method for calculating the internal element force vectors from element deformations. Possibly because the finite element formulation is based on the complementary principle of virtual work and the corresponding flexibility-based 2D beam-column elements do not have shape functions that relate deformation field inside the element with element nodal displacement vector.

Since the global finite element formulation is based on the stiffness (displacement) formulation, the flexibility (force) based element formulation will have to be reconciled with the global formulation. Furthermore, internal element force vectors of all elements should be determined during the phase of state determination. Hence, the state determination is obtained from the mixed stiffness-based and flexibility-based methods.

The nonlinear algorithm for the mixed stiffness-based and flexibility-based methods will be divided into two methods (a) with Newton-Raphson iteration in the element level to determine element state, (b) without iteration in the element level to determine element state. The former is based on the formulation of (?) and the later on the one of (?).

**1.2.2.3.1 With element iterations** As with the state determination of stiffness-based 2D beam-column in a nonlinear structural analysis the state determination process for the mixed stiffness-based and flexibility-based methods with Newton-Raphson iteration loop in the element level is made up of three parts as shown in Fig. 1.14 (which is the counterpart of Fig. 1.3).

1. Section state determination, Fig. 1.14(c)
2. Element state determination, Fig. 1.14(b)
3. Structure state determination, Fig. 1.14(a)

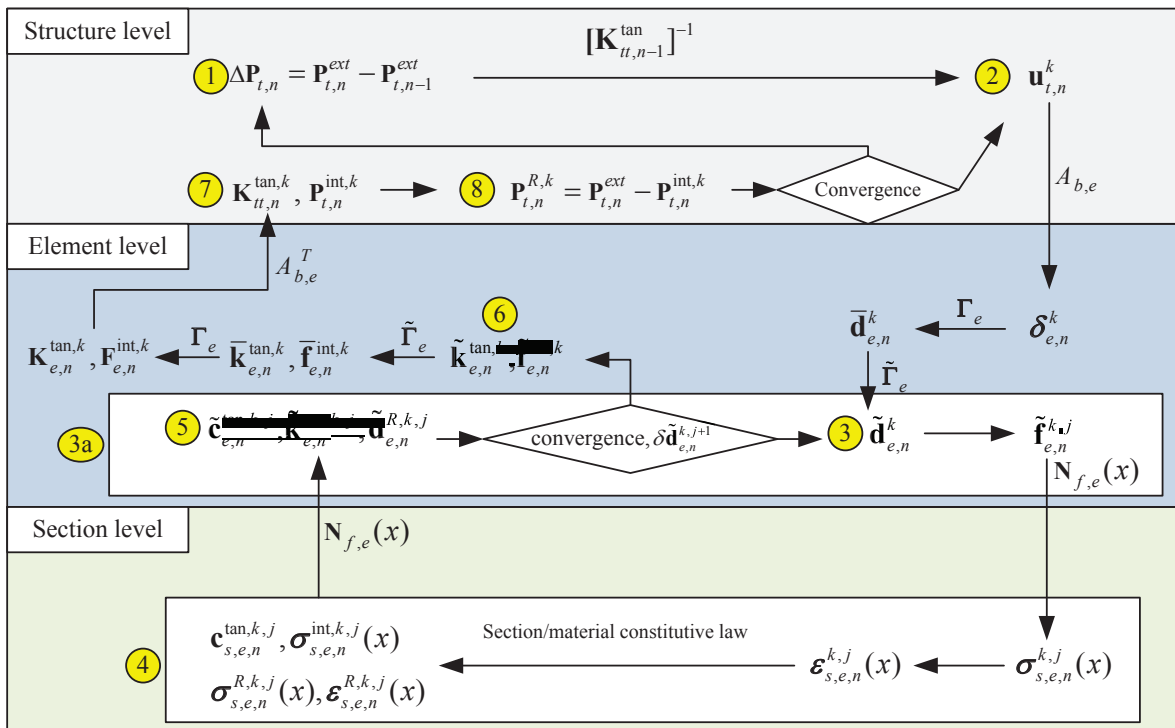
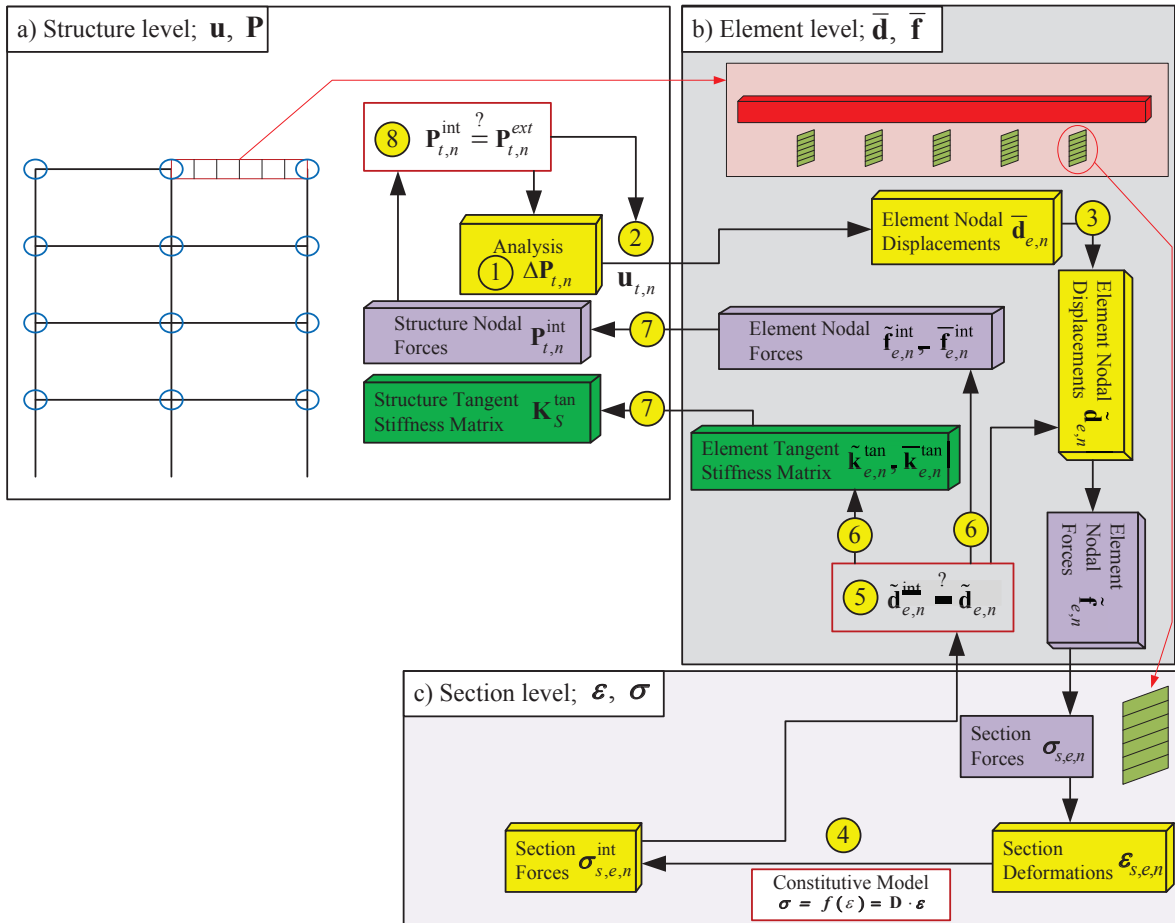


Figure 1.12: State determination procedure for flexibility-based method with Newton-Raphson iteration in the element

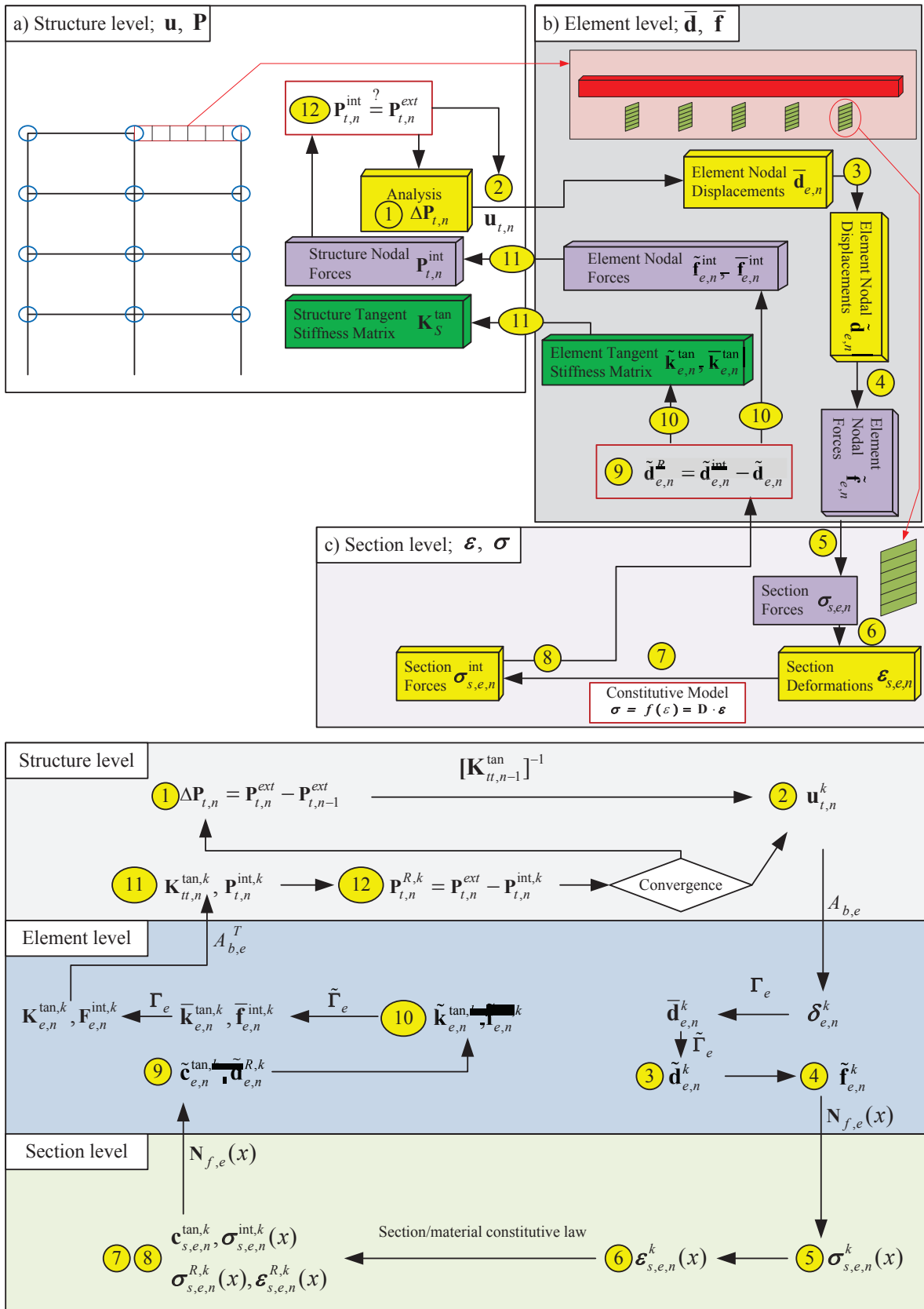


Figure 1.13: State determination procedure for flexibility-based method without Newton-Raphson iteration in the element

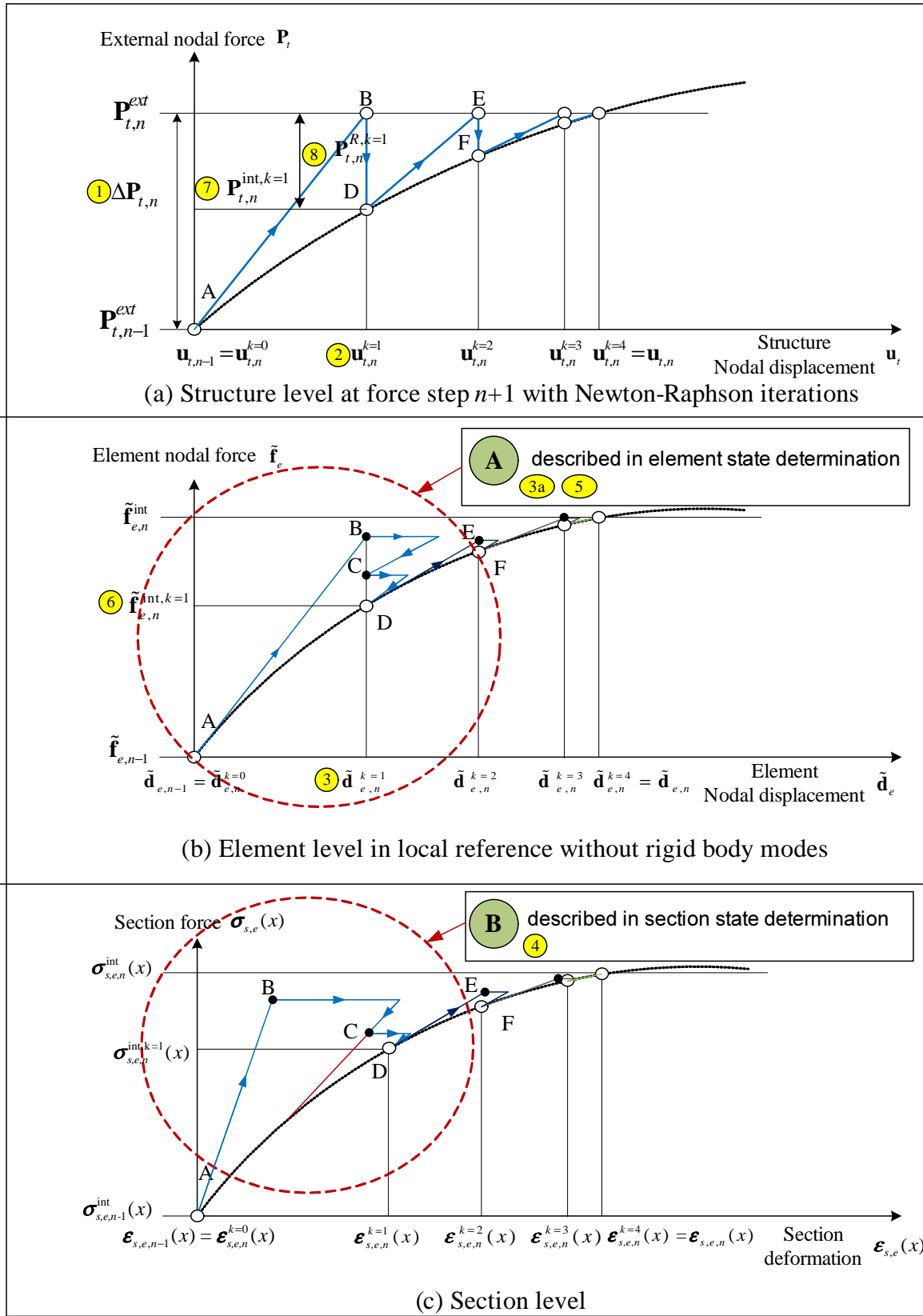


Figure 1.14: State determination for flexibility-based method with element iteration (?)

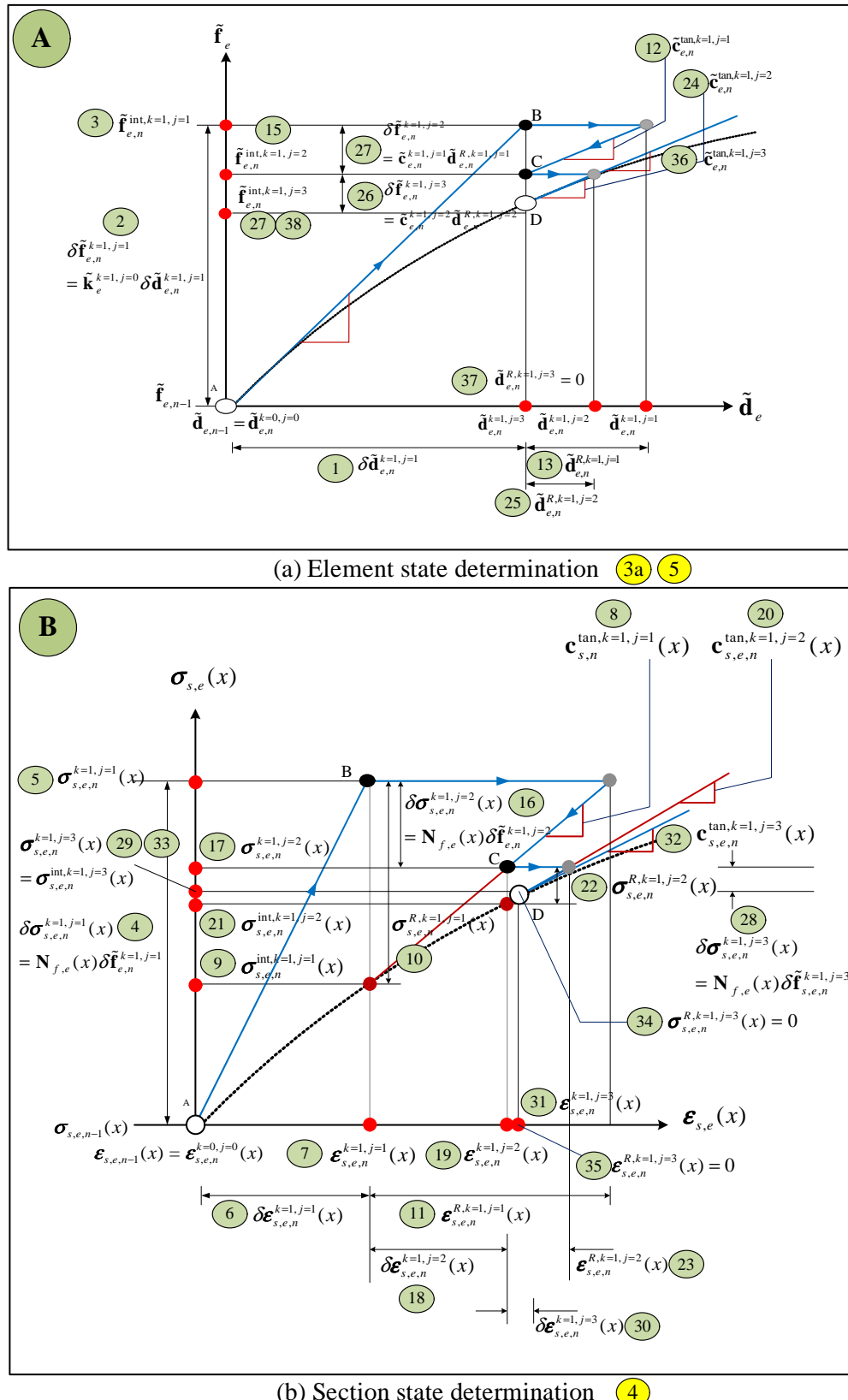


Figure 1.15: Element and section state determinations for flexibility-based 2D beam-column element with Newton-Raphson iteration loop in the element level

Where, superscript  $j$  in Fig. 1.14(b) denotes the iteration scheme at the element level in the element state determination process. This iteration loop is necessary for the determination of the internal element nodal force vector  $\tilde{\mathbf{f}}_e^{int,k}$  that correspond to the element nodal displacement vector  $\tilde{\mathbf{d}}_e^k$  at the  $k^{th}$  Newton-Raphson iteration.

It is again assumed that the Newton-Raphson is used for the iteration process in the structural level and that this does not affect the iterative scheme in the element level (which determines the internal element nodal force vector  $\tilde{\mathbf{f}}_e^{int}$  for the element nodal displacement vector  $\tilde{\mathbf{d}}_e$ ).

Broadly speaking, this formulation can be decomposed as follows:

1. First, determine the element nodal force vector  $\tilde{\mathbf{f}}_{e,n}^{k,j}$  (6) from the current element nodal displacement vector using the element tangent stiffness matrix  $\tilde{\mathbf{k}}_{e,n}^{tan,k,j-1}$  (3) of the previous iteration.
2. Through the force interpolation functions  $\mathbf{N}_{f,e}(x)$  determine the section force vectors  $\sigma_{s,e,n}^{k,j}(x)$  along the element. These are two complications in this procedure.
  - a) The determination of the section deformation vectors  $\epsilon_{s,e,n}^{k,j}(x)$  from section force vectors since the nonlinear section force-deformation relation is commonly expressed as an explicit function of section deformation vector (4).
  - b) Changes in the section tangent stiffness matrices  $\mathbf{k}_{s,e,n}^{tan}(x)$  produce a new element tangent stiffness matrix which, in turn, changes the element nodal force vector for the given element nodal displacement vector (6).

These problems are solved through a nonlinear approach which first determines residual element nodal displacement vector  $\tilde{\mathbf{d}}_{e,n}^{R,k,j}$  at each iteration. Then, compatibility of displacement at the structural level requires that this residual element nodal displacement vector be corrected.

This is accomplished at the element level by applying corrective element nodal force vector based on the current element tangent stiffness matrix. The corresponding section force vectors are then determined from the force interpolation functions so that equilibrium will always be satisfied along the element. These section force vectors will not change during the section state determination in order to maintain equilibrium along the element.

Finally, the linear approximation of the section force-deformation relation about the present state results in residual section deformation vectors  $\sigma_{s,e,n}^{R,k,j}(x)$ . These are then integrated along the element to obtain new residual element nodal displacement vector (5) and the whole process is repeated until convergence occurs. It is important to stress that compatibility of element nodal displacement vector and equilibrium along the element are always satisfied in this process.

The nonlinear solution procedure for the element and section state determinations in Fig. 1.14 are illustrated in details in Fig. 1.15 for one Newton-Raphson iteration  $k$ . For illustrative purposes, convergence in loop  $j$  is reached in three iterations in Fig. 1.15.

The goal of the Newton-Raphson iteration loop in the element level is to determine the internal element nodal force vector (6) for the current element nodal displacement vector at the  $k^{th}$  Newton-Raphson iteration, hence

$$\tilde{\mathbf{d}}_{e,n}^k = \tilde{\mathbf{d}}_{e,n}^{k-1} + \delta\tilde{\mathbf{d}}_{e,n}^k$$

An iterative process in the element level denoted through the superscript  $j$  will be introduced inside the  $k^{th}$  Newton-Raphson iteration, and the first iteration corresponds to  $j = 1$ .

The initial state of the element, represented by the point  $\mathbf{A}$ , and  $j = 0$  and  $k = 0$  in Fig. 1.15, corresponds to the state at the end of the last convergence in structural level. With the initial element tangent stiffness matrix given by

$$\tilde{\mathbf{c}}_{e,n}^{tan,k=1,j=0} = \tilde{\mathbf{c}}_{e,n}^{tan}$$

and the given incremental element nodal displacement vector

$$\delta\tilde{\mathbf{d}}_{e,n}^{k=1,j=1} = \delta\tilde{\mathbf{d}}_{e,n}^{k=1}$$

hence, the corresponding incremental element nodal force vector is

$$\delta\tilde{\mathbf{f}}_{e,n}^{k=1,j=1} = [\tilde{\mathbf{c}}_{e,n}^{tan,k=1,j=0}]^{-1} \cdot \delta\tilde{\mathbf{d}}_{e,n}^{k=1,j=1} = \tilde{\mathbf{k}}_{e,n}^{tan,k=1,j=0} \cdot \delta\tilde{\mathbf{d}}_{e,n}^{k=1,j=1}$$

The incremental section force vectors can now be determined from the force interpolation functions

$$\delta\sigma_{s,e,n}^{k=1,j=1}(x) = \mathbf{N}_{f,e}(x) \cdot \delta\tilde{\mathbf{f}}_{e,n}^{k=1,j=1}$$

With the section tangent flexibility matrices at end of the last convergence in structural level given by

$$\mathbf{c}_{s,e,n}^{tan,k=1,j=0}(x) = \mathbf{c}_{s,e,n-1}^{tan}(x)$$

the linearization of the section force-deformation relation yields the incremental section deformation vectors.

$$\delta\boldsymbol{\epsilon}_{s,e,n}^{k=1,j=1}(x) = \mathbf{c}_{s,e,n}^{tan,k=1,j=0}(x) \cdot \delta\boldsymbol{\sigma}_{s,e,n}^{k=1,j=1}(x)$$

The section deformation vectors are updated to the state that corresponds to point **B** in Fig. 1.15(b), and the updated section deformation vector (4) will be given by

$$\boldsymbol{\epsilon}_{s,e,n}^{k=1,j=1}(x) = \boldsymbol{\epsilon}_{s,e,n}^{k=1,j=0}(x) + \delta\boldsymbol{\epsilon}_{s,e,n}^{k=1,j=1}(x)$$

For the sake of simplicity we will assume that the section force-deformation relation is explicitly known, then the section deformation vectors  $\boldsymbol{\epsilon}_{s,e,n}^{k=1,j=1}(x)$  will correspond to internal section force vectors  $\boldsymbol{\sigma}_{s,e,n}^{int,k=1,j=1}(x)$  and updated section tangent flexibility matrices  $\mathbf{c}_{s,e,n}^{tan,k=1,j=1}(x)$  in Fig. 1.15(b) can be defined.

The residual section force vectors are then determined

$$\boldsymbol{\sigma}_{s,e,n}^{R,k=1,j=1}(x) = \boldsymbol{\sigma}_{s,e,n}^{k=1,j=1}(x) - \boldsymbol{\sigma}_{s,e,n}^{int,k=1,j=1}(x)$$

and are transformed into residual section deformation vectors  $\boldsymbol{\epsilon}_{s,e,n}^{R,k=1,j=1}(x)$

$$\boldsymbol{\epsilon}_{s,e,n}^{R,k=1,j=1}(x) = \mathbf{c}_{s,e,n}^{tan,k=1,j=1}(x) \cdot \boldsymbol{\sigma}_{s,e,n}^{R,k=1,j=1}(x)$$

The residual section deformation vectors are thus the linear approximation of the deformation error made in the linearization of the section force-deformation relation (Fig. 1.15(b)). While any suitable section flexibility matrix can be used to calculate the residual section deformation vector, the section tangent flexibility matrices offer the fastest convergence rate.

The residual section deformation vectors are integrated along the element using the complimentary principle of virtual work to obtain the residual element nodal displacement vector (5).

$$\tilde{\mathbf{d}}_{e,n}^{R,k=1,j=1} = \int_0^{L_e} \mathbf{N}_{f,e}(x)^T \cdot \boldsymbol{\epsilon}_{s,e,n}^{R,k=1,j=1}(x) dx$$

At this stage the first iteration ( $j = 1$ ) is completed. The final element and section states for  $j = 1$  correspond to point **B** in Fig. 1.15. The residual section deformation vectors  $\boldsymbol{\epsilon}_{s,e,n}^{R,k=1,j=1}(x)$  and the residual element nodal displacement vector  $\tilde{\mathbf{d}}_{e,n}^{R,k=1,j=1}$  were determined in the first iteration, but the corresponding element nodal displacement vector have not yet been updated. Instead, they constitute the starting point of the remaining steps within iteration loop  $j$ .

The presence of residual element nodal displacement vector  $\tilde{\mathbf{d}}_{e,n}^{R,k=1,j=1}$  will violate compatibility, since elements sharing a common node would now have different element nodal displacement vector. In order to restore the inter-element compatibility, corrective force vector  $\delta\tilde{\mathbf{f}}_{e,n}^{k=1,j=2}$  must be applied at the ends of the element as follows

$$\begin{aligned} \delta\tilde{\mathbf{f}}_{e,n}^{k=1,j=2} &= -[\tilde{\mathbf{c}}_{e,n}^{k=1,j=1}]^{-1} \cdot \tilde{\mathbf{d}}_{e,n}^{R,k=1,j=1} \\ \tilde{\mathbf{c}}_{e,n}^{k=1,j=1} &= \int_0^{L_e} \mathbf{N}_{f,e}(x)^T \cdot \mathbf{c}_{s,e,n}^{tan,k=1,j=1}(x) \cdot \mathbf{N}_{f,e}(x) dx \end{aligned} \quad (1.24)$$

Thus, in the second iteration ( $j = 2$ ), the element nodal force vector (6) is updated as

$$\tilde{\mathbf{f}}_{e,n}^{k=1,j=2} = \tilde{\mathbf{f}}_{e,n}^{k=1,j=1} + \delta\tilde{\mathbf{f}}_{e,n}^{k=1,j=2}$$

and the section force and deformation vectors are also updated to

$$\begin{aligned} \delta\boldsymbol{\sigma}_{s,e,n}^{k=1,j=2}(x) &= \mathbf{N}_{f,e}(x) \cdot \delta\tilde{\mathbf{f}}_{e,n}^{k=1,j=2} \\ \boldsymbol{\sigma}_{s,e,n}^{k=1,j=2}(x) &= \boldsymbol{\sigma}_{s,e,n}^{k=1,j=1}(x) + \delta\boldsymbol{\sigma}_{s,e,n}^{k=1,j=2}(x) \\ \delta\boldsymbol{\epsilon}_{s,e,n}^{k=1,j=2}(x) &= \boldsymbol{\epsilon}_{s,e,n}^{R,k=1,j=1}(x) + \mathbf{c}_{s,e,n}^{tan,k=1,j=1}(x) \cdot \delta\boldsymbol{\sigma}_{s,e,n}^{k=1,j=2}(x) \\ \boldsymbol{\epsilon}_{s,e,n}^{k=1,j=2}(x) &= \boldsymbol{\epsilon}_{s,e,n}^{k=1,j=1}(x) + \delta\boldsymbol{\epsilon}_{s,e,n}^{k=1,j=2}(x) \end{aligned}$$

The state of the element and sections within the element at the end of the second iteration  $j = 2$  corresponds to point **C** in Fig. 1.15. It should be noted that the updated tangent flexibility matrices  $\mathbf{c}_{s,e,n}^{tan,k=1,j=2}(x)$  and residual section deformation vectors  $\boldsymbol{\epsilon}_{s,e,n}^{R,k=1,j=2}(x)$  are computed for all sections.

The residual section deformation vectors are then integrated to obtain the residual element nodal deformation vector  $\tilde{\mathbf{d}}_{e,n}^{R,k=1,j=2}$  and the new element tangent flexibility matrix  $\tilde{\mathbf{c}}_{e,n}^{k=1,j=2}$  is determined by integration of the section flexibility matrices  $\mathbf{c}_{s,e,n}^{tan,k=1,j=2}(x)$  according to Eq. 1.24. This completes the second iteration within loop  $j$ .

The third and subsequent iterations follow exactly the same scheme. Convergence is achieved when the selected convergence criterion is satisfied. With the conclusion of iteration loop  $j$  the internal element nodal force vector for the given element nodal displacement vector  $\tilde{\mathbf{d}}_{e,n}^{k=1}$  are established, as represented by point **D** in Fig. 1.14 and Fig. 1.15. The Newton-Raphson iteration process can now proceed with step  $k + 1$ .

When incremental element nodal displacement vector  $\delta\tilde{\mathbf{d}}_{e,n}^{k,j=1} = \delta\tilde{\mathbf{d}}_{e,n}^k$  is added to the element nodal displacement vector  $\tilde{\mathbf{d}}_{e,n}^{k-1}$  at the end of the previous Newton-Raphson iteration, it is important to make sure that the element nodal displacement vector  $\tilde{\mathbf{d}}_{e,n}^k$  do not change except in the first iteration  $j = 1$  during iteration loop  $j$ .

Equilibrium along the element is always strictly satisfied since section force vectors (④) are derived from element nodal force vector by the force interpolation functions.

$$\sigma_{s,e,n}^k(x) = \mathbf{N}_{f,e}(x) \cdot \tilde{\mathbf{f}}_{e,n}^k \quad \text{and} \quad \delta\sigma_{s,e,n}^k(x) = \mathbf{N}_{f,e}(x) \cdot \delta\tilde{\mathbf{f}}_{e,n}^k$$

Compatibility is also satisfied, not only at the element ends, but also along the element.

$$\begin{aligned} \delta\tilde{\mathbf{f}}_{e,n}^{k,j} &= -\left[\tilde{\mathbf{c}}_{e,n}^{k,j-1}\right]^{-1} \cdot \tilde{\mathbf{d}}_{e,n}^{R,k,j-1} \\ \delta\sigma_{s,e,n}^{k,j}(x) &= \mathbf{N}_{f,e}(x) \cdot \delta\tilde{\mathbf{f}}_{e,n}^{k,j} \\ \delta\epsilon_{s,e,n}^{k,j}(x) &= \epsilon_{s,e,n}^{R,k,j-1}(x) + \mathbf{c}_{s,e,n}^{tan,k,j-1}(x) \cdot \delta\sigma_{s,e,n}^{k,j}(x) \end{aligned} \quad (1.25)$$

The second term of Eq. 1.25 expresses the relation between section deformation vectors and element nodal displacement vector. However, it should be noted that residual section deformation vectors  $\epsilon_{s,e,n}^{R,k,j-1}(x)$  do not strictly satisfy this compatibility condition. This requirement can only be satisfied by integrating the residual section deformation vectors  $\epsilon_{s,e,n}^{R,k,j-1}(x)$  to obtain  $\tilde{\mathbf{d}}_{e,n}^{R,k,j-1}$ . Since this is rather inefficient from a computational standpoint, the small compatibility error in the calculation of residual section deformation vectors  $\epsilon_{s,e,n}^{R,k,j-1}(x)$  will be neglected.

While equilibrium and compatibility are satisfied along the element during each iteration of loop  $j$ , the section force-deformation relation and the element force-deformation relation is only satisfied within a specified tolerance when convergence is achieved at point in Fig. 1.15.

**1.2.2.3.2 Without element iterations** This alternative method, first introduced by (?) has the added advantage (over the previous approach) of avoiding an inner element loop, at the expenses however of additional iterations at the structural level.

As with the state determination of stiffness-based 2D beam-column in a nonlinear structural analysis the state determination process for the mixed stiffness-based and flexibility-based method without iteration in the element level is made up of three phases as shown in Fig. 1.16.

1. Section state determination, Fig. 1.16(c)
2. Element state determination, Fig. 1.16(b)
3. Structure state determination, Fig. 1.16(a)

Starting with completion of the structure state determination, the internal nodal force vector at  $k^{th}$  iteration  $\mathbf{P}_{t,n}^{int,k}$  is compared with the total applied external nodal force vector  $\mathbf{P}_{t,n}^{ext}$  and the difference, if any, yields the residual nodal force vector  $\mathbf{P}_{t,n}^{R,k}$  (①) which is then reapplied to the structure in an iterative solution process until the difference of total applied external force vector and internal nodal force vector satisfies within a specified tolerance.

The state determination procedure is straightforward for a flexibility-based 2D beam-column element without element iteration like stiffness-based 2D beam-column element. The element nodal displacement vector  $\tilde{\mathbf{d}}_{e,n}^k$  (③) without rigid body modes at the  $k^{th}$  iteration is determined from Eq. 1.22

$$\begin{aligned} \delta\tilde{\mathbf{d}}_{e,n}^k &= \tilde{\Gamma}_e \cdot \delta\tilde{\mathbf{f}}_{e,n}^k \\ \tilde{\mathbf{d}}_{e,n}^k &= \tilde{\mathbf{d}}_{e,n}^{k-1} + \delta\tilde{\mathbf{d}}_{e,n}^k \end{aligned}$$

and the element nodal force vector  $\tilde{\mathbf{f}}_{e,n}^k$  (④) without rigid body modes is determined from Eq. 1.20

$$\begin{aligned} \delta\tilde{\mathbf{f}}_{e,n}^k &= \tilde{\mathbf{k}}_{e,n}^{tan,k-1} \cdot \delta\tilde{\mathbf{d}}_{e,n}^k \\ \tilde{\mathbf{f}}_{e,n}^k &= \tilde{\mathbf{f}}_{e,n}^{k-1} + \delta\tilde{\mathbf{f}}_{e,n}^k \end{aligned} \quad (1.26)$$

The section force vectors at the  $k^{th}$  iteration  $\sigma_{s,e,n}^k(x)$  (⑤) are determined from the element nodal force vector  $\tilde{\mathbf{f}}_{e,n}^k$ , and then the section deformation vectors at  $k^{th}$  iteration  $\epsilon_{s,e,n}^k(x)$  (⑥) are determined from the section force vectors

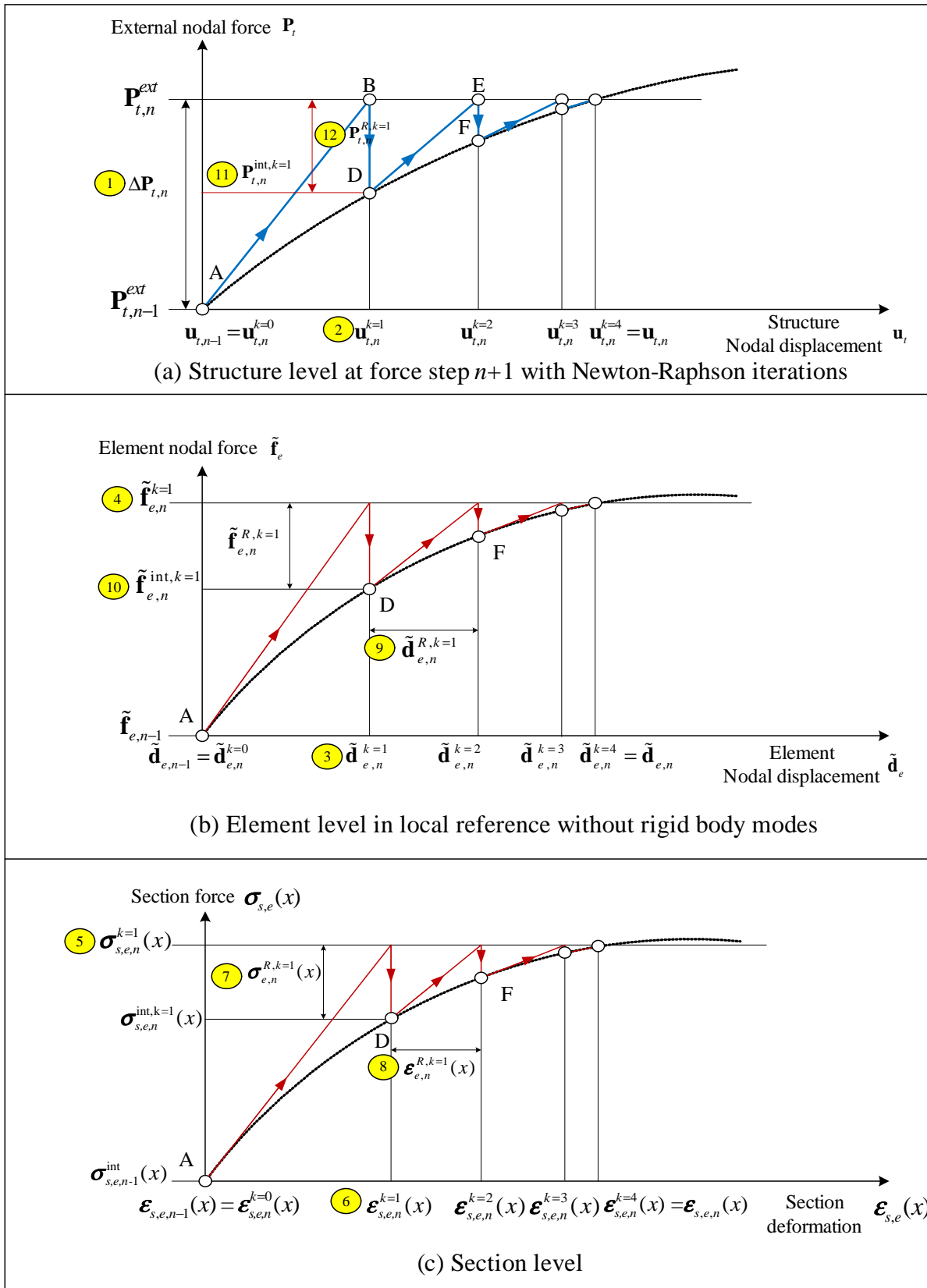


Figure 1.16: State determination for flexibility-based method without element iteration (?)

$$\boldsymbol{\sigma}_{s,e,n}^k(x).$$

$$\begin{aligned}\delta\boldsymbol{\sigma}_{s,e,n}^k(x) &= \mathbf{N}_{f,e} \cdot \delta\tilde{\mathbf{f}}_{e,n}^k \\ \boldsymbol{\sigma}_{s,e,n}^k(x) &= \boldsymbol{\sigma}_{s,e,n}^{k-1}(x) + \delta\boldsymbol{\sigma}_{s,e,n}^k(x) \\ \delta\boldsymbol{\varepsilon}_{s,e,n}^k(x) &= \mathbf{c}_{s,e,n}^{tan,k-1}(x) \cdot \delta\boldsymbol{\sigma}_{s,e,n}^k(x) \\ \boldsymbol{\varepsilon}_{s,e,n}^k(x) &= \boldsymbol{\varepsilon}_{s,e,n}^{k-1}(x) + \delta\boldsymbol{\varepsilon}_{s,e,n}^k(x)\end{aligned}$$

Assuming that the section constitutive law is explicitly known, the section tangent flexibility matrices  $\mathbf{c}_{s,e,n}^k(x)$  and the internal section force vectors  $\boldsymbol{\sigma}_{s,e,n}^{int,k}(x)$  (7) are readily computed from  $\boldsymbol{\varepsilon}_{s,e,n}^k(x)$  (8).

In this approach the residual section force and deformation vectors are first determined from the section tangent flexibility matrices  $\mathbf{c}_{s,e,n}^k(x)$ .

$$\begin{aligned}\boldsymbol{\sigma}_{s,e,n}^{R,k}(x) &= \boldsymbol{\sigma}_{s,e,n}^k(x) - \boldsymbol{\sigma}_{s,e,n}^{int,k}(x) \\ \boldsymbol{\varepsilon}_{s,e,n}^{R,k}(x) &= \mathbf{c}_{s,e,n}^k(x) \cdot \boldsymbol{\sigma}_{s,e,n}^{R,k}(x)\end{aligned}$$

The residual section deformation vectors are integrated along the element using the complimentary principle of virtual work to obtain the residual element nodal displacement vector (9).

$$\tilde{\mathbf{d}}_{e,n}^{R,k} = \int_0^{L_e} \mathbf{N}_{f,e}(x)^T \cdot \boldsymbol{\varepsilon}_{s,e,n}^{R,k}(x)$$

The element flexibility matrix without rigid body modes  $\tilde{\mathbf{c}}_{e,n}^k$  is determined from Eq. 1.20, and then the residual element nodal force vector will be determined form the residual element nodal displacement vector.

$$\tilde{\mathbf{f}}_{e,n}^{R,k} = [\tilde{\mathbf{c}}_{e,n}^k]^{-1} \cdot \tilde{\mathbf{d}}_{e,n}^{R,k} \quad (1.27)$$

The internal element nodal force vector (10) without rigid body modes is determined from Eq. 1.26 and Eq. 1.27.

$$\tilde{\mathbf{f}}_{e,n}^{int,k} = \tilde{\mathbf{f}}_{e,n}^k - \tilde{\mathbf{f}}_{e,n}^{R,k}$$

Finally, the internal element nodal force vector is obtained from Eq. 1.22.

$$\bar{\mathbf{f}}_{e,n}^{int,k} = \tilde{\mathbf{f}}_e^T \cdot \tilde{\mathbf{f}}_{e,n}^{int,k}$$

The flexibility-based 2D beam-column element without iteration in the element level to determine element state is straightforward method for the state determination procedure unlike the flexibility-based 2D beam-column element with Newton-Raphson iteration in the element level to do. This element formulation uses the force interpolation functions without any assumption unlike stiffness based element with displacement interpolation functions. Due to the exact character of the force interpolation functions, no intrinsic errors exist in the flexibility-based 2D beam-column element formulation without iteration in the element level to do. In addition, there are no limitations to the size of the elements, if the element has consistent section along longitudinal axis, for this reason (?)

#### 1.2.2.4 Nonlinear analysis using flexibility-based method

With reference to Fig. 1.14 and 1.15, and Fig. 1.17 to Fig. 1.19 for the method with Newton-Raphson iteration loop in the element level and Fig. 1.20 to Fig. 1.22 for The method without iteration in the element level, we will examine one single step of the Newton-Raphson method in structural level for nonlinear analysis using the flexibility-based method with section constitutive law due to force and displacement control. Force and displacement control are discussed in Sec. ???. Layer/fiber section procedure in Fig. 1.7 will be described in Sec. 1.3.

**1.2.2.4.1 With element iterations** We first examine the nonlinear analysis of flexibility-based 2D beam-column element with element iterations with reference to Fig. 1.17 to 1.19.

Step numbers are shown in Fig. 1.14, and numbers in Fig. 1.15 indicate the procedure for element and section determination during iterations.

- ① Compute the incremental nodal force vector  $\Delta\mathbf{P}_{t,n}^{ext}$ .

$$\Delta\mathbf{P}_{t,n}^{ext} = \mathbf{P}_{t,n}^{ext} - \mathbf{P}_{t,n-1}^{ext}$$

- ② Compute the incremental nodal displacement vector  $\delta\mathbf{u}_{t,n}$  and total nodal displacement vector  $\mathbf{u}_{t,n}$  in structure level. Initially, iteration started from Eq. 1.28 and  $k = 1$ .

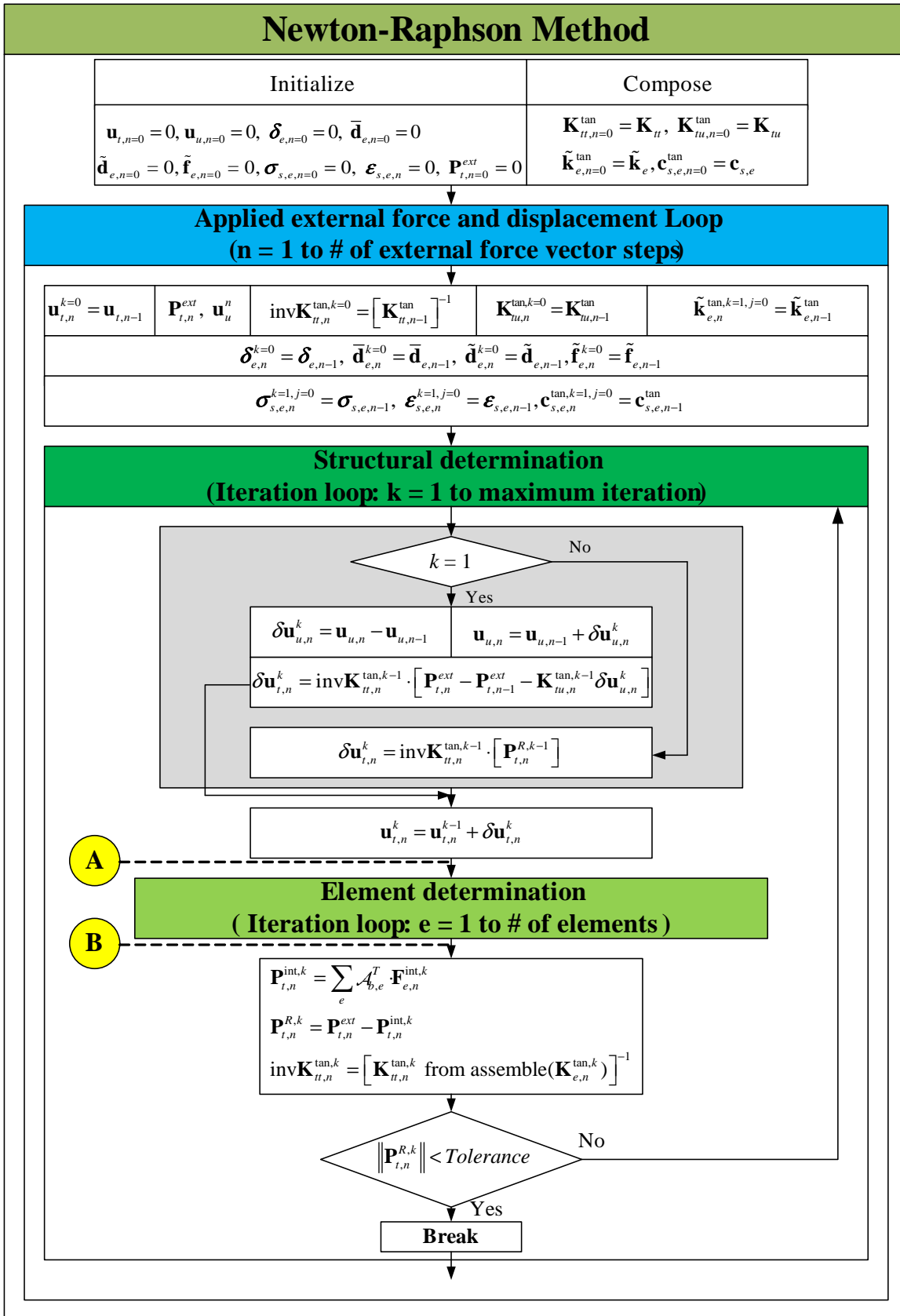


Figure 1.17: Flow chart of nonlinear analysis using flexibility-based method with Newton-Raphson iteration in the element level (1)

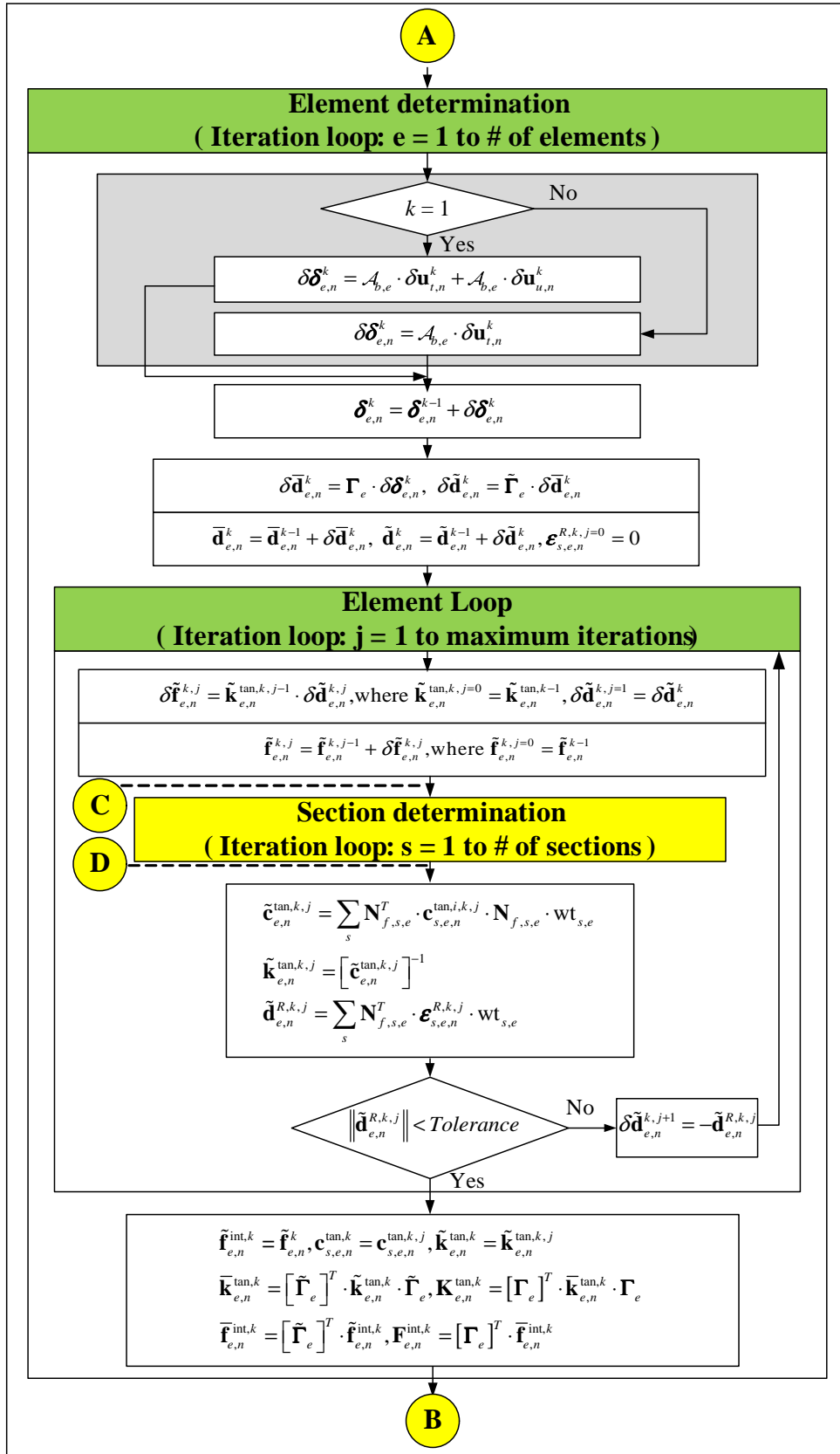


Figure 1.18: Flow chart of nonlinear analysis using flexibility-based method with Newton-Raphson iteration in the element level (2)

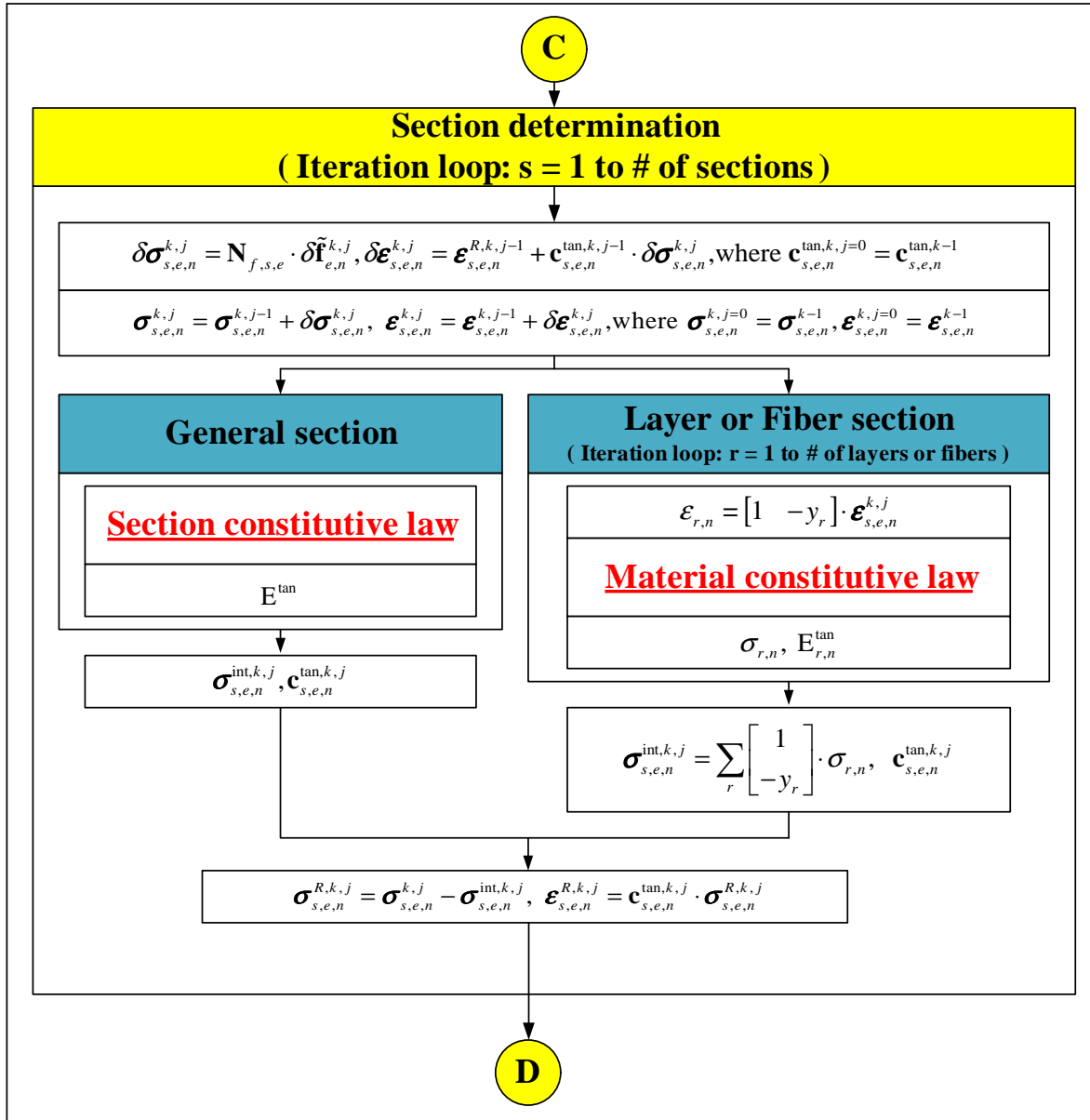


Figure 1.19: Flow chart of nonlinear analysis using flexibility-based method with Newton-Raphson iteration in the element level (3)

If  $k = 1$ ,

$$\begin{aligned}\delta \mathbf{u}_{u,n}^k &= \mathbf{u}_{u,n} - \mathbf{u}_{u,n-1} \\ \mathbf{u}_{u,n} &= \mathbf{u}_{u,n-1} + \delta \mathbf{u}_{u,n}^k \\ \delta \mathbf{u}_{t,n}^k &= [\mathbf{K}_{tt,n}^{tan,k-1}]^{-1} \cdot [\mathbf{P}_{t,n}^{ext} - \mathbf{P}_{t,n-1}^{ext} - \mathbf{K}_{tu,n}^{tan,k-1} \delta \mathbf{u}_{u,n}^k] \\ \mathbf{u}_{t,n}^k &= \mathbf{u}_{t,n}^{k-1} + \delta \mathbf{u}_{t,n}^k\end{aligned}\tag{1.28}$$

If  $k \neq 1$ ,

$$\begin{aligned}\mathbf{P}_{t,n}^{R,k} &= \mathbf{P}_{t,n}^{ext} - \mathbf{P}_{t,n}^{int,k} \\ \delta \mathbf{u}_{t,n}^{k+1} &= [\mathbf{K}_{tt,n}^{tan,k}]^{-1} \cdot \mathbf{P}_{t,n}^{R,k} \\ \mathbf{u}_{t,n}^{k+1} &= \mathbf{u}_{t,n-1} + \Delta \mathbf{u}_{t,n}^{k+1} = \mathbf{u}_{t,n}^k + \delta \mathbf{u}_{t,n}^{k+1}\end{aligned}\tag{1.29}$$

where, superscript  $k$  is the iteration counter,  $\mathbf{P}_t^R$  the residual nodal force vector in structural level,  $\Delta \mathbf{u}_{t,n}^{k+1}$  the total incremental displacement vector from the last converged step, and  $\delta \mathbf{u}_n^{k+1}$  the last incremental displacement vector.

③ Loop over all the elements and determine their state.

- Determine the element nodal displacement vector in global reference.

If  $k = 1$ ,

$$\delta \boldsymbol{\delta}_{e,n}^k = \mathcal{A}_{b,e} \cdot \delta \mathbf{u}_{t,n}^k + \mathcal{A}_{b,e} \cdot \delta \mathbf{u}_{u,n}^k$$

If  $k \neq 1$ ,

$$\delta \boldsymbol{\delta}_{e,n}^k = \mathcal{A}_{b,e} \cdot \delta \mathbf{u}_{t,n}^k$$

where,  $\mathcal{A}_{b,e}$  is displacement extracting operator.

$$\delta_{e,n}^k = \delta_{e,n}^{k-1} + \delta \boldsymbol{\delta}_{e,n}^k$$

and  $\delta_{e,n}^0$  corresponds to  $\boldsymbol{\delta}_{e,n-1}$ .

- Determine the element nodal displacement vector in local reference.

$$\begin{aligned}\delta \bar{\mathbf{d}}_{e,n}^k &= \boldsymbol{\Gamma}_e \cdot \delta \boldsymbol{\delta}_{e,n}^k \\ \bar{\mathbf{d}}_{e,n}^k &= \bar{\mathbf{d}}_{e,n}^{k-1} + \delta \bar{\mathbf{d}}_{e,n}^k\end{aligned}$$

and  $\bar{\mathbf{d}}_{e,n}^0$  corresponds to  $\bar{\mathbf{d}}_{e,n-1}$ .

- Determine the element nodal displacement vector without rigid body modes in local reference.

$$\begin{aligned}\delta \tilde{\mathbf{d}}_{e,n}^k &= \tilde{\boldsymbol{\Gamma}}_e \cdot \delta \bar{\mathbf{d}}_{e,n}^k \\ \tilde{\mathbf{d}}_{e,n}^k &= \tilde{\mathbf{d}}_{e,n}^{k-1} + \delta \tilde{\mathbf{d}}_{e,n}^k\end{aligned}$$

and,  $\bar{\mathbf{d}}_{e,n}^0$  and  $\tilde{\mathbf{d}}_{e,n}^0$  correspond to  $\bar{\mathbf{d}}_{e,n-1}$  and  $\tilde{\mathbf{d}}_{e,n-1}$ .

③a Start the element state determination. Loop over all elements in the structure. The state determination of each element is performed within loop  $j$ .

- Determine the element nodal force vector without rigid body modes

$$\begin{aligned}\delta \tilde{\mathbf{f}}_{e,n}^{k,j} &= \tilde{\mathbf{k}}_{e,n}^{tan,k,j-1} \cdot \delta \tilde{\mathbf{d}}_{e,n}^k \\ \tilde{\mathbf{f}}_{e,n}^{k,j} &= \tilde{\mathbf{f}}_{e,n}^{k,j-1} + \delta \tilde{\mathbf{f}}_{e,n}^{k,j}\end{aligned}$$

$\delta \tilde{\mathbf{d}}_{e,n}^{k,j=1}$ ,  $\tilde{\mathbf{f}}_{e,n}^{k,j=0}$ , and and,  $\tilde{\mathbf{k}}_{e,n}^{tan,k,j=0}$  correspond to  $\delta \tilde{\mathbf{d}}_e^k$ ,  $\tilde{\mathbf{f}}_{e,n}^{k-1}$ , and  $\tilde{\mathbf{k}}_{e,n}^{tan,k-1}$ .

④ Start the section state determination by looping over the element's sections. The total number of section may vary from element to element. Therefore, the total number of sections in an element is  $nIp_e$  and it depends on the number of integration points in the Gauss Lobatto quadrature rule.

- Determine the section force vector.

For the section state determination, we first need to differentiate between general section and layer/fiber section as described in Sec. 1.3. For the sake of this description we consider general section only. The state determination of each section is performed within loop  $s$  where the subscript corresponds to the  $s^{th}$  section.

$$\begin{aligned}\delta\sigma_{s,e,n}^{k,j} &= \mathbf{N}_{f,s,e} \cdot \tilde{\mathbf{f}}_{e,n}^{k,j} \\ \sigma_{s,e,n}^{k,j} &= \sigma_{s,e,n}^{k,j-1} + \delta\sigma_{s,e,n}^{k,j}\end{aligned}$$

where,  $\mathbf{N}_{f,s,e}$  is the matrix derived from the force interpolation functions at  $s^{th}$  section of  $e^{th}$  element, and  $\sigma_{s,e,n}^{k,j=0}$  corresponds to  $\sigma_{s,e,n}^{k-1}$ .

- Determine section deformation vector.

$$\begin{aligned}\delta\varepsilon_{s,e,n}^{k,j} &= \varepsilon_{s,e,n}^{R,k,j-1} + \mathbf{c}_{s,e,n}^{tan,k,j-1} \cdot \delta\sigma_{s,e,n}^{k,j} \\ \varepsilon_{s,e,n}^{k,j} &= \varepsilon_{s,e,n}^{k,j-1} + \delta\varepsilon_{s,e,n}^{k,j}\end{aligned}$$

and,  $\varepsilon_{s,e,n}^{k,j=0}$  and  $\mathbf{c}_{s,e,n}^{tan,k,j=0}$  correspond to  $\varepsilon_{s,e,n}^{k-1}$  and  $\mathbf{c}_{s,e,n}^{tan,k-1}$ , and  $\varepsilon_{s,e,n}^{R,k,j=0} = 0$ .

- Determine the section tangent flexibility matrix and the internal section force vector. If we assume that the section constitutive law is explicitly known,  $\mathbf{c}_{s,e,n}^{tan,k,j}$  and  $\sigma_{s,e,n}^{int,k,j}$  are both determined from  $\varepsilon_{s,e,n}^{k,j}$ . However, in elastic section, we need not compute  $\mathbf{c}_{s,e,n}^{tan,k,j}$  again as it is identical to the initial section flexibility matrix  $\tilde{\mathbf{c}}_{s,e}$ .

- Determine the residual section force and deformation vector.

$$\begin{aligned}\sigma_{s,e,n}^{R,k,j} &= \sigma_{s,e,n}^{k,j} - \sigma_{s,e,n}^{int,k,j} \\ \varepsilon_{s,e,n}^{R,k,j} &= \mathbf{c}_{s,e,n}^{tan,k,j} \cdot \sigma_{s,e,n}^{R,k,j}\end{aligned}$$

- ⑤ Determine the updated element flexibility matrix and the residual element nodal displacement vector.

The residual section deformation vectors and the section tangent flexibility matrices are integrated along the element using the complimentary principle of virtual work to obtain the residual element nodal displacement vector and the element tangent flexibility matrix.

$$\begin{aligned}\tilde{\mathbf{d}}_{e,n}^{R,k,j} &= \sum_s \mathbf{N}_{f,s,e}^T \cdot \varepsilon_{s,e,n}^{R,k,j} \cdot \text{wt}_{s,e} \\ \tilde{\mathbf{c}}_{e,n}^{tan,k,j} &= \sum_s \mathbf{N}_{f,s,e}^T \cdot \mathbf{c}_{s,e,n}^{tan,k,j} \cdot \mathbf{N}_{f,s,e} \cdot \text{wt}_{s,e} \\ \tilde{\mathbf{k}}_{e,n}^{tan,k,j} &= [\tilde{\mathbf{c}}_{e,n}^{tan,k,j}]^{-1}\end{aligned}$$

where,  $\text{wt}_{s,e}$  is the weight coefficient associated with the Jacobian at the  $s^{th}$  section of the  $e^{th}$  element.

Convergence at the element level must be satisfied with the residual element nodal displacement vector.

- If  $\tilde{\mathbf{d}}_{e,n}^{R,k,j}$  is within the specified tolerance, go to ⑥.
- If  $\tilde{\mathbf{d}}_{e,n}^{R,k,j}$  is not within the specified tolerance,  $j$  and  $\delta\tilde{\mathbf{d}}_{e,n}^{k,j+1}$  are updated to  $j+1$  and  $-\tilde{\mathbf{d}}_{e,n}^{R,k,j}$ , and the next Newton-Raphson iteration initiates. We then repeat ③a through ⑤ until convergence occurs at the element level.

- ⑥ Determine the internal element nodal force vector and the element tangent stiffness matrix.

$$\begin{aligned}\tilde{\mathbf{f}}_{e,n}^{int,k} &= \tilde{\mathbf{f}}_{e,n}^{int,k,j} \\ \tilde{\mathbf{F}}_{e,n}^{int,k} &= \tilde{\boldsymbol{\Gamma}}_e^T \cdot \tilde{\mathbf{f}}_{e,n}^{int,k} \\ \mathbf{F}_{e,n}^{int,k} &= \boldsymbol{\Gamma}_e^T \cdot \tilde{\mathbf{F}}_{e,n}^{int,k}\end{aligned}$$

$$\begin{aligned}\mathbf{c}_{s,e,n}^{tan,k} &= \mathbf{c}_{s,e,n}^{tan,k,j} \\ \tilde{\mathbf{k}}_{e,n}^{tan,k} &= \tilde{\mathbf{k}}_{e,n}^{tan,k,j} \\ \bar{\mathbf{k}}_{e,n}^{tan,k} &= \tilde{\boldsymbol{\Gamma}}_e^T \cdot \tilde{\mathbf{k}}_{e,n}^{tan,k} \cdot \tilde{\boldsymbol{\Gamma}}_e \\ \mathbf{K}_{e,n}^{tan,k} &= \boldsymbol{\Gamma}_e^T \cdot \bar{\mathbf{k}}_{e,n}^{tan,k} \cdot \boldsymbol{\Gamma}_e\end{aligned}$$

⑦ Determine the internal nodal force vector and the augmented tangent stiffness matrix.

$$\begin{aligned}\mathbf{P}_{t,n}^{int,k} &= \sum_e \mathcal{A}_{b,e}^T \cdot \mathbf{F}_{e,n}^{int,k} \\ \mathbf{K}_{S,n}^{tan,k} &= \sum_e \mathcal{A}_{b,e}^T \cdot \mathbf{K}_{e,n}^{tan,k} \cdot \mathcal{A}_{b,e}\end{aligned}$$

where,  $\mathcal{A}_{b,e}^T$  is force assembling operator, and  $\mathbf{K}_{S,n}^{tan,k}$  is consist of  $\mathbf{K}_{tt,n}^{tan,k}$ ,  $\mathbf{K}_{tu,n}^{tan,k}$ ,  $\mathbf{K}_{ut,n}^{tan,k}$ , and  $\mathbf{K}_{uu,n}^{tan,k}$ .

⑧ Compute the residual nodal force vector at the structural level from Eq. 1.29. We then satisfy convergence with the residual nodal force vector.

- If  $\mathbf{P}_{t,n}^{R,k}$  is within the specified tolerance, go to next force increment.
- If  $\mathbf{P}_{t,n}^{R,k}$  is not within the specified tolerance,  $k$  is updated to  $k+1$  and the next Newton-Raphson iteration initiates. Eq. 1.29 in ② through ⑧ are repeated until convergence occurs at the structure level.

**1.2.2.4.2 Without element iterations** We then consider the methodology first proposed by (?) in which there are no element iteration with reference to Fig. 1.16 and Fig. 1.20 to 1.22.

① Compute the incremental nodal force vector  $\Delta\mathbf{P}_{t,n}^{ext}$ .

$$\Delta\mathbf{P}_{t,n}^{ext} = \mathbf{P}_{t,n}^{ext} - \mathbf{P}_{t,n-1}^{ext}$$

② Compute the incremental nodal displacement vector  $\delta\mathbf{u}_{t,n}$  and total nodal displacement vector  $\mathbf{u}_{t,n}$  in structure level. Initially, iteration started from Eq. 1.30 and  $k=1$ .

If  $k=1$ ,

$$\begin{aligned}\delta\mathbf{u}_{u,n}^k &= \mathbf{u}_{u,n} - \mathbf{u}_{u,n-1} \\ \mathbf{u}_{u,n} &= \mathbf{u}_{u,n-1} + \delta\mathbf{u}_{u,n}^k \\ \delta\mathbf{u}_{t,n}^k &= [\mathbf{K}_{tt,n}^{tan,k-1}]^{-1} \cdot [\mathbf{P}_{t,n}^{ext} - \mathbf{P}_{t,n-1}^{ext} - \mathbf{K}_{tu,n}^{tan,k-1} \delta\mathbf{u}_{u,n}^k] \\ \mathbf{u}_{t,n}^k &= \mathbf{u}_{t,n-1}^{k-1} + \delta\mathbf{u}_{t,n}^k\end{aligned}\tag{1.30}$$

If  $k \neq 1$ ,

$$\begin{aligned}\mathbf{P}_{t,n}^{R,k} &= \mathbf{P}_{t,n}^{ext} - \mathbf{P}_{t,n}^{int,k} \\ \delta\mathbf{u}_{t,n}^{k+1} &= [\mathbf{K}_{tt,n}^{tan,k}]^{-1} \cdot \mathbf{P}_{t,n}^{R,k} \\ \mathbf{u}_{t,n}^{k+1} &= \mathbf{u}_{t,n-1} + \Delta\mathbf{u}_{t,n}^{k+1} = \mathbf{u}_{t,n}^k + \delta\mathbf{u}_{t,n}^{k+1}\end{aligned}\tag{1.31}$$

where, superscript  $k$  is the iteration counter,  $\mathbf{P}_t^R$  the residual nodal force vector in structural level,  $\Delta\mathbf{u}_{t,n}^{k+1}$  the total incremental displacement vector from the last converged step, and  $\delta\mathbf{u}_n^{k+1}$  the last incremental displacement vector.

③ Loop over all the elements and determine their state.

- Determine the element nodal displacement vector in global reference.

If  $k=1$ ,

$$\delta\boldsymbol{\delta}_{e,n}^k = \mathcal{A}_{b,e} \cdot \delta\mathbf{u}_{t,n}^k + \mathcal{A}_{b,e} \cdot \delta\mathbf{u}_{u,n}^k$$

If  $k \neq 1$ ,

$$\delta\boldsymbol{\delta}_{e,n}^k = \mathcal{A}_{b,e} \cdot \delta\mathbf{u}_{t,n}^k$$

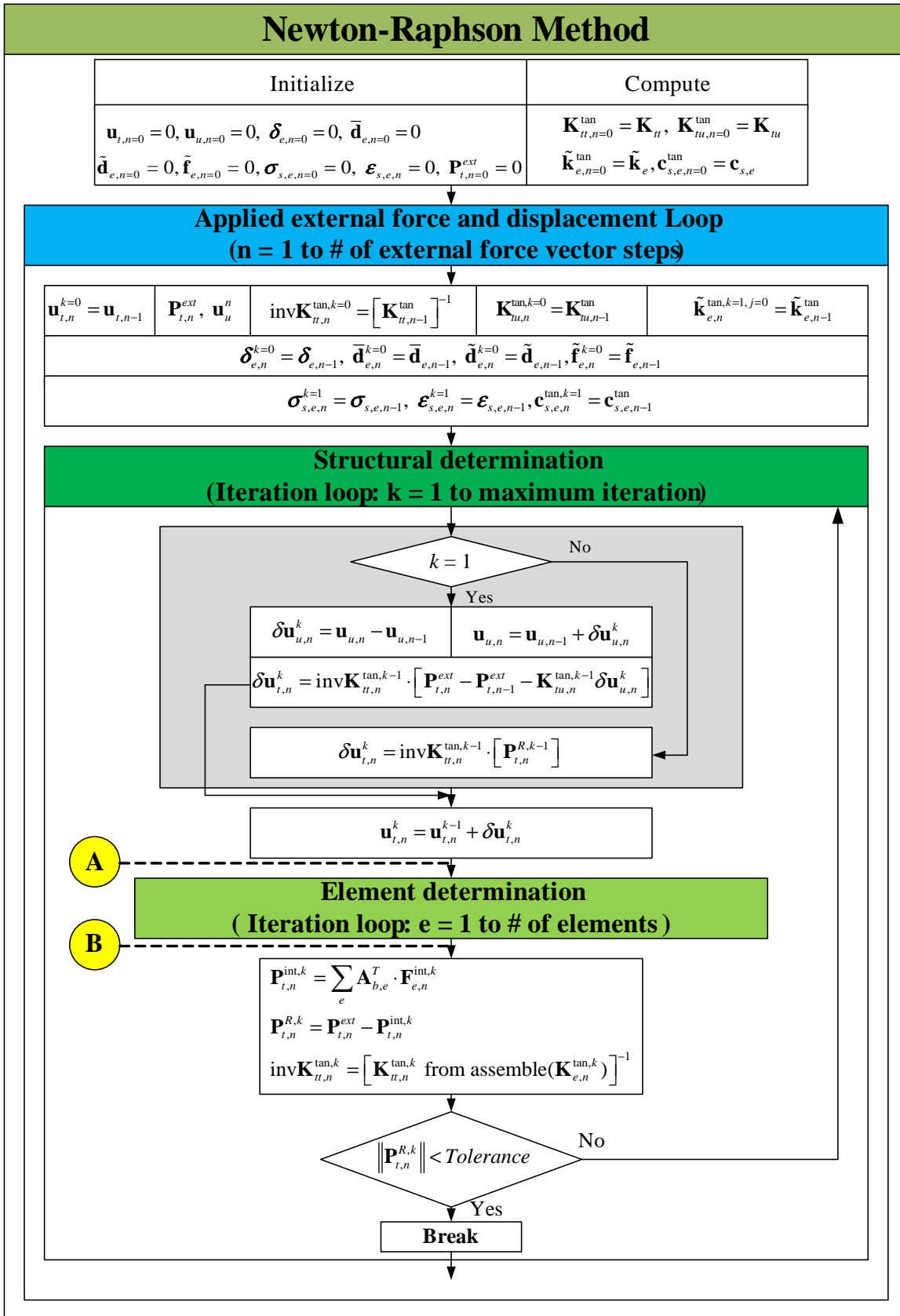


Figure 1.20: Flow chart of nonlinear analysis using flexibility-based method without iteration in the element level (1)

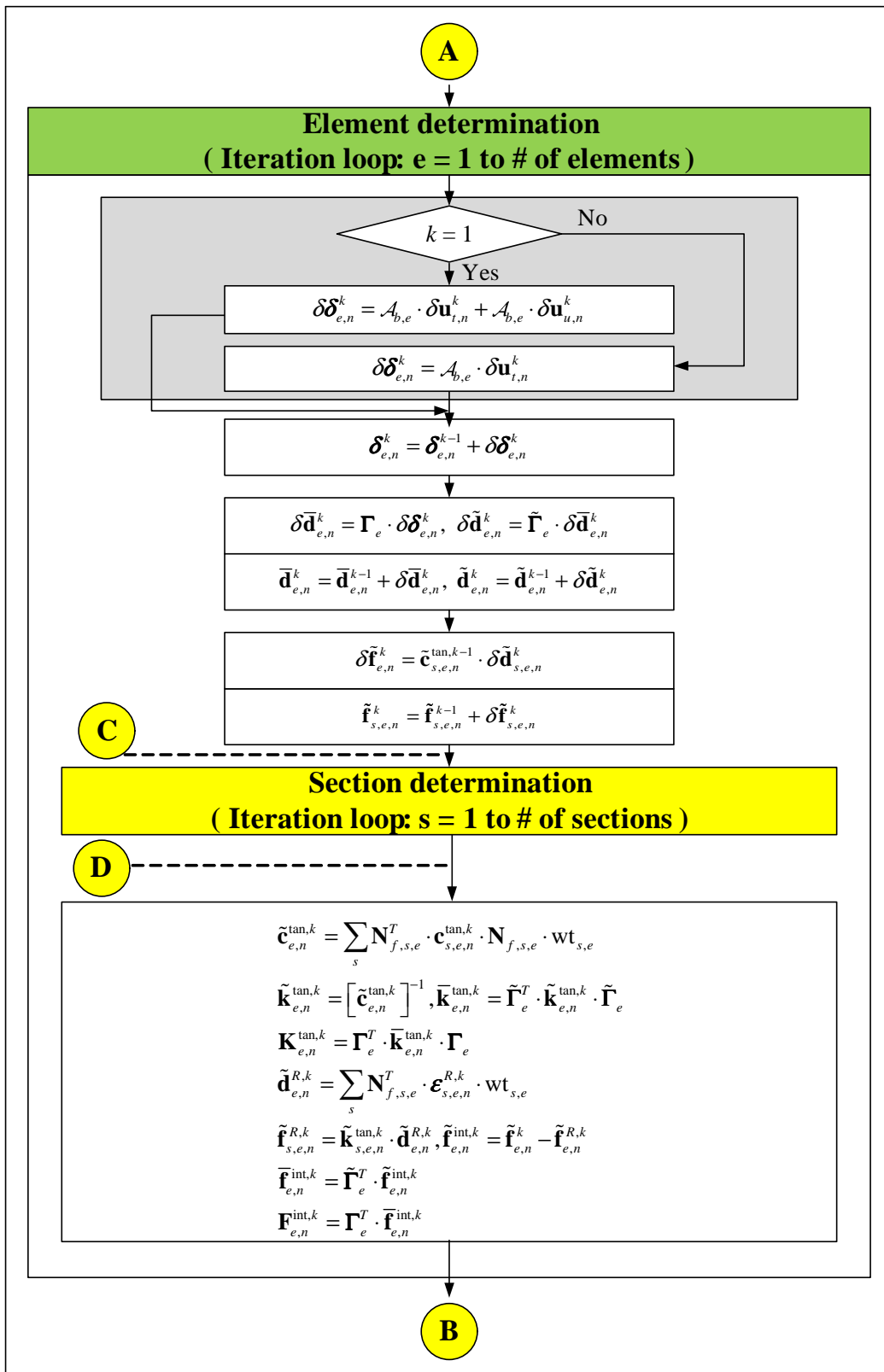


Figure 1.21: Flow chart of nonlinear analysis using flexibility-based method without iteration in the element level (2)

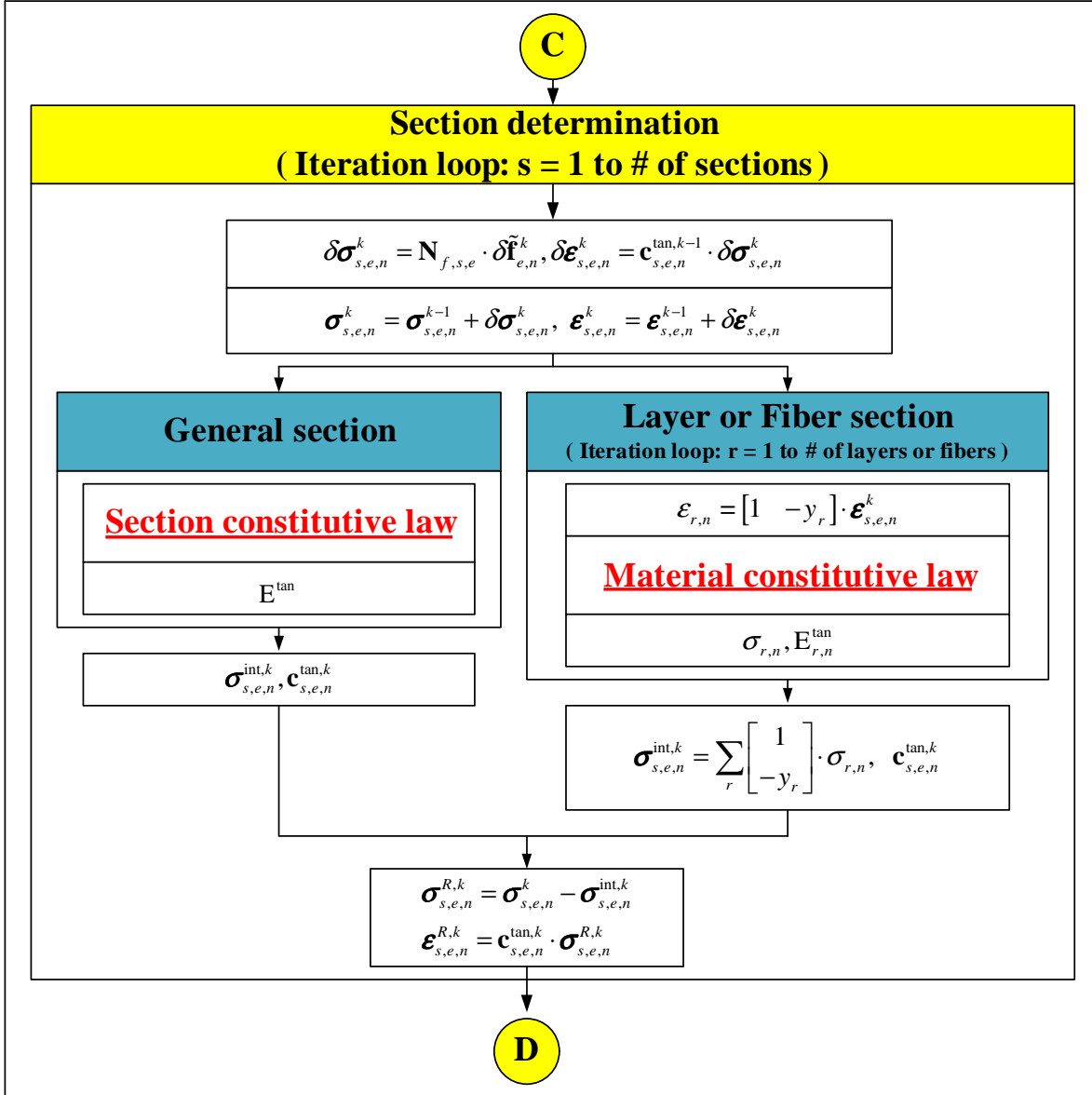


Figure 1.22: Flow chart of nonlinear analysis using flexibility-based method without iteration in the element level (3)

where,  $\mathcal{A}_{b,e}$  is displacement extracting operator.

$$\delta\mathbf{d}_{e,n}^k = \mathbf{d}_{e,n}^{k-1} + \delta\mathbf{d}_{e,n}^k$$

and  $\mathbf{d}_{e,n}^0$  corresponds to  $\mathbf{d}_{e,n-1}$ .

- Determine the element nodal displacement vector in local reference.

$$\delta\bar{\mathbf{d}}_{e,n}^k = \boldsymbol{\Gamma}_e \cdot \delta\mathbf{d}_{e,n}^k$$

$$\bar{\mathbf{d}}_{e,n}^k = \bar{\mathbf{d}}_{e,n}^{k-1} + \delta\bar{\mathbf{d}}_{e,n}^k$$

and  $\bar{\mathbf{d}}_{e,n}^0$  corresponds to  $\bar{\mathbf{d}}_{e,n-1}$ .

- Determine the element nodal displacement vector without rigid body modes in local reference.

$$\delta\tilde{\mathbf{d}}_{e,n}^k = \tilde{\boldsymbol{\Gamma}}_e \cdot \delta\bar{\mathbf{d}}_{e,n}^k$$

$$\tilde{\mathbf{d}}_{e,n}^k = \tilde{\mathbf{d}}_{e,n}^{k-1} + \delta\tilde{\mathbf{d}}_{e,n}^k$$

and,  $\bar{\mathbf{d}}_{e,n}^0$  and  $\tilde{\mathbf{d}}_{e,n}^0$  correspond to  $\bar{\mathbf{d}}_{e,n-1}$  and  $\tilde{\mathbf{d}}_{e,n-1}$ .

- ④ Determine the element nodal force vector without rigid body modes

$$\delta\tilde{\mathbf{f}}_{e,n}^k = \tilde{\mathbf{k}}_{e,n}^{tan,k-1} \cdot \delta\tilde{\mathbf{d}}_{e,n}^k$$

$$\tilde{\mathbf{f}}_{e,n}^k = \tilde{\mathbf{f}}_{e,n}^{k-1} + \delta\tilde{\mathbf{f}}_{e,n}^k$$

and,  $\tilde{\mathbf{f}}_{e,n}^{k=0}$  and  $\tilde{\mathbf{k}}_{e,n}^{tan,k=0}$  correspond to  $\tilde{\mathbf{f}}_{e,n-1}$ , and  $\tilde{\mathbf{k}}_{e,n-1}^{tan}$ .

- ⑤ Start the section state determination by looping over the element's sections. The total number of section may vary from element to element. Therefore, the total number of sections in an element is  $nIp_e$  and it depends on the number of integration points in the Gauss Lobatto quadrature rule.

- Determine the section force vector.

$$\delta\sigma_{s,e,n}^k = \mathbf{N}_{f,s,e} \cdot \delta\tilde{\mathbf{f}}_{e,n}^k$$

$$\sigma_{s,e,n}^k = \sigma_{s,e,n}^{k-1} + \delta\sigma_{s,e,n}^k$$

where,  $\mathbf{N}_{f,s,e}$  is the matrix derived from the force interpolation functions at the  $s^{th}$  section of the  $e^{th}$  element, and  $\sigma_{s,e,n}^{k=0}$  corresponds to  $\sigma_{s,e,n-1}$ .

- ⑥ Determine the section deformation vector. We again assume a general section. The state determination of each section is performed in loop  $s$ .

$$\delta\epsilon_{s,e,n}^k = \mathbf{c}_{s,e,n}^{tan,k-1} \cdot \delta\sigma_{s,e,n}^k$$

$$\epsilon_{s,e,n}^k = \epsilon_{s,e,n}^{k-1} + \delta\epsilon_{s,e,n}^k$$

and,  $\mathbf{c}_{s,e,n}^{tan,k=0}$  and  $\epsilon_{s,e,n}^{k=0}$  correspond to  $\mathbf{c}_{s,e,n-1}^{tan}$  and  $\epsilon_{s,e,n-1}$ .

- ⑦ Determine the section tangent flexibility matrix and the internal section force vector. If we assume that the section constitutive law is explicitly known,  $\mathbf{c}_{s,e,n}^{tan,k}$  and  $\sigma_{s,e,n}^{int,k}$  are both determined from  $\epsilon_{s,e,n}^k$ . However, in elastic section, we need not to compute  $\mathbf{c}_{s,e,n}^{tan,k}$  again as it is identical to the initial section flexibility matrix  $\tilde{\mathbf{c}}_{s,e}$ .

- Determine the residual section force vector.

$$\sigma_{s,e,n}^{R,k} = \sigma_{s,e,n}^k - \sigma_{s,e,n}^{int,k}$$

- ⑧ Determine the residual section deformation vector.

$$\epsilon_{s,e,n}^{R,k} = \mathbf{c}_{s,e,n}^{tan,k} \cdot \sigma_{s,e,n}^{R,k}$$

- ⑨ Determine updated element flexibility matrix and the residual element nodal displacement vector.

The residual section deformation vectors and the section tangent flexibility matrices are integrated along the element using on the complimentary principle of virtual work to obtain the residual element nodal displacement

vector and the element tangent flexibility matrix.

$$\begin{aligned}\tilde{\mathbf{d}}_{e,n}^{R,k} &= \sum_s \mathbf{N}_{f,s,e}^T \cdot \boldsymbol{\epsilon}_{s,e,n}^{R,k} \cdot \text{wt}_{s,e} \\ \tilde{\mathbf{c}}_{e,n}^{tan,k} &= \sum_s \mathbf{N}_{f,s,e}^T \cdot \mathbf{c}_{s,e,n}^{tan,k} \cdot \mathbf{N}_{f,s,e} \cdot \text{wt}_{s,e} \\ \tilde{\mathbf{k}}_{e,n}^{tan,k} &= [\tilde{\mathbf{c}}_{e,n}^{tan,k}]^{-1}\end{aligned}$$

where,  $\text{wt}_{s,e}$  is the weight coefficient associated with the Jacobian at the  $s^{th}$  section of the  $e^{th}$  element.

- ⑩ Determine the internal element nodal force vector and the element tangent stiffness matrix.

$$\begin{aligned}\tilde{\mathbf{f}}_{e,n}^{R,k} &= \tilde{\mathbf{k}}_{e,n}^{tan,k} \cdot \tilde{\mathbf{d}}_{e,n}^{R,k} \\ \tilde{\mathbf{f}}_{e,n}^{int,k} &= \tilde{\mathbf{f}}_{e,n}^{R,k} - \tilde{\mathbf{f}}_{e,n}^{R,k} \\ \bar{\mathbf{f}}_{e,n}^{int,k} &= \tilde{\boldsymbol{\Gamma}}_e^T \cdot \tilde{\mathbf{f}}_{e,n}^{int,k} \\ \mathbf{F}_{e,n}^{int,k} &= \boldsymbol{\Gamma}_e^T \cdot \bar{\mathbf{f}}_{e,n}^{int,k} \\ \bar{\mathbf{k}}_{e,n}^{tan,k} &= \tilde{\boldsymbol{\Gamma}}_e^T \cdot \tilde{\mathbf{k}}_{e,n}^{tan,k} \cdot \tilde{\boldsymbol{\Gamma}}_e \\ \mathbf{K}_{e,n}^{tan,k} &= \boldsymbol{\Gamma}_e^T \cdot \bar{\mathbf{k}}_{e,n}^{tan,k} \cdot \boldsymbol{\Gamma}_e\end{aligned}$$

- ⑪ Determine the internal nodal force vector and the augmented tangent stiffness matrix.

$$\begin{aligned}\mathbf{P}_{t,n}^{int,k} &= \sum_e \mathcal{A}_{b,e}^T \cdot \mathbf{F}_{e,n}^{int,k} \\ \mathbf{K}_{S,n}^{tan,k} &= \sum_e \mathcal{A}_{b,e}^T \cdot \mathbf{K}_{e,n}^{tan,k} \cdot \mathcal{A}_{b,e}\end{aligned}$$

where,  $\mathcal{A}_{b,e}^T$  is force assembling operator.

- ⑫ Compute the residual nodal force vector at the structural level from Eq. 1.29. We then satisfy convergence with the residual nodal force vector.

Check convergence

- If  $\mathbf{P}_{t,n}^{R,k}$  is within the specified tolerance, go to next force increment.
- If  $\mathbf{P}_{t,n}^{R,k}$  is not within the specified tolerance,  $k$  is updated to  $k + 1$  and the next Newton-Raphson iteration initiates. Eq. 1.31 in ② through ⑫ are repeated until convergence occurs at the structure level.

### 1.3 Layer/Fiber Section

So far, we have assumed that a section is characterized by a moment curvature relation, and that when the moment reaches the plastic/yield moment, it instantaneously plastifies. This is only an approximation, as in reality there is a gradual plastification starting from the outer fibers, and this plastification zone gradually spreads inward until the whole section ultimately becomes plastic. To capture this gradual spread one can either resort to continuum 2D/3D solid (finite) elements, which is computationally expensive/inefficient, or use layered elements. Hence, our objective is to derive  $\mathbf{k}_{s,e}^{tan}(x)$  such that

$$\left\{ \begin{array}{l} N(x) \\ M_z(x) \end{array} \right\} = \mathbf{k}_{s,e}^{tan}(x) \left\{ \begin{array}{l} \varepsilon(x) \\ \phi_z(x) \end{array} \right\}$$

Ignoring the effects of transverse shear deformation (accounted for in the so-called Timoshenko beam), and thus assuming a linear strain distribution (Euler-Bernouilli beam), but a non linear stress-stain behavior, the stress distribution can be readily determined from

$$\sigma_t(x) = \frac{N_x(x)}{A(x)} \pm \frac{M_z(x)}{I_z(x)} y$$

At this point, from the nodal displacement, we can determine the section deformations (axial strain,  $\varepsilon(x)$  and curvature,  $\phi(x)$ ) (and thus the linear strain distribution), and since we have a nonlinear material, the exact location

of the neutral axis is not yet known, and at each fiber elevation we do have a different  $E_r^{tan}(x)$ . Hence, with reference to Fig. 1.23.

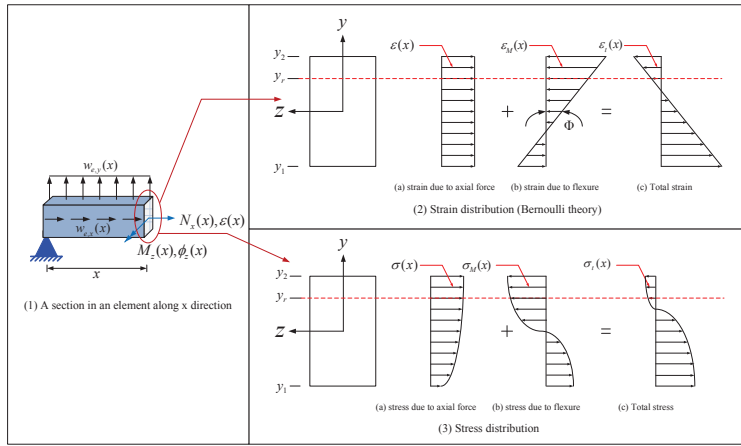


Figure 1.23: Stress and strain distribution of nonlinear material

**Primary Terms** are those due to pure axial and flexure:

**Pure axial force due to  $\sigma(x)$**  is simply determined from

$$\begin{aligned} N_x(x) &= \int_{-y_1}^{y_2} \sigma(x) dA = \int_{-y_1}^{y_2} E_r^{tan}(x) \cdot \varepsilon(x) dA \\ &\simeq \sum_r E_r^{tan}(x) \cdot A_r(x) \cdot \varepsilon(x) \end{aligned} \quad (1.32)$$

**Pure moment due to  $\sigma_M(x)$**  is considered next, and again we seek an expression of  $(M(x))$  in terms of the curvature and  $E_r^{tan}(x)$ , and recalling that  $I = \int y^2 dA$  and  $\sigma_M(x)@y_r = E_r^{tan}(x) \cdot \phi_z(x) \cdot y_r$

$$\begin{aligned} M_z(x) &= \int_{-y_1}^{y_2} \sigma_M(x) \cdot y dA \\ &= \int_{-y_1}^{y_2} E_r^{tan}(x) \cdot \phi_z(x) \cdot y \cdot y dA \\ &= \phi_z(x) \int_{-y_1}^{y_2} E_r^{tan}(x) \cdot \phi_z(x) \cdot y^2 dA \\ &\simeq \sum_r E_r^{tan}(x) \cdot A_r(x) \cdot y_r^2 \cdot \phi_z(x) \end{aligned} \quad (1.33)$$

**Secondary Terms** of axial force or moment are thus caused by curvature or axial strain.

**Second axial force due to curvature**

$$\begin{aligned} dN_x(x) &= -E_r^{tan}(x) \cdot \varepsilon_M(x) dA = -E_r^{tan}(x) \cdot \phi_z(x) \cdot y dA \\ N_x(x) &= - \int_{-y_1}^{y_2} E_r^{tan}(x) \cdot \phi_z(x) \cdot y dA \\ &\simeq - \sum_r E_r^{tan}(x) \cdot A_r(x) \cdot y_r \cdot \phi_z(x) \end{aligned} \quad (1.34)$$

where the strain ( $\varepsilon_M(x)$ ) is obtained from the curvature ( $\phi_z(x)$ ).

### Secondary moment due to axial strain

$$\begin{aligned}
 dM_z(x) &= -E_r^{tan}(x) \cdot \varepsilon(x) \cdot y \cdot dA \\
 M_z(x) &= - \int_{-y_1}^{y_2} E_r^{tan}(x) \cdot \varepsilon(x) \cdot y dA \\
 &\simeq - \sum_r E_r^{tan}(x) \cdot A_r(x) \cdot y_r \cdot \varepsilon(x)
 \end{aligned} \tag{1.35}$$

Summing up from Eq. 1.32 to 1.35 within a matrix,  $\mathbf{k}_{s,e}^{tan}(x)$  takes the form:

$$\begin{Bmatrix} N \\ M \end{Bmatrix} = \sum_r \begin{bmatrix} E_r^{tan}(x) \cdot A_r(x) & -E_r^{tan}(x) \cdot A_r(x) \cdot y_r \\ -E_r^{tan}(x) \cdot A_r(x) \cdot y_r & E_r^{tan}(x) \cdot A_r(x) \cdot y_r^2 \end{bmatrix} \begin{Bmatrix} \varepsilon(x) \\ \phi_z(x) \end{Bmatrix} \tag{1.36}$$

The implementation of this layer or fiber section will require an additional discretization of the cross section into layers or fibers as shown in Fig. 1.24.

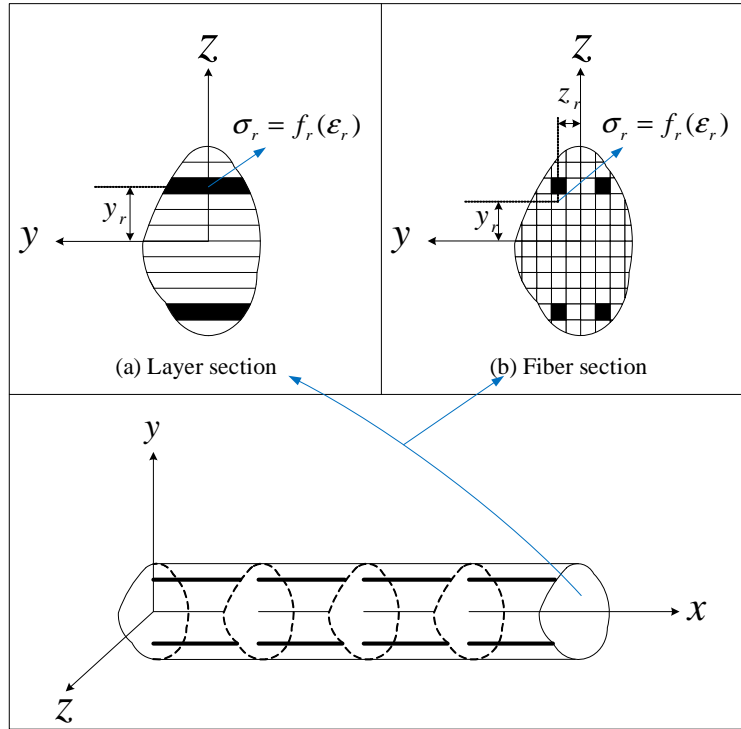


Figure 1.24: Layer/fiber sections-Distribution of control sections and section subdivision into layers/fibers

Noting that layer/fiber stress-strain relations are typically expressed as explicit functions of strain, state determination is shown in Fig. 1.25,

We note that this cross sectional definition allows us to easily specify longitudinal steel reinforcement. Shear reinforcement, on the other hand, can not be explicitly modeled, however, common practice is to assign modified properties to the confined concrete (?).

## 1.4 Zero-Length 2D Element Formulation

As discussed in Sec. ?? a methodology to account for nonlinearities in frame analysis is lumped plasticity. In this approach we consider that plastic hinges (or their formulation) contribute for the structural nonlinearity. Those hinges typically form at the end node regions. Therefore, zero-length element can be used at the end of beam or beam-column elements.

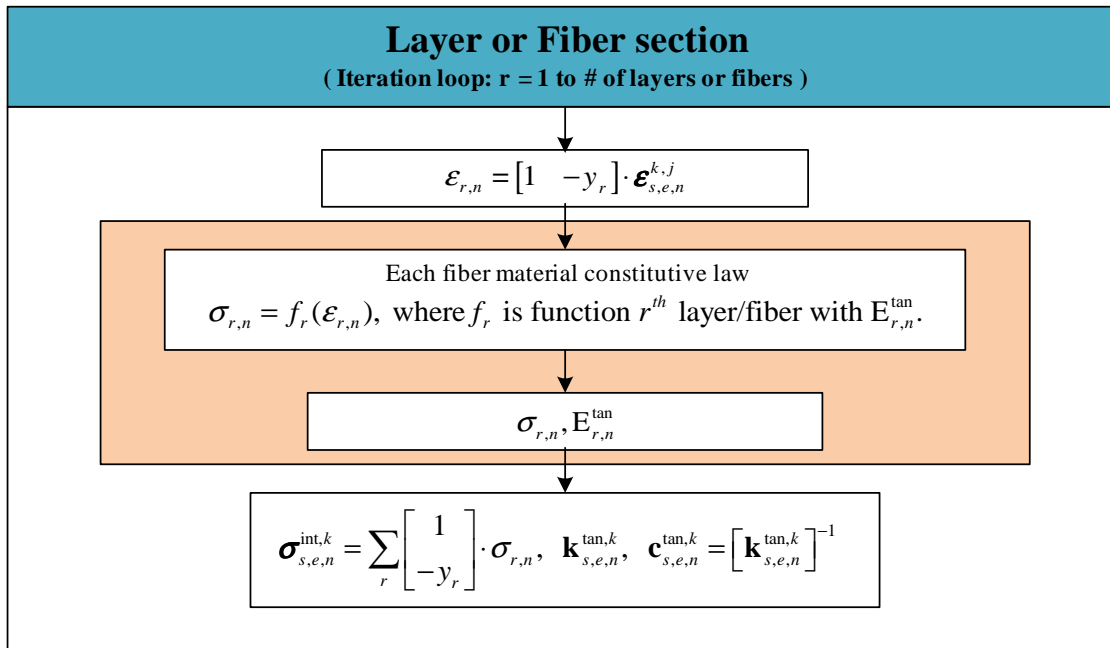


Figure 1.25: Layer/fiber section state determination

#### 1.4.1 Formulation

The element end deformations in the reinforced concrete are composed of two types:

- flexural deformation that causes inelastic strains
- element end rotation which may be caused by the slip of longitudinal reinforcement in reinforced concrete or plastic hinges in steel members.

Fig. 1.26 describes zero-length 2D element and examples for usage. Its formulation does not account for coupling of the three possible degrees of freedom.

**Constitutive law** Section constitutive law is expressed as

$$\underbrace{\begin{Bmatrix} N_x \\ V_y \\ M_z \end{Bmatrix}}_{\boldsymbol{\sigma}_s} = \underbrace{\begin{bmatrix} [EA]^{\tan} & 0 & 0 \\ 0 & [GA]^{\tan} & 0 \\ 0 & 0 & [EI_z]^{\tan} \end{bmatrix}}_{\mathbf{k}_s^{\tan}} \underbrace{\begin{Bmatrix} \bar{u}_{x2} - \bar{u}_{x1} \\ \bar{v}_{y2} - \bar{v}_{y1} \\ \bar{\theta}_{z2} - \bar{\theta}_{z1} \end{Bmatrix}}_{\boldsymbol{\epsilon}_s}$$

where,  $[EA]^{\tan}$ ,  $[GA]^{\tan}$  and  $[EI_z]^{\tan}$  are tangent stiffnesses associated with axial, shear and moment.

#### Equilibrium

Composing equilibrium equations between point A and point B in Fig. 1.27,

$$\begin{aligned} \bar{N}_{x1} &= [EA]^{\tan} \cdot (\bar{u}_{x1} - \bar{u}_{x2}) \\ \bar{V}_{y1} &= [GA]^{\tan} \cdot (\bar{v}_{y1} - \bar{v}_{y2}) \\ \bar{M}_{z1} &= [EI_z]^{\tan} \cdot (\bar{\theta}_{z1} - \bar{\theta}_{z2}) \end{aligned} \tag{1.37}$$

Likewise between point B and point C,

$$\begin{aligned} \bar{N}_{x2} &= [EA]^{\tan} \cdot (\bar{u}_{x2} - \bar{u}_{x1}) \\ \bar{V}_{y2} &= [GA]^{\tan} \cdot (\bar{v}_{y2} - \bar{v}_{y1}) \\ \bar{M}_{z2} &= [EI_z]^{\tan} \cdot (\bar{\theta}_{z2} - \bar{\theta}_{z1}) \end{aligned} \tag{1.38}$$

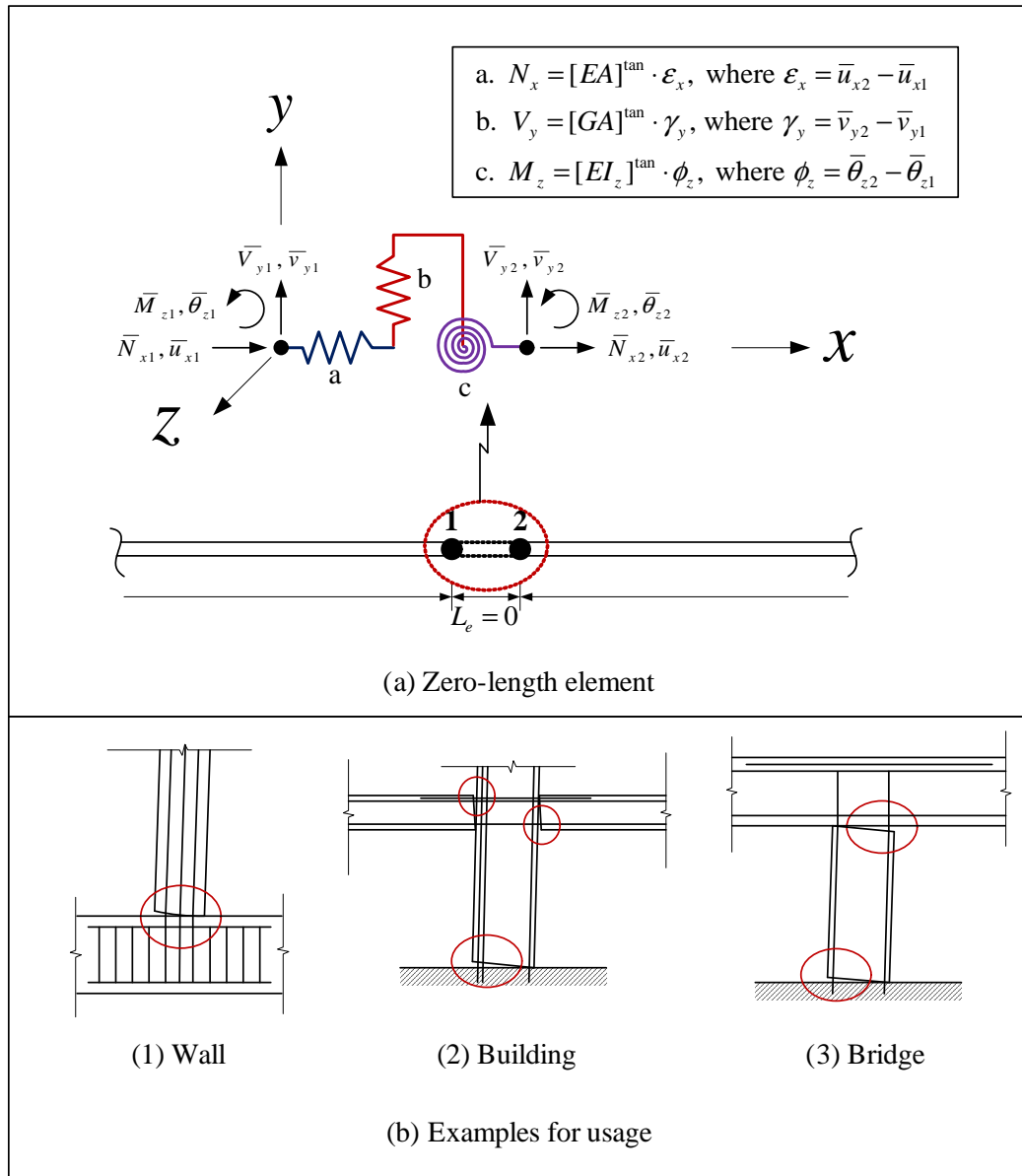


Figure 1.26: Zero-length 2D element(1)

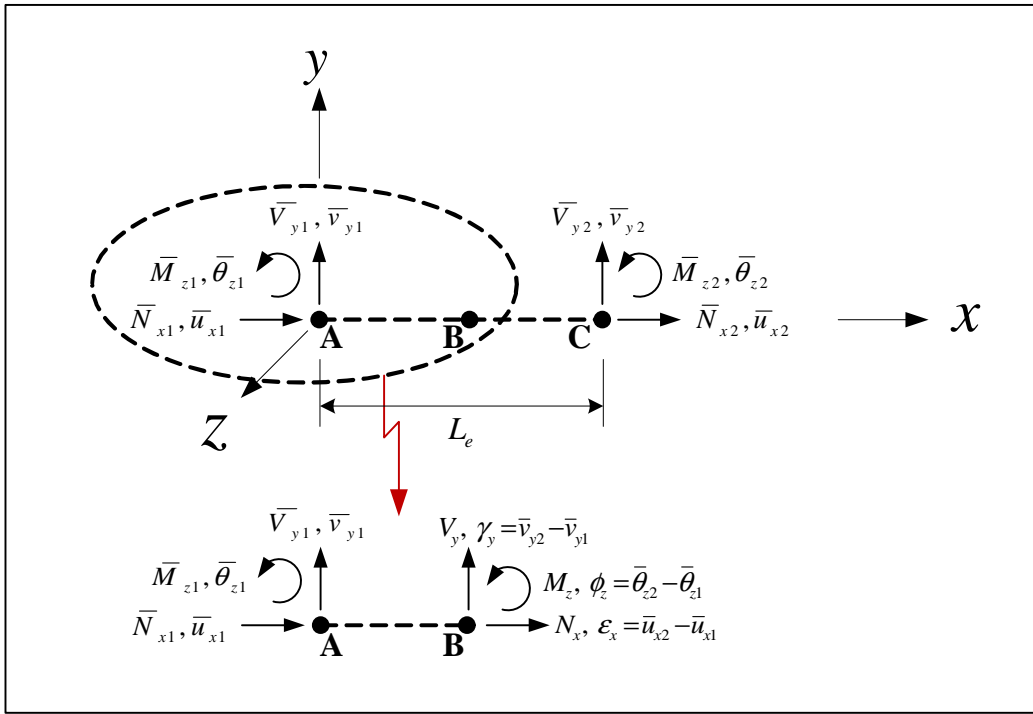


Figure 1.27: Zero-length 2D element(2)

Rewriting Eq. 1.37 and 1.38 to matrix form, the relationship between element nodal force and displacement vector is given by

$$\begin{Bmatrix} \bar{N}_{x1} \\ \bar{V}_{y1} \\ \bar{M}_{z1} \\ \bar{N}_{x2} \\ \bar{V}_{y2} \\ \bar{M}_{z2} \end{Bmatrix} = \bar{k}_e^{tan} \begin{Bmatrix} \bar{u}_{x1} \\ \bar{v}_{y1} \\ \bar{\theta}_{z1} \\ \bar{u}_{x2} \\ \bar{v}_{y2} \\ \bar{\theta}_{z2} \end{Bmatrix}$$

$$\bar{f}_e$$

$$\bar{d}_e$$

where,  $\bar{k}_e^{tan}$  is the element stiffness matrix in local reference.

$$\bar{k}_e^{tan} = \begin{bmatrix} [EA]^{tan} & 0 & 0 & -[EA]^{tan} & 0 & 0 \\ 0 & [GA]^{tan} & 0 & 0 & -[GA]^{tan} & 0 \\ 0 & 0 & [EI_z]^{tan} & 0 & 0 & -[EI_z]^{tan} \\ -[EA]^{tan} & 0 & 0 & [EA]^{tan} & 0 & 0 \\ 0 & -[GA]^{tan} & 0 & 0 & [GA]^{tan} & 0 \\ 0 & 0 & -[EI_z]^{tan} & 0 & 0 & [EI_z]^{tan} \end{bmatrix} \quad (1.39)$$

#### 1.4.2 Coordinate system in zero-length 2D element

Coordinate system in zero-length 2D element is same as in Sec. 1.2.1.2, Fig. 1.2.

#### 1.4.3 Element state determination with 2 Dimension and 3 degrees of freedom per node

With reference Fig. 1.28, we will examine one single step of zero-length 2D element for nonlinear analysis.

Step 1: Determine the section deformation vector, axial deformation, shear deformation and curvature.

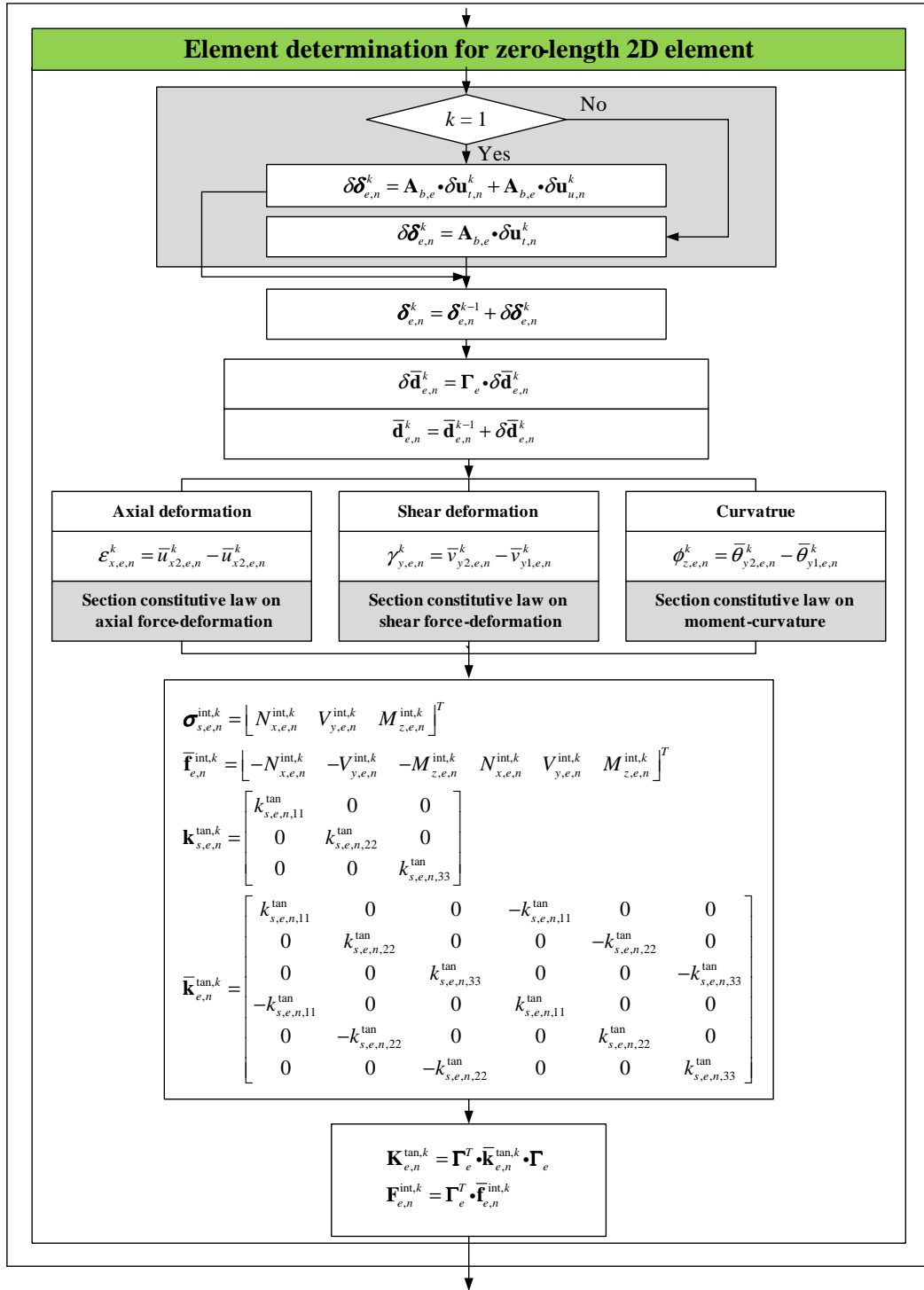


Figure 1.28: Flow chart of zero-length 2D element for element state determination

For each deformation, we extract the associated components from  $\bar{\mathbf{d}}_{e,n}^k$ .

$$\bar{\mathbf{d}}_{e,n}^k = [\bar{u}_{x1,e,n}^k \ \bar{v}_{y1,e,n}^k \ \bar{\theta}_{z1,e,n}^k \ \bar{u}_{x2,e,n}^k \ \bar{v}_{y2,e,n}^k \ \bar{\theta}_{z2,e,n}^k]^T \quad (1.40)$$

$$\boldsymbol{\epsilon}_{s,e,n}^k = [\varepsilon_{x,e,n}^k \ \gamma_{y,e,n}^k \ \phi_{z,e,n}^k]^T$$

$$\varepsilon_{x,e,n}^k = \bar{u}_{x2,e,n}^k - \bar{u}_{x1,e,n}^k$$

$$\gamma_{y,e,n}^k = \bar{v}_{y2,e,n}^k - \bar{v}_{y1,e,n}^k \quad (1.41)$$

$$\phi_{z,e,n}^k = \bar{\theta}_{z2,e,n}^k - \bar{\theta}_{z1,e,n}^k \quad (1.42)$$

where, Eq. 1.40 defines axial section deformation, Eq. 1.41 the shear deformation, and Eq. 1.42 the curvature.

Step 2: Determine the section tangent stiffness associated with axial force-deformation, shear force-deformation, and moment-curvature in the section constitutive laws. Section constitutive laws modified with several variables in function of material constitutive law associated with uniaxial stress-strain relationship can be used (?). The internal section force vector is determined next. If we assume that the section constitutive law is explicitly known,  $\mathbf{k}_{s,e,n}^{tan,k}$  and  $\boldsymbol{\sigma}_{s,e,n}^{int,k}$  are determined from  $\boldsymbol{\epsilon}_{s,e,n}^k$ . However, in elastic section, we need not to compute  $\mathbf{k}_{s,e,n}^{tan,k}$  again as it is identical to the initial section stiffness matrix  $\mathbf{k}_{s,e}$ .

For an elastic section,

$$\begin{aligned} \mathbf{k}_{s,e,n}^{tan} &= \mathbf{k}_{s,e} \\ \underbrace{\begin{Bmatrix} N_{x,e,n}^{int,k} \\ V_{y,e,n}^{int,k} \\ M_{z,e,n}^{int,k} \end{Bmatrix}}_{\boldsymbol{\sigma}_{s,e,n}^{int,k}} &= \mathbf{k}_{s,e,n}^{tan} \underbrace{\begin{Bmatrix} \varepsilon_{x,e,n}^k \\ \gamma_{y,e,n}^k \\ \phi_{z,e,n}^k \end{Bmatrix}}_{\boldsymbol{\epsilon}_{s,e,n}^k} \end{aligned}$$

where,  $\mathbf{k}_{s,e,n}^{tan,k}$  is the section tangent stiffness matrix at  $k^{th}$  iteration.

Step 3: Determine the internal element nodal force vector and the element tangent stiffness matrix from Eq. 1.39.

$$\bar{\mathbf{f}}_{e,n}^{int,k} = [N_{x,e,n}^{int,k} \ V_{y,e,n}^{int,k} \ M_{z,e,n}^{int,k} \ -N_{x,e,n}^{int,k} \ -V_{y,e,n}^{int,k} \ -M_{z,e,n}^{int,k}]^T$$

$$\bar{\mathbf{k}}_e^{tan,k} = \begin{bmatrix} EA_{e,n}^{tan,k} & 0 & 0 & -EA_{e,n}^{tan,k} & 0 & 0 \\ 0 & GA_{e,n}^{tan,k} & 0 & 0 & -GA_{e,n}^{tan,k} & 0 \\ 0 & 0 & EI_{z,e,n}^{tan,k} & 0 & 0 & -EI_{z,e,n}^{tan,k} \\ -EA_{e,n}^{tan,k} & 0 & 0 & EA_{e,n}^{tan,k} & 0 & 0 \\ 0 & -GA_{e,n}^{tan,k} & 0 & 0 & GA_{e,n}^{tan,k} & 0 \\ 0 & 0 & -EI_{z,e,n}^{tan,k} & 0 & 0 & EI_{z,e,n}^{tan,k} \end{bmatrix}$$

where,  $\bar{\mathbf{k}}_e^{tan,k}$  is the element tangent stiffness matrix in local reference.

We determine  $\mathbf{F}_{e,n}^{int,k}$  and  $\mathbf{K}_{e,n}^{tan,k}$ .

$$\mathbf{F}_{e,n}^{int,k} = \boldsymbol{\Gamma}_e^T \cdot \bar{\mathbf{f}}_{e,n}^{int,k}$$

$$\mathbf{K}_{e,n}^{tan,k} = \boldsymbol{\Gamma}_e^T \cdot \bar{\mathbf{k}}_e^{tan,k} \cdot \boldsymbol{\Gamma}_e$$

## 1.5 Zero-Length Section Element Formulation

Zero-length section element is analogous to the zero length element, however, it uses layer/fiber. This element enables us to model the shift in center of section rotation which may occur (in bar-slip for example). The element is formulated on the basis of coupled axial force and moment.

Fig. 1.29 describes zero-length 2D section element.

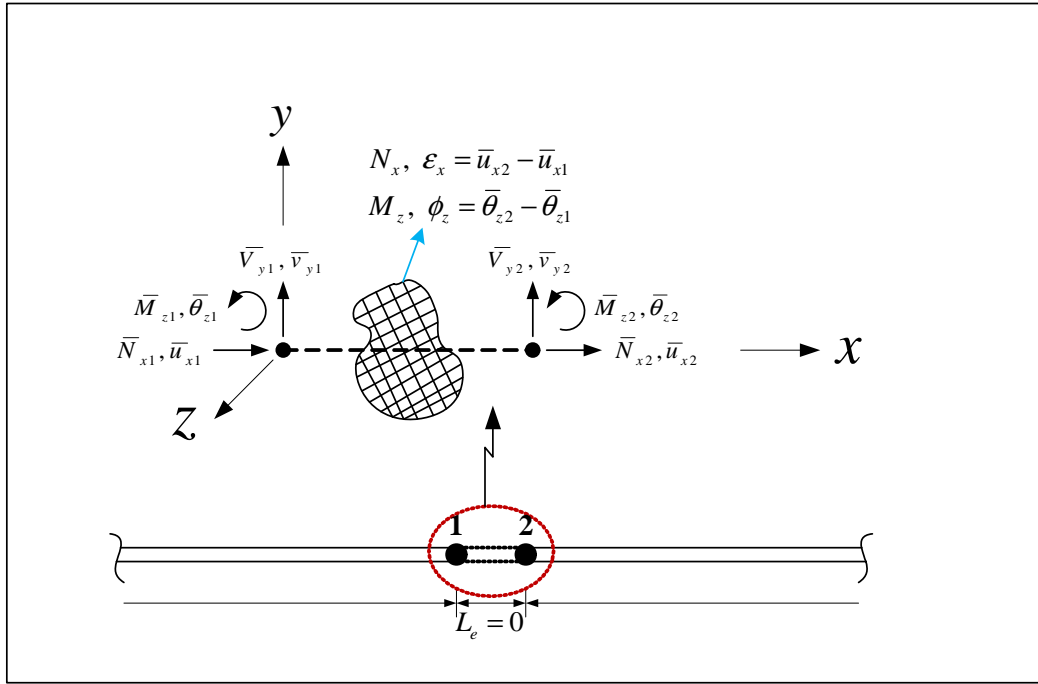


Figure 1.29: Zero-length 2D section element(1)

### 1.5.1 Formulation

**Constitutive law** Section constitutive law is expressed as

$$\underbrace{\begin{Bmatrix} N_x \\ M_z \end{Bmatrix}}_{\sigma_s} = \underbrace{\begin{bmatrix} k_{s,11}^{tan} & k_{s,12}^{tan} \\ k_{s,21}^{tan} & k_{s,22}^{tan} \end{bmatrix}}_{k_s^{tan}} \cdot \underbrace{\begin{Bmatrix} \bar{u}_{x2} - \bar{u}_{x1} \\ \bar{\theta}_{z2} - \bar{\theta}_{z1} \end{Bmatrix}}_{\epsilon_s}$$

where,  $k_s^{tan}$  is the section tangent stiffness matrix obtained from layer/fiber state determination.

**Equilibrium** Zero-length section element is based on Bernoulli beam theory.

Composing equilibrium equations between point A and point B in Fig. 1.30,

$$\begin{aligned} \bar{N}_{x1} &= k_{s,11}^{tan} \cdot (\bar{u}_{x1} - \bar{u}_{x2}) + k_{s,12}^{tan} \cdot (\bar{\theta}_{z1} - \bar{\theta}_{z2}) \\ \bar{M}_{z1} &= k_{s,21}^{tan} \cdot (\bar{u}_{x1} - \bar{u}_{x2}) + k_{s,22}^{tan} \cdot (\bar{\theta}_{z1} - \bar{\theta}_{z2}) \end{aligned} \quad (1.43)$$

Likewise between point B and point C,

$$\begin{aligned} \bar{N}_{x2} &= k_{s,11}^{tan} \cdot (\bar{u}_{x2} - \bar{u}_{x1}) + k_{s,12}^{tan} \cdot (\bar{\theta}_{z2} - \bar{\theta}_{z1}) \\ \bar{M}_{z2} &= k_{s,21}^{tan} \cdot (\bar{u}_{x2} - \bar{u}_{x1}) + k_{s,22}^{tan} \cdot (\bar{\theta}_{z2} - \bar{\theta}_{z1}) \end{aligned} \quad (1.44)$$

Rewriting Eq. 1.43 and 1.44 to matrix form, the relationship between element nodal force and displacement vector is given by

$$\underbrace{\begin{Bmatrix} \bar{N}_{x1} \\ 0 \\ \bar{M}_{z1} \\ \bar{N}_{x2} \\ 0 \\ \bar{M}_{z2} \end{Bmatrix}}_{\bar{\mathbf{f}}_e} = \bar{k}_e^{tan} \underbrace{\begin{Bmatrix} \bar{u}_{x1} \\ 0 \\ \bar{\theta}_{z1} \\ \bar{u}_{x2} \\ 0 \\ \bar{\theta}_{z2} \end{Bmatrix}}_{\bar{\mathbf{d}}_e}$$

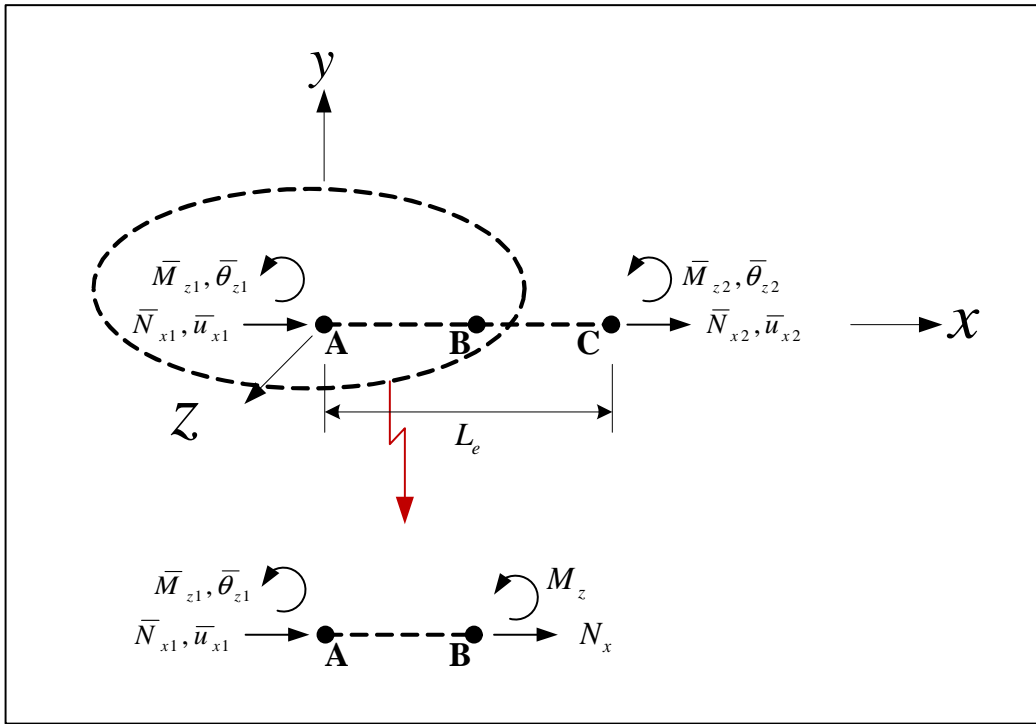


Figure 1.30: Zero-length 2D section element(2)

where,  $\bar{\mathbf{k}}_e^{tan}$  is the element stiffness matrix in local reference.

$$\bar{\mathbf{k}}_e^{tan} = \begin{bmatrix} k_{s,11}^{tan} & 0 & k_{s,12}^{tan} & -k_{s,11}^{tan} & 0 & -k_{s,12}^{tan} \\ 0 & 0 & 0 & 0 & 0 & 0 \\ k_{s,21}^{tan} & 0 & k_{s,22}^{tan} & -k_{s,21}^{tan} & 0 & -k_{s,22}^{tan} \\ -k_{s,11}^{tan} & 0 & -k_{s,12}^{tan} & k_{s,11}^{tan} & 0 & k_{s,12}^{tan} \\ 0 & 0 & 0 & 0 & 0 & 0 \\ -k_{s,21}^{tan} & 0 & -k_{s,22}^{tan} & k_{s,21}^{tan} & 0 & k_{s,22}^{tan} \end{bmatrix} \quad (1.45)$$

### 1.5.2 Coordinate system in zero-length 2D section element

Coordinate system in zero-length 2D element is same as in Sec. 1.2.1.2, Fig. 1.2.

### 1.5.3 Element state determination with 2 Dimension and 3 degrees of freedom per node

With reference Fig. 1.31, we will examine one single step of zero-length 2D section element for nonlinear analysis.

Step 1: Determine the section deformation vector, axial deformation and curvature.

For each deformation, we extracts the associated components from  $\bar{\mathbf{d}}_{e,n}^k$ .

$$\begin{aligned} \bar{\mathbf{d}}_{e,n}^k &= [\bar{u}_{x1,e,n}^k \ 0 \ \bar{\theta}_{z1,e,n}^k \ \bar{u}_{x2,e,n}^k \ 0 \ \bar{\theta}_{z2,e,n}^k]^T \\ \boldsymbol{\varepsilon}_{s,e,n}^k &= [\varepsilon_{x,e,n}^k, \ \phi_{z,e,n}^k]^T \\ \varepsilon_{x,e,n}^k &= \bar{u}_{x2,e,n}^k - \bar{u}_{x1,e,n}^k \\ \phi_{z,e,n}^k &= \bar{\theta}_{z2,e,n}^k - \bar{\theta}_{z1,e,n}^k \end{aligned}$$

Step 2: Determine the section tangent stiffness associated with axial force-deformation and moment-curvature using layer/fiber state determination in Sec. 1.3. Determine next the internal section force vector. If we assume that the material constitutive law is explicitly known,  $\mathbf{k}_{s,e,n}^{tan,k}$  and  $\boldsymbol{\sigma}_{s,e,n}^{int,k}$  are determined from  $\boldsymbol{\varepsilon}_{s,e,n}^k$ . However, in the section with elastic material, we need not to compute  $\mathbf{k}_{s,e,n}^{tan,k}$  again as it is identical to the initial section stiffness matrix  $\mathbf{k}_{s,e}$ .

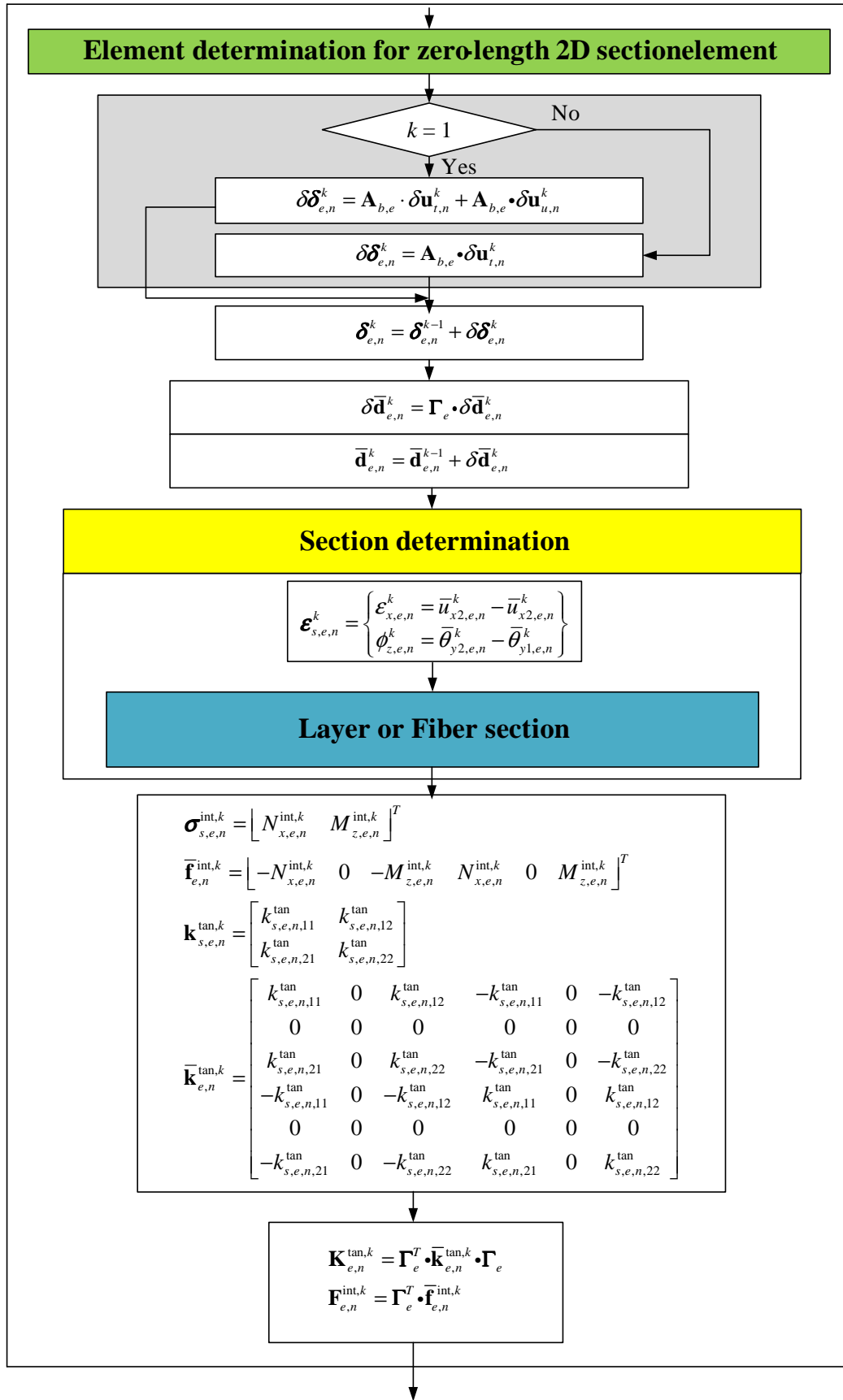


Figure 1.31: Flow chart of zero-length 2D section element for element state determination

If we have a section with elastic material, then

$$\underbrace{\begin{Bmatrix} \mathbf{k}_{s,e,n}^{tan} \\ \begin{Bmatrix} N_{x,e,n}^{int,k} \\ M_{z,e,n}^{int,k} \end{Bmatrix} \\ \boldsymbol{\sigma}_{s,e,n}^{int,k} \end{Bmatrix}}_{\bar{\mathbf{k}}_{e,n}^{int,k}} = \mathbf{k}_{s,e,n}^{tan} \underbrace{\begin{Bmatrix} \varepsilon_{x,e,n}^k \\ \phi_{z,e,n}^k \\ \boldsymbol{\varepsilon}_{s,e,n}^k \end{Bmatrix}}_{\bar{\boldsymbol{\varepsilon}}_{s,e,n}^k}$$

where,  $\mathbf{k}_{s,e,n}^{tan,k}$  is the section tangent stiffness matrix at  $k^{th}$  iteration.

Step 3: Determine the internal element nodal force vector and the element tangent stiffness matrix from Eq. 1.45.

$$\bar{\mathbf{f}}_{e,n}^{int,k} = [N_{x,e,n}^{int,k}, 0, M_{z,e,n}^{int,k}, -N_{x,e,n}^{int,k}, 0, -M_{z,e,n}^{int,k}]^T$$

$$\bar{\mathbf{k}}_{e,n}^{tan,k} = \begin{bmatrix} k_{s,e,n,11}^{tan,k} & 0 & k_{s,e,n,12}^{tan,k} & -k_{s,e,n,11}^{tan,k} & 0 & -k_{s,e,n,12}^{tan,k} \\ 0 & 0 & 0 & 0 & 0 & 0 \\ k_{s,e,n,21}^{tan,k} & 0 & k_{s,e,n,22}^{tan,k} & -k_{s,e,n,21}^{tan,k} & 0 & -k_{s,e,n,22}^{tan,k} \\ -k_{s,e,n,11}^{tan,k} & 0 & -k_{s,e,n,21}^{tan,k} & k_{s,e,n,11}^{tan,k} & 0 & k_{s,e,n,12}^{tan,k} \\ 0 & 0 & 0 & 0 & 0 & 0 \\ -k_{s,e,n,21}^{tan,k} & 0 & -k_{s,e,n,22}^{tan,k} & k_{s,e,n,21}^{tan,k} & 0 & k_{s,e,n,22}^{tan,k} \end{bmatrix}$$

where,  $\bar{\mathbf{k}}_{e,n}^{tan,k}$  is the element tangent stiffness matrix in local reference.

We determine  $\mathbf{F}_{e,n}^{int,k}$  and  $\mathbf{K}_{e,n}^{tan,k}$ .

$$\begin{aligned} \mathbf{F}_{e,n}^{int,k} &= \boldsymbol{\Gamma}_e^T \cdot \bar{\mathbf{f}}_{e,n}^{int,k} \\ \mathbf{K}_{e,n}^{tan,k} &= \boldsymbol{\Gamma}_e^T \cdot \bar{\mathbf{k}}_{e,n}^{tan,k} \cdot \boldsymbol{\Gamma}_e \end{aligned}$$

## 1.6 Element Force

Structures should resist applied external forces. Applicable external forces of an element basically are divided into three forces; element nodal forces, element distributed forces and element nodal displacements such as settlements or pushover tests due to displacement control. These external forces are shown in Fig. 1.32.

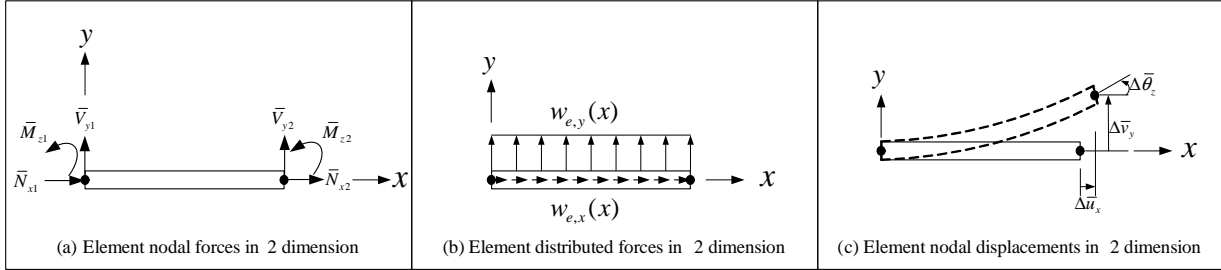


Figure 1.32: Forces of an element

Element nodal forces shown in Fig. 1.32 (a) are applied directly at the corresponding degrees of freedom. However, so far we have not accounted for the element forces  $\mathbf{w}_e(x)$  (as defined in Eq. 1.14) shown in Fig. 1.32 (b). Those can be lumped as concentrated forces at suitably selected arbitrary nodes, and the degrees of freedom at these and the actual joints are treated as the unknowns. For element distributed forces, we should consider the nodal equivalent forces  $\bar{\mathbf{f}}_e^{nef}$  of element distributed forces in structural level irrespective of whether we use the stiffness-based or the mixed stiffness-based and flexibility-based method.  $\bar{\mathbf{f}}_e^{nef}$  on element distributed forces of an element is based on stiffness-based formulation.

$$\begin{aligned}
 \mathbf{N}_d(x) &= \begin{bmatrix} 1 - \frac{x}{L_e} & 0 & 0 & \frac{x}{L_e} & 0 & 0 \\ 0 & \frac{2x^3}{L_e^3} - \frac{3x^2}{L_e^2} + 1 & \frac{x^3}{L_e^2} - \frac{2x^2}{L_e} + x & 0 & \frac{3x^2}{L_e^2} - \frac{2x^3}{L_e^3} & \frac{x^3}{L_e^2} - \frac{x^2}{L_e} \end{bmatrix} \\
 \mathbf{w}_e(x) &= \begin{Bmatrix} w_{e,x}(x) \\ w_{e,y}(x) \end{Bmatrix} \\
 \bar{\mathbf{f}}_e^{nef} &= \int_o^{L_e} \mathbf{N}_d(x) \cdot \mathbf{w}_e(x) dx
 \end{aligned} \tag{1.46}$$

For a uniformly distributed force vector  $\mathbf{w}_e(x) = \begin{Bmatrix} w_x \\ w_y \end{Bmatrix}$ , then Eq. 1.46 reduces to the classical

$$\bar{\mathbf{f}}_e^{nef} = \left[ \frac{w_x \cdot L_e}{2}, \frac{w_y \cdot L_e}{2}, \frac{w_y \cdot L_e^2}{12}, \frac{w_x \cdot L_e}{2}, \frac{w_y \cdot L_e}{2}, -\frac{w_y \cdot L_e^2}{12} \right]^T \tag{1.47}$$

which are shown in Fig. 1.33.

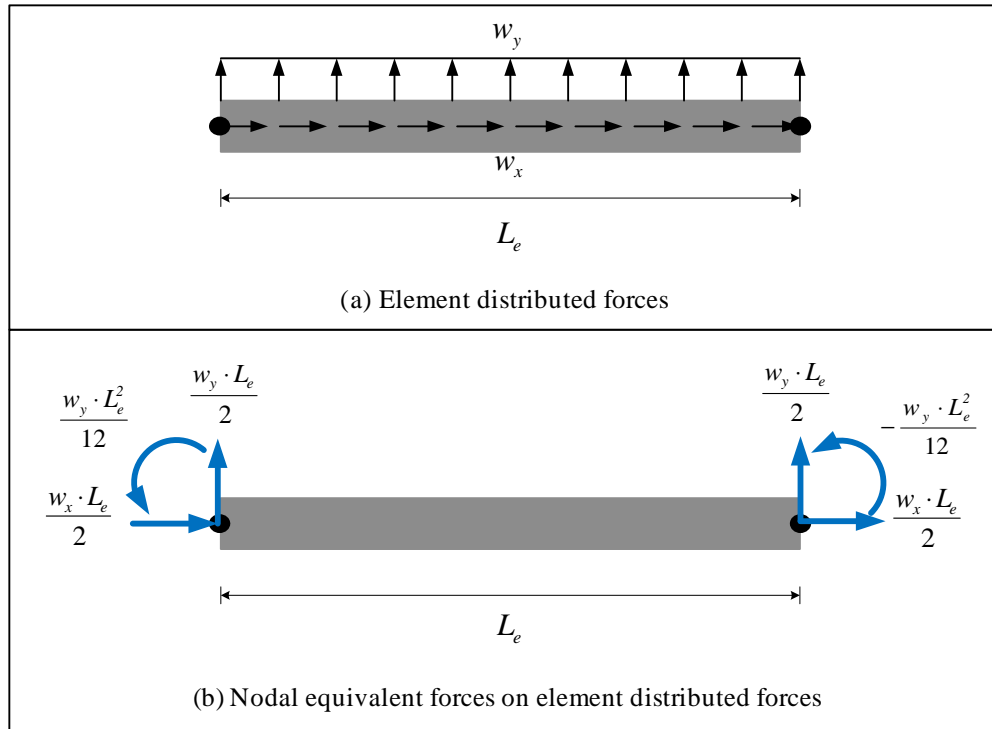


Figure 1.33: Nodal equivalent forces of an element

Element nodal displacements considered as external forces are shown in Fig. 1.32 (c). Those are applied as constraint degrees of freedom.

Let us consider the equilibrium equation considered by element nodal forces, element distributed forces, and element nodal displacements in an element shown in Fig. 1.34.

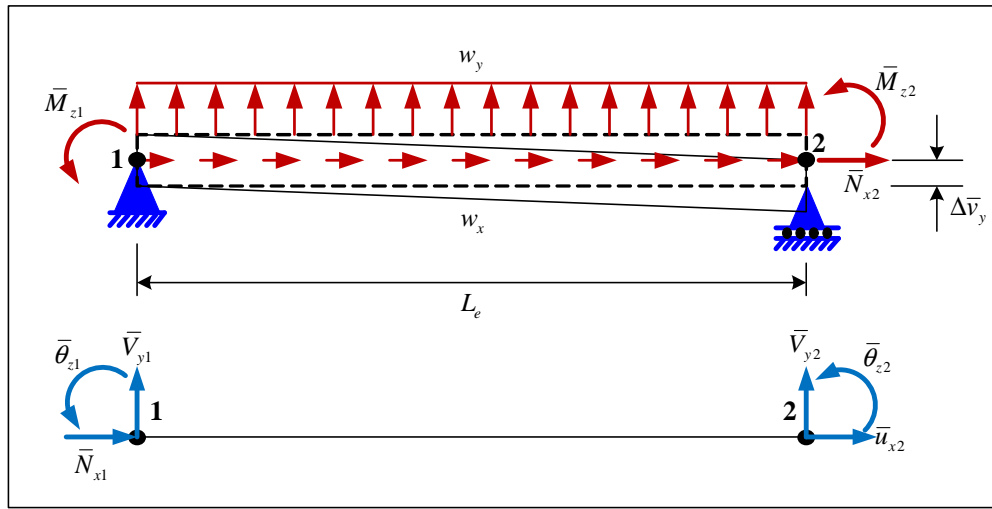


Figure 1.34: Example with element distributed forces and nodal displacement applied at constraint degree of freedom

If the element has elastic section, we obtain equilibrium equation, Eq. 1.48.

$$\underbrace{\begin{Bmatrix} \bar{N}_{x1}^? \\ \bar{V}_{y1}^? \\ \bar{M}_{z1}^? \\ \bar{N}_{x2}^? \\ \bar{V}_{y2}^? \\ \bar{M}_{z2}^? \end{Bmatrix}}_{\bar{\mathbf{f}}_e} = \underbrace{\begin{bmatrix} \frac{EA}{L_e} & 0 & 0 & -\frac{EA}{L_e} & 0 & 0 \\ 0 & \frac{12EI_z}{L_e^3} & \frac{6EI_z}{L_e^2} & 0 & -\frac{12EI_z}{L_e^3} & \frac{6EI_z}{L_e^2} \\ 0 & \frac{6EI_z}{L_e^2} & \frac{4EI_z}{L_e} & 0 & -\frac{6EI_z}{L_e^2} & \frac{2EI_z}{L_e} \\ -\frac{EA}{L_e} & \frac{L_e^2}{L_e} & \frac{L_e}{L_e} & 0 & \frac{EA}{L_e} & 0 \\ -\frac{12EI_z}{L_e} & -\frac{6EI_z}{L_e^2} & -\frac{2EI_z}{L_e} & 0 & \frac{12EI_z}{L_e^3} & -\frac{6EI_z}{L_e^2} \\ 0 & \frac{6EI_z}{L_e^2} & \frac{2EI_z}{L_e} & 0 & -\frac{6EI_z}{L_e^2} & \frac{4EI_z}{L_e} \end{bmatrix}}_{\bar{\mathbf{k}}_e} \cdot \underbrace{\begin{Bmatrix} 0^\checkmark \\ 0^\checkmark \\ \bar{\theta}_{z1}^? \\ \bar{u}_{x2}^? \\ \Delta \bar{v}_y^\checkmark \\ \bar{\theta}_{z2}^? \end{Bmatrix}}_{\bar{\mathbf{d}}_e} - \underbrace{\begin{Bmatrix} \frac{w_x \cdot L_e}{2} \\ \frac{w_y \cdot L_e}{2} \\ \frac{w_y \cdot L_e^2}{12} \\ \frac{w_x \cdot L_e}{2} \\ \frac{w_y \cdot L_e}{2} \\ -\frac{w_y \cdot L_e^2}{12} \end{Bmatrix}}_{\bar{\mathbf{F}}_e^{ref}} \quad (1.48)$$

where, superscript ? indicates unknown forces and displacements, and  $\checkmark$  known forces and displacements.

## 1.7 Summary

This chapter has presented the details of the element formulation coded in Mercury. The Mercury supports most of the elements (in particular flexibility based fiber elements, zero length and zero length section elements). These elements are widely used and tested and would enable the analysis of complex structure such as reinforced concrete frame.

## Chapter 2

### CONSTITUTIVE MODELS

The nonlinear analysis of structures hinges on the constitutive relation relating strains to stresses, better yet incremental strains to incremental stresses through  $E^{tan}$ . This chapter is devoted to the derivation of such relations for steel and concrete. In each case we will consider both analytically (or thermodynamically) derived models as well as heuristic ones which are found to be acceptable.

It should be noted that the constitutive models expressed in terms of stress-strain relationships are to be used in fiber/layered sections (though the simplified bilinear model can be used in zero-length elements).

#### 2.1 Steel Models

Most metallic materials, when subjected to high stress level, exhibit plasticity behavior, i.e. when force is removed, the body does not return to its original shape, but has some permanent plastic deformation associated with it.

Materials such as steel or concrete, commonly used in structures, show yielding and plastic deformation. A typical uniaxial stress-strain curve for steel is shown in Fig. 2.1. Following a linear response, steel exhibits an abrupt change

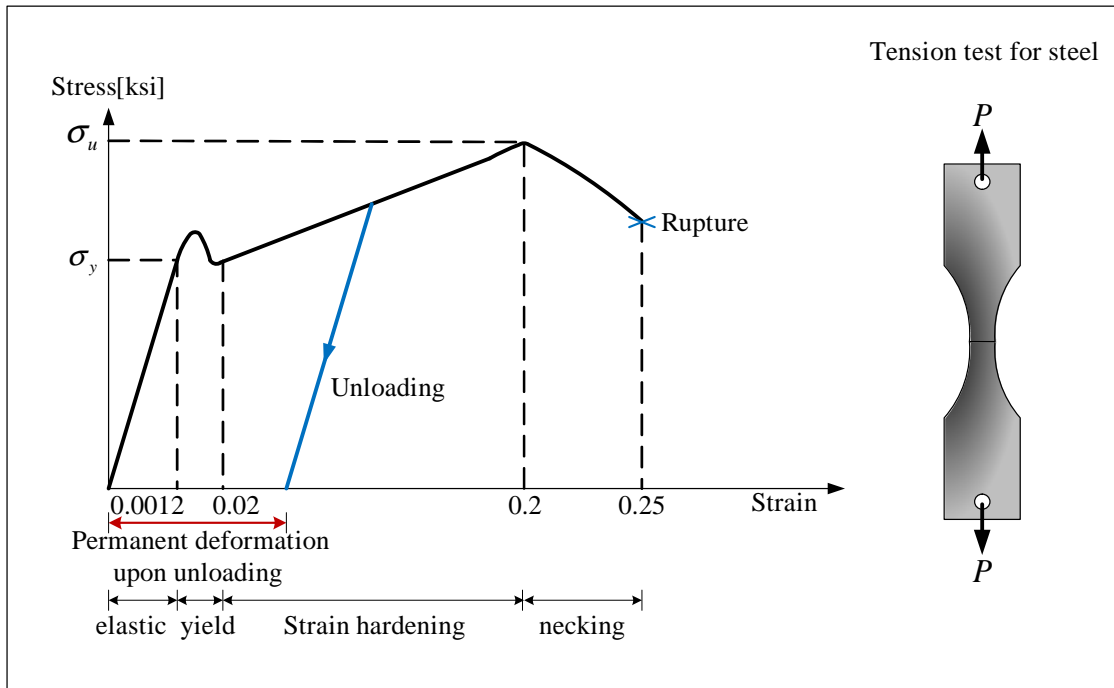


Figure 2.1: Uniaxial stress-strain curve for steel

in stiffness which occurs at the yield point. Beyond yielding, a permanent deformation is introduced upon unloading. This behavior can be idealized by a bilinear stress-strain relationship with two slopes, the second being called the tangent modulus  $E^{tan}$ . After reaching the yield point, the slope could be smaller, equal, or greater than zero as shown in Fig. 2.2(a).

Fig. 2.2(b) illustrates an elastic-perfectly plastic situation, that is after reaching the yield stress, the material starts flowing plastically without any further increase or decrease. The specimen is first loaded to point A, reaches its yield stress, and then flows plastically at point B, we unload the specimen until we reach a zero-load condition at point C. However, since we have loaded the specimen beyond the yield point, we observe that a permanent deformation or a permanent strain has been introduced in the material. We denote this permanent strain in one dimension the plastic strain  $\varepsilon^p$  which is permanent deformation.

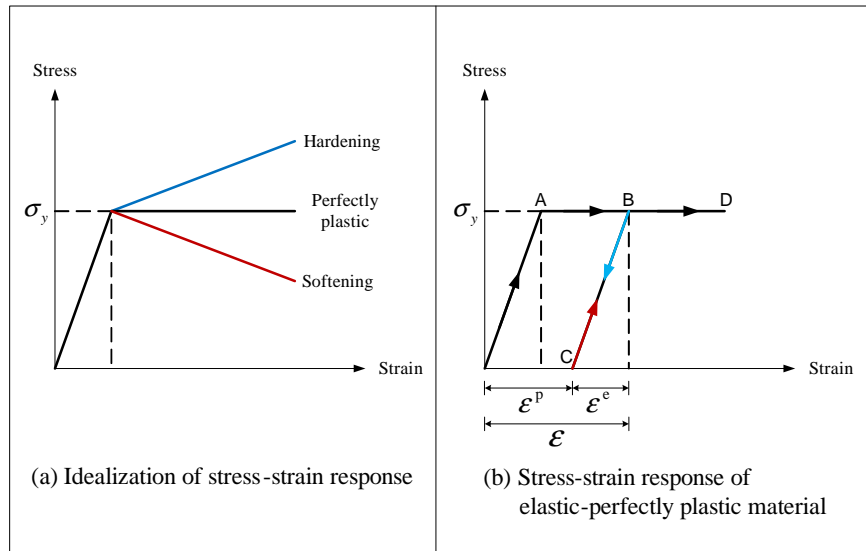


Figure 2.2: Idealized stress-strain response hardening material

The total strain  $\varepsilon$  can thus be decomposed into an elastic strain  $\varepsilon^e$  and a plastic one.

$$\begin{aligned}\varepsilon &= \varepsilon^e + \varepsilon^p \\ \sigma &= E \cdot \varepsilon^e \\ \sigma &= E \cdot (\varepsilon - \varepsilon^p)\end{aligned}\tag{2.1}$$

Eq. 2.1 describes the stress-strain relation with plastic behavior for the elastic-perfectly plastic uniaxial loading conditions.

Next we will present the mathematical structure of two classical phenomenological isotropic hardening model (?).

## 2.1.1 “Exact” Models

### 2.1.1.1 Isotropic hardening model

Formulation of this constitutive law is based on classical theory of plasticity and is thus developed as follows:

**Helmholtz free energy potential** The general format of associated dissipative models starts from the Helmholtz free energy expansion. Expanding the free energy into two terms, an elastic and a plastic one, we have

$$\rho \cdot \phi(\varepsilon^e, \xi) = \underbrace{\frac{1}{2} \varepsilon^e \cdot E \cdot \varepsilon^e}_{\text{Elastic}} + \underbrace{\frac{1}{2} \cdot \xi \cdot H \cdot \xi}_{\text{Plastic}}$$

where  $\rho$  is density,  $\phi(\varepsilon^e, \xi)$  the Helmholtz free energy potential function in terms of elastic strain  $\varepsilon^e$  and a strain-like internal variable  $\xi$ ,  $E$  elastic modulus, and  $H$  plastic modulus.

The elastic and plastic moduli  $E$  and  $H$  are shown in Fig. 2.3. The elastic and plastic stress,  $\sigma$  and  $q$  respectively, are (by definition) given by

$$\text{Linear elasticity: } \sigma := \rho \cdot \frac{\partial \phi}{\partial \varepsilon^e} = E \cdot \varepsilon^e\tag{2.2}$$

$$\text{Plasticity: } q := \rho \cdot \frac{\partial \phi}{\partial \xi} = H \cdot \xi\tag{2.3}$$

where,  $q$  is the initial yield stress  $\sigma_y$  at  $\xi = 0$ .

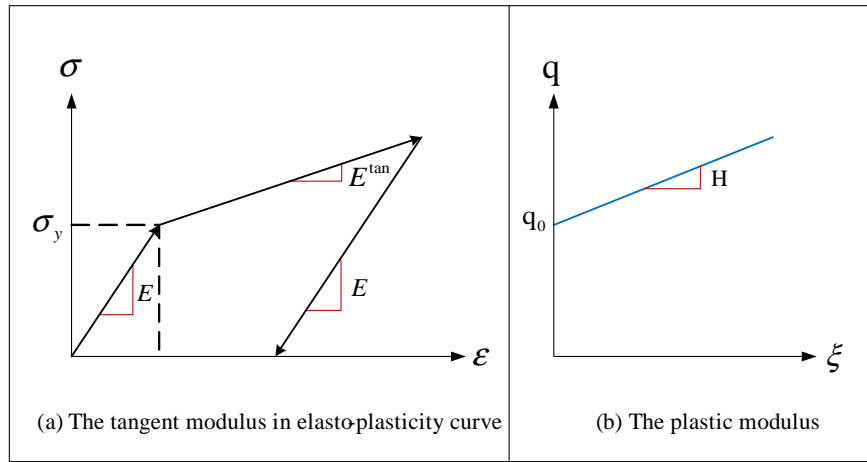


Figure 2.3: The tangent modulus for isotropic hardening model

Assuming  $E$  and  $H$  constant, we can rewrite Eq. 2.2 and Eq. 2.3 in rate form as

$$\dot{\sigma} = E \cdot \dot{\epsilon}^e = E \cdot (\dot{\epsilon} - \dot{\epsilon}^p) \quad (2.4)$$

$$\dot{q} = H \cdot \dot{\xi} \quad (2.5)$$

**Yield function** The yield function (in 1D) is defined as

$$f(\sigma, q) := |\sigma| - q$$

Thus if  $f(\sigma, q) < 0$ , then the stress is within the elastic domain. Alternatively, if  $f(\sigma, q) = 0$ , the stress has reached its plastic limit. Fig. 2.4 shows the evolution of the elastic domain. First the strain reaches yielding

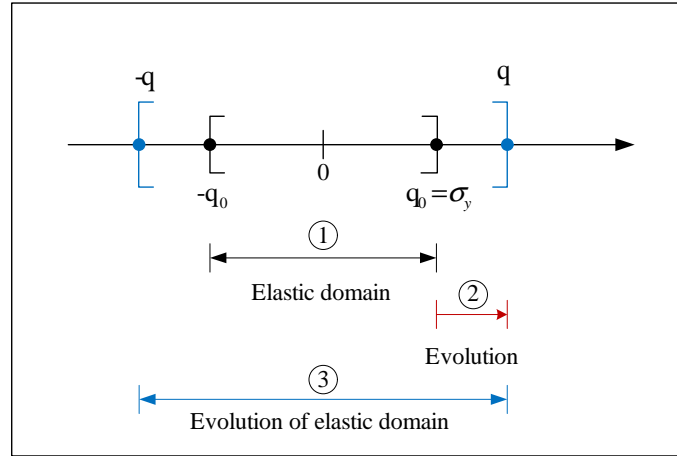


Figure 2.4: The evolution of elastic domain in isotropic hardening model

( $q_0 = \sigma_y$ ), and then at that point further increase in strain results in an expansion of  $q$  this will in turn expand the elastic domain.

**Evolution equation** We must define two of them<sup>1</sup>:

<sup>1</sup>We have established a yield criterion. When the stress is inside the yield surface, it is elastic, Hooke's law is applicable, strains are recoverable, and there is no dissipation of energy. However, when the load on the structure pushes the stress tensor to be beyond the yield surface, the stress tensor locks up on the yield surface, and the structure deforms plastically (if the material exhibits

1. Plastic flow for  $\dot{\varepsilon}^p$  defined by

$$\dot{\varepsilon}^p := \dot{\gamma} \cdot \frac{\partial g}{\partial \sigma} \quad (2.6)$$

where,  $\dot{\gamma}$  is a plastic multiplier or consistency parameter (as we shall see later, this term will ultimately drop off from  $E^{tan}$ , and  $g$  is the plastic potential function in terms of  $\sigma$  and  $q$ .

In isotropic hardening models, we assume  $g(\sigma, q) = f(\sigma, q)$ , thus  $\frac{\partial g}{\partial \sigma} = \text{sign}(\sigma)$  where  $\text{sign}(\sigma)$  is 1 if  $\sigma \geq 0$  or -1 if  $\sigma < 0$ . Then, we rewrite Eq. 2.6 as

$$\dot{\varepsilon}^p = \dot{\gamma} \cdot \text{sign}(\sigma)$$

or

$$\dot{\gamma} = |\dot{\varepsilon}^p| \geq 0$$

2. The second plastic flow is associated with the strain-like internal state variable associated with plasticity.

$$\dot{\xi} := \dot{\gamma} \cdot h(\sigma, q)$$

where,  $h(\sigma, q)$  is a dimensionless hardening function. For simplicity and under the assumption of elasto-plastic hardening material with bilinear curve,

$$h(\sigma, q) = -\frac{\partial g}{\partial q} = 1$$

Therefore, we can rewrite Eq. 2.4 and Eq. 2.5 as follows

$$\begin{aligned} \dot{\sigma} &= E \cdot (\dot{\varepsilon} - \dot{\gamma} \cdot \frac{\partial g}{\partial \sigma}) \\ &= E \cdot (\dot{\varepsilon} - \dot{\gamma} \cdot \text{sign}(\sigma)) \end{aligned} \quad (2.7)$$

and

$$\begin{aligned} \dot{q} &= H \cdot \dot{\gamma} \cdot h(\sigma, q) \\ &= H \cdot \dot{\gamma} \end{aligned} \quad (2.8)$$

**Kuhn-Tucker conditions and consistency condition** In the elastic regime, the yield function  $f$  must remain negative and the plastic multiplier is zero. On the other hand, during plastic flow the yield function  $f$  must be zero while plastic multiplier is positive. This is succinctly expressed by the so-called Kuhn-Tucker condition,

$$\text{Elastic loading and unloading : } f < 0, \quad \dot{\gamma} = 0 \quad (2.9)$$

$$\text{Plastic loading : } f = 0, \quad \dot{\gamma} > 0 \quad (2.10)$$

Eq. 2.9 and Eq. 2.10 can be combined for the general case of  $f \leq 0$  and  $\dot{\gamma} \geq 0$ , then

$$f \cdot \dot{\gamma} = 0 \quad (2.11)$$

**Consistency Condition:** During plastic loading the stress path is constrained to move along the yield surface, thus this consistency condition precludes us from going beyond the yield surface and is mathematically expressed as  $\dot{f}(\sigma, 1) = 0$ , or

$$\begin{aligned} \dot{f}(\sigma, q) &= \frac{\partial f}{\partial \sigma} \cdot \frac{\partial \sigma}{\partial t} + \frac{\partial f}{\partial q} \cdot \frac{\partial q}{\partial t} \\ &= \frac{\partial f}{\partial \sigma} \cdot \dot{\sigma} + \frac{\partial f}{\partial q} \cdot \dot{q} = 0 \end{aligned} \quad (2.12)$$

**Tangent Modulus** Finally, we need to evaluate tangent modulus  $E^{tan}$  such that  $\dot{\sigma} = E^{tan}\dot{\varepsilon}$ . Substituting Eq. 2.7

---

hardening as opposed to elastic-perfectly plastic response, then the yield surface expands or moves with the stress point still on the yield surface). At this point, the crucial question is what will be direction of the plastic flow (that is the relative magnitude of the components of  $\dot{\varepsilon}^P$ ). This question is addressed by the **flow rule**, or **normality rule**

and Eq. 2.8 into Eq. 2.12, we obtain

$$\frac{\partial f}{\partial \sigma} \cdot E \cdot \left( \dot{\varepsilon} - \dot{\gamma} \cdot \frac{\partial g}{\partial \sigma} \right) + \frac{\partial f}{\partial q} \cdot H \cdot \dot{\gamma} \cdot h(\sigma, q) = 0$$

Therefore,

$$\dot{\gamma} = \frac{\frac{\partial f}{\partial \sigma} \cdot E \cdot \dot{\varepsilon}}{\frac{\partial f}{\partial \sigma} \cdot E \cdot \frac{\partial g}{\partial \sigma} - \frac{\partial f}{\partial q} \cdot H \cdot h(\sigma, q)} \quad (2.13)$$

Substituting Eq. 2.13 into Eq. 2.7, we obtain an explicit expression for the incremental stress,

$$\begin{aligned} \dot{\sigma} &= E \cdot \left( \dot{\varepsilon} - \dot{\gamma} \cdot \frac{\partial g}{\partial \sigma} \right) \\ &= \left( E - \frac{\frac{\partial f}{\partial \sigma} \cdot E^2 \cdot \frac{\partial g}{\partial \sigma}}{\frac{\partial f}{\partial \sigma} \cdot E \cdot \frac{\partial g}{\partial \sigma} - \frac{\partial f}{\partial q} \cdot H \cdot h(\sigma, q)} \right) \cdot \dot{\varepsilon} \\ &= E^{tan} \cdot \dot{\varepsilon} \end{aligned}$$

For elasto-plastic hardening material with bilinear curve in one dimension,

$$\dot{\gamma} = \frac{\text{sign}(\sigma) \cdot E \cdot \dot{\varepsilon}}{E + H}$$

and the tangent modulus reduces to

$$\begin{aligned} E^{tan} &= E - \frac{\text{sign}(\sigma) \cdot E^2 \cdot \text{sign}(\sigma)}{\text{sign}(\sigma) \cdot E \cdot \text{sign}(\sigma) - (-1) \cdot H \cdot (1)} \\ &= E - \frac{E^2}{E + H} \\ &= \frac{E \cdot H}{E + H} \end{aligned}$$

### 2.1.1.2 Combined isotropic and kinematic hardening model

We describe isotropic and kinematic hardening model. Finally, we summarize the major equations governing plasticity.

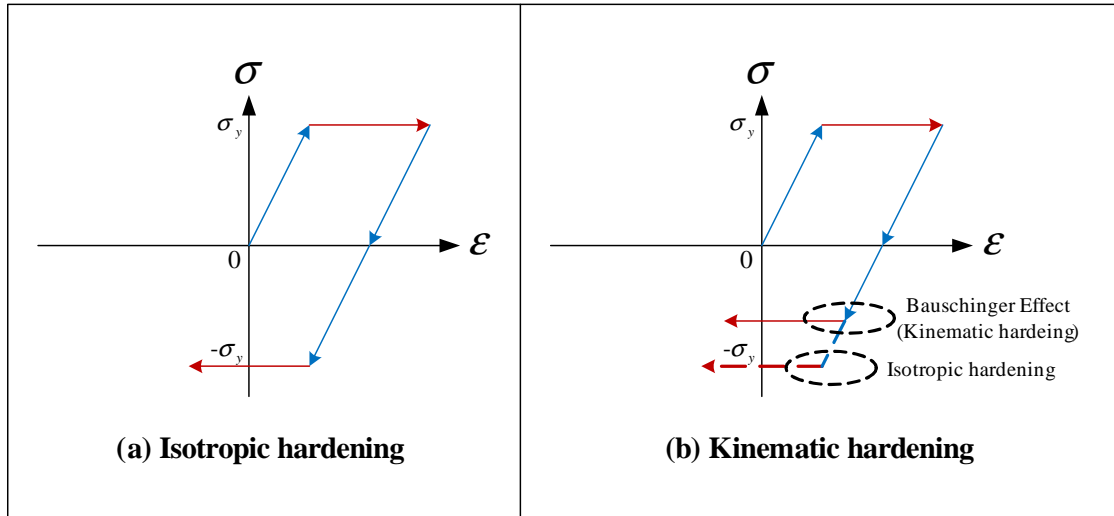


Figure 2.5: Isotropic and kinematic hardening plasticity

Yield surface of isotropic hardening plasticity is symmetric about the origin at  $\sigma = 0$ , Fig. 2.5(a), whereas for kinematic hardening plasticity the yield surface is unsymmetric, Fig. 2.5(b). This lack of symmetry is caused by the classical Bauschinger effect.

**Helmholtz free energy potential** The Helmholtz free energy function is now enriched by a set of strain-like internal state variables for combined isotropic and kinematic hardening (as opposed to a single value previously):

$$\rho \cdot \phi(\varepsilon^e, \boldsymbol{\xi}) = \underbrace{\frac{1}{2} \cdot \varepsilon^e \cdot E \cdot \varepsilon^e}_{\text{Elastic}} + \underbrace{\frac{1}{2} \cdot \boldsymbol{\xi}^T \cdot \mathbf{H} \cdot \boldsymbol{\xi}}_{\text{Plastic}}$$

where,  $\boldsymbol{\xi}$  is a strain-like vector of internal state variables, and  $\mathbf{H}$  is the hardening matrix.

$$\boldsymbol{\xi} = [\xi^{iso}, \xi^{kin}]^T$$

$$\mathbf{H} = \begin{bmatrix} H^{iso} & 0 \\ 0 & H^{kin} \end{bmatrix}$$

where,  $\xi^{iso}$  is a strain-like internal state variable of isotropic plasticity,  $\xi^{kin}$  a strain-like internal state variable of kinematic plasticity,  $H^{iso}$  the isotropic plastic modulus, and  $H^{kin}$  the kinematic plastic modulus. The thermodynamically stress-like vector of internal state variables is thus given by

$$\mathbf{q}^\xi = \mathbf{H} \cdot \boldsymbol{\xi}$$

$$= [H^{iso} \cdot \xi^{iso}, H^{kin} \cdot \xi^{kin}]^T$$

$$= [\mathbf{q}^{iso}, \mathbf{q}^{kin}]^T$$

where,  $\mathbf{q}^{iso}$  is an isotropic stress-like internal state variable and  $\mathbf{q}^{kin}$  a kinematic stress-like internal state variable. Therefore, the rate form of stress-like vector of internal state variables becomes

$$\dot{\mathbf{q}}^\xi = \mathbf{H} \cdot \dot{\boldsymbol{\xi}}$$

$$= [H^{iso} \cdot \dot{\xi}^{iso}, H^{kin} \cdot \dot{\xi}^{kin}]^T$$

$$= [\dot{\mathbf{q}}^{iso}, \dot{\mathbf{q}}^{kin}]^T \quad (2.14)$$

**Yield function** Having stress-like internal state variable  $\mathbf{q}^{iso}$ , we redefine the yield function as

$$f(\sigma, \mathbf{q}^\xi) := |\sigma - \mathbf{q}^{kin}| - \mathbf{q}^{iso}$$

As mentioned above, if  $f(\sigma, \mathbf{q}^\xi) < 0$ , the stress is in the elastic domain, otherwise, if  $f(\sigma, \mathbf{q}^\xi) = 0$ , the stress reaches plasticity.

**Evolution Equations** Again, we consider two of them:

1. Plastic flow of  $\dot{\varepsilon}^p$  is again given by

$$\dot{\varepsilon}^p := \dot{\gamma} \cdot \frac{\partial g}{\partial \sigma} \quad (2.15)$$

and we again assume that  $g(\sigma, \mathbf{q}^{iso})$  to be the same as  $f(\sigma, \mathbf{q}^{iso})$ .

Fig. 2.6 depicts the evolution of the elastic domain for  $H^{iso} = 0$  (isotropic perfectly plastic) and  $H^{kin} > 0$ . The size of elastic domains is the same after evolution.

2. The evolution of  $\dot{\boldsymbol{\xi}}$  is defined by

$$\dot{\boldsymbol{\xi}} := \dot{\gamma} \cdot \mathbf{h}(\sigma, \mathbf{q}^\xi) \quad (2.16)$$

where,  $\mathbf{h}(\sigma, \mathbf{q}^\xi)$  is a dimensionless hardening function.

$$\mathbf{h}(\sigma, \mathbf{q}^\xi) = -\frac{\partial g}{\partial \mathbf{q}^\xi}$$

$$= [-\frac{\partial g}{\partial \mathbf{q}^{iso}}, -\frac{\partial g}{\partial \mathbf{q}^{kin}}]^T$$

$$= [1, \text{sign}(\sigma - \mathbf{q}^{kin})]^T$$

Combining Eq. 2.14 and Eq. 2.16,

$$\dot{\mathbf{q}}^\xi = \mathbf{H} \cdot \dot{\boldsymbol{\xi}} = \mathbf{H} \cdot \dot{\gamma} \cdot \mathbf{h}(\sigma, \mathbf{q}^\xi) \quad (2.17)$$

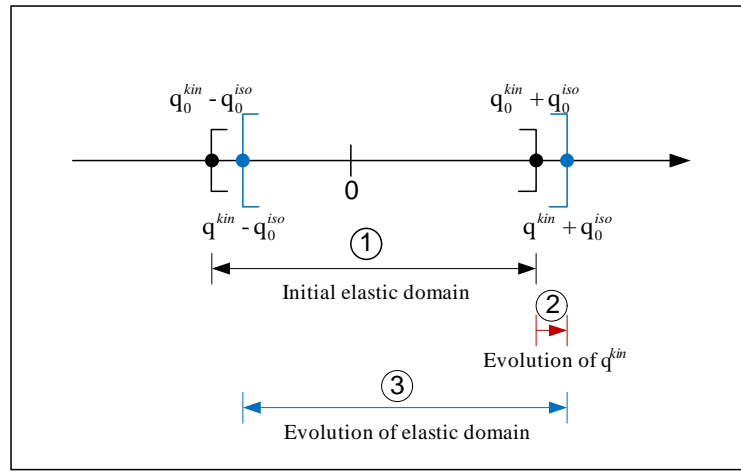


Figure 2.6: The evolution of elastic domain in isotropic and kinematic hardening model for  $H^{iso} = 0$  (isotropic perfectly plastic) and  $H^{kin} > 0$

**Tangent Modulus** To determine  $E^{tan}$ , we again invoke the consistency condition given by Eq. 2.12 and where  $\dot{\mathbf{q}}$  has now been replaced by  $\dot{\mathbf{q}}^\xi$

$$\dot{f}(\sigma, \mathbf{q}^\xi) = \frac{\partial f}{\partial \sigma} \cdot \dot{\sigma} + \frac{\partial f}{\partial \mathbf{q}^\xi} \cdot \dot{\mathbf{q}}^\xi = 0 \quad (2.18)$$

Substituting Eq. 2.7 and Eq. 2.17 into Eq. 2.18,

$$\frac{\partial f}{\partial \sigma} \cdot E \cdot \left( \dot{\varepsilon} - \dot{\gamma} \cdot \frac{\partial g}{\partial \sigma} \right) + \frac{\partial f}{\partial \mathbf{q}^\xi} \cdot \mathbf{H} \cdot \dot{\gamma} \cdot \mathbf{h}(\sigma, \mathbf{q}^\xi) = 0 \quad (2.19)$$

$\dot{\gamma}$  is determined from Eq. 2.19

$$\dot{\gamma} = \frac{\frac{\partial f}{\partial \sigma} \cdot E \cdot \dot{\varepsilon}}{\frac{\partial f}{\partial \sigma} \cdot E \cdot \frac{\partial g}{\partial \sigma} - \frac{\partial f}{\partial \mathbf{q}^\xi} \cdot \mathbf{H} \cdot \mathbf{h}(\sigma, \mathbf{q}^\xi)} \quad (2.20)$$

From Eq. 2.7,

$$\begin{aligned} \dot{\sigma} &= E \cdot \left( \dot{\varepsilon} - \dot{\gamma} \cdot \frac{\partial g}{\partial \sigma} \right) \\ &= \left( E - \frac{\frac{\partial f}{\partial \sigma} \cdot E^2 \cdot \frac{\partial g}{\partial \sigma}}{\frac{\partial f}{\partial \sigma} \cdot E \cdot \frac{\partial g}{\partial \sigma} - \frac{\partial f}{\partial \mathbf{q}^\xi} \cdot \mathbf{H} \cdot \mathbf{h}(\sigma, \mathbf{q}^\xi)} \right) \cdot \dot{\varepsilon} \\ &= E^{tan} \cdot \dot{\varepsilon} \end{aligned}$$

Thus, for elasto-plastic hardening material with bilinear curve, Eq. 2.20 reduces to:

$$\dot{\gamma} = \frac{\text{sign}(\sigma - q^{kin}) \cdot E \cdot \dot{\varepsilon}}{E + H^{iso} + H^{kin}}$$

Finally, we determine the tangent modulus,  $E^{tan}$ ,

$$\begin{aligned} E^{tan} &= E - \frac{\frac{\partial f}{\partial \sigma} \cdot E^2 \cdot \frac{\partial g}{\partial \sigma}}{\frac{\partial f}{\partial \sigma} \cdot E \cdot \frac{\partial g}{\partial \sigma} - \frac{\partial f}{\partial q^k} \cdot \mathbf{H} \cdot \mathbf{h}(\sigma, \mathbf{q}^k)} \\ &= E - \frac{\text{sign}(\sigma - q^{kin})^2 \cdot E^2}{\text{sign}(\sigma - q^{kin})^2 \cdot E - [-1, -\text{sign}(\sigma - q^{kin})] \begin{bmatrix} H^{iso} & 0 \\ 0 & H^{kin} \end{bmatrix} \left\{ \begin{array}{c} 1 \\ \text{sign}(\sigma - q^{kin}) \end{array} \right\}} \\ &= \frac{E \cdot (H^{iso} + H^{kin})}{E + H^{iso} + H^{kin}} \end{aligned}$$

### 2.1.1.3 Determination for isotropic and kinematic hardening parameters

Fig. 2.7 illustrates the procedure to determine uniaxial stress  $\sigma$  and tangent modulus  $E^{tan}$  from uniaxial strain  $\varepsilon$ .

## 2.1.2 Heuristic Models

### 2.1.2.1 Simplified Bilinear model with isotropic hardening

Whereas the proceeding model is rooted in plasticity theory, its implementation may be problematic. Alternatively, a phenomenologically similar model can be derived based on (?) and as implemented in (?).

**2.1.2.1.1 Stress-strain relation** Instead of determining the  $E^{tan}$  with  $H$  in Sec. 2.1.1.1, the simplified bilinear model computes it through a strain-hardening coefficient  $b$  which is the ratio of the post-yield tangent modulus  $E^{tan}$  and the initial elastic modulus  $E$ , and only considers isotropic hardening with Eq. 2.21 and Eq. 2.22 (?). Fig. 2.8 describes this simplified bilinear model.

$$E^{tan} = b \cdot E$$

To account for the evolution of elastic domain in isotropic hardening, a stress shift  $\sigma_\Delta$  is determined as follow:

- If the incremental strain  $\Delta\varepsilon$  changes a positive value into a negative one:

$$\begin{aligned} \Delta^N &= 1 + a_1 \cdot \left( \frac{\varepsilon_{max} - \varepsilon_{min}}{2 \cdot a_2 \cdot \varepsilon_y} \right)^{0.8} \\ \sigma_\Delta &= \Delta^N \cdot \sigma_y \cdot (1 - b) \end{aligned} \tag{2.21}$$

- If the incremental strain  $\Delta\varepsilon$  changes a negative value into a positive one:

$$\begin{aligned} \Delta^P &= 1 + a_3 \cdot \left( \frac{\varepsilon_{max} - \varepsilon_{min}}{2 \cdot a_4 \cdot \varepsilon_y} \right)^{0.8} \\ \sigma_\Delta &= \Delta^P \cdot \sigma_y \cdot (1 - b) \end{aligned} \tag{2.22}$$

where,  $a_1$  and  $a_3$  are isotropic hardening parameter which reflect an increase of the compression yield envelope through a fraction of the yield strength after a plastic strain  $a_2 \cdot \frac{\sigma_u}{E}$ , and tension yield envelope as a fraction of the yield strength after a plastic strain of  $a_4 \cdot \frac{\sigma_u}{E}$ .  $a_2$  and  $a_4$  are isotropic hardening parameter with respect to  $a_1$  and  $a_3$ , and  $\varepsilon_{max}$  and  $\varepsilon_{min}$  are the strain at the maximum and minimum strain reversal point. Limiting factor of this model is that  $a_1$ ,  $a_2$ ,  $a_3$  and  $a_4$  must be determined through curve fitting of the model with experimental results. Default values are  $a_1 = 0$ ,  $a_2 = 55$ ,  $a_3 = 0$ , and  $a_4 = 55$  in (?).

**2.1.2.1.2 Determination for simplified bilinear model** Fig. 2.9 shows the procedure to obtain uniaxial stress  $\sigma$  and tangent modulus  $E^{tan}$  from uniaxial strain  $\varepsilon$ .

### 2.1.2.2 Giuffre-Menegotto-Pinto Model Modified by Filippou et al.

This section is based on doctoral dissertation of ?.

**2.1.2.2.1 Stress-strain relationship** The reinforcing steel stress-strain behavior is described by the nonlinear model of ?, as modified by ?, to include isotropic strain hardening. This model introduces smooth curve to describe similar behavior to experimental one instead of bilinear curve.

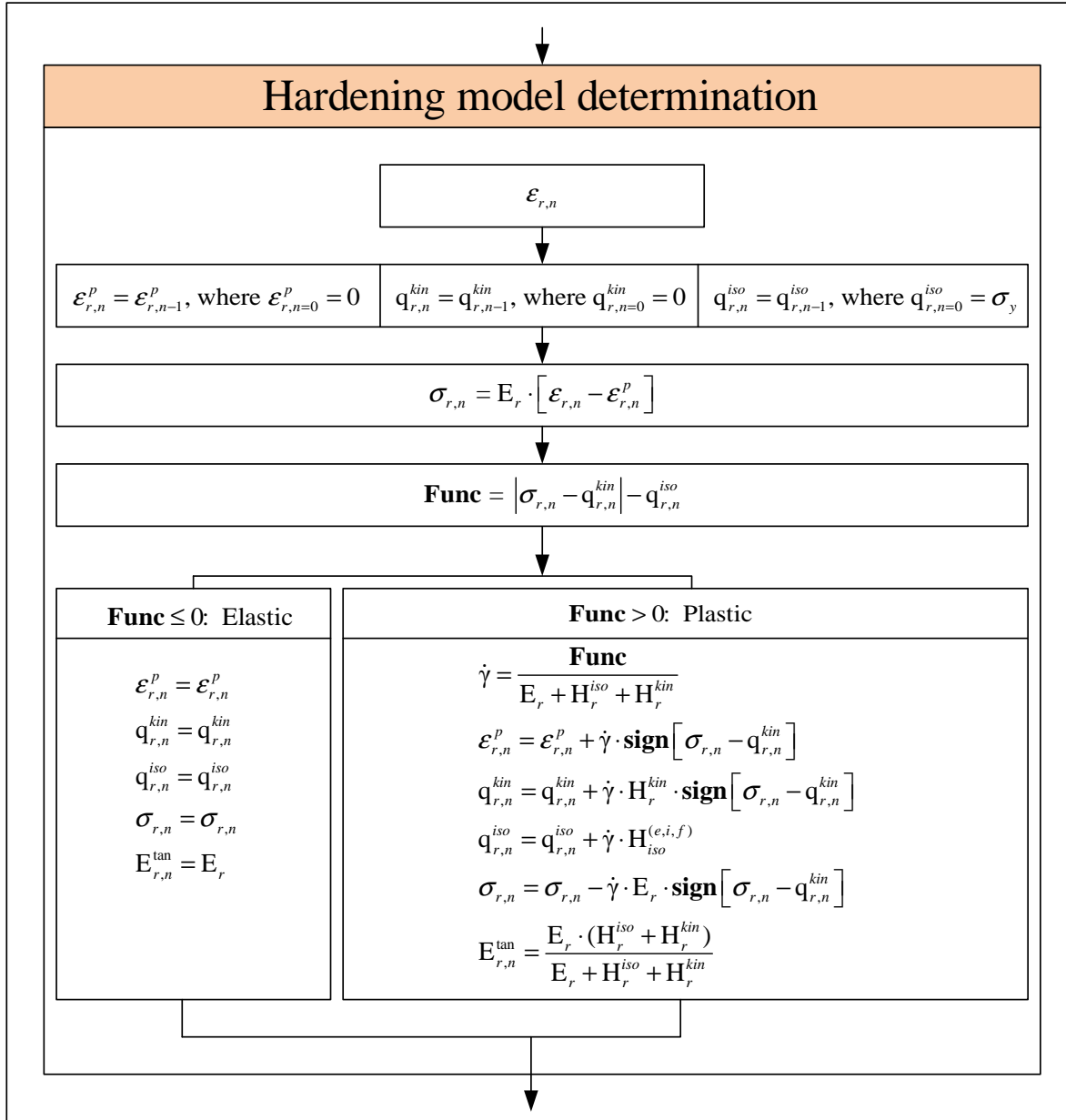


Figure 2.7: Determination for isotropic and kinematic hardening model

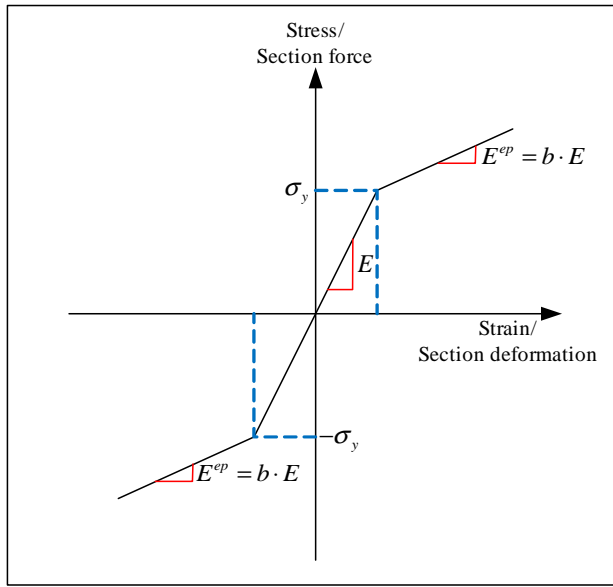


Figure 2.8: Bilinear model

The model presented in ? starts from the following empirical form of the stress-strain relation which is found to be close enough to experimentally determined ones.

$$\sigma^* = b \cdot \varepsilon^* + \frac{(1-b) \cdot \varepsilon^*}{(1 + \varepsilon^{*R})^{1/R}} \quad (2.23)$$

where,

$$\begin{aligned} \varepsilon^* &= \frac{\varepsilon - \varepsilon_{rev}}{\varepsilon_0 - \varepsilon_{rev}} \\ \sigma^* &= \frac{\sigma - \sigma_{rev}}{\sigma_0 - \sigma_{rev}} \end{aligned} \quad (2.24)$$

The tangent modulus  $E^{tan}$  is obtained by differentiating Eq. 2.23 and 2.24,

$$E^{tan} = \frac{d\sigma}{d\varepsilon} = \frac{\sigma_0 - \sigma_{rev}}{\varepsilon_0 - \varepsilon_{rev}} \cdot \frac{d\varepsilon^*}{d\varepsilon^*} \quad (2.25)$$

where,

$$\frac{d\varepsilon^*}{d\varepsilon} = b + \left[ \frac{1-b}{(1 + \varepsilon^{*R})^{1/R}} \right] \cdot \left[ 1 - \frac{\varepsilon^{*R}}{1 + \varepsilon^{*R}} \right] \quad (2.26)$$

In Fig. 2.10, Eq. 2.24 represents a curved transition from a straight line asymptote with slope  $E$  (a) to another asymptote with slope  $E^{tan}$  (b),  $\sigma_{rev}$  and  $\varepsilon_{rev}$  are the stress and strain at the point of strain reversal (point A), which also forms the origin of the asymptote with slope  $E$  (a), and  $\sigma_0$  and  $\varepsilon_0$  are the stress and strain at the point of intersection of the two asymptotes (point B).

$b$  is the strain hardening ratio between slope  $E^{tan}$  and  $E$ , and  $R$  is a parameter that influences the curvature of the transition curve between the two asymptotes and permits a good representation of the Bauschinger effect. As indicated in Fig. 2.10,  $\sigma_0$ ,  $\varepsilon_0$ ,  $\sigma_{rev}$  and  $\varepsilon_{rev}$  are updated after each strain reversal.

In Fig. 2.11,  $R$  is dependent on the absolute strain difference between the current asymptote intersection point (point B) and the previous maximum or minimum strain reversal point (point C) depending on whether the current strain is increasing or decreasing, respectively. There are two reported expression for  $R(\xi)$ :

- Menegotto-Pinto original model (?),

$$R(\xi) = R_0 - \frac{cR_1 \cdot \xi}{cR_2 + \xi} \quad (2.27)$$

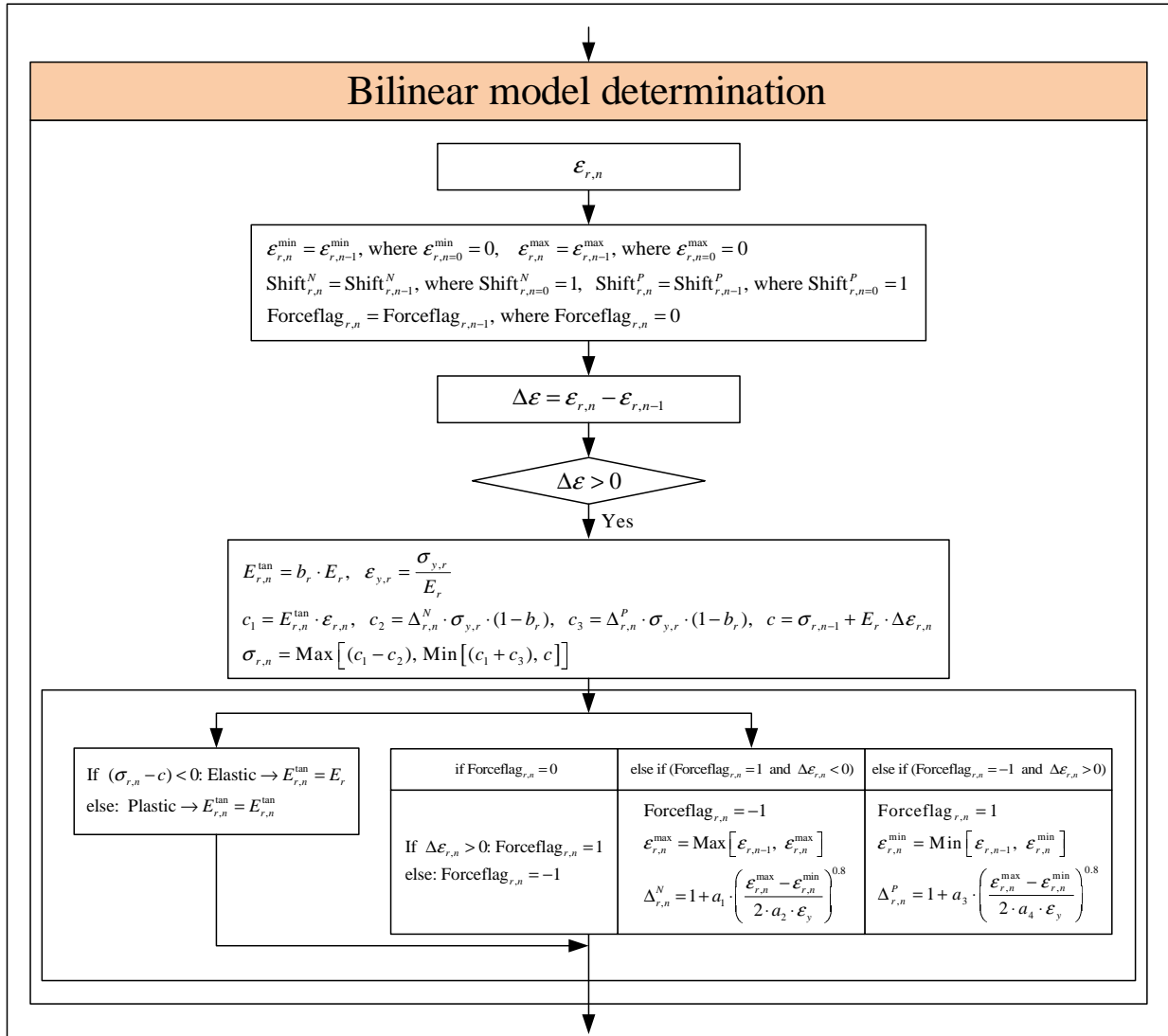


Figure 2.9: Determination for simplified bilinear model

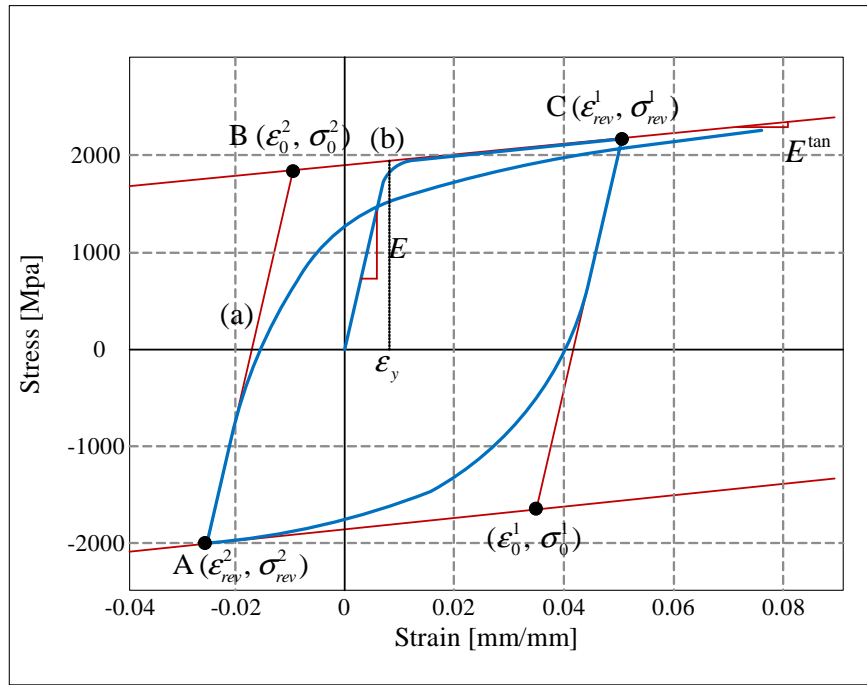


Figure 2.10: Menegotto-Pinto steel model  
(?)

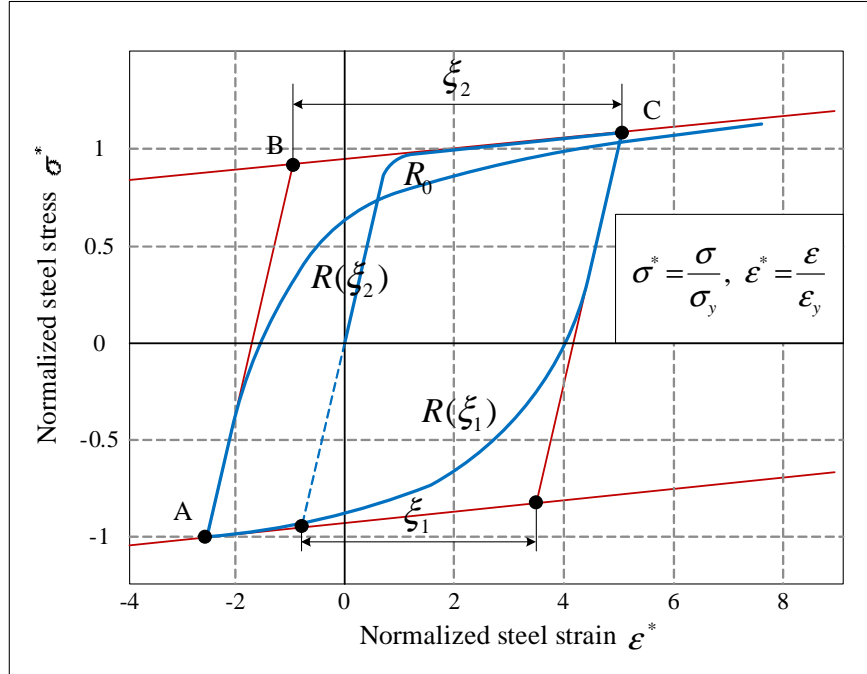


Figure 2.11: Definition of curvature parameter  $R$  in Menegotto-Pinto steel model  
(?)

- Steel2 in OpenSees (?),

$$R(\xi) = R_0 \left( 1 - \frac{cR_1 \cdot \xi}{cR_2 + \xi} \right) \quad (2.28)$$

where,  $R_0$  is the value of the parameter  $R$  during first loading, and  $cR_1$  and  $cR_2$  are experimentally determined parameters to be defined together with  $R_0$ .  $\xi$  can be expressed as

$$\xi = \left| \frac{\varepsilon^m - \varepsilon_0}{\varepsilon_y} \right| \quad (2.29)$$

where,  $\varepsilon^m$  is the strain at the previous maximum or minimum strain reversal point depending on whether the current strain is increasing or decreasing, respectively.  $\varepsilon_0$  is the strain at the current intersection point of the two asymptotes.

As shown in Fig. 2.10, both  $\varepsilon^m$  and  $\varepsilon_0$  lie along the same asymptote and  $\varepsilon_y$  is the initial yield strain. Fig. 2.11 shows how  $\xi$  is updated following a strain reversal.

Some clarification is needed in connection with the set of rules for unloading and reloading which are implied by Eq. 2.23 to 2.29, allowing for a generalized load history. If the analytical model had a memory extending over all previous branches of the stress-strain history, then it would allow for the resumption of the previous reloading branch, as soon as the new reloading curve reached it. However, this would require that the model store all necessary information to retrace all previous incomplete reloading curves, and this is clearly impractical from a computational standpoint. Memory of the past stress-strain history is therefore limited to a predefined number of parameters, which in the present model are:

1. stress and strain at the last state of the model
2. stress and strain at the last state reversal point
3. stress and strain at the last asymptote intersection point
4. flag indication whether the last branch is ascending or descending
5. strain at the previous minimum strain reversal point
6. strain at the previous maximum strain reversal point

As a result of these restrictions reloading following partial unloading does not hit the original curve following unloading started, but, instead, continues on the new reloading curve until reaching the monotonic envelope. However, the discrepancy between the analytical model and the actual behavior is typically very small, ?.

The above implementation of the model corresponds to its simplest form, as proposed by ?: elastic and yield asymptotes are assumed to be straight lines, the position of the limiting asymptotes corresponding to the yield surface is assumed to be fixed at all times and the slope  $E$  remains constant, Fig. 2.10.

In spite of the simplicity in formulation, the model is capable of reproducing well experimental results and its major drawback stems from its failure to allow for isotropic hardening. To account for this effect ? proposed a shift of  $\sigma_0$  and  $\varepsilon_0$  in the linearly yield asymptote as follows:

- If the incremental strain  $\Delta\varepsilon$  changes a positive value to a negative value:

$$\begin{aligned} \Delta^N &= 1 + a_1 \cdot \left( \frac{\varepsilon^{max} - \varepsilon^{min}}{2 \cdot a_2 \cdot \varepsilon_y} \right)^{0.8} \\ \varepsilon_0 &= \frac{-\sigma_y \cdot \Delta^N + E^{tan} \cdot \varepsilon_y \cdot \Delta^N - \sigma_{rev} + E \cdot \varepsilon_{rev}}{E - E^{tan}} \\ \sigma_0 &= -\sigma_y \cdot \Delta^N + E^{tan} \cdot (\varepsilon_o + \varepsilon_y \cdot \Delta^N) \end{aligned} \quad (2.30)$$

- If the incremental strain  $\Delta\varepsilon$  changes a negative value to a positive value,

$$\begin{aligned} \Delta^P &= 1 + a_3 \cdot \left( \frac{\varepsilon^{max} - \varepsilon^{min}}{2 \cdot a_4 \cdot \varepsilon_y} \right)^{0.8} \\ \varepsilon_0 &= \frac{\sigma_y \cdot \Delta^P - E^{tan} \cdot \varepsilon_y \cdot \Delta^P - \sigma_{rev} + E \cdot \varepsilon_{rev}}{E - E^{tan}} \\ \sigma_0 &= \sigma_y \cdot \Delta^P + E^{tan} \cdot (\varepsilon_o - \varepsilon_y \cdot \Delta^P) \end{aligned} \quad (2.31)$$

where,  $a_1$  and  $a_3$  are isotropic hardening parameter which reflect an increase of the compression yield envelope through a fraction of the yield strength after a plastic strain  $a_2 \cdot \frac{\sigma_y}{E}$ , and tension yield envelope as a fraction of the yield strength after a plastic strain of  $a_4 \cdot \frac{\sigma_y}{E}$ .  $a_2$  and  $a_4$  are isotropic hardening parameter with respect to  $a_1$  and  $a_3$ , and  $\varepsilon_{max}$  and  $\varepsilon_{min}$  are the strain at the maximum and minimum strain reversal point. Limiting factor of this model is that  $a_1$ ,  $a_2$ ,  $a_3$  and  $a_4$  must be determined through curve fitting of the model with experimental results. Default values are  $a_1 = 0$ ,  $a_2 = 55$ ,  $a_3 = 0$ , and  $a_4 = 55$  in (?).

**2.1.2.2.2 Determination for modified Giuffre-Menegotto-Pinto Model** Fig. 2.12 to 2.15 show the procedure to obtain uniaxial stress  $\sigma$  and tangent modulus  $E^{tan}$  from uniaxial strain  $\varepsilon$ .

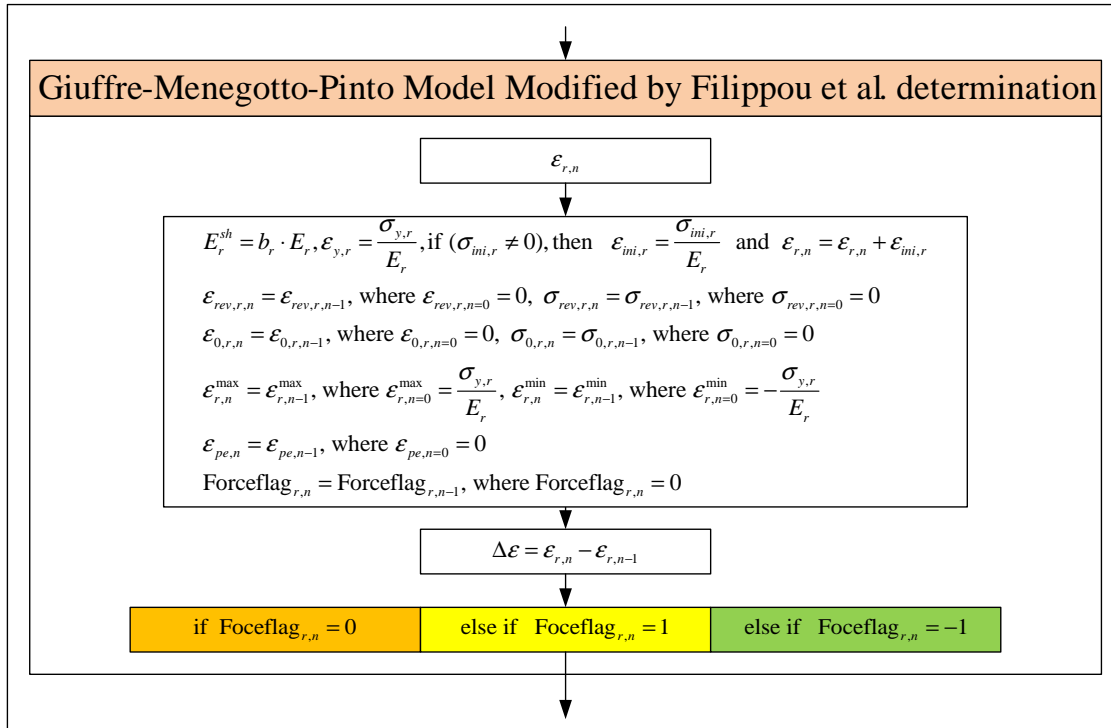


Figure 2.12: Determination (1) for Giuffre-Menegotto-Pinto Model Modified by Filippou et al.

## 2.2 Concrete Models

### 2.2.1 Heuristic Models

#### 2.2.1.1 Modified Kent And Park Model

This section is based on doctoral dissertation of (?).

**2.2.1.1.1 Stress-strain relation** The concrete model describes the concrete stress-strain relation under an arbitrary cyclic strain history. In particular, the model implemented takes into account four important factors:

1. effect of concrete confinement on the monotonic envelope curve in compression
2. successive degradation of stiffness of both the unloading and reloading curves, for increasing values of compressive strain
3. effect of tension stiffening
4. hysteretic response under cyclic loading in compression

if $\text{Forceflag}_{r,n} = 0$		
if $\Delta\epsilon = 0$	else if $\Delta\epsilon < 0$	else if $\Delta\epsilon > 0$
$\epsilon_{rev,r,n} = 0$	$\epsilon_{rev,r,n} = 0$	$\epsilon_{rev,r,n} = 0$
$\sigma_{rev,r,n} = 0$	$\sigma_{rev,r,n} = 0$	$\sigma_{rev,r,n} = 0$
$\epsilon_{0,r,n} = 0$	$\epsilon_{0,r,n} = \sigma_{y,r} / E_r$	$\epsilon_{0,r,n} = -\sigma_{y,r} / E_r$
$\sigma_{0,r,n} = 0$	$\sigma_{0,r,n} = \sigma_{y,r}$	$\sigma_{0,r,n} = -\sigma_{y,r}$
$\epsilon_{r,n}^{\max} = \sigma_{y,r} / E_r$	$\epsilon_{r,n}^{\max} = \sigma_{y,r} / E_r$	$\epsilon_{r,n}^{\max} = \sigma_{y,r} / E_r$
$\epsilon_{r,n}^{\min} = -\sigma_{y,r} / E_r$	$\epsilon_{r,n}^{\min} = -\sigma_{y,r} / E_r$	$\epsilon_{r,n}^{\min} = -\sigma_{y,r} / E_r$
$\text{Forceflag}_{r,n} = 0$	$\text{Forceflag}_{r,n} = \epsilon_{pe,n}^{\min}$	$\text{Forceflag}_{r,n} = \epsilon_{pe,n}^{\max}$
$\sigma_{r,n} = \sigma_{ini,r}$	$\text{Forceflag}_{r,n} = 1$	$\text{Forceflag}_{r,n} = -1$
$E_{r,n}^{\tan} = E_r$	$\xi = \left  \frac{\epsilon_{pe,n} - \epsilon_{0,r,n}}{\epsilon_{y,r}} \right $ $R = R_0 - R_0^{ratio} \cdot \frac{cR_1 \cdot \xi}{cR_2 + \xi}$ $\dot{\epsilon} = \frac{\epsilon_{r,n} - \epsilon_{rev,r,n}}{\epsilon_{0,r,n} - \epsilon_{rev,r,n}}$ $c_1 = 1 +  \dot{\epsilon} ^R$ $c_2 = c_1^{1/R}$ $\sigma_{r,n} = b_r \cdot \dot{\epsilon} + (1 - b_r) \cdot \frac{\dot{\epsilon}}{c_2}$ $\sigma_{r,n} = \sigma_{r,n} \cdot (\sigma_{0,r,n} - \sigma_{rev,r,n}) + \sigma_{rev,r,n}$ $E_{r,n}^{\tan} = b_r + \frac{(1 - b_r)}{c_1 \cdot c_2}$ $E_{r,n}^{\tan} = E_{r,n}^{\tan} \cdot \frac{\sigma_{0,r,n} - \sigma_{rev,r,n}}{\epsilon_{0,r,n} - \epsilon_{rev,r,n}}$	$\xi = \left  \frac{\epsilon_{pe,n} - \epsilon_{0,r,n}}{\epsilon_{y,r}} \right $ $R = R_0 - R_0^{ratio} \cdot \frac{cR_1 \cdot \xi}{cR_2 + \xi}$ $\dot{\epsilon} = \frac{\epsilon_{r,n} - \epsilon_{rev,r,n}}{\epsilon_{0,r,n} - \epsilon_{rev,r,n}}$ $c_1 = 1 +  \dot{\epsilon} ^R$ $c_2 = c_1^{1/R}$ $\sigma_{r,n} = b_r \cdot \dot{\epsilon} + (1 - b_r) \cdot \frac{\dot{\epsilon}}{c_2}$ $\sigma_{r,n} = \sigma_{r,n} \cdot (\sigma_{0,r,n} - \sigma_{rev,r,n}) + \sigma_{rev,r,n}$ $E_{r,n}^{\tan} = b_r + \frac{(1 - b_r)}{c_1 \cdot c_2}$ $E_{r,n}^{\tan} = E_{r,n}^{\tan} \cdot \frac{\sigma_{0,r,n} - \sigma_{rev,r,n}}{\epsilon_{0,r,n} - \epsilon_{rev,r,n}}$

Figure 2.13: Determination (2) for Giuffre-Menegotto-Pinto Model Modified by Filippou et al.

else if $\text{Foceflag}_{r,n} = 1$	
if $\Delta\epsilon < 0$	else if $\Delta\epsilon > 0$
$\mathcal{E}_{rev,r,n}, \sigma_{rev,r,n}$ $\Delta^N = 1 + a_1 \cdot \left( \frac{\mathcal{E}_{r,n}^{\max} - \mathcal{E}_{r,n}^{\min}}{2 \cdot a_2 \cdot \mathcal{E}_y} \right)^{0.8}$ $\mathcal{E}_{0,r,n} = \frac{-\sigma_{y,r} \cdot \Delta^N + E_r^{sh} \cdot \mathcal{E}_{y,r} \cdot \Delta^N - \sigma_{rev,r,n} + E_r \cdot \epsilon_{rev,r,n}}{E_r - E_r^{sh}}$ $\sigma_{0,r,n} = -\sigma_{y,r} \cdot \Delta^N + E_r^{sh} \cdot (\mathcal{E}_{0,r,n} + \mathcal{E}_{y,r} \cdot \Delta^N)$ $\mathcal{E}_{r,n}^{\max} = \text{Max} [\mathcal{E}_{r,n}^{\max}, \mathcal{E}_{r,n-1}]$ $\mathcal{E}_{r,n}^{\min} = \text{Min} [\mathcal{E}_{r,n}^{\min}, \mathcal{E}_{r,n-1}]$ $\epsilon_{pe,n} = \mathcal{E}_{r,n}^{\min}$ $\text{Forceflag}_{r,n} = -1$ $\xi = \left  \frac{\mathcal{E}_{pe,n} - \mathcal{E}_{0,r,n}}{\mathcal{E}_{y,r}} \right $ $R = R_0 - R_0^{nratio} \cdot \frac{cR_1 \cdot \xi}{cR_2 + \xi}$ $\dot{\mathcal{E}} = \frac{\mathcal{E}_{r,n} - \mathcal{E}_{rev,r,n}}{\mathcal{E}_{0,r,n} - \mathcal{E}_{rev,r,n}}$ $c_1 = 1 +  \dot{\mathcal{E}} ^R$ $c_2 = c_1^{1/R}$ $\sigma_{r,n} = b_r \cdot \dot{\mathcal{E}} + (1 - b_r) \cdot \frac{\dot{\mathcal{E}}}{c_2}$ $\sigma_{r,n} = \sigma_{r,n} \cdot (\sigma_{0,r,n} - \sigma_{rev,r,n}) + \sigma_{rev,r,n}$ $E_{r,n}^{\tan} = b_r + \frac{(1 - b_r)}{c_1 \cdot c_2}$ $E_{r,n}^{\tan} = E_{r,n}^{\tan} \cdot \frac{\sigma_{0,r,n} - \sigma_{rev,r,n}}{\mathcal{E}_{0,r,n} - \mathcal{E}_{rev,r,n}}$	$\mathcal{E}_{rev,r,n}, \sigma_{rev,r,n}, \mathcal{E}_{0,r,n}, \sigma_{0,r,n}$ $\mathcal{E}_{r,n}^{\max} = \text{Max} [\mathcal{E}_{r,n}^{\max}, \mathcal{E}_{r,n-1}]$ $\mathcal{E}_{r,n}^{\min} = \text{Min} [\mathcal{E}_{r,n}^{\min}, \mathcal{E}_{r,n-1}]$ $\epsilon_{pe,n} = \mathcal{E}_{r,n}^{\max}$ $\text{Forceflag}_{r,n} = 1$ $\xi = \left  \frac{\mathcal{E}_{pe,n} - \mathcal{E}_{0,r,n}}{\mathcal{E}_{y,r}} \right $ $R = R_0 - R_0^{nratio} \cdot \frac{cR_1 \cdot \xi}{cR_2 + \xi}$ $\dot{\mathcal{E}} = \frac{\mathcal{E}_{r,n} - \mathcal{E}_{rev,r,n}}{\mathcal{E}_{0,r,n} - \mathcal{E}_{rev,r,n}}$ $c_1 = 1 +  \dot{\mathcal{E}} ^R$ $c_2 = c_1^{1/R}$ $\sigma_{r,n} = b_r \cdot \dot{\mathcal{E}} + (1 - b_r) \cdot \frac{\dot{\mathcal{E}}}{c_2}$ $\sigma_{r,n} = \sigma_{r,n} \cdot (\sigma_{0,r,n} - \sigma_{rev,r,n}) + \sigma_{rev,r,n}$ $E_{r,n}^{\tan} = b_r + \frac{(1 - b_r)}{c_1 \cdot c_2}$ $E_{r,n}^{\tan} = E_{r,n}^{\tan} \cdot \frac{\sigma_{0,r,n} - \sigma_{rev,r,n}}{\mathcal{E}_{0,r,n} - \mathcal{E}_{rev,r,n}}$

Figure 2.14: Determination (3) for Giuffre-Menegotto-Pinto Model Modified by Filippou et al.

else if $\text{Foceflag}_{r,n} = -1$	
if $\Delta\epsilon > 0$	else if $\Delta\epsilon < 0$
$\epsilon_{rev,r,n}, \sigma_{rev,r,n}$ $\Delta^P = 1 + a_3 \cdot \left( \frac{\epsilon_{r,n}^{\max} - \epsilon_{r,n}^{\min}}{2 \cdot a_4 \cdot \epsilon_y} \right)^{0.8}$ $\epsilon_{0,r,n} = \frac{\sigma_{y,r} \cdot \Delta^P - E_r^{sh} \cdot \epsilon_{y,r} \cdot \Delta^P - \sigma_{rev,r,n} + E_r \cdot \epsilon_{rev,r,n}}{E_r - E_r^{sh}}$ $\sigma_{0,r,n} = \sigma_{y,r} \cdot \Delta^P + E_r^{sh} \cdot (\epsilon_{0,r,n} - \epsilon_{y,r} \cdot \Delta^P)$ $\epsilon_{r,n}^{\max} = \text{Max}[\epsilon_{r,n}^{\max}, \epsilon_{r,n-1}]$ $\epsilon_{r,n}^{\min} = \text{Min}[\epsilon_{r,n}^{\min}, \epsilon_{r,n-1}]$ $\epsilon_{pe,n} = \epsilon_{r,n}^{\max}$ $\text{Forceflag}_{r,n} = 1$ $\xi = \left  \frac{\epsilon_{pe,n} - \epsilon_{0,r,n}}{\epsilon_{y,r}} \right $ $R = R_0 - R_0^{nratio} \cdot \frac{cR_1 \cdot \xi}{cR_2 + \xi}$ $\dot{\epsilon} = \frac{\epsilon_{r,n} - \epsilon_{rev,r,n}}{\epsilon_{0,r,n} - \epsilon_{rev,r,n}}$ $c_1 = 1 +  \dot{\epsilon} ^R$ $c_2 = c_1^{1/R}$ $\sigma_{r,n} = b_r \cdot \dot{\epsilon} + (1 - b_r) \cdot \frac{\dot{\epsilon}}{c_2}$ $\sigma_{r,n} = \sigma_{r,n} \cdot (\sigma_{0,r,n} - \sigma_{rev,r,n}) + \sigma_{rev,r,n}$ $E_{r,n}^{\tan} = b_r + \frac{(1 - b_r)}{c_1 \cdot c_2}$ $E_{r,n}^{\tan} = E_{r,n}^{\tan} \cdot \frac{\sigma_{0,r,n} - \sigma_{rev,r,n}}{\epsilon_{0,r,n} - \epsilon_{rev,r,n}}$	$\epsilon_{rev,r,n}, \sigma_{rev,r,n}, \epsilon_{0,r,n}, \sigma_{0,r,n}$ $\epsilon_{r,n}^{\max} = \text{Max}[\epsilon_{r,n}^{\max}, \epsilon_{r,n-1}]$ $\epsilon_{r,n}^{\min} = \text{Min}[\epsilon_{r,n}^{\min}, \epsilon_{r,n-1}]$ $\epsilon_{pe,n} = \epsilon_{r,n}^{\min}$ $\text{Forceflag}_{r,n} = -1$ $\xi = \left  \frac{\epsilon_{pe,n} - \epsilon_{0,r,n}}{\epsilon_{y,r}} \right $ $R = R_0 - R_0^{nratio} \cdot \frac{cR_1 \cdot \xi}{cR_2 + \xi}$ $\dot{\epsilon} = \frac{\epsilon_{r,n} - \epsilon_{rev,r,n}}{\epsilon_{0,r,n} - \epsilon_{rev,r,n}}$ $c_1 = 1 +  \dot{\epsilon} ^R$ $c_2 = c_1^{1/R}$ $\sigma_{r,n} = b_r \cdot \dot{\epsilon} + (1 - b_r) \cdot \frac{\dot{\epsilon}}{c_2}$ $\sigma_{r,n} = \sigma_{r,n} \cdot (\sigma_{0,r,n} - \sigma_{rev,r,n}) + \sigma_{rev,r,n}$ $E_{r,n}^{\tan} = b_r + \frac{(1 - b_r)}{c_1 \cdot c_2}$ $E_{r,n}^{\tan} = E_{r,n}^{\tan} \cdot \frac{\sigma_{0,r,n} - \sigma_{rev,r,n}}{\epsilon_{0,r,n} - \epsilon_{rev,r,n}}$

Figure 2.15: Determination (4) for Giuffre-Menegotto-Pinto Model Modified by Filippou et al.

The monotonic envelope curve of concrete in compression follows the original model of ? and extended by ?. Even though more accurate and complete models have been published since, the so-called modified Kent and Park model offers a good balance between simplicity and accuracy.

Tension stiffening is the ability of concrete between cracks to resist tensile stress and contribute to the flexural stiffness of the member. Due to the discrete nature of the cracks, concrete in between cracks remains bonded to the reinforcement and, thus, contributes to the stiffness of the member. However, as the magnitude of load increases, additional cracks form at closer intervals, hence reducing the tensile stress that can be developed in the concrete. Therefore tension stiffening is gradually reduced as load is increased in the post-cracking stage. Past investigators have taken tension stiffening into account by modifying the concrete stress-strain relation such that, after reaching the tensile strength (cracking), the tensile stress reduces gradually to zero as tensile strain is increased. The gradual reduction of tensile strength is often approximated as linear, multi-linear or exponential. A similar approach with a linear rate of reduction is adopted. However, the results indicate that the application of tension stiffening over all fibers of a member can lead to significant overestimation of the ultimate strength. Rather tension stiffening is a localized phenomenon that affects the concrete in the immediate vicinity of the reinforcement. In analytical studies, only the concrete fibers within an effective area around the reinforcements are assigned tension softening. Clearly, the size of the effective area has a significant effect on tension stiffening behavior of the member.

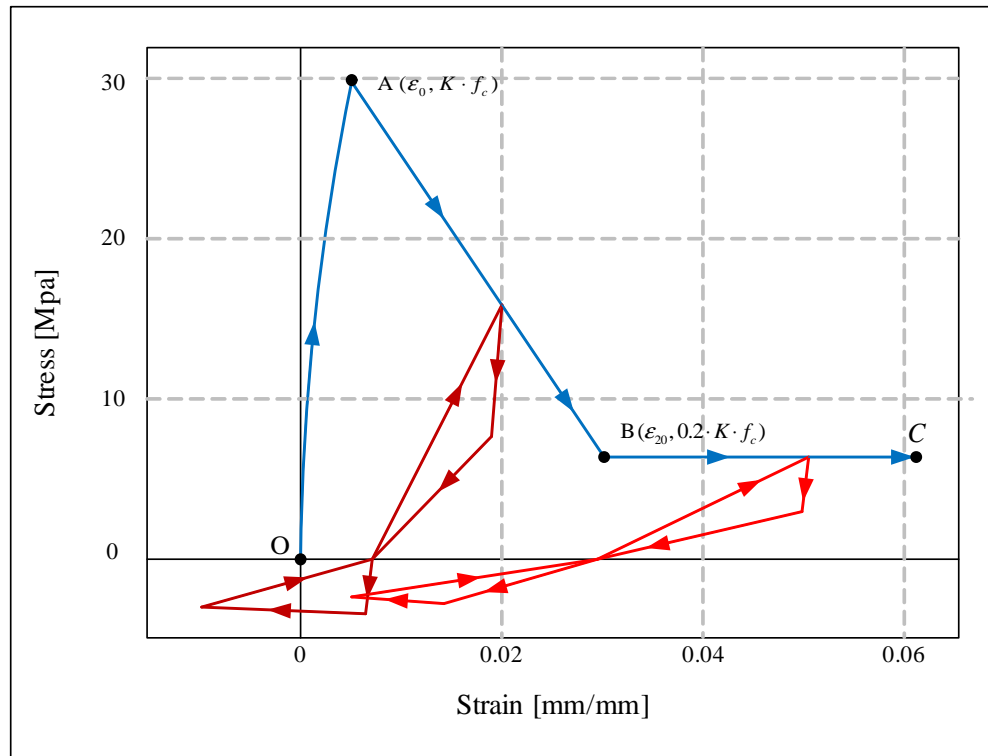


Figure 2.16: Concrete material model in compression  
(?)

In the modified Kent and Park model (?) shown in Fig. 2.16, the monotonic concrete stress-strain relation in compression is empirically defined by three regions. Adopting the convention that compression is positive, the three regions are,

- Segment  $OA$ :  $\varepsilon_c \leq \varepsilon_0$

$$\sigma_c = K \cdot f_c \cdot \left[ 2 \cdot \frac{\varepsilon_c}{\varepsilon_0} - \left( \frac{\varepsilon_c}{\varepsilon_0} \right)^2 \right]$$

From this equation, we can determine the maximum compressive strength of confined concrete:

$$f'_{c,confined} = K f'_c \quad (2.32)$$

- Segment AB:  $\varepsilon_0 < \varepsilon_c \leq \varepsilon_{20}$

$$\sigma_c = K \cdot f_c \cdot [1 - Z(\varepsilon_c - \varepsilon_0)]$$

- Segment BC:  $\varepsilon_c > \varepsilon_{20}$

$$\sigma_c = 0.2 \cdot K \cdot f_c$$

The corresponding tangent moduli are given by the following equations

- Segment OA:  $\varepsilon_c \leq \varepsilon_0$

$$E^{tan} = \frac{2 \cdot K \cdot f_c}{\varepsilon_0} \cdot \left(1 - \frac{\varepsilon_c}{\varepsilon_0}\right)$$

- Segment AB:  $\varepsilon_0 < \varepsilon_c \leq \varepsilon_{20}$

$$E^{tan} = -Z \cdot K \cdot f_c$$

- Segment BC:  $\varepsilon_c > \varepsilon_{20}$

$$E^{tan} = 0$$

where,

$$\varepsilon_0 = 0.002 \cdot K$$

$$K = 1 + \frac{\rho_s \cdot f_{ys}}{f_c}$$

$$Z = \frac{0.5}{\frac{3+0.29 \cdot f_c}{145 \cdot f_c - 1000} + 0.75 \cdot \rho_s \cdot \sqrt{\frac{h}{s_h}} - 0.002 \cdot K}$$

$\varepsilon_0$  is the concrete strain corresponding maximum stress,  $\varepsilon_{20}$  the concrete strain at 20 percent of maximum stress,  $K$  a factor which accounts for the strength increase due to confinement,  $Z$  the strain softening slope,  $f_c$  the concrete compressive cylinder strength in MPa (1 MPa = 145 psi),  $f_{ys}$  the yield strength of stirrups in MPa,  $\rho_s$  the ratio of the volume of hoop reinforcement to the volume of concrete core measured to outside of stirrups,  $h$  the width of concrete core measured to outside of stirrups, and  $s_h$  the center to center spacing of stirrups or hoop sets.

From the previous equations,  $\varepsilon_{20}$  can be determined from

$$\varepsilon_{20} = \varepsilon_0 + \frac{K f'_c - 0.2 f'_{c,confined}}{Z K f'_c} \quad (2.33)$$

The cyclic unloading and reloading behavior is represented by a set of straight lines. Fig. 2.16 shows that hysteretic behavior occurs under, both, tensile and compressive stress. Although the compressive and tensile hysteresis loops are continuous, they will be discussed separately for the sake of clarity.

On the compressive side of the model, there is a successive degradation of stiffness of both the unloading and reloading lines for increasing values of maximum strain, as shown in Fig. 2.16. The degradation of stiffness is such that the projections of all reloading lines intersect at a common point R in Fig. 2.17. Point R is determined by the intersection of the tangent to the monotonic envelope curve at the origin and the projection of the unloading line from point B that corresponds to concrete strength of  $0.2 \cdot f_c$  (Fig. 2.17). The strain and stress at the intersection point are given by the following expressions

$$\begin{aligned} \varepsilon_R &= \frac{0.2 \cdot K \cdot f_c - E_{20} \cdot \varepsilon_{20}}{E_c - E_{20}} \\ \sigma_R &= E_c \cdot \varepsilon_R \end{aligned} \quad (2.34)$$

where  $E_c$  is the tangent modulus of the monotonic envelope curve at the origin,  $E_{20}$  is the unloading modulus at point B of the monotonic envelope curve with a strength of  $0.2 \cdot f_c$ . The magnitude of  $E_{20}$  has to be determined experimentally.

After unloading from a point on the compressive monotonic envelope (point D in Fig. 2.17), and before reaching the zero stress axis (point H in Fig. 2.17), the model response follows two smaller envelopes that are defined by the following equations,

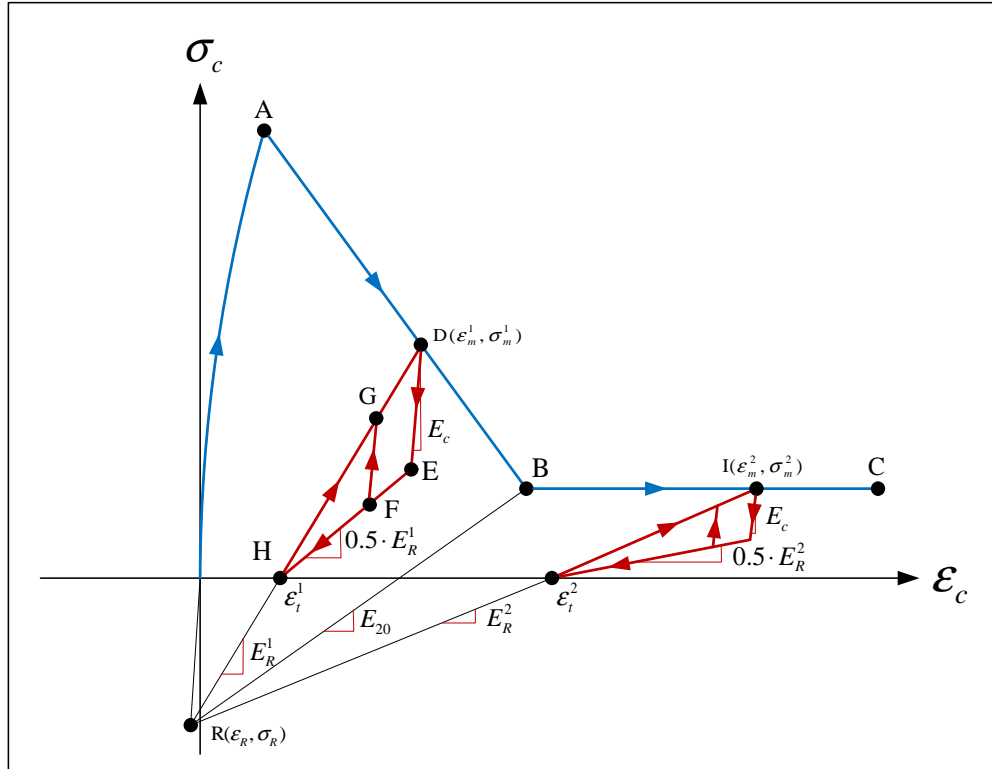


Figure 2.17: Concrete material model under cyclic loading in compression  
(?)

- Maximum envelope (line HD)

$$\sigma_{max} = \sigma_m + E_R \cdot (\varepsilon_c - \varepsilon_m) \quad (2.35)$$

- Minimum envelope (line HE)

$$\sigma_{min} = 0.5 \cdot E_R \cdot (\varepsilon_c - \varepsilon_t) \quad (2.36)$$

where,

$$\begin{aligned} E_R &= \frac{\sigma_m - \sigma_R}{\varepsilon_m - \varepsilon_R} \\ \varepsilon_t &= \varepsilon_m - \frac{\sigma_m}{E_R} \end{aligned} \quad (2.37)$$

$\sigma_m$  and  $\varepsilon_m$  are the stress and strain at the unloading point on the compressive monotonic envelope, respectively. Therefore, the positions of the two smaller envelopes depend on the position of the unloading point. For partial loading and unloading cycles within the smaller envelopes the model follows straight line with modulus  $E_c$ .

In the numerical implementation a trial stress and tangent modulus are assumed based on linear elastic behavior with slope  $E_c$ ,

$$\sigma_{c,n}^{tr} = \sigma_{c,n-1} + E_c \cdot \Delta\varepsilon_{c,n} \quad (2.38)$$

where  $\sigma_{c,n}^{tr}$  is the updated trial stress,  $\sigma_{c,n-1}$  is the previous stress state and  $\Delta\varepsilon_{c,n}$  is the strain increment. The following rules are then used to determine actual stress and modulus of the model

$$\begin{aligned} \text{if } \sigma_{min} \leq \sigma_{c,n}^{tr} \leq \sigma_{max} \text{ then } \sigma_{c,n} = \sigma_{c,n}^{tr} \text{ and } E^{tan} = E_c \\ \text{if } \sigma_{c,n}^{tr} < \sigma_{min} \text{ then } \sigma_{c,n} = \sigma_{min} \text{ and } E^{tan} = 0.5 \cdot E_R \\ \text{if } \sigma_{c,n}^{tr} > \sigma_{max} \text{ then } \sigma_{c,n} = \sigma_{max} \text{ and } E^{tan} = E_R \end{aligned} \quad (2.39)$$

The rules governing the hysteretic behavior of the model in compression according to Eq. 2.34 to 2.39 are illustrated by a sample history in Fig. 2.17. If unloading occurs from point D to point E, reloading will be on the same path back to D. If unloading reaches point F, the hysteresis loop DEFGD will result upon reloading. If complete unloading to point H occurs, reloading will result in the hysteresis loop DEHD. It is important to note that the reloading line will always rejoin the compression monotonic envelope at the point of initial unloading. For the case when unloading continues past point H and the model starts reloading in tension, a different set of rules govern the hysteretic behavior. However upon reloading in compression, the model will reenter the compression region at the point on the zero stress axis at the completion of unloading (point H) and whatever happens in the tension region will not affect the behavior of the model, once it returns to the compression region.

The tensile behavior of the model, as shown in Fig. 2.18, takes into account tension stiffening and the degradation of the unloading and reloading stiffness for increasing values of maximum tensile strain after initial cracking. The maximum tensile strength of the concrete (modulus of rupture) is assumed equal to,

$$f_t = 0.6228\sqrt{f_c} \quad (2.40)$$

where  $f_t$  and  $f_c$  are expressed in MPa.

Fig. 2.18 shows two consecutive tensile hysteresis loops which are part of a sample cyclic history that also include compressive stresses. The model assumes that tensile stress can occur anywhere along the strain axis, either as a result of initial tensile loading or as a result of unloading from a compressive state. In the latter case a tensile stress occurs under a compressive strain. The tensile stress-strain relation is defined by three points with coordinates  $(\varepsilon_t, 0)$ ,  $(\varepsilon_{tp}, \sigma_{tp})$  and  $(\varepsilon_u, 0)$ , as represented by points J, K and M in Fig. 2.18, respectively.  $\varepsilon_t$  is the strain at the point where the unloading line from the compressive stress region crosses the strain axis.  $\varepsilon_t$  is given by Eq. 2.37 and changes with maximum compressive strain.  $\varepsilon_{tp}$  and  $\sigma_{tp}$  are the strain and stress at the peak of the tensile stress-strain relation and are given by the following expressions,

$$\begin{aligned} \varepsilon_{tp} &= \varepsilon_t + \Delta\varepsilon_t \\ \sigma_{tp} &= f_t \cdot \left(1 + \frac{E_t}{E_c}\right) - E_t \cdot \Delta\varepsilon_t \end{aligned} \quad (2.41)$$

where  $\Delta\varepsilon_t$  is the previous maximum differential between tensile strain and  $\varepsilon_t$  as shown in Fig. 2.18. Before initial cracking,  $\Delta\varepsilon_t$  is equal to  $f_t/E_c$ .  $E_t$  is the slope of the softening branch of concrete in tension (typically  $-1/10$  to  $-1/5$

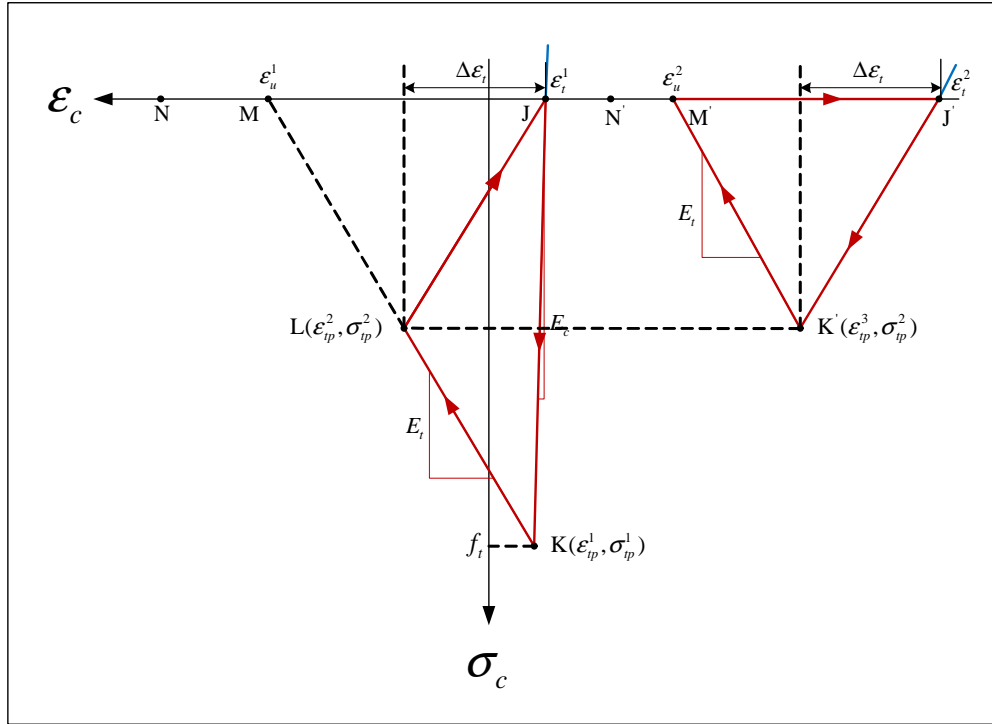


Figure 2.18: Concrete material model under cyclic loading in tension  
(?)

of  $E_c$ ),  $\varepsilon_u$  is the strain at the point where the tensile stress is reduced to zero and is given by the expression,

$$\varepsilon_u = \varepsilon_t + f_t \cdot \left( \frac{1}{E_t} + \frac{1}{E_c} \right) \quad (2.42)$$

Given these three control points, the tensile stress-strain relation and tangent moduli are defined by the following equations (tension is positive),

- Segment JK:  $\varepsilon_t < \varepsilon_c \leq \varepsilon_{tp}$

$$\sigma_c = E^{tan} \cdot (\varepsilon_c - \varepsilon_t), \quad E^{tan} = \frac{\sigma_{tp}}{\varepsilon_{tp} - \varepsilon_t} \quad (2.43)$$

- Segment KM:  $\varepsilon_{tp} < \varepsilon_c \leq \varepsilon_u$

$$\sigma_c = \sigma_{tp} + E^{tan} \cdot (\varepsilon_c - \varepsilon_{tp}), \quad E^{tan} = -E_t \quad (2.44)$$

- Segment MN:  $\varepsilon_c > \varepsilon_u$

$$\sigma_c = 0, \quad E^{tan} = 0 \quad (2.45)$$

If  $\varepsilon_{tp} \geq \varepsilon_u$  then  $\sigma_{tp}$ ,  $\sigma_c$  and  $E^{tan}$  are all assumed to be zero. The modulus  $E_t$  controls the degree of tension stiffening by controlling the slope of Eq. 2.44. The steeper the slope, the smaller will be the effect of tension stiffening. Tensile unloading and reloading are governed by Eq. 2.43 which also includes stiffness degradation for increasing values of strain differential  $\Delta\varepsilon_t$ . The value of  $\Delta\varepsilon_t$  changes whenever  $\varepsilon_c - \varepsilon_{tp}$ .

The tensile behavior of the model, as characterized by Eq. 2.40 to 2.45, can be better understood by following the example load paths in Fig. 2.18. As the model unloads from compression, it crosses the strain axis at the point J. It then loads in tension until initial cracking occurs at point K. Beyond point K softening commences until the strain reversal point L. The unloading path follows a straight line from point L to point J where the model reloads in compression. The second time the model goes into tension is at point J'. The reloading path J'K' is exactly the duplication of the previous unloading path LJ that has been shifted a distance JJ' along the strain axis. At point K' the model rejoins the softening branch which continues until the tensile stress is reduced to zero at point M'. The stress remains zero through the strain reversal point N' until the model reloads in compression at point J'. Henceforth,

the tensile stress capacity of the model is reduced to zero.

The present concrete model is relatively economical in terms of the amount of memory required of the past stress-strain history. The parameters that are used as memory can be listed as follows:

1. the stress and strain at the point corresponding to the last model state
2. the strain at the last unloading point on the compressive monotonic envelope,  $\varepsilon_m$
3. The differential  $\Delta\varepsilon_t$  between maximum previous tensile strain and  $\varepsilon_t$

The concrete damage considered in the present model is in the form of unloading and reloading stiffness degradation for increasing values of maximum strain. But actual concrete damage also includes the reduction of the monotonic envelopes under cyclic loading.

### 2.2.1.1.2 Data preparation for modified Kent and Park model

Listing 2.1: Data Preparation for Modified Kent and Park Model

```

1  %% Modified Kent and Park Model for CORE CONCRETE
2  clear
3  clc
4  %
5  %
6  %% User input data
7  % Units 1: MPa; 2 ksi
8  units=2;
9  % concrete compressive strength
10 f_c_unconfined = 5;
11 %
12 fys = 60;      %Yield strength of stirrups
13 f_y = 1.25*fys; %To account for rate effect
14 %
15 b = 14;        %Member width (in)
16 d = 20;        %Member height (in)
17 L = 12*13.5;   %Member length
18 cover = 2;     %Cover to stirrup
19 sh = 12;        %Center to center spacing of stirrups
20 stirrup_dia = 3/8; %in
21 n_stirrup = 15; %Number shear reinforcing bars in member
22 %
23 %
24 % Compute intermediary values
25 A_core = (b-2*cover)*(d-2*cover); %in^2
26 P_core = 2*((b-2*cover) + 2*(d-2*cover)); %Perimeter of core approx. equal to length of single stirrup
27 V_stirrup = n_stirrup*(pi/4*stirrup_dia)^2*P_core); %Total volume of shear reinforcement
28 rhos = V_stirrup/(A_core*L); %Ratio of volume of shear reinforcement to volume of
29 %concrete core measured to outside of stirrups
30 h = d-2*cover; %width of concrete core measured to outside of stirrups
31 %
32 % Compute parameters
33 lambda = 0.3; %Ratio of unloading slope at epsilon_c to slope E0, Default value 0.3
34 % Factor to account for strength increase due to confinement
35 K = 1 + (rhos*f_y)/f_c_unconfined;
36 % Controls the descending branch of the compressive stress strain curve
37 switch units
38   case 1 % MPa
39     Z = 0.5/(((3+0.29*f_c_unconfined)/(0.145*f_c_unconfined - 1))+(0.75*rhos*sqrt(h/sh))-0.002*K); %Strain softening slope
40   case 2 % psi
41     Z = 0.5/(((3+0.29*f_c_unconfined/0.145)/(f_c_unconfined - 1))+(0.75*rhos*sqrt(h/sh))-0.002*K); %Strain softening slope
42 end
43 %
44 % Compressive strain corresponding to peak stress in compression CONFINED
45 epsilon_0_unconfined=0.003;
46 epsilon_0_confined = 0.002*K;
47 % Peak stress in CONFINED concrete
48 f_c_c_confined = K*f_c_unconfined;
49 % Ultimate strain in compression
50 f_c_20_unconfined=f_c_unconfined/3;
51 f_c_20_confined=0.2*f_c_c_confined;
52 epsilon_20_unconfined = epsilon_0_unconfined+(K*f_c_unconfined-f_c_20_unconfined)/(Z*K*f_c_unconfined );
53 epsilon_20_unconfined = 3*epsilon_0_unconfined;
54 % Initial E in compression (same for confined and unconfined concrete)
55 E_0_unconfined=2*f_c_unconfined/epsilon_0_unconfined;
56 E_0_confined=2*f_c_c_confined/epsilon_0_confined;
57 %
58 % Initial E in tension
59 E_t_unconfined=E_0_unconfined/5;
60 E_t_confined=E_0_confined/5;
61 %
62 % Tensile strength
63 switch units
64   case 1 % MPa
65     sigma_t_unconfined=0.6228*sqrt(f_c_unconfined);
66     sigma_t_confined=0.6228*sqrt(f_c_c_confined);
67   case 2 % psi
68     sigma_t_unconfined = 7.5*sqrt(f_c_unconfined*1000);
69     sigma_t_confined = 7.5*sqrt(f_c_c_confined*1000);
70 end
71 %
72 fid=fopen('Concrete-Properties.out','w+');
73 fprintf(fid,' Preparation of Concrete input data in Mercury\n');
74 fprintf(fid,' for the Modified Kent and Park Model\n\n');
75 switch units
76   case 1
77     fprintf(fid,' Units MPa\n\n')
78   case 2
79     fprintf(fid,' Units Ksi\n\n')

```

```

78 end
79 fprintf(fid , ' UNCONFINED CONCRETE\n\n');
80 fprintf(fid , ' Intial tangent modulus in tension.....%8.2f\n', E_t_unconfined);
81 fprintf(fid , ' Confined compressive strength.....%8.2f\n', f_c_unconfined);
82 fprintf(fid , ' Peak strain in compression .....%8.2f\n', -epsilon_0_unconfined);
83 fprintf(fid , ' Strain at 20 percent of peak stress....%8.2f\n', -epsilon_20_unconfined);
84 fprintf(fid , ' Stress at 20 percent of peak stress....%8.2f\n', -f_c_20_unconfined);
85 fprintf(fid , ' Tensile strength .....%8.2f\n', sigma_t_unconfined);
86 fprintf(fid , ' Coefficient Lambda.....%8.2f\n', lambda);
87
88 fprintf(fid , ' CONFINED CONCRETE\n\n');
89 fprintf(fid , ' Intial tangent modulus in tension.....%8.2f\n', E_t_confined);
90 fprintf(fid , ' Confined compressive strength.....%8.2f\n', f_c_confined);
91 fprintf(fid , ' Peak strain in compression .....%8.2f\n', -epsilon_0_confined);
92 fprintf(fid , ' Strain at 20 percent of peak stress....%8.2f\n', -epsilon_20_confined);
93 fprintf(fid , ' Stress at 20 percent of peak stress....%8.2f\n', -f_c_20_confined);
94 fprintf(fid , ' Tensile strength .....%8.2f\n', sigma_t_confined);
95 fprintf(fid , ' Coefficient Lambda.....%8.2f\n', lambda);
96 fclose(fid)

```

**2.2.1.1.3 Determination for modified Kent and Park model** Fig. 2.19 and 2.20 show the procedure to obtain uniaxial stress  $\sigma$  and tangent modulus  $E^{tan}$  from uniaxial strain  $\varepsilon$ .

## 2.2.2 “Exact” Models

### 2.2.2.1 Anisotropic damage model with effective damage and stiffness recovery

Whereas the modified Kent-Park model has been successfully used in many applications, it remains a heuristic empirical model which accurate performance may not be assured within the context of real-time hybrid simulation with limited number of iterations. To address this possible handicap amore, rigorous and thermodynamically correct constitutive model for concrete is implemented<sup>2</sup>. Such a model was developed by ?.

#### 2.2.2.1.1 Constitutive model

**Thermodynamic potential** The Gibbs potential  $\rho \cdot \phi^*$  is based on the Ladeveze's framework (?) for anisotropic damage model. The splitting of the stress tensor into deviatoric and hydrostatic components allows us to consider separately the shear and the hydrostatic parts. Furthermore, each component is again splitted into two additional ones: the positive and the negative in order to model the unilateral effect, Fig. 2.21. The damage influences only the positive part through the damage tensor  $\mathbf{D}$ .

$$\rho \cdot \phi^* = \frac{1 + \nu}{2 \cdot E} \left[ \text{Tr} \left( \mathbf{H} \cdot \boldsymbol{\sigma}_+^D \mathbf{H} \cdot \boldsymbol{\sigma}_+^D \right) + \text{Tr} \left( \langle \boldsymbol{\sigma}^D \rangle_- \langle \boldsymbol{\sigma}^D \rangle_- \right) \right] + \frac{1 - 2\nu}{6 \cdot E} \left[ \frac{\langle \text{Tr} \boldsymbol{\sigma} \rangle_+^2}{1 - D_H} + \langle \text{Tr} \boldsymbol{\sigma} \rangle_-^2 \right] \quad (2.46)$$

where  $\rho$ ,  $\nu$  and  $E$  are respectively the density, the Poisson's ratio and Young modulus. The tensor  $\mathbf{H}$  is defined by

$$\mathbf{H} = (\mathbf{1} - \mathbf{D})^{\frac{1}{2}}$$

where  $(\cdot)^D$  is the deviatoric of  $(\cdot)$ ,

$$(\cdot)^D = (\cdot) - \frac{1}{3} \text{Tr}(\cdot) \cdot \mathbf{1}$$

$\langle \cdot \rangle_{+,-}$  is the positive or negative part of  $(\cdot)$ , and  $D_H$  is the hydrostatic part of  $\mathbf{D}$ ,

$$D_H = \frac{1}{3} \text{Tr} \mathbf{D}$$

In Ladeveze's framework (?),  $\boldsymbol{\sigma}_+^D$  is an unusual positive part of  $\boldsymbol{\sigma}^D$ : if  $\lambda_I$  are the eigenvalues of  $\mathbf{H}\boldsymbol{\sigma}^D$  and  $\mathbf{T}^I$  the corresponding eigenvectors,  $\boldsymbol{\sigma}_+^D$  is

$$\boldsymbol{\sigma}_+^D = \sum_I \langle \lambda_I \rangle_+ \left( \mathbf{H}^{-1} \cdot \mathbf{T}^I \right) \left( \mathbf{H}^{-1} \cdot \mathbf{T}^I \right)^T$$

---

<sup>2</sup>Implementation of this model was made possible through the collaboration of Prof. Ragueneau and Mr. Lebon from ENS/Cachen

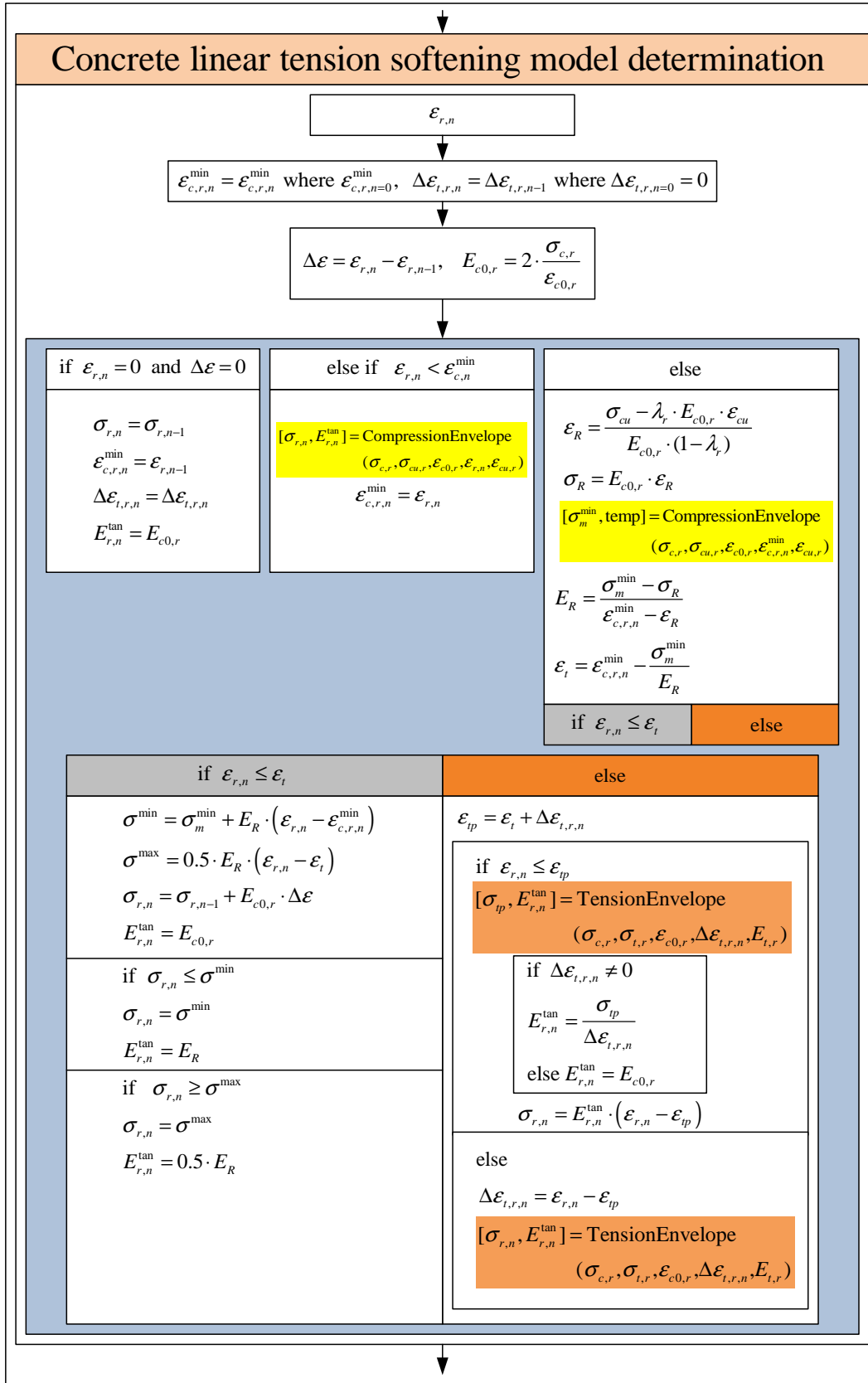


Figure 2.19: Determination (1) for modified Kent and Park model

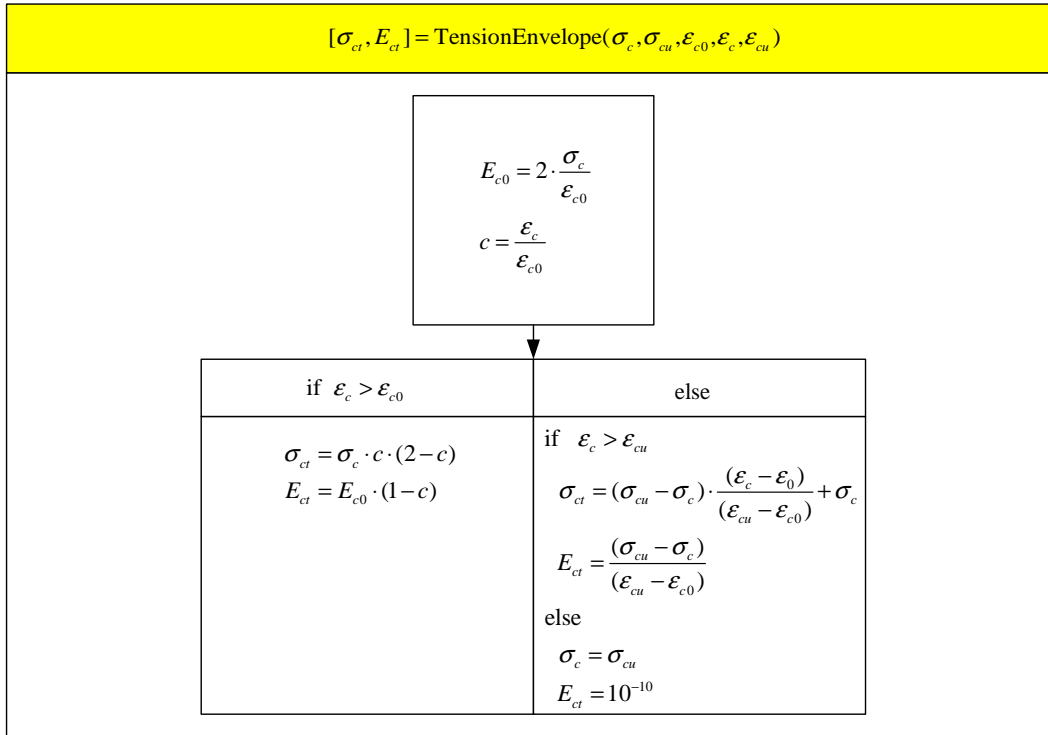
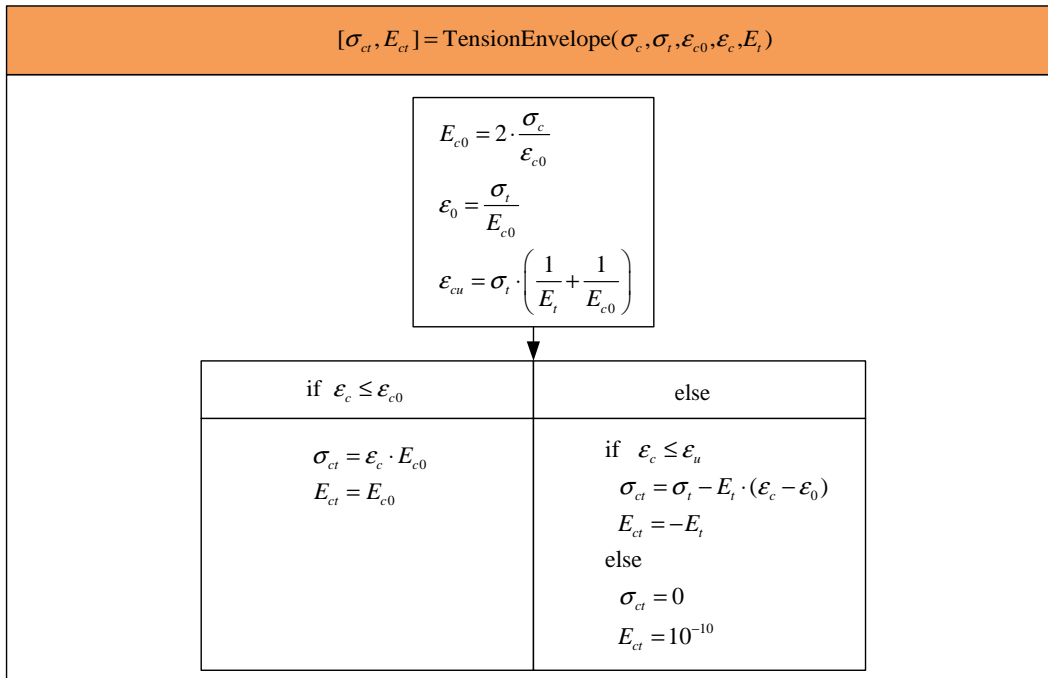


Figure 2.20: Determination (2) for modified Kent and Park model

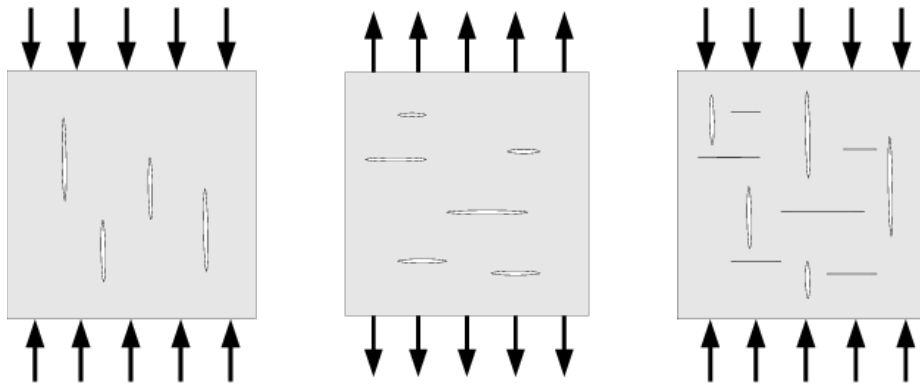


Figure 2.21: Cracks induced by compression, tension, tension and compression

**Constitutive law** The constitutive law is derived from Gibbs potential using Eq. 2.46:

$$\begin{aligned}\boldsymbol{\varepsilon} &= \rho \cdot \frac{\partial \phi^*}{\partial \boldsymbol{\sigma}} \\ &= \frac{1+\nu}{E} \left[ (\mathbf{H} \cdot \boldsymbol{\sigma}_+^D \mathbf{H})^D + \langle \boldsymbol{\sigma}^D \rangle_-^D \right] + \frac{1-2\nu}{3 \cdot E} \left[ \frac{\langle \text{Tr}(\boldsymbol{\sigma}) \rangle_+}{1-D_H} + \langle \text{Tr}(\boldsymbol{\sigma}) \rangle_- \right] \cdot \mathbf{I} \\ &= \frac{1+\nu}{E} \cdot \tilde{\boldsymbol{\sigma}} - \frac{\nu}{E} \cdot \text{Tr}(\tilde{\boldsymbol{\sigma}}) \cdot \mathbf{I}\end{aligned}$$

where  $\tilde{\boldsymbol{\sigma}}$  is the effective stress obtained by rewriting the stress strain law in terms of the effective stress:

$$\tilde{\boldsymbol{\sigma}} = \left[ (\mathbf{H} \cdot \boldsymbol{\sigma}_+^D \mathbf{H})^D + \langle \boldsymbol{\sigma}^D \rangle_-^D \right] + \left[ \frac{\langle \text{Tr}(\boldsymbol{\sigma}) \rangle_+}{1-D_H} + \langle \text{Tr}(\boldsymbol{\sigma}) \rangle_- \right] \cdot \mathbf{I}$$

**Damage evolution law** The damage evolution law should account for cyclic loading. Hence, the damage criterion  $f$  should depend on an effective damage  $d_\varepsilon$  (?) such that

$$\begin{aligned}f &= \hat{\varepsilon} - \kappa(d_\varepsilon) \\ d_\varepsilon &= \frac{\mathbf{D} : \langle \boldsymbol{\varepsilon} \rangle_+}{\max(\langle \boldsymbol{\varepsilon} \rangle_I)}\end{aligned}$$

where  $\hat{\varepsilon}$  is Mazars strain defined by

$$\hat{\varepsilon} = \sqrt{\langle \boldsymbol{\varepsilon} \rangle_+ : \langle \boldsymbol{\varepsilon} \rangle_+}$$

and  $\kappa$  the consolidation function,

$$\kappa(d_\varepsilon) = a \cdot \tan \left[ \frac{d_\varepsilon}{aA} + \arctan \left( \frac{\kappa_0}{a} \right) \right]$$

where  $A$  and  $a$  are two damage coefficients, and  $\kappa_0$  is initial elasticity threshold.

Thus, if the damage criterion is negative, the material is in the linear elastic range, and if it is positive, the damage increases along the positive strain:

$$\dot{\mathbf{D}} = \dot{\lambda} \langle \boldsymbol{\varepsilon} \rangle_+$$

where the damage Lagrange multiplier  $\dot{\lambda}$  is determined from the Kuhn-Tucker condition ( $f = 0$  and  $f' = 0$ ).

**2.2.2.1.2 Uniaxial multi-fiber formulation** Multi-fiber formulation based on Euler-Bernoulli beam theory is equivalent to a uniaxial loading. Hence, the stress tensor and the strain tensor are reduced to

$$\boldsymbol{\sigma} = \begin{pmatrix} \sigma_{11} & 0 & 0 \\ 0 & 0 & 0 \\ 0 & 0 & 0 \end{pmatrix}$$

and,

$$\boldsymbol{\epsilon} = \begin{pmatrix} \varepsilon_{11} & 0 & 0 \\ 0 & \varepsilon_{22} & 0 \\ 0 & 0 & \varepsilon_{33} \end{pmatrix}$$

The damage tensor becomes diagonal and the constitutive law can be rewritten as (?),

$$\boldsymbol{\sigma} = \mathbf{B}(D_1, D_2) \cdot \frac{\boldsymbol{\sigma}}{E} \quad (2.47)$$

where  $\mathbf{B}$  is a diagonal tensor which depends on the damage variable and loading, and  $D_1$  and  $D_2$  are associated with tension and compression damage respectively.

Rewriting Eq. 2.47 with matrix form,

$$\boldsymbol{\sigma} = \begin{pmatrix} \sigma & 0 & 0 \\ 0 & 0 & 0 \\ 0 & 0 & 0 \end{pmatrix} \boldsymbol{\epsilon} = \begin{pmatrix} \epsilon_1 & 0 & 0 \\ 0 & \epsilon_2 & 0 \\ 0 & 0 & \epsilon_2 \end{pmatrix} \mathbf{D} = \begin{pmatrix} D_1 & 0 & 0 \\ 0 & D_2 & 0 \\ 0 & 0 & D_2 \end{pmatrix}$$

so

$$\boldsymbol{\sigma}^D = \begin{pmatrix} \frac{2\sigma}{3} & 0 & 0 \\ 0 & \frac{-1\sigma}{3} & 0 \\ 0 & 0 & \frac{-1\sigma}{3} \end{pmatrix} \mathbf{H} = \begin{pmatrix} \frac{1}{\sqrt{1-D_1}} & 0 & 0 \\ 0 & \frac{1}{\sqrt{1-D_2}} & 0 \\ 0 & 0 & \frac{1}{\sqrt{1-D_2}} \end{pmatrix}$$

$$\text{Tr}(\boldsymbol{\sigma}) = \sigma \quad D_H = D_1 + 2D_2$$

$$\epsilon_e = \frac{1+\nu}{E} \left( (\mathbf{H} \boldsymbol{\sigma}_+^D \mathbf{H})^D + \boldsymbol{\sigma}_-^D \right) + \frac{1-2\nu}{3E} \left[ \frac{\langle \text{Tr}(\boldsymbol{\sigma}) \rangle_+}{1-D_H} + \frac{\langle \text{Tr}(\boldsymbol{\sigma}) \rangle_-}{1-D_H} \right] \mathbf{Id}$$

For tension ( $\sigma > 0$ ), we assume that only  $D_1$  increases.

$$\begin{aligned} \boldsymbol{\epsilon}_e &= \begin{pmatrix} \epsilon_1 & 0 \\ 0 & \epsilon_2 \end{pmatrix} = \frac{\sigma}{E} \mathbf{B}^t = \frac{\sigma}{E} \begin{pmatrix} B_1^t & 0 \\ 0 & B_2^t \end{pmatrix} \\ B_1^t &= \frac{1+\nu}{9} \left( \frac{4}{1-D_1} + \frac{2}{1-D_2} \right) + \frac{1-2\nu}{3} \frac{1}{1-(D_1+2D_2)} \\ B_2^t &= \frac{1+\nu}{9} \left( \frac{-2}{1-D_1} - \frac{1}{1-D_2} \right) + \frac{1-2\nu}{3} \frac{1}{1-(D_1+2D_2)} \end{aligned}$$

For compression ( $\sigma < 0$ ), we assume that only  $D_2$  increases.

$$\begin{aligned} \boldsymbol{\epsilon}_e &= \begin{pmatrix} \epsilon_1 & 0 \\ 0 & \epsilon_2 \end{pmatrix} = \frac{\sigma}{E} \mathbf{B}^c = \frac{\sigma}{E} \begin{pmatrix} B_1^c & 0 \\ 0 & B_2^c \end{pmatrix} \\ B_1^c &= \frac{1+\nu}{9} \left( \frac{4}{1-D_1} + \frac{2}{1-D_2} \right) + \frac{1-2\nu}{3} \\ B_2^c &= \frac{1+\nu}{9} \left( \frac{-2}{1-D_1} - \frac{1}{1-D_2} \right) + \frac{1-2\nu}{3} \end{aligned}$$

### 2.2.2.1.3 Determination for anisotropic damage model

#### 2.2.2.1.3.1 Tension loading: $\varepsilon_{11} > 0$

- Constitutive equations

If  $f = \hat{\varepsilon} - \kappa_0 \geq 0$  and  $\eta_t = 1$  then:

$$\begin{aligned} \sigma &= \frac{E}{B_{11}^t} \epsilon \\ \sigma &= \frac{E}{\frac{1+\nu}{9} \cdot \left( \frac{4}{1-D_1} + 2 \right) + \frac{1-2\nu}{3} \left( 1 - \frac{D_1+2D_2}{3} \right)} \cdot \varepsilon \\ D_1 &= a \cdot A \left( \text{atan} \left( \frac{\varepsilon_{11}}{a} \right) - \text{atan} \left( \frac{\kappa_0}{a} \right) \right) \end{aligned} \quad (2.48)$$

where,  $\hat{\varepsilon} = \sqrt{\langle \boldsymbol{\varepsilon} \rangle_+ : \langle \boldsymbol{\varepsilon} \rangle_+} = \varepsilon_{11} \geq 0$ ,

$$\langle \boldsymbol{\varepsilon} \rangle_+ = \begin{pmatrix} \varepsilon_{11} & 0 & 0 \\ 0 & 0 & 0 \\ 0 & 0 & 0 \end{pmatrix}$$

$D_2$  is constant and tangent modulus is determined with Eq. 2.48:

$$\dot{\sigma} = E^{tan} \cdot \dot{\varepsilon} \quad (2.49)$$

However, if  $f = \hat{\varepsilon} - \kappa_0 < 0$ , the tangent modulus is equal to the secant one.

$$E^{tan} = \frac{E}{B_{11}^t}$$

- Coherent tangent stiffness modulus in numerical implementation

If  $f = \hat{\varepsilon} - \kappa_0 \geq 0$  and  $\eta_t = 1$ , tangent modulus is determined with Eq. 2.48 and 2.49:

$$\begin{aligned} E_n^{tan} &= \frac{\partial \sigma_n}{\partial \varepsilon_n} \\ B_{11,n}^t &= \frac{1+\nu}{9} \cdot \left( \frac{4}{1-D_{1,n}} + 2 \right) + \frac{1-2\nu}{3 \cdot \left( 1 - \frac{(D_{1,n}+2 \cdot D_{2,n-1})}{3} \right)} \\ D_{1,n} &= a \cdot A \left( \text{atan} \left( \frac{\varepsilon_{11,n}}{a} \right) - \text{atan} \left( \frac{\kappa_0}{a} \right) \right) \end{aligned}$$

where n is current excitation step.

$$\frac{\partial \sigma_n}{\partial \varepsilon_n} = \frac{\partial}{\partial \varepsilon_n} \left( \frac{E}{B_{11,n}^t} \cdot \varepsilon_n \right) = \frac{E}{B_{11,n}^t} - E \cdot \varepsilon_n \frac{1}{(B_{11,n}^t)^2} \cdot \frac{\partial B_{11,n}^t}{\partial \varepsilon_n}$$

where,

$$\begin{aligned} \frac{\partial B_{11,n}^t}{\partial \varepsilon_n} &= \frac{\partial B_{11,n}^t}{\partial D_{1,n}} \cdot \frac{\partial D_{1,n}}{\partial \varepsilon_n} \\ C_1 &= \frac{\partial B_{11,n}^t}{\partial D_{1,n}} = \frac{1+\nu}{9} \cdot \frac{4}{(1-D_{1,n})^2} + \frac{1-2\nu}{9 \left( 1 - \frac{D_{1,n}+2D_{2,n-1}}{3} \right)} \\ C_2 &= \frac{\partial D_{1,n}}{\partial \varepsilon_n} = \frac{\partial}{\partial \varepsilon_n} \left( a \cdot A \left( \text{atan} \left( \frac{\varepsilon_n}{a} \right) - \text{atan} \left( \frac{\kappa_0}{a} \right) \right) \right) = \frac{A}{1 + \left( \frac{\varepsilon_n}{a} \right)^2} \end{aligned}$$

Finally, we obtain tangent modulus:

$$E_n^{tan} = \frac{E}{B_{11,n}^t} - E \cdot \varepsilon_n \cdot \frac{1}{(B_{11,n}^t)^2} \cdot C_1 \cdot C_2$$

### 2.2.2.1.3.2 Compressive loading: $\varepsilon_{11} < 0$

- Constitutive equations

If  $f = \hat{\varepsilon} - \kappa_0 \geq 0$  and  $\eta_t = 1$  then:

$$\begin{aligned} \sigma &= \frac{E}{\frac{1+\nu}{9} \cdot \left( \frac{2}{1-D_2} + 4 \right) + \frac{1-2\nu}{3}} \cdot \varepsilon \\ D_2 &= \frac{a \cdot A}{2} \left( \text{atan} \left( \frac{\sqrt{2} \cdot \varepsilon_{22}}{a} \right) - \text{atan} \left( \frac{\kappa_0}{a} \right) \right) \\ \varepsilon_{22} &= \frac{B_{22}^c}{B_{11}^c} \cdot \varepsilon_{11} \end{aligned} \quad (2.50)$$

where,  $\hat{\varepsilon} = \sqrt{\langle \boldsymbol{\varepsilon} \rangle_+ : \langle \boldsymbol{\varepsilon} \rangle_+} = \sqrt{2 \cdot \varepsilon_{22}^2} \geq 0$ ,

$$\langle \boldsymbol{\varepsilon} \rangle_+ = \begin{pmatrix} 0 & 0 & 0 \\ 0 & \varepsilon_{22} & 0 \\ 0 & 0 & \varepsilon_{33} = \varepsilon_{22} \end{pmatrix}$$

$D_1$  is constant and tangent modulus is determined with Eq. 2.50:

$$\dot{\sigma} = E^{tan} \cdot \dot{\varepsilon} \quad (2.51)$$

However, if  $f = \hat{\varepsilon} - \kappa_0 < 0$ , the tangent modulus is equal to the secant one.

$$E^{tan} = \frac{E}{B_{11}^c}$$

- Coherent tangent stiffness modulus in numerical implementation

If  $f = \hat{\varepsilon} - \kappa_0 \geq 0$  and  $\eta_t = 1$ , tangent modulus is determined with Eq. 2.50 and 2.51:

$$\begin{aligned} E_n^{tan} &= \frac{\partial \sigma_n}{\partial \varepsilon_n} \\ B_{11,n-1}^c &= \frac{1+\nu}{9} \cdot \left( 4 + \frac{2}{1-D_{2,n-1}} \right) + \frac{1-2\nu}{3} \\ B_{22,n-1}^c &= -\frac{1+\nu}{9} \cdot \left( 2 + \frac{1}{1-D_{2,n-1}} \right) + \frac{1-2\nu}{3} \\ B_{11,n}^c &= \frac{1+\nu}{9} \cdot \left( 4 + \frac{2}{1-D_{2,n}} \right) + \frac{1-2\nu}{3} \\ B_{22,n}^c &= -\frac{1+\nu}{9} \cdot \left( 2 + \frac{1}{1-D_{2,n}} \right) + \frac{1-2\nu}{3} \end{aligned}$$

where n is current excitation step.

$$\begin{aligned} \tilde{\nu}_{n-1} &= -\frac{B_{22,n-1}^c}{B_{11,n-1}^c}, \quad \varepsilon_{22,n}^{tr} = -\tilde{\nu}_{n-1} \cdot \varepsilon_{11,n} \\ \tilde{\nu}_n &= -\frac{B_{22,n}^c}{B_{11,n}^c}, \quad \varepsilon_{22,n} = -\tilde{\nu}_n \cdot \varepsilon_{11,n} \end{aligned}$$

where,  $\varepsilon_{22,n}^{tr}$  is trial strain on  $\varepsilon_{22}$ .

$$\frac{\partial \sigma_n}{\partial \varepsilon_n} = \frac{\partial}{\partial \varepsilon_n} \left( \frac{E}{B_{11,n}^c} \cdot \varepsilon_n \right) = \frac{E}{B_{11,n}^c} - E \cdot \varepsilon_n \frac{1}{(B_{11,n}^c)^2} \cdot \frac{\partial B_{11,n}^c}{\partial \varepsilon_n}$$

where,

$$\begin{aligned} \frac{\partial B_{11,n}^c}{\partial \varepsilon_n} &= \frac{\partial B_{11,n}^c}{\partial D_{2,n}} \cdot \frac{\partial D_{2,n}}{\partial \varepsilon_n} \\ C_1 &= \frac{\partial B_{11,n}^c}{\partial D_{2,n}} = \frac{2(1+\nu)}{9(1-D_{2,n})^2} \\ C_2 &= \frac{\partial D_{2,n}}{\partial \varepsilon_n} = \frac{\partial}{\partial \varepsilon_n} \left( a \cdot A \left( \text{atan} \left( \frac{-\tilde{\nu}_{n-1} \cdot \sqrt{2} \cdot \varepsilon_{11,n}}{a} \right) - \text{atan} \left( \frac{\kappa_0}{a} \right) \right) \right) \\ &= -\tilde{\nu}_{n-1} \frac{A}{\sqrt{2}} \cdot \frac{1}{1 + \left( \frac{-\tilde{\nu}_{n-1} \cdot \sqrt{2} \cdot \varepsilon_{11,n}}{a} \right)^2} \end{aligned}$$

Finally, we obtain tangent modulus:

$$E_n^{tan} = \frac{E}{B_{11,n}^c} - E \cdot \varepsilon_n \cdot \frac{1}{(B_{11,n}^c)^2} \cdot C_1 \cdot C_2$$

Fig. 2.22 describes the relationship between strain and stress in anisotropic damage model without permanent strain.

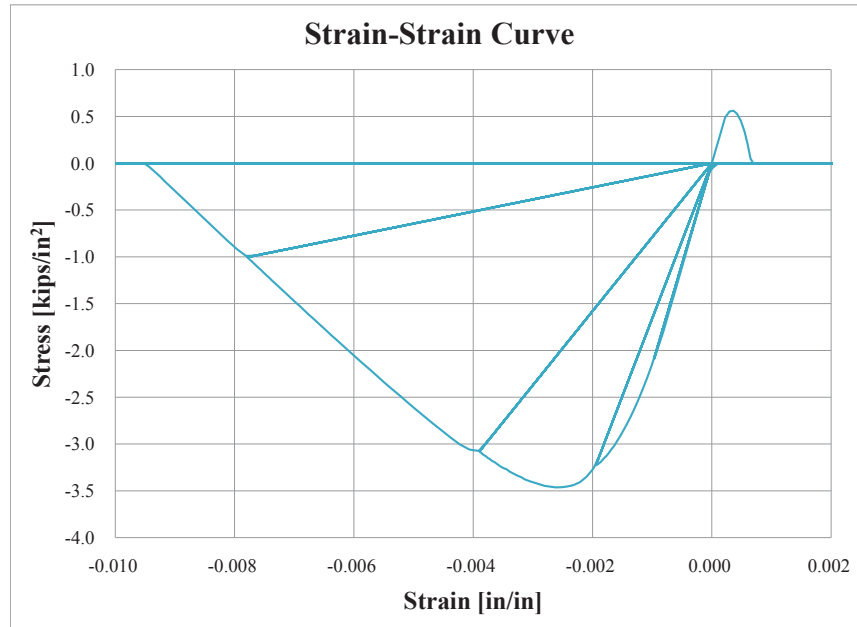


Figure 2.22: Strain-stress curve for anisotropic damage model without permanent strain

Fig 2.23 to 2.25 show the procedure to obtain uniaxial stress  $\sigma$  and tangent modulus  $E^{tan}$  from uniaxial strain  $\varepsilon$ .

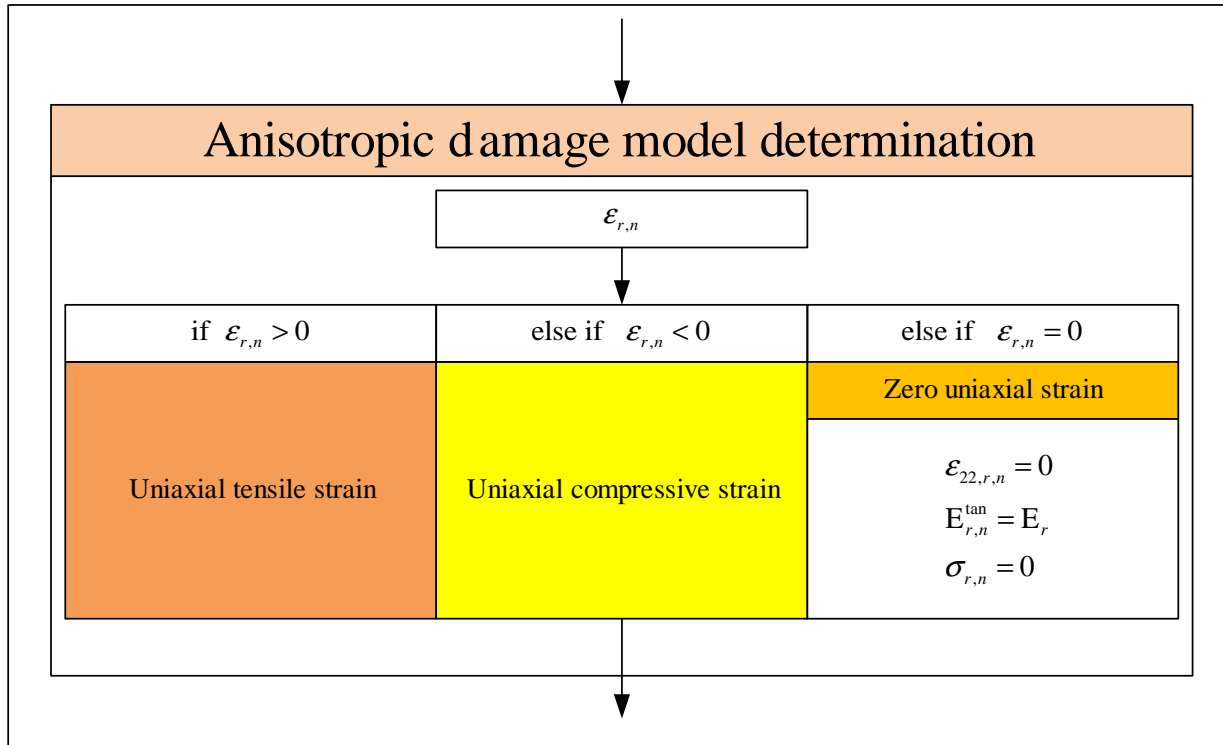


Figure 2.23: Determination (1) for the anisotropic damage model

### 2.2.2.2 Anisotropic damage model with effective damage, stiffness recovery and permanent strains $\epsilon_{an}$

The proceeding anisotropic damage model did not account for permanent deformations. The following extension of the model shell address this limitation.

This model is based on the anisotropic damage model  $\psi_e^*$  previously identified as  $\psi^*$ .

$$\rho\psi^* = \rho\psi_e^* + \rho\psi_{an}^* \quad (2.52)$$

For the damaged part of the model, the consolidation function is altered to take into consideration the elastic feedback in compression:

$$\kappa(d_\epsilon) = \frac{d_\epsilon}{A} + \kappa_0 \quad (2.53)$$

where  $A$  and  $\kappa_0$  are two parameters which depend on the material.

The damage criterion will depend on the elastic strains and not on total ones:

$$f = \hat{\epsilon}_{el} - \kappa(d_\epsilon) \quad (2.54)$$

The anelastic part of the model is:

$$\rho\psi_{an}^* = \sigma : \epsilon_{an} \quad (2.55)$$

This corresponds to the partition of the total strain into an elastic and permanent component.

$$\epsilon = \frac{\partial \rho\psi^*}{\partial \sigma} = \frac{\partial \rho\psi_e^*}{\partial \sigma} + \frac{\partial \rho\psi_{an}^*}{\partial \sigma} = \epsilon_e + \epsilon_{an} \quad (2.56)$$

The evolution of the permanent strains are derived by the following equations:

$$\dot{\epsilon}_{an} = g_D(d_\epsilon) \dot{D}^D + g_H(d_\epsilon) \dot{d}_\epsilon \mathbf{Id} \quad (2.57)$$

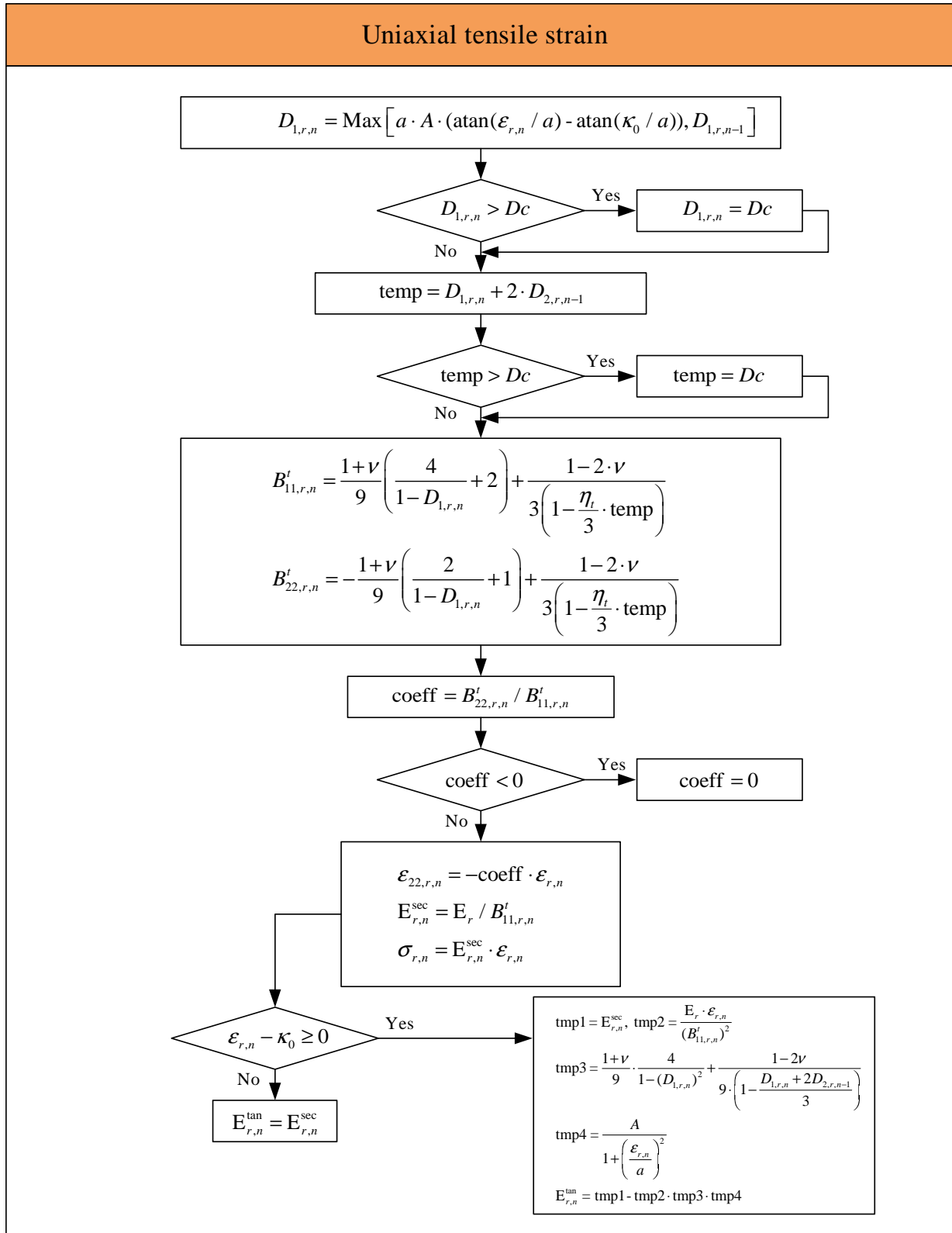


Figure 2.24: Determination (2) for the anisotropic damage model

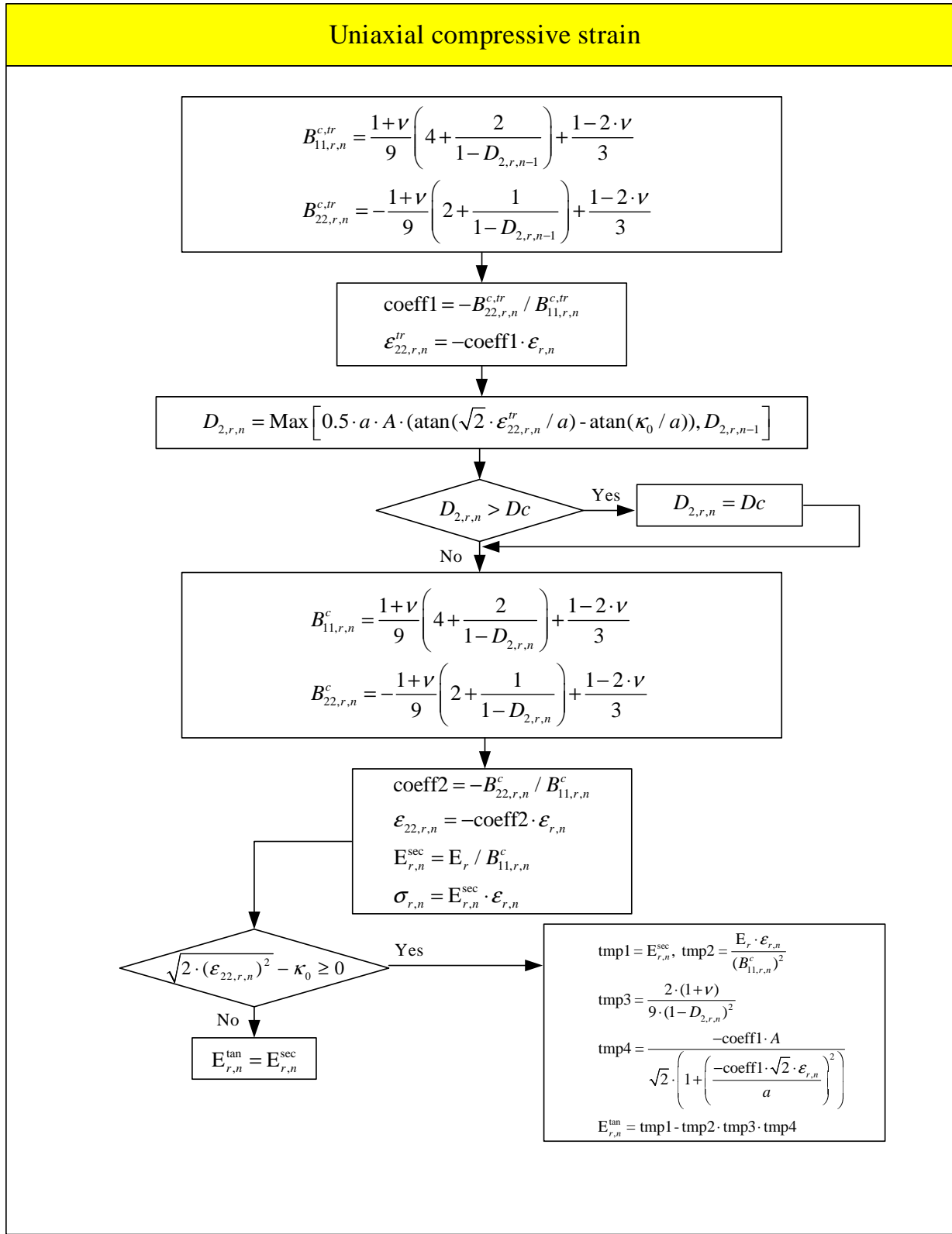


Figure 2.25: Determination (3) for the anisotropic damage model

with  $g_D(d_\epsilon)$   $g_H(d_\epsilon)$  two functions depending on the activate damage to respect the dissymmetry tension/compression. Two continuum bilinear functions are proposed here:

$$\begin{array}{lll} \text{if } d_\epsilon < 1 & g_D(d_\epsilon) = \frac{k_D}{K_D} d_\epsilon & \text{else } g_D(d_\epsilon) = \frac{k_D}{K_D} + k_D(d_\epsilon - 1) \\ g_H(d_\epsilon) = \frac{k_H}{K_H} d_\epsilon & & g_H(d_\epsilon) = \frac{k_H}{K_H} + k_H(d_\epsilon - 1) \end{array} \quad (2.58)$$

**2.2.2.2.1 Uniaxial numerical scheme** The loading state is defined by the sign of the elastic strain. Thus to determine the loading state at the timestep  $n$ , the increment of strain  $\Delta\epsilon$  is compared with the elastic strain at timestep  $n-1$ : If  $\epsilon_{n-1}^e < 0$  and  $\Delta\epsilon < -\epsilon_{n-1}^e$ , the loading state remains in compression, else it switches to tension. If  $\epsilon_{n-1}^e > 0$  and  $\Delta\epsilon < -\epsilon_{n-1}^e$ , the loading state remains in tension, else it switches to compression.

In tension:

- Elastic forecast :  $\epsilon_{1,n}^e = \epsilon_{1,n-1}^e + \Delta\epsilon_1$
- Damage criterion test:  $f$ 
  - if  $f < 0$ , elastic behavior:

$$\begin{array}{lll} D_{1,n} & = & D_{1,n-1} \\ D_{2,n} & = & D_{2,n-1} \\ \epsilon_{1,n}^{an} & = & \epsilon_{1,n-1}^{an} \\ \epsilon_{2,n}^{an} & = & \epsilon_{2,n-1}^{an} \end{array} \quad (2.59)$$

– else, damaging behavior:

$$\begin{array}{lll} D_{1,n} & = & A(\epsilon_{1,n}^e - \kappa_0) \\ D_{2,n} & = & D_{2,n-1} \\ \epsilon_{1,n}^{an} & = & \epsilon_{1,n-1}^{an} + \left( \frac{2k_D}{3K_D} + \frac{k_H}{K_H} \right) D_{1,n} \\ \epsilon_{2,n}^{an} & = & \epsilon_{2,n-1}^{an} + \left( \frac{-k_D}{3K_D} + \frac{k_H}{K_H} \right) D_{1,n} \end{array} \quad (2.60)$$

- Computation of  $\sigma$  and  $\epsilon_{2,n}^e$ :

$$\begin{array}{lll} B_{1,n} & = & \frac{1+\nu}{9} \cdot \left( \frac{4}{1-D_{1,n}} + 2 \right) + \frac{1-2\nu}{3 \cdot \left( 1 - \frac{(D_{1,n}+2 \cdot D_{2,n-1})}{3} \right)} \\ B_{2,n} & = & \frac{1+\nu}{9} \cdot \left( \frac{2}{1-D_{1,n}} + 1 \right) + \frac{1-2\nu}{3 \cdot \left[ 1 - \frac{\eta_t}{3} \cdot (D_{1,n} + 2 \cdot D_{2,n-1}) \right]} \\ \sigma_n & = & \frac{E}{B_{1,n}} \epsilon_n^e \\ \epsilon_{2,n}^e & = & \frac{B_{2,n}}{B_{1,n}} \epsilon_{1,n}^e \end{array} \quad (2.61)$$

In compression:

- Elastic forecast :  $\epsilon_{1,n}^e = \epsilon_{1,n-1}^e + \Delta\epsilon_1$
- Damage criterion test:  $f$ 
  - if  $f < 0$ , elastic behavior:

$$\begin{array}{lll} D_{1,n} & = & D_{1,n-1} \\ D_{2,n} & = & D_{2,n-1} \\ \epsilon_{1,n}^{an} & = & \epsilon_{1,n-1}^{an} \\ \epsilon_{2,n}^{an} & = & \epsilon_{2,n-1}^{an} \end{array} \quad (2.62)$$

– else, damaging behavior:

The evolution of the permanent strain must be estimate:

$$\begin{array}{ll} \dot{\epsilon}_{1,n}^{an} & = \gamma(d_{\epsilon n-1}) * d_{\epsilon 2,n} \\ \dot{\epsilon}_{1,n}^{an} & = 2\gamma(d_{\epsilon n-1}) * (D_{2,n} - D_{2,n-1}) \end{array} \quad (2.63)$$

The damage evolution becomes:

$$D_{2,n} = \frac{A(-\sqrt{2}\tilde{n}u_{n-1}(\epsilon - \epsilon_{1,n-1}^{an} - \dot{\epsilon}_{1,n}^{an}) - \kappa_0)}{2} \quad (2.64)$$

$$D_{2,n} = \frac{A \left( -\sqrt{2}n\tilde{u}_{n-1} (\epsilon - \epsilon_{1,n-1}^{an} + 2\gamma (d_{\epsilon n-1}) D_{2,n-1} - \kappa_0) \right)}{2 \left( \sqrt{2}A\tilde{u}_{n-1}\gamma (d_{\epsilon n-1}) \right)} \quad (2.65)$$

$$\begin{aligned} \epsilon_{2,n}^{e, trial} &= \frac{B_{2,n-1}}{B_{1,n-1}} \epsilon_{1,n}^e \\ D_{1,n} &= D_{1,n-1} \\ \epsilon_{1,n}^{an} &= \epsilon_{1,n-1}^{an} + \left( \frac{-2k_D}{3K_D} + \frac{k_H}{K_H} \right) D_{1,n} \\ \epsilon_{2,n}^{an} &= \epsilon_{2,n-1}^{an} + \left( \frac{k_D}{3K_D} + \frac{k_H}{K_H} \right) D_{1,n} \end{aligned} \quad (2.66)$$

- Computation of  $\sigma$  and  $\epsilon_{2,n}^e$ :

$$\begin{aligned} B_{1,n} &= \frac{1+\nu}{9} \cdot \left( 4 + \frac{2}{1-D_{2,n}} \right) + \frac{1-2\nu}{3} \\ B_{2,n} &= -\frac{1+\nu}{9} \cdot \left( 2 + \frac{1}{1-D_{2,n}} \right) + \frac{1-2\nu}{3} \\ \sigma_n &= \frac{E}{B_{1,n}} \epsilon_n^e \\ \epsilon_{2,n}^e &= \frac{B_{2,n}}{B_{1,n}} \epsilon_{1,n}^e \end{aligned} \quad (2.67)$$

Fig. 2.26 describes the relationship between strain and stress in anisotropic damage model with permanent strain.

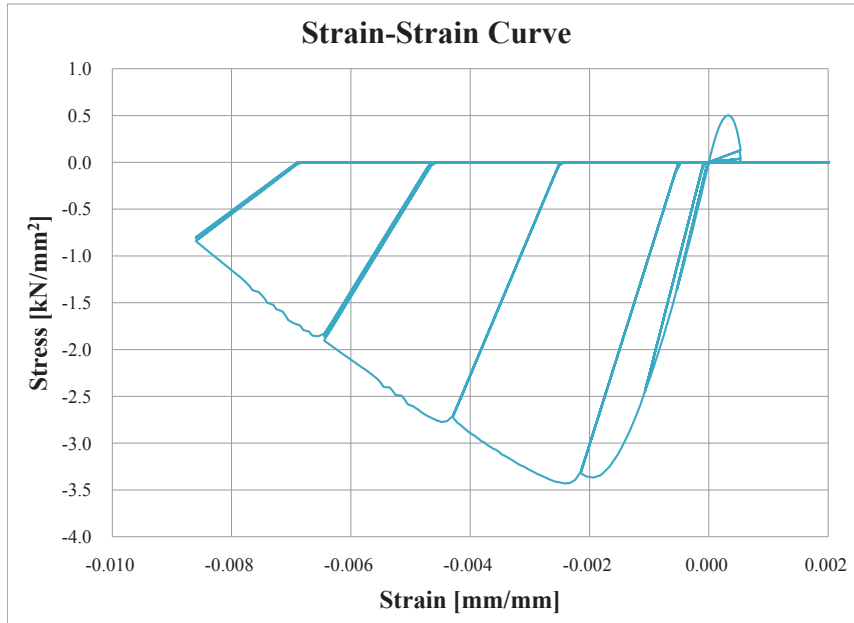


Figure 2.26: Strain-stress curve for anisotropic damage model with permanent strain

### 2.3 Bond-Slip

Slip due to longitudinal reinforcing bar near the column and from the anchorage can be easily determined if we assume a uniform bond stress  $u_b$  along the bars within the development length inside the footing or the beam-column

joint, (?). From equilibrium

$$u_b(\pi d_b)l_d = \frac{\pi d_b^2}{4} f_s \quad (2.68)$$

where  $d_b$  is the bar diameter,  $l_d$  is the development length over which the slip occurs, solving for  $l_d$

$$l_d = \frac{d_b f_s}{4 u_b} \quad (2.69)$$

Assuming that the maximum strain occurs at the end of the column, and a linear variation of strain along the development length, the integral of the strain curve will give the total bar slip at the footing-column interface or beam-column interface

$$S = \frac{\varepsilon_s l_d}{2} = \frac{f_s l_d}{2 E_s} \quad (2.70)$$

Substituting Eq. 2.69 for  $l_d$  in the preceding equation

$$S = \frac{\varepsilon_s d_b f_s}{8 u_b} \quad (2.71)$$

Finally, assuming that the cross section rotates about its neutral axis when slip occurs ( $\phi_y = \varepsilon_y/(d - c)$ ), the displacement related to the bar slip at a point at a distance  $L$  from the column base will be

$$\Delta_{\text{slip}} = \frac{\phi_y d_b f_y L}{8 u_b} \quad (2.72)$$

? presented a simplified bond model for bond stress in terms of the actual steel stress. It assumes a constant bond stress of  $u_e = 12\sqrt{f'_c}$  prior to steel yielding, and another constant bond stress of  $u_p = 6\sqrt{f'_c}$  past steel yielding, Fig. 2.27. Based on this assumption, the total bar slip at the edge of the anchorage is obtained by integrating the steel

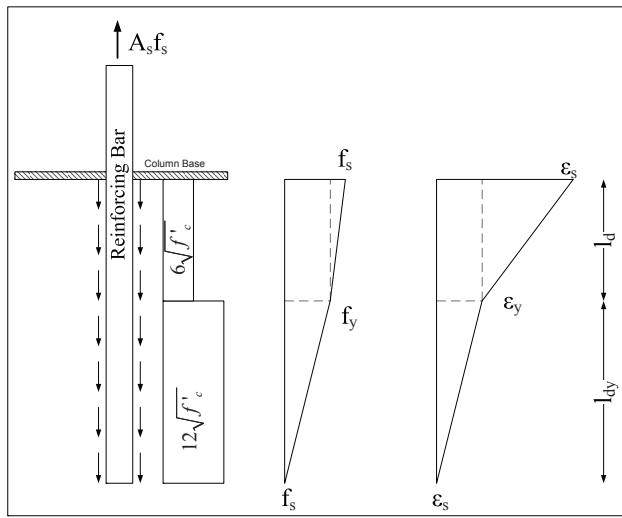


Figure 2.27: Longitudinal bar bond stress, steel stress, and strain profiles, (?)

strains over the embedded length.

? used this model to obtain a monotonic relation for bar slip versus bar stress at the column base. Assuming sufficient anchorage:

$$S_1 = \frac{\varepsilon_s f_s}{8 u_e} d_b; \quad \varepsilon_s \leq \varepsilon_y \quad (2.73)$$

$$S_2 = \frac{\varepsilon_y f_y}{8 u_e} d_b + \frac{(\varepsilon_s + \varepsilon_y)(f_s - f_y)}{8 u_p} d_b; \quad \varepsilon_s > \varepsilon_y \quad (2.74)$$

where  $d_b$  is the bar diameter,  $u_e$  is the elastic bond stress  $= 12\sqrt{f'_c}$  (psi), and  $u_p$  is the plastic bond stress  $= 6\sqrt{f'_c}$ . The following Matlab code generates a plot of normalized stress versus bond slip.

Listing 2.2: Bond-slip

```

1 clear
2 %+++++
3 %% Input parameters
4 d_b=3/8; % bar diameter in inches
5 f_c=4000; % compressive strength (psi)
6 E_s=27300000; % psi
7 b=0.01; %
8 fy=64000;% original yield stress in psi
9 f_y=1.25*fy; % yield stress increased by 25% for rate effect
10 %f_u=100000; % ksi
11 %
12 epsilon_y=f_y/E_s;
13 %% Bond
14 u_e=12*sqrt(f_c);
15 u_p=6*sqrt(f_c);
16 %
17 k=0;
18 epsilon_final=30*epsilon_y;
19 delta_epsilon=epsilon_final/100;
20 for epsilon_s=0:delta_epsilon:epsilon_final
21 k=k+1;
22 if epsilon_s<=epsilon_y
23 f_s=epsilon_s*E_s;
24 slip_y=epsilon_s*f_s*d_b/(8*u_e);
25 slip(k)=slip_y;
26 else
27 f_s=epsilon_y*E_s+b*(epsilon_s-epsilon_y)*E_s;
28 slip_u=epsilon_y*f_y*d_b/(8*u_e)+(epsilon_s+epsilon_y)*(f_s-f_y)*d_b/(8*u_p);
29 slip(k)=slip_u;
30 end
31 normalized_stress(k)=f_s/f_y;
32 end
33 plot(slip,normalized_stress,'linewidth',2);grid;xlim([0,max(slip)]);
34 xlabel('Slip [in]', 'fontsize',14);ylabel('f_s/f_y', 'fontsize',14);
35 print -deps 'bond-slip-curve.eps';

```

This code generates the stress slip curve shown in Fig. 2.27.

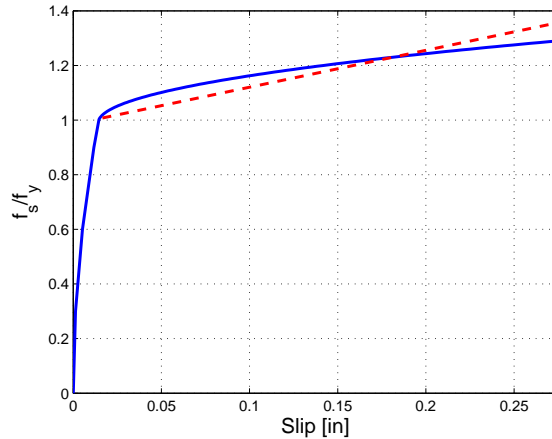


Figure 2.28: Stress slip curve

## 2.4 Lumped Plasticity Model

To be completed later

## 2.5 Constitutive models for zero length and zero length section elements

### 2.5.1 Zero Length Element

Zero length elements are used primarily for lumped plasticity models. In fiber models, they are used to provide a finite shear stiffness, whereas the axial and flexural ones can be considered as rigid (no corresponding entries in Mercury implies rigid connection).

$$K_S = \frac{\alpha G A_g}{L} \quad (2.75)$$

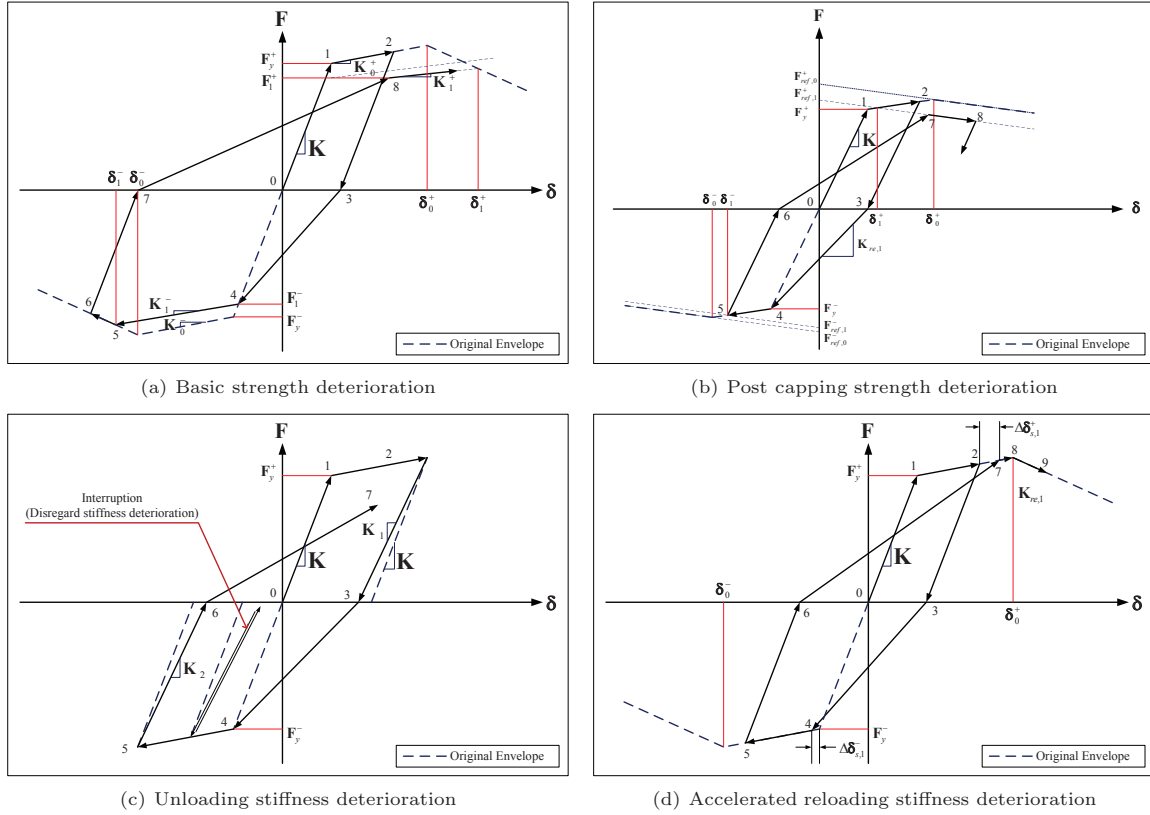


Figure 2.29: Hysteretic model with strength and stiffness deterioration, (?)

where  $\alpha$  is the shape section coefficient (5/6 for rectangular section),  $G$  is the shear modulus ( $G = E_c/2(1 + \nu)$ ); Concrete Poisson ratio is about 0.25.

Future release of Mercury, should have zero length elements enriched by limit state material properties to act as a fuse to possible failure.

### 2.5.2 Zero length section element

This section is an adaptation of ?

Zero length section element should be used only when fiber elements are used if we want to capture the bond slip between concrete and rebar. Though many models have been proposed for bond-slip, we will adopt the model of ? as it is the most rational one in handling the shifting position of the neutral axis (essential to determine the bond slip displacement).

From Fig. 2.28 we have a nonlinear post-peak response, and we need to linearize it, and then solve for  $u_p$  (which will be different than the previously given value of  $6\sqrt{f'_c}$  suitable for the nonlinear hardening segment).

We seek to have the linearized segment intersect the nonlinear one at  $1.25f_y$ , hence

$$\varepsilon_u = \varepsilon_y + 0.25 \frac{f_y}{E_s/h} = \frac{f_y}{E_s} + 0.25h \frac{f_y}{E_s} = 0.26h\varepsilon_y \quad (2.76)$$

where  $h$  is the hardening parameter set to 100. Substituting in Eq. 2.74

$$S_u = \frac{\varepsilon_y f_y}{8u_e} d_b + \frac{(26\varepsilon_y + \varepsilon_y)(1.25f_y - f_y)}{8u_p} d_b \quad (2.77)$$

$$= S_y + \frac{27\varepsilon_y \times 0.25f_y}{8u_p} d_b \quad (2.78)$$

$$= S_y + \frac{6.75\varepsilon_y f_y}{8u_p} d_b \quad (2.79)$$

We can reasonably assume that

$$S_u = \varepsilon_s \frac{S_y}{\varepsilon_y} = 26S_y \quad (2.80)$$

Substituting in Eq. 2.79

$$26S_y = S_y + \frac{6.75\varepsilon_y f_y}{8u_p} d_b \quad (2.81)$$

or

$$25 \frac{\varepsilon_y f_y}{8u_e} d_b = \frac{6.75\varepsilon_y f_y}{8u_p} d_b \quad (2.82)$$

$$u_p = \frac{6.75}{25} u_e \quad (2.83)$$

$$= \frac{6.75}{25} 12\sqrt{f'_c} \quad (2.84)$$

$$= 3.24\sqrt{f'_c} \quad (2.85)$$

$u_p$  may be used in so-called limit state elements to assess bond slip induced failure.

Irrespective of which steel model is used in the beam-column, it is recommended to use the bilinear one for this element. Using a bilinear model, with  $h = 0.01$  will be equivalent to having a bar slip curve such that the second segment intersect the exact one at  $f_s = 1.25f_y$  with  $u_p = 3.24\sqrt{f'_c}$ .

In the steel bilinear model, the Young's modulus should be adjusted to reflect bond slip, by replacing  $E_s$  by  $E_{bs}$  which is equal to

$$E_{bs} = \frac{f_y}{S_y} \quad (2.86)$$

It should be noted that inherent in this assumption is a *unit length* of the zero length element.

Finally, to maintain the same material stiffness ratio between bar-slip steel in the zero length section element, and the one in the frame element (longitudinal steel), we multiply the bar slip concrete material strains by  $E_s/E_{bs}$ .

The concrete properties for the zero length section element are such that the location of the neutral axis in the beam-column element and the zero length fiber section is the same. Thus

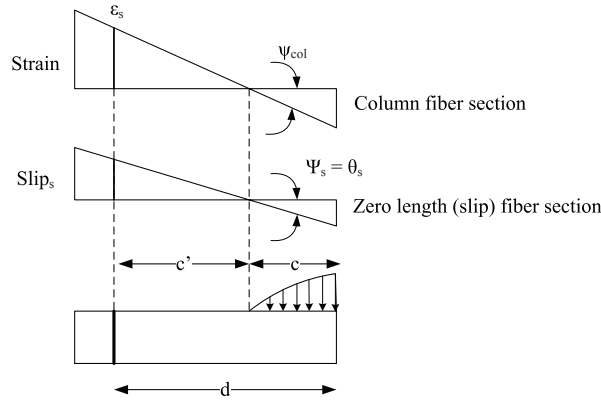


Figure 2.30: Compatibility of NA between beam-column and zero length fiber section

$$\begin{aligned} \theta_s &= \frac{S_s}{c'} \\ \Psi_{col} &= \frac{\varepsilon_s}{c'} \end{aligned} \quad \left\{ \theta_s = \Psi_{col} \frac{S_s}{\varepsilon_s} \right. \quad (2.87)$$

Hence all fiber strains (corresponding to steel and concrete) in the zero length section must be scaled by  $\frac{S_s}{\varepsilon_s}$ . This can be easily achieved in altering the material input data such that

1. All stress values remain unchanged
2. Strains are scaled by  $\frac{S_y}{\varepsilon_y}$

### 2.5.3 Summary

Fig. 2.31 highlight the modeling of the zero length element and section.

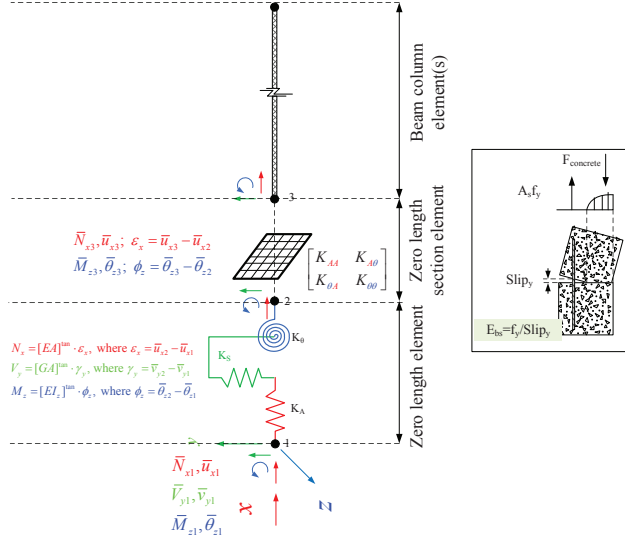


Figure 2.31: Zero length element and section

### 2.6 Summary

This chapter has presented the details of the constitutive models coded in Mercury. The model selected are well known and tested and would enable the analysis of complex steel or reinforced concrete frame.



## Chapter 3

### Structural Modeling

This chapter addresses the major issues in modeling structure for a nonlinear static or transient analysis.

Table. ?? provides a concise summary of the example validation problems. In it, we adopt the following shortcuts:

- SBC: Stiffness-based 2D beam-column
- FBC1: Flexibility-based 2D beam-column with element iteration
- FBC2: Flexibility-based 2D beam-column without element iteration
- Damage1: Anisotropic damage 1D material model without permanent strain
- Damage2: Anisotropic damage 1D material model with permanent strain
- ModKP: Modified Kent-Park material model
- ModGMP: Modified Giuffre-Monegotto-Pinto material model
- Disp(displ): Displacement.

### 3.1 Truss, Material Nonlinearity, Static and Dynamic

This is a transient nonlinear analysis of a truss based on the HHT algorithm ( $\alpha$  method), and the elements are modeled by the modified Giuffre-Monegotto-Pinto materials. Truss, and results are shown in Fig. 3.1.

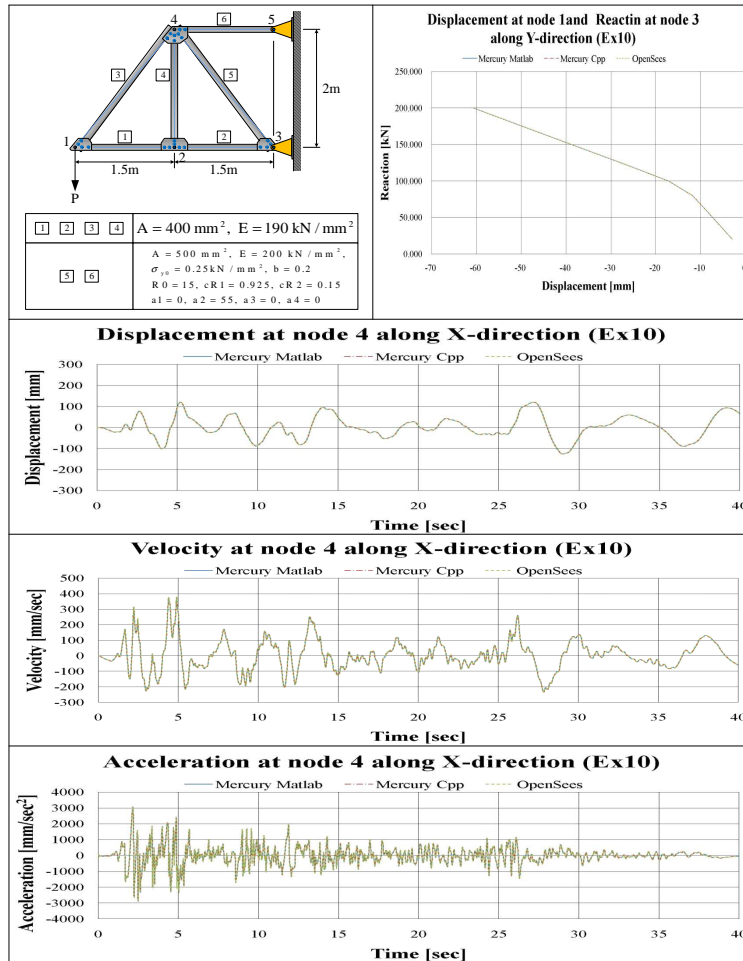


Figure 3.1: Ex10: Truss, ModGMP material, load control, HHT

In static analysis, incremental forces that increase by  $-20\text{kN}$  from  $-20\text{kN}$  to  $-200\text{kN}$  at node 1 along the  $Y$  direction are applied.

Document Section	ID	Element	Zero Length	Formulation	Section
3.1	Ex10	Truss		Stiffness	General
3.2	Ex11				
	Ex12				
3.3	Ex16				
	Ex17				
	Ex18				
	Ex19				
	Ex20				
3.4	Ex21	Beam Column		Flexibility, With Iteration	Fiber
	Ex22				
	Ex23				
3.5	Ex24		Element	Stiffness Based	General
3.6	Ex25				
3.7	Ex26			Flexibility, iteration	Fiber
	Ex27				
3.8	Ex28		Element & Section	Flexibility (itera- tion)	
3.9	Ex29				
Section					

Document Section	ID	Constitutive Model	Hardening	Load Control	Transient		
3.1	Ex10	Elastic and ModGMP	Kinematic	& Static Stiffness control	HHT		
3.2	Ex11	Damage					
	Ex12	ModKP					
3.3	Ex16	Simplified Bilinear	No				
	Ex17	Simplified Bilinear	Isotropic				
	Ex18	ModGMP	Kinematic				
	Ex19	ModGMP	Kinematic & Isotropic				
3.4	Ex20	Classical Hardening	Isotropic	Cyclic disp control	HHT		
	Ex21		Kinematic				
	Ex22		Kinematic & Isotropic				
3.5	Ex23	Elastic and Simplified Bilinear	No		Shing		
3.6	Ex24	Elastic and Bilinear	Isotropic				
3.7	Ex25	Classical Hardening		Pushover			
	Ex26						
3.8	Ex27	ModGMP and ModKP	Kinematic	&	HHT/Shing		
3.9	Ex29	Multiple	&				
Cyclic disp control							

SBC: Stiffness-based 2D beam-column Isotropic  
 FBC1: Flexibility-based 2D beam-column with element iteration  
 FBC2: Flexibility-based 2D beam-column without element iteration  
 Damage1: Anisotropic damage 1D material model without permanent strain  
 Damage2: Anisotropic damage 1D material model with permanent strain  
 ModKP: Modified Kent-Park material model  
 ModGMP: Modified Giuffre-Monegotto-Pinto material model  
 Disp(displ): Displacement.

Table 3.1: Features of Example Problems

In the second part, the transient analysis without self-weight and nodal forces is performed with HHT integration scheme.

### 3.1.1 MATLAB

Listing 3.1: MATLAB; Truss

```

1 % Mercury Matlab Version 1.0.1
2 % Written by Dae-Hung Kang, CU-NEES
3 % Copyright 2009, CU-NEES
4 % Written : September 2009.
5 % File name: Ex10.m
6 %
7 %
8 %
9 % Description
10 % 1. Static and transient analysis
11 % 2. Load control
12 % 3. Iterative method
13 % 4. Simple 2D truss element
14 % 5. General section
15 % 6. Elastic and modified Giuffre-Monegotto-Pinto material
16 %
17 % Select type of analysis.
18 % AnalysisType = 1: Static analysis
19 % AnalysisType = 2: Transient analysis
20 AnalysisType = 2;
21 %
22 % Preface
23 Unit      = {'kN', 'mm'};
24 %          ndim, ndofpn
25 StrMode   = {2, 2};
26 %
27 % Control block
28 Iteration = {'static', { {'NewtonRaphson', 10, 1.0e-8, 'DisplNorm'} ;
29                      {'ModifiedNewtonRaphson', 20, 1.0e-8, 'EnergyNorm'} ;
30                      {'InitialStiffness', 30, 1.0e-8, 'ForceNorm'} ;
31                  } ;
32 'transient', { {'NewtonRaphson', 10, 1.0e-8, 'DisplNorm'} ;
33                  {'ModifiedNewtonRaphson', 20, 1.0e-8, 'EnergyNorm'} ;
34                  {'InitialStiffness', 30, 1.0e-8, 'ForceNorm'} ;
35              } ;
36 };
37 if (AnalysisType == 2)
38     Integration = {'HHT', 0, -0.1, 0.3025, 0.6, 0, 0};
39     eigens     = {0.02, 0.02};
40 end
41 %
42 % Geometry block
43 %          nodtag, x, y
44 nodcoord = {1, 0, 0;
45             2, 1500, 0;
46             3, 3000, 0;
47             4, 1500, 2000;
48             5, 3000, 2000};
49 %          nodtag, x, y
50 constraint = {3, 1, 1;
51               5, 1, 1};
52 %
53 % Element block
54 %          eletag, 'Simple2DTruss', in, jn, sectag
55 elements = { {1, 'Simple2DTruss', 1, 2, 1};
56             {2, 'Simple2DTruss', 2, 3, 1};
57             {3, 'Simple2DTruss', 1, 4, 1};
58             {4, 'Simple2DTruss', 2, 4, 1};
59             {5, 'Simple2DTruss', 3, 4, 2};
60             {6, 'Simple2DTruss', 4, 5, 2} };
61 %
62 % Section block
63 %          sectag, 'General', {mattag, A, Ix, Iy, Iz}
64 sections = { {1, 'General', {1, 400, 0, 0, 0}};
65             {2, 'General', {2, 500, 0, 0, 0}}};
66 %
67 % Material block
68 %          mattag, 'Elastic', E, G, density
69 materials = { {1, 'Elastic', 190, 0, 7850*10^-9}
70 %             mattag, 'ModGMP', E, sy, b, R0, cR1, cR2, density, a1, a2, a3, a4
71             {2, 'ModGMP', 200, 0.25, 0.2, 15, 0.925, 0.15, 7850*10^-9, 0, 55, 0, 55} };
72 %
73 % Force block
74 if (AnalysisType == 1)
75     forces = { 1, 'Static', {'NodalForces', {1, 2, -20}};
76                 2, 'LoadCtrl', {1, 2, {-40, -60, -80, -100, -120, -140, -160, -180, -200}} };
77 elseif (AnalysisType == 2)
78     ga = load('ElCentro.g=0.01.Matlab.txt');
79     nga = size(ga, 1);
80     for i = 1:nga
81         groundacceleration{i,1} = ga(i,1);
82         groundacceleration{i,2} = ga(i,2);
83         groundacceleration{i,3} = ga(i,3);
84     end
85     forces = { 1, 'Static', {'NodalForces', {1, 2, 0} },
86                 2, 'Acceleration', {9810, groundacceleration} };
87 end
88 %

```

### 3.1.2 C++

Listing 3.2: C++; Truss

```

1 --- **** AnalysisType = 1: Static analysis
2 --- **** AnalysisType = 2: Transient analysis
3 AnalysisType = 2
4
5 --- ****
6 %nodes = { {1, 0, 0, 'mass', 6.28, 6.28},
7     {2, 1500, 0, 'mass', 7.85, 7.85},
8     {3, 3000, 0},
9     {4, 1500, 2000, 'mass', 14.915, 14.915},
10    {5, 3000, 2000} }
11
12 Simple2DTruss = 'truss2d',
13 elements = { {1, Simple2DTruss, 1, 2, 400, 1},
14     {2, Simple2DTruss, 2, 3, 400, 1},
15     {3, Simple2DTruss, 1, 4, 400, 1},
16     {4, Simple2DTruss, 2, 4, 400, 1},
17     {5, Simple2DTruss, 3, 4, 500, 2},
18     {6, Simple2DTruss, 4, 5, 500, 2}, }
19 --{tag, 'modifiedGMPsteel', E, rho, fy, b_ratio, R0, cR1, cR2, a1, a2, a3, a4, sigma_init}
20 materials = { {1,'elastic',190,0.0};
21     {2,'modifiedGMPsteel', 200, 0, 0.25, 0.2, 15, 0.925, 0.15, 0, 55, 0, 55, 0} }
22 --- ****
23 model = StructureModel(2,2)
24 model:addNodes(nodes)
25 model:addMaterials(materials)
26 model:addElements(elements)
27 model:constrainNode(3,1,1)
28 model:constrainNode(5,1,1)
29 --- ****
30 -- Static analysis
31 if (AnalysisType == 1) then
32     print(" Static analysis started\n")
33     staticloading = LoadDescription()
34     staticloading:addLoad({ 'incrementalnodalload', 1, 2, -20,-40,-60,-80,-100,-120,-140,-160,-180,-200 })
35 --- ****
36 displ = {}
37 function displperstep(increment)
38     dx1,dy1 = model:nodeDisplacements(1)
39     dx2,dy2 = model:nodeDisplacements(2)
40     dx4,dy4 = model:nodeDisplacements(4)
41     table.insert(displ, dx1)
42     table.insert(displ, dy1)
43     table.insert(displ, dx2)
44     table.insert(displ, dy2)
45     table.insert(displ, dx4)
46     table.insert(displ, dy4)
47 end
48
49 react = {}
50 function reactperstep(increment)
51     fx3,fy3 = model:nodeRestoringForces(3)
52     fx5,fy5 = model:nodeRestoringForces(5)
53     table.insert(react, fx3)
54     table.insert(react, fy3)
55     table.insert(react, fx5)
56     table.insert(react, fy5)
57 end
58
59 solver = NonlinearSolver("newtonraphson", { displacementdeltatolerance=1e-3, iterations=100})
60 analysis = StaticAnalysis(solver)
61 analysis:setStructureModel(model)
62 analysis:adccallback(displperstep,"increment")
63 analysis:adccallback(reactperstep,"increment")
64 analysis:solve(staticloading)
65 --- ****
66 -- Set output file
67 function writedata6(x, fname)
68     local f = assert(io.open(fname, 'w'))
69     local writenl = 0
70     for i,v in ipairs(x) do
71         f:write(v, " ")
72         writenl = writenl + 1
73         -- length of row size: writenl
74         if (writenl > 5) then
75             writenl = 0
76             f:write("\n")
77         end
78     end
79     f:close()
80 end
81
82 function writedata4(x, fname)
83     local f = assert(io.open(fname, 'w'))
84     local writenl = 0
85     for i,v in ipairs(x) do
86         f:write(v, " ")
87         writenl = writenl + 1
88         -- length of row size: writenl
89         if (writenl > 3) then
90             writenl = 0
91             f:write("\n")
92         end
93     end
94     f:close()
95 end
96
97 writedata6(displ, 'Ex10StaticNodalDisp1_2_4.dat')
98 writedata4(react, 'Ex10StaticReact_3_5.dat')
99 print(" Static analysis ended\n")
100 end
101 --- ****
102 if (AnalysisType == 2) then
103     print(" Transient analysis started\n")
104     earthquakeloading = LoadDescription()
105     accelamp = 9810
106     earthquakeloading:addLoad({ 'groundmotion', 'ElCentro-g-0-01-OpenSees.txt', dt=0.01, 1,accelamp })
107 --- ****

```

```

108    displ = {}
109    function displpertime(time)
110        dx1,dy1 = model:nodeDisplacements(1)
111        dx2,dy2 = model:nodeDisplacements(2)
112        dx4,dy4 = model:nodeDisplacements(4)
113        table.insert(displ, dx1)
114        table.insert(displ, dy1)
115        table.insert(displ, dx2)
116        table.insert(displ, dy2)
117        table.insert(displ, dx4)
118        table.insert(displ, dy4)
119    end
120
121    react = {}
122    function reactpertime(time)
123        fx3,fy3 = model:nodeRestoringForces(3)
124        fx5,fy5 = model:nodeRestoringForces(5)
125        table.insert(react, fx3)
126        table.insert(react, fy3)
127        table.insert(react, fx5)
128        table.insert(react, fy5)
129    end
130
131    veloc = {}
132    function velocpertime(time)
133        vx1,vy1 = model:nodeVelocities(1)
134        vx2,vy2 = model:nodeVelocities(2)
135        vx4,vy4 = model:nodeVelocities(4)
136        table.insert(veloc, vx1)
137        table.insert(veloc, vy1)
138        table.insert(veloc, vx2)
139        table.insert(veloc, vy2)
140        table.insert(veloc, vx4)
141        table.insert(veloc, vy4)
142    end
143
144    accel = {}
145    function accelpertime(time)
146        ax1,ay1 = model:nodeAccelerations(1)
147        ax2,ay2 = model:nodeAccelerations(2)
148        ax4,ay4 = model:nodeAccelerations(4)
149        table.insert(accel, ax1)
150        table.insert(accel, ay1)
151        table.insert(accel, ax2)
152        table.insert(accel, ay2)
153        table.insert(accel, ax4)
154        table.insert(accel, ay4)
155    end
156
157    *****
158    solver = NonlinearSolver("newtonraphson", { displacementdeltatolerance=le-6, iterations=10})
159    transientanalysis = DynamicAnalysis("HHT", model, solver, earthquakeloading, 0.01, -0.1, 0.3025, 0.6)
160    transientanalysis:adccallback(displpertime, "timestep")
161    transientanalysis:adccallback(reactpertime, "timestep")
162    transientanalysis:adccallback(velocpertime, "timestep")
163    model:setRayleighCoefficients(0.025533,0.007826)
164    transientanalysis:solve(4000)
165
166    *****
167    function writedata6(x, fname)
168        local f = assert(io.open(fname, 'w'))
169        local writenl = 0
170        for i,v in ipairs(x) do
171            f:write(v, "\n")
172            writenl = writenl + 1
173            length of row size: writenl
174            if (writenl > 5) then
175                writenl = 0
176                f:write("\n")
177            end
178        end
179        f:close()
180
181    function writedata4(x, fname)
182        local f = assert(io.open(fname, 'w'))
183        local writenl = 0
184        for i,v in ipairs(x) do
185            f:write(v, "\n")
186            writenl = writenl + 1
187            length of row size: writenl
188            if (writenl > 3) then
189                writenl = 0
190                f:write("\n")
191            end
192        end
193        f:close()
194    end
195
196    writedata6(displ, 'Ex10TransientNodalDisp_1_2_4.dat')
197    writedata6(react, 'Ex10TransientReact_3_5.dat')
198    writedata6(veloc, 'Ex10TransientNodalVelo_1_2_4.dat')
199    writedata6(accel, 'Ex10TransientNodalAccel_1_2_4.dat')
200    print(" Transient analysis ended\n")
201 end
202
203    *****

```

### 3.2 Uniaxial Concrete Nonlinear Element, Cyclic Displacement

These examples assume concrete members and seek to compare the modified Kent-Park model with the anisotropic damage model with permanent strain when subjected to cyclic displacement statically, Fig. 3.2. Fig. 3.3 describes the static analysis with cyclic displacements applied at node 2 in the X direction.

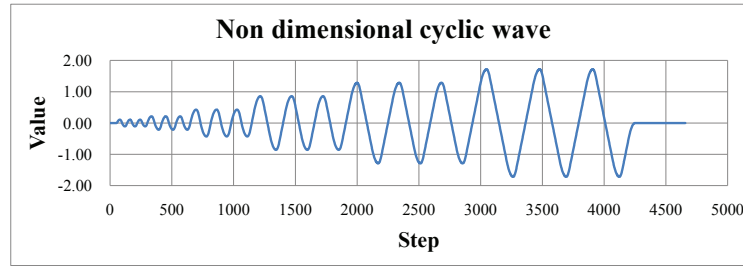


Figure 3.2: Cyclic wave without dimension

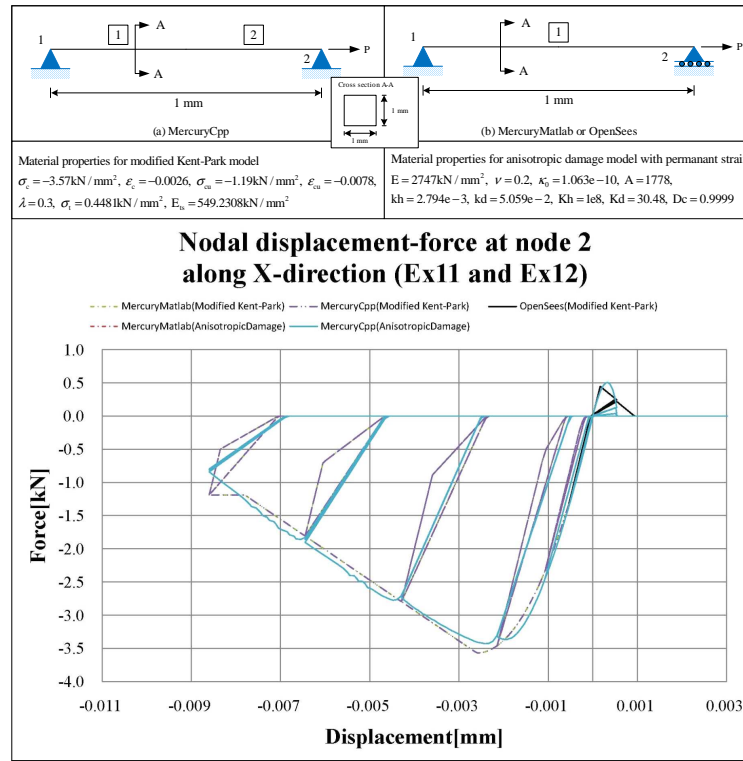


Figure 3.3: Examples 11- 12

### 3.2.1 MATLAB

```

1 % Mercury Matlab Version 1.0.1
2 % Written by Dae-Hung Kang, CU-NEES
3 % Copyright 2009, CU-NEES
4 % Written : November 2009.
5 % File name: Ex11to12.m
6 %
7 %
8 %
9 % Description
10 % 1. Static analysis
11 % 2. Displacement control
12 % 3. Iterative method
13 % 4. Simple 2D truss element
14 % 5. General section
15 % 6. Anisotropic damage material(Ex11)
16 % and modified Kent-Park material(Ex12)
17 %
18 % Select material type
19 % MatType = 1: anisotropic damage material with permanent strain (Ex11)
20 % MatType = 2: modified Kent-Park material (Ex12)
21 MatType = 1;
22 %
23 % Preface
24 Unit = {'kN', 'mm'};
25 StrMode = {2, 2};
26 %
27 % Control block
28 Iteration = {'static', { {'NewtonRaphson', 10, 1.0e-8, 'DisplNorm'},
29                         {'ModifiedNewtonRaphson', 20, 1.0e-8, 'EnergyNorm'},
30                         {'InitialStiffness', 30, 1.0e-8, 'ForceNorm'}},
31                     };
32 };
33 %
34 % Geometry block
35 nodcoord = {1, 0, 0;
36              2, 1, 0;};
37 constraint = {1, 1, 1;
38                2, 0, 1;};
39 %
40 % Element block
41 elements = { {1, 'Simple2DTruss', 1, 2, 1} };
42 %
43 % Section block
44 sections = { 1, 'General', {1, 1, 0, 0, 0} };
45 %
46 % Material block
47 if (MatType == 1)
48   % {tag, 'AnisotropicDamage', E, nu, kappa0, A, kh, kd, Kh, Kd, Dc, density};
49   materials = { {1, 'AnisotropicDamage', 2.747e+003, 0.2, 1.063e-010, 1.778e+003, 2.794e-003, 5.059e-002, 1.000e+008, 3.048e+001, 0} };
50 end
51 if (MatType == 2)
52   % {tag, 'ModKP', sc, ecu, scu, lambda, st, Ets, density};
53   materials = { {1, 'ModKP', -3.57, -0.0026, -1.19, -0.0078, 0.3, 0.448121077, 549.2307692, 0} };
54 end
55 %
56 % Force block
57 DispInput = load('cyclicwave.txt');
58 row = size(DispInput,1);
59 for i = 1:row
60   DispCell{i} = 0.005*DispInput(i);
61 end
62 % force{tag, 'Static', {NodalForces, {nodnum, globalaxis, m}}
63 forces = { 1, 'Static', {'NodalForces', {2, 1, 0}};
64           2, 'DispCtrl', {2, 1, DispCell} };
65 %

```

### 3.2.2 C++

```

1 --- ****
2 --- MatType = 1: Anisotropic damage model with permanent strain
3 --- MatType = 2: Modified Kent-Park model
4 MatType = 2
5 ---
6 nodes = { {1, 0, 0},
7           {2, 1, 0} };
8 ---
9 Simple2DTruss = 'truss2d';
10 elements = { {1, Simple2DTruss, 1, 2, 1, 1} };
11 ---
12 if (MatType == 1) then
13   materials = { {1, 'anisotropicdamage2', 2.747e+003, 0, 0.2, 1.063e-010, 1.778e+003, 2.794e-003, 5.059e-002, 1.000e+008, 3.048e+001} };
14 end
15 if (MatType == 2) then
16   concretemat = 'ConcreteLinearTensionSoftening';
17   materials = { {1, concretemat, 549.2307692, 0, -3.57, -0.0026, -1.19, -0.0078, 0.3, 0.448121077} };
18 end
19 ---
20 model = StructureModel(2,2)
21 model:addNodes(nodes)
22 model:addMaterials(materials)
23 model:addElements(elements)
24 model:constrainNode(1,1,1)
25 model:constrainNode(2,1,1)
26 ---
27 function generateincrementalload()
28   --- format:                                     tag          node dof
29   local loadform = {'incrementalnodaldisplacement', 2, 1}
30   local f = assert(io.open('cyclicwave.txt','r'))
31   local n = f:read('*number')
32   while (n ~= nil) do

```

```

33     table.insert(loadform, 0.005*n)
34     n = f:read("*number")
35   end
36   f:close()
37   return loadform
38 end
39 --- ****
40 staticloading = LoadDescription()
41 --- format: 'staticnodalload' <node> <dof> <amplitude>
42 l = generateincrementalload()
43 staticloading:addLoad(l)
44 --- ****
45 --- Static analysis
46 print(" Static analysis started\n")
47 displ = {}
48 function displperstep(increment)
49   dx2,dy2 = model:nodeDisplacements(2)
50   table.insert(displ, dx2)
51 end
52 ---
53 react = {}
54 function reactperstep(increment)
55   fx1,fy1 = model:nodeRestoringForces(1)
56   table.insert(react, fx1)
57 end
58 ---
59 solver = NonlinearSolver("initialstiffness", { displacementdeltatolerance=1e-3, iterations=10000})
60 analysis = StaticAnalysis(solver)
61 analysis:setStructureModel(model)
62 ---analysis:adDCALLBACK(displperstep,"increment")
63 ---analysis:adDCALLBACK(reactperstep,"increment")
64 analysis:solve(staticloading)
65 --- ****
66 --- Set output file
67 function writedata(x, fname)
68   local f = assert(io.open(fname, 'w'))
69   local writenl = 0
70   for i,v in ipairs(x) do
71     f:write(v, " ")
72     writenl = writenl + 1
73     --- length of row size: writenl
74     if (writenl > 0) then
75       writenl = 0
76       f:write("\n")
77     end
78   end
79   f:close()
80 end
81 ---
82 if (MatType == 1) then
83   writedata1(displ, 'Ex11StaticDamageNodalDisp_2.dat')
84   writedata1(react, 'Ex11StaticDamageReact_1.dat')
85 end
86 if (MatType == 2) then
87   writedata1(displ, 'Ex12StaticModKPNodalDisp_2.dat')
88   writedata1(react, 'Ex12StaticModKPReact_1.dat')
89 end
90 print(" Static analysis ended\n")

```

### 3.3 Uniaxial Steel Nonlinear Element, Cyclic Displacement

Bilinear and modified Giuffre-Monegotto-Pinto constitutive models with cyclic displacement are examined next, Fig. 3.2. Fig. ?? shows the results of the static analysis with cyclic displacements applied at node 2 in the  $X$  direction. Ex16 has bilinear material without isotropic hardening, Ex17 has bilinear material with isotropic hardening, Ex18 has modified Giuffre-Monegotto-Pinto material without isotropic hardening, and Ex19 has modified Giuffre-Monegotto-Pinto material with isotropic hardening material.

#### 3.3.1 MATLAB

```

1 %
2 % Mercury Matlab Version 1.0.1
3 % Written by Dae-Hung Kang, CU-NEES
4 % Copyright 2009, CU-NEES
5 % Written : October 2009.
6 % File name: Ex16to17.m
7 %
8 % Description
9 % 1. Static analysis
10 % 2. Displacement control
11 % 3. Iterative method
12 % 4. Simple 2D truss element
13 % 5. General sections
14 % 6. Bilinear material
15 %
16 % A36 Steel properties
17 % Density of 7.8 g/cm^3
18 % Minimum yield strength of 250 MPa(0.25 GPa)
19 % Ultimate tensile strength of 400-550 MPa(0.4-0.55 GPa)
20 %
21 % Select material type
22 % MatType = 1: Bilinear material without isotropic hardening
23 % MatType = 2: Bilinear material with isotropic hardening
24 MatType = 2;
25 %
26 % Preface
27 Unit = {'kN', 'mm'};
28 StrMode = {2, 2};
29 %
30 % Control block
31 Iteration = {'static', { {'NewtonRaphson', 10, 1.0e-8, 'DisplNorm'} ;
32                           {'ModifiedNewtonRaphson', 20, 1.0e-8, 'EnergyNorm'}};

```

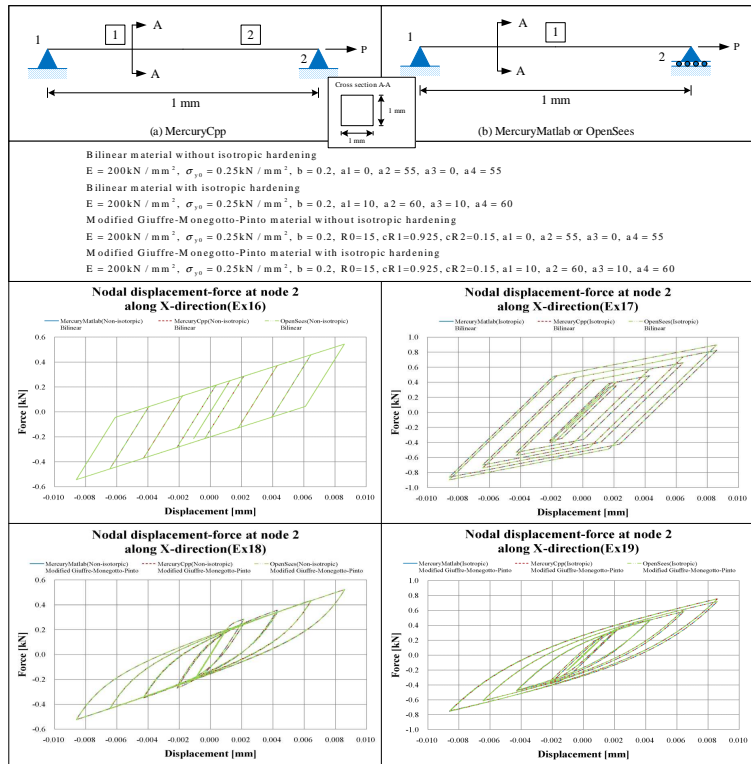


Figure 3.4: Examples 16- 19

```

33 %' InitialStiffness', 30, 1.0e-8, 'ForceNorm');
34 %
35 %
36 % Geometry block
37 nodcoord = {1, 0, 0;
38             2, 1, 0};
39 constraint = {1, 1, 1;
40                2, 0, 1};
41 %
42 % Element block
43 elements = {1, 'Simple2DTruss', 1, 2, 1};
44 %
45 % Section block
46 sections = {1, 'General', {1, 1, 0, 0, 0}};
47 %
48 % Material block
49 if MatType == 1
50     materials = {1, 'Bilinear', 200, 0.25, 0.2, 0, 0, 55, 0, 55};
51 elseif MatType == 2
52     materials = {1, 'Bilinear', 200, 0.25, 0.2, 0, 10, 60, 10, 60};
53 end
54 %
55 % Force block
56 DispInput = load('cyclicwave.txt');
57 row = size(DispInput, 1);
58 for i = 1:row
59     DispCell{i} = 0.005 * DispInput(i);
60 end
61 %    forctag, 'Static', {'NodalForces', {nodnum, globalaxis, m}}
62 forces = {1, 'Static', {'NodalForces', {2, 1, 0}};
63           2, 'DispCtrl', {2, 1, DispCell} };
64 %

```

### 3.3.2 C++

```

1 --- ****
2 --- MatType == 1: Bilinear material without isotropic hardening
3 --- MatType == 2: Bilinear material with isotropic hardening
4 MatType = 2
5 ---
6 nodes = { {1, 0, 0},
7           {2, 1, 0} };
8 ---
9 Simple2DTruss = 'truss2d';
10 elements = { {1, Simple2DTruss, 1, 2, 1, 1} }
11 ---
12 if (MatType == 1) then
13 --- materials = {tag, 'bilinear', E, rho, fy, b_ratio, a1,a2, a3, a4}
14     materials = { {1,'bilinear', 200, 0, 0.25, 0.2, 0, 55, 0, 55} };

```

```

15 end
16 if (MatType == 2) then
17     materials = { {1,'bilinear', 200, 0, 0.25, 0.2, 10, 60, 10, 60} }
18 end
19 *****
20 model = StructureModel(2,2)
21 model:addNodes(nodes)
22 model:addMaterials(materials)
23 model:addElements(elements)
24 model:constrainNode(1,1,1)
25 model:constrainNode(2,1,1)
26 *****
27 function generateincrementalload()
28     format:  
         tag          node dof
29     local loadform = {'incrementalnodaldisplacement', 2, 1}
30     local f = assert(io.open('cyclicwave.txt','r'))
31     local n = f:read('*number')
32     while (n ~= nil) do
33         table.insert(loadform, 0.005*n)
34         n = f:read('*number')
35     end
36     f:close()
37     return loadform
38 end
39 *****
40 staticloading = LoadDescription()
41 format: 'staticnodalload' <bnode> <bdof> <amplitude>
42 l = generateincrementalload()
43 staticloading:addLoad(l)
44 *****
45 Static analysis
46 print("Static analysis started\n")
47 displ = {}
48 function displperstep(increment)
49     dx2,dy2 = model:nodeDisplacements(2)
50     table.insert(displ, dx2)
51 end
52 ---
53 react = {}
54 function reactperstep(increment)
55     fx1,fy1 = model:nodeRestoringForces(1)
56     table.insert(react, fx1)
57 end
58 ---
59 solver = NonlinearSolver("initialstiffness", { displacementdeltatolerance=1e-3, iterations=10000})
60 analysis = StaticAnalysis(solver)
61 analysis:setStructureModel(model)
62 analysis:adccallback(displperstep,'increment')
63 analysis:adccallback(reactperstep,'increment')
64 analysis:solve(staticloading)
65 *****
66 Set output file
67 function writedata1(x, fname)
68     local f = assert(io.open(fname,'w'))
69     local writenl = 0
70     for i,v in ipairs(x) do
71         f:write(v, " ")
72         writenl = writenl + 1
73         -- length of row size: writenl
74         if (writenl > 0) then
75             writenl = 0
76             f:write("\n")
77         end
78     end
79     f:close()
80 end
81 if (MatType == 1) then
82     writedata1(displ,'Ex16StaticNonIsotropicNodalDisp_2.dat')
83     writedata1(react,'Ex16StaticNonIsotropicReact_1.dat')
84 end
85 if (MatType == 2) then
86     writedata1(displ,'Ex17StaticIsotropicNodalDisp_2.dat')
87     writedata1(react,'Ex17StaticIsotropicReact_1.dat')
88 end
89 print(" Static analysis ended\n")

```

```

1 %
2 % Mercury Matlab Version 1.0.1
3 % Written by Dae-Hung Kang, CU-NEES
4 % Copyright 2009, CU-NEES
5 % Written : October 2009.
6 % File name: Ex18to19.m
7 %
8 % Description
9 % 1. Static analysis
10 % 2. Displacement control
11 % 3. Iterative method
12 % 4. Simple 2D truss element
13 % 5. General sections
14 % 6. Modified Giuffre-Monegotto-Pinto material
15 %
16 % A36 Steel properties
17 % Density of 7.8 g/cm^3
18 % Minimum yield strength of 250 MPa(0.25 GPa)
19 % Ultimate tensile strength of 400–550 MPa(0.4–0.55 GPa)
20 %
21 % Select material type
22 % MatType = 1: ModGMP material without isotropic hardening
23 % MatType = 2: ModGMP material with isotropic hardening
24 MatType = 2;
25 %
26 % Preface
27 Unit      = {'kN', 'mm'};
StrMode = {2, 2};

```

```

29 %
30 % Control block
31 Iteration = {'static', { {'NewtonRaphson', 10, 1.0e-8, 'DisplNorm'} ;
32             {'ModifiedNewtonRaphson', 20, 1.0e-8, 'EnergyNorm'} ;
33             {'InitialStiffness', 30, 1.0e-8, 'ForceNorm'} ;
34         }};
35 %
36 % Geometry block
37 nodcoord = {1, 0, 0;
38             2, 1, 0};
39 constraint = {1, 1, 1;
40             2, 0, 1};
41 %
42 % Element block
43 elements = { 1, 'Simple2DTruss', 1, 2, 1}; };
44 %
45 % Section block
46 sections = { 1, 'General', {1, 1, 0, 0, 0}}; };
47 %
48 % Material block
49 if MatType == 1
50     mattag, 'ModGMP', E, sy, b, R0, cR1, cR2, density, a1, a2, a3, a4
51     materials = { {1, 'ModGMP', 200, 0.25, 0.2, 15, 0.925, 0.15, 0, 0, 55, 0, 55} };
52 elseif MatType == 2
53     materials = { {1, 'ModGMP', 200, 0.25, 0.2, 15, 0.925, 0.15, 0, 10, 60, 10, 60} };
54 end
55 %
56 % Force block
57 DispInput = load('cyclicwave.txt');
58 row = size(DispInput,1);
59 for i = 1:row
60     DispCell{i} = 0.005*DispInput(i);
61 end
62 %      forcetag, 'Static', {'NodalForces', {nodnum, globalaxis, m}}
63 forces = { 1, 'Static', {'NodalForces', {2, 1, 0}};
64             2, 'DispCtrl', {2, 1, DispCell} };
65 %

```

```

1 --- ****
2 --- MatType = 1: ModGMP material without isotropic hardening
3 --- MatType = 2: ModGMP material with isotropic hardening
4 MatType = 2
5 --- ****
6 nodes = { {1, 0, 0},
7             {2, 1, 0} };
8 --- ****
9 Simple2DTruss = 'truss2d'
10 elements = { {1, Simple2DTruss, 1, 2, 1, 1} };
11 --- ****
12 if (MatType == 1) then
13     materials = {{tag, 'modifiedGMPsteel', E, rho, fy, b_ratio, R0, cR1, cR2, a1, a2, a3, a4, sigma_init} }
14     materials = { {1,'modifiedGMPsteel', 200, 0, 0.25, 0.2, 15, 0.925, 0.15, 0.0, 55, 0, 55, 0} }
15 end
16 if (MatType == 2) then
17     materials = { {1,'modifiedGMPsteel', 200, 0, 0.25, 0.2, 15, 0.925, 0.15, 10, 60, 10, 60, 0} }
18 end
19 --- ****
20 model = StructureModel(2,2)
21 model:addNodes(nodes)
22 model:addMaterials(materials)
23 model:addElements(elements)
24 model:constrainNode(1,1,1)
25 model:constrainNode(2,1,1)
26 --- ****
27 function generateincrementalload()
28     --- format:           tag           node dof
29     local loadform = {'incrementalnodaldisplacement', 2, 1}
30     local f = assert(io.open('cyclicwave.txt','r'))
31     local n = f:read('*number')
32     while (n ~= nil) do
33         table.insert(loadform, 0.005*n)
34         n = f:read('*number')
35     end
36     f:close()
37     return loadform
38 end
39 --- ****
40 staticloading = LoadDescription()
41 --- format: 'staticnodalload' <node> <dof> <amplitude>
42 l = generateincrementalload()
43 staticloading:addLoad(l)
44 --- ****
45 --- Static analysis
46 print(" Static analysis started\n")
47 displ = {}
48 function displperstep(increment)
49     dx2,dy2 = model:nodeDisplacements(2)
50     table.insert(displ, dx2)
51 end
52 ---
53 react = {}
54 function reactperstep(increment)
55     fx1,fy1 = model:nodeRestoringForces(1)
56     table.insert(react, fx1)
57 end
58 ---
59 solver = NonlinearSolver("initialstiffness", { displacementdeltatolerance=1e-3, iterations=10000})
60 analysis = StaticAnalysis(solver)
61 analysis:setStructureModel(model)
62 analysis:adDCALLBACK(displperstep,"increment")
63 analysis:adDCALLBACK(reactperstep,"increment")
64 analysis:solve(staticloading)
65 --- ****
66 --- Set output file
67 function writedata(x, fname)

```

```

68 local f = assert(io.open(fname, 'w'))
69 local writenl = 0
70 for i,v in ipairs(x) do
71   f:write(v, " ")
72   writenl = writenl + 1
73   if length of row size: writenl
74   if (writenl > 0) then
75     writenl = 0
76     f:write("\n")
77   end
78 end
79 f:close()
80
81 if (MatType == 1) then
82   writedata1(displ, 'Ex18StaticNonIsotropicNodalDisp_2.dat')
83   writedata1(react, 'Ex18StaticNonIsotropicReact_1.dat')
84 end
85 if (MatType == 2) then
86   writedata1(displ, 'Ex19StaticIsotropicNodalDisp_2.dat')
87   writedata1(react, 'Ex19StaticIsotropicReact_1.dat')
88 end
89 print(" Static analysis ended\n")
90

```

### 3.4 Steel Beam-columns, Fiber Section, Static, Transient (HHT and Shing)

Beam column elements with layered section, and hardening material are analyzed next, Fig. ???. The Cyclic displacement shown in Fig. 3.2, magnified by a factor of 50 are applied on node 3 in the  $X$  direction. Ex20 has stiffness-based beam-column, Ex21 has flexibility-based beam-column with element iteration, and Ex22 has flexibility-based beam-column without element iteration. For transient analysis, HHT integration scheme in Ex20 and Shing method in Ex21 are used with  $\alpha = -0.1$ ,  $\beta = 0.3025$  and  $\gamma = 0.6$ .

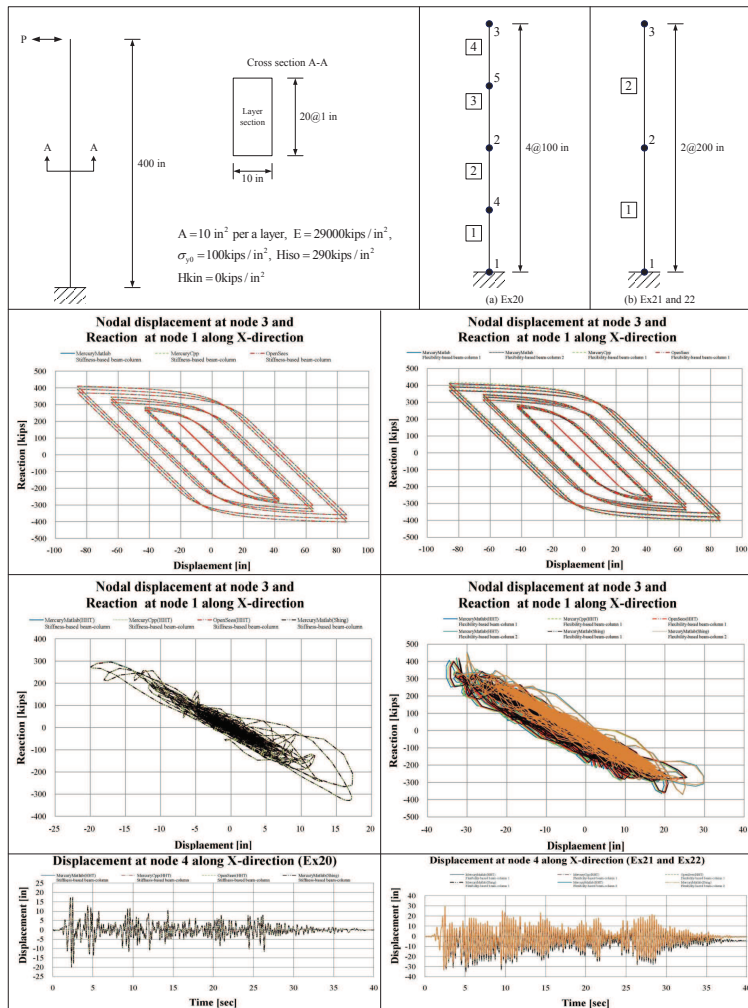


Figure 3.5: Examples 20- 22

```

1 %%%%%%%%%%%%%%%%%%%%%%%%%%%%%%%%%%%%%%
2 % Mercury Matlab Version 1.0.1
3 % Written by Dae-Hung Kang, CU-NEES
4 % Copyright 2009, CU-NEES
5 % Written : October 2009.
6 % File name: Ex20to22.m
7 %
8 % Description
9 % 1. Static and transient analysis
10 % 2. Load control
11 % 3. Iterative method
12 % 4. Stiffness-based 2D beam-column,
13 %    flexibility-based 2D beam-column 1 and 2
14 % 5. Layer sections
15 % 6. Hardening material
16 %
17 % Section AnalysisType
18 % AnalysisType = 1: Displacement Control
19 % AnalysisType = 2: Transient analysis
20 AnalysisType = 2;
21 %
22 % Section DynType
23 % DynType = 1: Newmark beta
24 % DynType = 2: HHT
25 % DynType = 3: Shing
26 % DynType = 4: None
27 DynType = 3;
28 %
29 % Section EleType
30 % EleType = 1: Stiffness-based 2D beam-column
31 % EleType = 2: Flexibility-based 2D beam-column by Spacone
32 % EleType = 3: Flexibility-based 2D beam-column by Carol
33 EleType = 2;
34 %
35 % Preface
36 Unit      = {'kip', 'in'};
37 StrMode   = {2, 3};
38 %
39 % Control block
40 if ( (EleType == 1 || EleType == 2) && (DynType == 1 || DynType == 2) )
41     Iteration = {'static', { {'NewtonRaphson', 100, 1.0e-6, 'ForceNorm'},
42                     {'ModifiedNewtonRaphson', 1000, 1.0e-6, 'ForceNorm'},
43                     {'InitialStiffness', 10000, 1.0e-6, 'ForceNorm'}},
44                     'transient', { {'NewtonRaphson', 10, 1.0e-3, 'DisplNorm'},
45                     {'ModifiedNewtonRaphson', 100, 1.0e-3, 'DisplNorm'},
46                     {'InitialStiffness', 1000, 1.0e-3, 'DisplNorm'}},
47                     'element', { {'NewtonRaphson', 100, 1.0e-3, 'DisplNorm'},
48                     {'ModifiedNewtonRaphson', 1000, 1.0e-3, 'DisplNorm'},
49                     {'InitialStiffness', 100000, 1.0e-3, 'DisplNorm'}},
50                     } };
51 else
52     Iteration = {'static', { {'InitialStiffness', 10000, 1.0e-6, 'ForceNorm'}},
53                     'transient', { {'InitialStiffness', 100000, 1.0e-3, 'DisplNorm'}},
54                     } };
55 elseif ( (EleType == 3) && (DynType == 1 || DynType == 2) )
56     Iteration = {'static', { {'InitialStiffness', 10000, 1.0e-6, 'ForceNorm'}},
57                     'transient', { {'InitialStiffness', 100000, 1.0e-3, 'DisplNorm'}},
58                     } };
59 else
60     if (DynType == 3)
61         Iteration = {'static', { {'NewtonRaphson', 100, 1.0e-6, 'ForceNorm'},
62                     {'ModifiedNewtonRaphson', 1000, 1.0e-6, 'ForceNorm'},
63                     {'InitialStiffness', 10000, 1.0e-6, 'ForceNorm'}},
64                     'transient', { {'InitialStiffness', 100000, 1.0e-3, 'DisplNorm'}}, % for shing method
65                     } };
66         'element', { {'NewtonRaphson', 100, 1.0e-3, 'DisplNorm'},
67                     {'ModifiedNewtonRaphson', 1000, 1.0e-3, 'DisplNorm'},
68                     {'InitialStiffness', 100000, 1.0e-3, 'DisplNorm'}},
69                     } };
70     end;
71 end
72 %
73 if (DynType == 1)
74     Integration = {'Newmark', 0, 1/4, 1/2, 0, 0};
75     eigens      = {0.02, 0.02};
76 end
77 if (DynType == 2)
78     Integration = {'HHT', 0, -0.1, 0.3025, 0.6, 0, 0};
79     eigens      = {0.02, 0.02};
80 end
81 if (DynType == 3)
82     Integration = {'Shing', 0, -0.1, 0.3025, 0.6, 0, 0, 10};
83     eigens      = {0.02, 0.02};
84 end
85 %
86 % Geometry block
87 if (EleType == 1)
88     nodcoord = {1, 0, 0;
89                 4, 0, 100;
90                 2, 0, 200;
91                 5, 0, 300;
92                 3, 0, 400};
93 else
94     nodcoord = {1, 0, 0;
95                 2, 0, 200;
96                 3, 0, 400};
97 end
98 %
99 % nodtag, x, y, z
100 constraint = {1, 1, 1, 1};
101 %
102 % Element block
103 % elements = { { eletag, 'eletype', in, jn, nIp, sectag } };
104 if (EleType == 1)
105     elements = { {1, 'StiffnessBased2DBeamColumn', 1, 4, 5, 1},
106                  {2, 'StiffnessBased2DBeamColumn', 4, 2, 5, 1},
107                  {3, 'StiffnessBased2DBeamColumn', 2, 5, 5, 1}};


```

```

108     {4, 'StiffnessBased2DBeamColumn', 5, 3, 5, 1};};
109 elseif (EleType == 2)
110     elements = { {1, 'FlexibilityBased2DBeamColumn1', 1, 2, 5, 1};
111                 {2, 'FlexibilityBased2DBeamColumn1', 2, 3, 5, 1};};
112 elseif (EleType == 3)
113     elements = { {1, 'FlexibilityBased2DBeamColumn2', 1, 2, 5, 1};
114                 {2, 'FlexibilityBased2DBeamColumn2', 2, 3, 5, 1};};
115 end
116 %
117 % Section block
118 % b = 10, h = 20, number of layer = 10, hlayer = 2
119 area = 10; mtag = 1; count = 0;
120 for ydis = -9.5:1.0:9.5
121     count = count + 1; lay(count,1:3) = [mtag, area, ydis];
122 end
123 nlay = size(lay,1);
124 for i = 1:nlay
125     laycell{i,1}=lay(i,1); laycell{i,2}=lay(i,2); laycell{i,3}=lay(i,3);
126 end
127 % sections = { sectag, 'Layer', {mattag, A, y} }
128 sections = { {1, 'Layer', laycell} };
129 clear area; clear mtag; clear count; clear nlay; clear lay;
130 clear laycell; clear i; clear ydis;
131 %
132 % Material block
133 % mass density = 15.2 (slug/ft^3)
134 % = 15.2 (lb*s^2/ft^3)
135 % = 15.2*(10^-3)/(12^4) (kips*s^2/in^4)
136 materials = { {1, 'Hardening', 29*10^-3, 100, 290, 0, 7.3302e-007} };
137 %
138 % Force block
139 if (AnalysisType == 1)
140     DispInput = load('cyclicwave.txt');
141     row = size(DispInput,1);
142     for i = 1:row
143         DispCell{i} = 50*DispInput(i);
144     end
145     forces = { {1, 'Static', {'NodalForces', {3, 1, 0} } },
146                 {2, 'DispCtrl', {3, 1, DispCell} } };
147     clear DispInput; clear row; clear i; clear DispCell;
148 elseif (AnalysisType == 2)
149     ga = load('ElCentro-g-0-01-Matlab.txt');
150     nga = size(ga, 1);
151     for i = 1:nga
152         groundacceleration{i,1} = ga(i,1);
153         groundacceleration{i,2} = ga(i,2);
154         groundacceleration{i,3} = ga(i,3);
155     end
156     forces = { {1, 'Static', {'NodalForces', {3, 1, 0} } },
157                 {2, 'Acceleration', {50*386.4, groundacceleration} } };
158     clear ga; clear nga; clear i; clear groundacceleration;
159 end
160 %

```

```

1 --- **** AnalysisType = 1: Static analysis
2 --- AnalysisType= 2: Trnsient analysis
3 AnalysisType = 2
4 EleType = 2
5 --- EleType = 1: Stiffness-based beam-column
6 --- EleType = 2: Flexibility-based beam-column
7 EleType = 1
8 ---
9 if (EleType == 1) then
10     nodes = {{1, 0, 0};
11                 {4, 0, 100, 'mass', 0.0146604, 0.0146604, 0};
12                 {2, 0, 200, 'mass', 0.0146604, 0.0146604, 0};
13                 {5, 0, 300, 'mass', 0.0146604, 0.0146604, 0};
14                 {3, 0, 400, 'mass', 0.0073302, 0.0073302, 0}};
15     elements = { {1, 'StiffnessBased2DBeamColumn', 1, 4, {1, 5} };
16                 {2, 'StiffnessBased2DBeamColumn', 4, 2, {1, 5} };
17                 {3, 'StiffnessBased2DBeamColumn', 2, 5, {1, 5} };
18                 {4, 'StiffnessBased2DBeamColumn', 5, 3, {1, 5} } };
19 end
20 if (EleType == 2) then
21     nodes = {{1, 0, 0};
22                 {2, 0, 200, 'mass', 0.0293208, 0.0293208, 0};
23                 {3, 0, 400, 'mass', 0.0146604, 0.0146604, 0}};
24     flexparams = {100000, 1e-3}
25     elements = { {1, 'FlexibilityBased2DBeamColumn', 1, 2, {1, 5}, flexparams },
26                 {2, 'FlexibilityBased2DBeamColumn', 2, 3, {1, 5}, flexparams } };
27 end
28 --
29
30 sections = {
31 1, 'Fiber',
32 --- MatTag, Area, y-loc, z-loc
33 { 1, 10, -9.5, 0;
34 1, 10, -8.5, 0;
35 1, 10, -7.5, 0;
36 1, 10, -6.5, 0;
37 1, 10, -5.5, 0;
38 1, 10, -4.5, 0;
39 1, 10, -3.5, 0;
40 1, 10, -2.5, 0;
41 1, 10, -1.5, 0;
42 1, 10, -0.5, 0;
43 1, 10, 0.5, 0;
44 1, 10, 1.5, 0;
45 1, 10, 2.5, 0;
46 1, 10, 3.5, 0;
47 1, 10, 4.5, 0;
48 1, 10, 5.5, 0;
49 1, 10, 6.5, 0;
50 1, 10, 7.5, 0;
51 1, 10, 8.5, 0;

```

```

52     1, 10, 9.5, 0; } };
53
54 materials = { {1,'hardening',29000, 0, 100, 290, 0} }
55
56 model = StructureModel(2,3)
57 model:addNodes(nodes)
58 model:addMaterials(materials)
59 model:addSections(sections)
60 model:addElements(elements)
61 model:constrainNode(1,1,1,1)
62 if (AnalysisType == 1) then
63     model:constrainNode(3,1,0,0)
64 end
65
66 -- Static analysis
67 if (AnalysisType == 1) then
68     print("Static analysis started\n")
69     function generateincrementalload()
70         format: tag node dof
71         local loadform = {'incrementalnodaldisplacement', 3, 1}
72         local f = assert(io.open('cyclicwave.txt','r'))
73         local n = f:read('*number')
74         while (n ~= nil) do
75             table.insert(loadform, 50*n)
76             n = f:read('*number')
77         end
78         f:close()
79         return loadform
80     end
81
82 staticloading = LoadDescription()
83 format: 'staticnodalload' <node> <dof> <amplitude>
84 l = generateincrementalload()
85 staticloading:addLoad(l)
86
87 displ = {}
88 function displperstep(increment)
89     dx3,dy3,dz3 = model:nodeDisplacements(3)
90     table.insert(displ, dx3)
91 end
92
93 react = {}
94 function reactperstep(increment)
95     fx1,fy1,fz1 = model:nodeRestoringForces(1)
96     table.insert(react, fx1)
97 end
98
99
100 --solver = NonlinearSolver("newtonraphson", { displacementdeltatolerance=1e-3, iterations=100})
101 solver = NonlinearSolver("initialstiffness", { displacementdeltatolerance=1e-3, iterations=1000000})
102 analysis = StaticAnalysis(solver)
103 analysis:setStructureModel(model)
104 analysis:adDCALLBACK(displperstep,"increment")
105 analysis:adDCALLBACK(reactperstep,"increment")
106 analysis:solve(staticloading)
107
108 -- Set output file
109 function writedata(x, fname)
110     local f = assert(io.open(fname,'w'))
111     local writenl = 0
112     for i,v in ipairs(x) do
113         f:write(v, "\n")
114         writenl = writenl + 1
115     end
116     if (writenl > 0) then
117         writenl = 0
118         f:write("\n")
119     end
120 end
121 f:close()
122 end
123
124 if (EleType == 1) then
125     writedata(displ,'Ex20StaticNodalDisp_3.dat')
126     writedata(react,'Ex20StaticReact_1.dat')
127 end
128 if (EleType == 2) then
129     writedata(displ,'Ex21StaticNodalDisp_3.dat')
130     writedata(react,'Ex21StaticReact_1.dat')
131 end
132 print("Static analysis ended\n")
133
134
135 if (AnalysisType == 2) then
136     print("Transient analysis started\n")
137     earthquakeloading = LoadDescription()
138     accelamp = 50*386.4
139     earthquakeloading:addLoad({'groundmotion','ElCentro_g_0_01_OpenSees.txt',dt=0.01, 1,accelamp})
140
141 displ = {}
142 function displpertime(time)
143     dx3,dy3,dz3 = model:nodeDisplacements(3)
144     table.insert(displ, dx3)
145 end
146
147 react = {}
148 function reactpertime(time)
149     fx1,fy1,fz1 = model:nodeRestoringForces(1)
150     table.insert(react, fx1)
151 end
152
153 --solver = NonlinearSolver("newtonraphson", { displacementdeltatolerance=1e-3, iterations=100})
154 solver = NonlinearSolver("initialstiffness", { displacementdeltatolerance=1e-3, iterations=1000})
155 transientanalysis = DynamicAnalysis("HHT", model, solver, earthquakeloading, 0.01, -0.1, 0.3025, 0.6)
156 transientanalysis:adDCALLBACK(displpertime, "timestep")
157 transientanalysis:adDCALLBACK(reactpertime, "timestep")
158 if (EleType == 1) then

```

```

159     model:setRayleighCoefficients(9.693343,0.000038)
160   end
161   if (EleType == 2) then
162     model:setRayleighCoefficients(0.757867,0.000287)
163   end
164   transientanalysis:solve(4000)
165   ****
166   function writedata1(x, fname)
167     local f = assert(io.open(fname, 'w'))
168     local writenl = 0
169     for i,v in ipairs(x) do
170       f:write(v, " ")
171       writenl = writenl + 1
172       if length of row size: writenl
173       if (writenl > 0) then
174         writenl = 0
175         f:write("\n")
176       end
177     end
178   f:close()
179 end
180 if (EleType == 1) then
181   writedata1(displ,'Ex20HHTNodalDisp_3.dat')
182   writedata1(react,'Ex20HHTReact_1.dat')
183 end
184 if (EleType == 2) then
185   writedata1(displ,'Ex21HHTNodalDisp_3.dat')
186   writedata1(react,'Ex21HHTReact_1.dat')
187 end
188 print(" Transient analysis ended\n")
190
191 ****

```

### 3.5 Zero-length and Beam Column, Nonlinear Steel Element, load control

The implementation of the zero-length element is examined next in combination with stiffness-based beam-column and zero-length element, elastic and bilinear materials, Fig. 3.6. The incremental forces are increase by -10kN up to -50kN at node 2 in the  $X$  direction.

```

1 % Mercury Matlab Version 1.0.1
2 % Written by Dae-Hung Kang, CU-NEES
3 % Copyright 2009, CU-NEES
4 % Written : October 2009.
5 % File name: Ex23.m
6 %
7 % Description
8 % 1. Static analysis
9 % 2. Static force and load control
10 % 3. Iterative method
11 % 4. Stiffness-based 2D beam column and Zero-Length 2D element
12 % 5. General section
13 % 6. Bilinear material
14 %
15 % Preface
16 Unit      = {'kip', 'in'};
17 StrMode   = {2, 3};
18 %
19 % Control block
20 Iteration = {'static', { 'InitialStiffness', 100, 1.0e-8, 'ForceNorm' };
21           }
22           };
23 %
24 % Geometry block
25 nodcoord  = {1, 0, 0;
26               2, 0, 0;
27               3, 0, 120};
28 constraint = {1, 1, 1, 1;
29                 3, 1, 1, 1};
30 %
31 % Element block
32 elements = { {1, 'ZeroLength2D', 1, 2, 0, 1, 0, deg2rad(90)}
33             {2, 'StiffnessBased2DBeamColumn', 2, 3, 1, 1} };
34 %
35 % Section block
36 sections = { 1, 'General', {2, 20, 0, 0, 1400} };
37 %
38 % Material block
39 materials = { {1, 'Bilinear', 1050, 21, 0.2, 0, 0, 1, 0, 1};
40             {2, 'Elastic', 30000, 0, 0} };
41 %
42 % Force block
43 forces = { 1, 'Static', { 'NodalForces', {2, 1, -10} };
44             2, 'LoadCtrl', {2, 1, {-20,-30,-40,-50} } };
45 %

```

```

1 --- ****
2 nodes = { {1, 0, 0};
3           {2, 0, 0};
4           {3, 0, 120} };
5 --- ****
6 --- { eleTag, 'InterfaceElement2D', inode, jnode, { {matTag, {1,0,0} } }, { {secTag}, {0,1,0},{-1,0,0} } }
7 elements = { {1, 'InterfaceElement2D', 1, 2, { {1, {1,0,0} } } }, {} };
8           {2, 'StiffnessBased2DBeamColumn', 2, 3, { {1, 1} } } };
9 --- ****
10 sections = { 1, 'general', {2, 20, 1400} };
11 ---
12 materials = { {1,'bilinear', 1050, 0, 21, 0.2, 0, 1, 0, 1};
13             {2,'elastic',30000, 0.0} };
14 --- ****

```

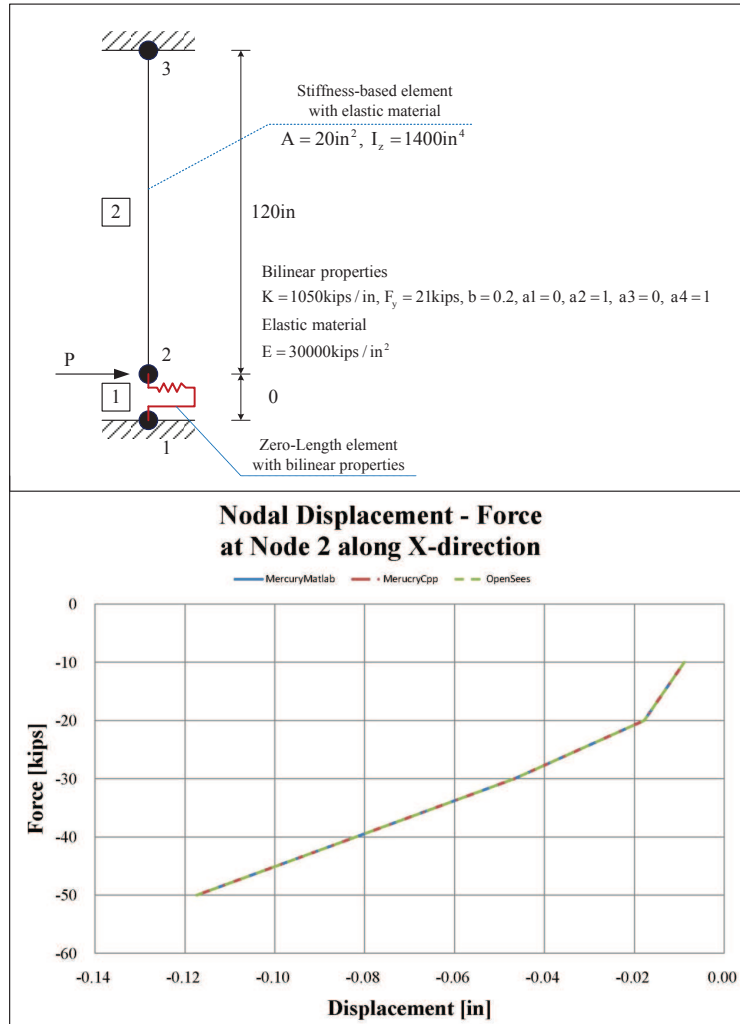


Figure 3.6: Examples 23

```

15 model = StructureModel(2,3)
16 model:addNodes(nodes)
17 model:addMaterials(materials)
18 model:addSections(sections)
19 model:addElements(elements)
20 *****
21 model:constrainNode(1,1,1,1)
22 model:constrainNode(3,1,1,1)
23 *****
24 staticloading = LoadDescription()
25 staticloading:addLoad({'incrementalnodalload', 2, 1, -10,-20,-30,-40,-50})
26 *****
27 displ = {}
28 function displperstep(increment)
29     dx2,dy2,dz2 = model:nodeDisplacements(2)
30     table.insert(displ, dx2)
31 end
32 solver = NonlinearSolver("newtonraphson", { displacementdeltatolerance=le-5, iterations=100})
33 analysis = StaticAnalysis(solver)
34 analysis:setStructureModel(model)
35 analysis:adDCALLBACK(displperstep,"increment")
36 analysis:solve(staticloading)
37 *****
38 Set output file
39 function writedata1(x, fname)
40     local f = assert(io.open(fname,'w'))
41     local writtenl = 0
42     for i,v in ipairs(x) do
43         f:write(v, " ")
44         writtenl = writtenl + 1
45         -- length of row size: writtenl
46         if (writtenl > 0) then
47             writtenl = 0
48             f:write("\n")
49         end
50     end
51     f:close()
52 end
53 writedata1(displ, 'Ex23NodalDisp-2.dat')

```

### 3.6 Zero-length Section, and Beam Column, Fiber, Nonlinear Steel Element, load control

The zero length section element is validated next in a similar way as in the preceding example, Fig. 3.7. Incremental forces of  $-20\text{kN}$  up to  $-400\text{kN}$  are applied on node 2 in the X direction.

```

1 % Mercury Matlab Version 1.0.1
2 % Written by Dae-Hung Kang, CU-NEES
3 % Copyright 2009, CU-NEES
4 % Written : October 2009.
5 % File name: Ex24.m
6 %
7 %
8 % Description
9 % 1. Static analysis
10 % 2. Static force and load control
11 % 3. Iterative method
12 % 4. Stiffness-based 2D beam column and Zero-Length 2D section element
13 % 5. General section
14 % 6. Bilinear material
15 %
16 % Preface
17 Unit      = {'kip', 'in'};
18 StrMode   = {2, 3};
19 %
20 % Control block
21 Iteration = {'static', { {'InitialStiffness', 100, 1.0e-8, 'ForceNorm'} ;
22           }};
23 %
24 %
25 % Geometry block
26 nodcoord = {1, 0, 0;
27             2, 0, 0;
28             3, 0, 120};
29 constraint = {1, 1, 1, 1;
30                 3, 1, 1, 1};
31 %
32 %
33 % Element block
34 elements = { {1, 'ZeroLength2DSection', 1, 2, deg2rad(90), 1}
35           {2, 'StiffnessBased2DBeamColumn', 2, 3, 3, 2} };
36 %
37 % Section block
38 sections = { 2, 'Layer', {2, 12, 5.5;
39                     2, 12, 4.5;
40                     2, 12, 3.5;
41                     2, 12, 2.5;
42                     2, 12, 1.5;
43                     2, 12, 0.5;
44                     2, 12, -0.5;
45                     2, 12, -1.5;
46                     2, 12, -2.5;
47                     2, 12, -3.5;
48                     2, 12, -4.5;
49                     2, 12, -5.5};
50           1, 'Layer', {1, 12, 5.5;
51                     1, 12, 4.5;
52                     1, 12, 3.5;
53                     1, 12, 2.5;
54                     1, 12, 1.5;
55                     1, 12, 0.5;
56                     1, 12, -0.5;
57                     1, 12, -1.5;
58                     1, 12, -2.5;
59                     1, 12, -3.5;
60                     1, 12, -4.5;
61                     1, 12, -5.5};
62           };
63

```

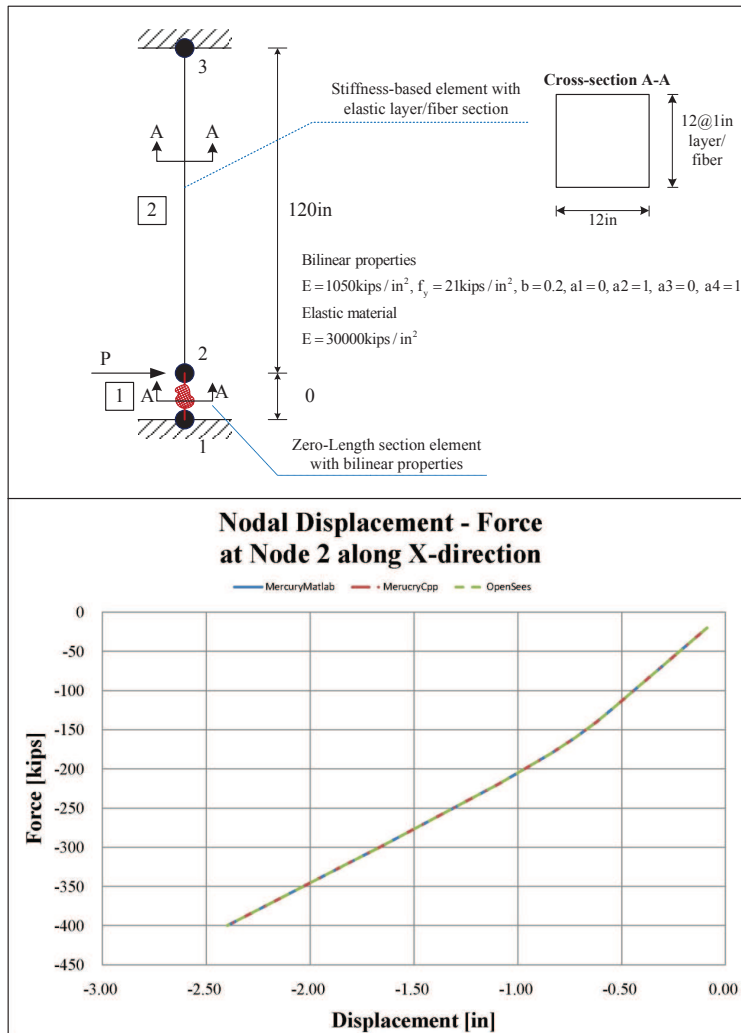


Figure 3.7: Examples 24

```

59           1, 12, -4.5;
60           1, 12, -5.5} } ;
61 %
62 % Material block
63 materials = { {1, 'Bilinear', 1050, 21, 0.2, 0, 0, 1, 0, 1};
64           {2, 'Elastic', 30000, 0, 0} } ;
65 %
66 % Force block
67 forces = { {1, 'Static', {'NodalForces', {2, 1, -20}}};
68           2, 'LoadCtrl', {2, 1, {-40, -60, -80, -100, -120,...,
69                         -140, -160, -180, -200, -220,...,
70                         -240, -260, -280, -300, -320,...,
71                         -340, -360, -380, -400} } } ;
72 %

```

```

1 -----
2 nodes = { {1, 0, 0};
3           {2, 0, 0};
4           {3, 0, 120} } ;
5 -----
6 { eleTag, 'InterfaceElement2D', inode, jnode, { {matTag, {1,0,0} } }, { {secTag} }, {0,1,0},{-1,0,0} } ;
7 elements = { {1, 'InterfaceElement2D', 1, 2, {}, {{1}}, {0,1,0},{-1,0,0} } ;
8           {2, 'StiffnessBased2DBeamColumn', 2, 3, {2, 3}} } ;
9 -----
10 sections = {1, 'Fiber', {1, 12, 5.5, 0;
11           1, 12, 4.5, 0;
12           1, 12, 3.5, 0;
13           1, 12, 2.5, 0;
14           1, 12, 1.5, 0;
15           1, 12, 0.5, 0;
16           1, 12, -0.5, 0;
17           1, 12, -1.5, 0;
18           1, 12, -2.5, 0;
19           1, 12, -3.5, 0;
20           1, 12, -4.5, 0;
21           1, 12, -5.5, 0};
22           2, 'Fiber', {2, 12, 5.5, 0;
23           2, 12, 4.5, 0;
24           2, 12, 3.5, 0;
25           2, 12, 2.5, 0;
26           2, 12, 1.5, 0;
27           2, 12, 0.5, 0;
28           2, 12, -0.5, 0;
29           2, 12, -1.5, 0;
30           2, 12, -2.5, 0;
31           2, 12, -3.5, 0;
32           2, 12, -4.5, 0;
33           2, 12, -5.5, 0};
34       };
35 -----
36 materials = { {1,'bilinear', 1050, 0, 21, 0.2, 0, 1, 0, 1};
37           {2,'elastic ',30000, 0.0} } ;
38 -----
39 model = StructureModel (2,3)
40 model: addNodes(nodes)
41 model: addMaterials(materials)
42 model: addSections(sections)
43 model: addElements(elements)
44 -----
45 model: constrainNode (1,1,1,1)
46 model: constrainNode (3,1,1,1)
47 -----
48 staticloading = LoadDescription()
49 staticloading: addLoad({ 'incrementalnodalload', 2, 1, -20,-40,-60,-80,-100,-120,-140,-160,-180,-200,-220,-240,-260,-280,-300,-320,-340 });
50 -----
51 displ = {}
52 function displperstep(increment)
53   dx2,dy2,dz2 = model: nodeDisplacements(2)
54   table.insert(displ, dx2)
55 end
56 solver = NonlinearSolver("newtonraphson", { displacementdeltatolerance=1e-5, iterations=100})
57 analysis = StaticAnalysis(solver)
58 analysis: setStructureModel(model)
59 analysis: addcallback(displperstep,'increment')
60 analysis: solve(staticloading)
61 -----
62 Set output file
63 function writedata1(x, fname)
64   local f = assert(io.open(fname,'w'))
65   local writenl = 0
66   for i,v in ipairs(x) do
67     f:write(v, " ")
68     writenl = writenl + 1
69     length of row size: writenl
70     if (writenl > 0) then
71       writenl = 0
72       f:write("\n")
73     end
74   end
75   f:close()
76 end
77 writedata1(displ, 'Ex24NodalDisp.2.dat')
```

### 3.7 Beam-column, Fiber Section, Nonlinear Material, multi-d.o.f.s displacement control, Pushover Analysis

Validation of displacement control at multiple free degrees of freedom, as described in 4.5 is performed next. Layered sections beam-column elements with hardening material are used, Fig. ???. Cyclic displacements shown in Fig. 3.2 are applied at node 2 and 3 magnified by a facotr of -30 and 50 respectively. Ex25 has stiffness-based beam-column and Ex26 has flexibility-based beam-column.

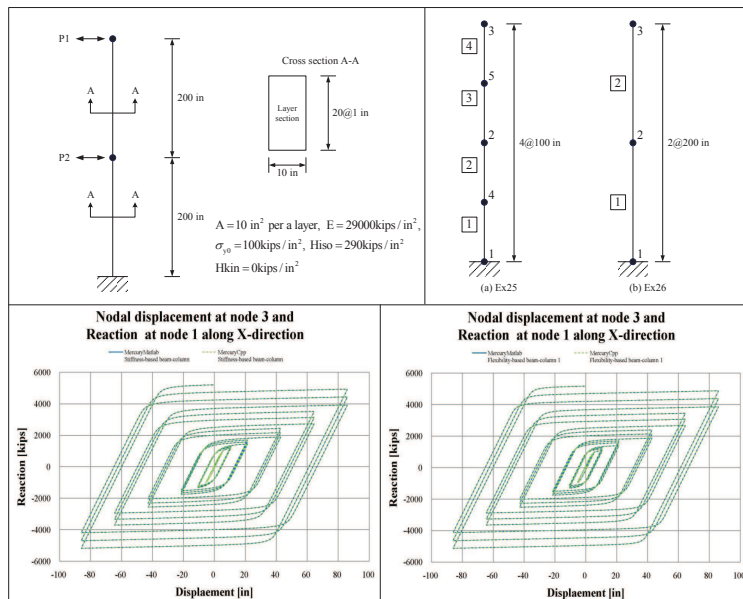


Figure 3.8: Examples 25- 26

```

1 %
2 % Mercury Matlab Version 1.0.1
3 % Written by Dae-Hung Kang, CU-NEES
4 % Copyright 2009, CU-NEES
5 % Written : October 2009.
6 % File name: Ex25to26.m
7 %
8 % Description
9 % 1. Static analysis
10 % 2. Multiple displacement control
11 % 3. Iterative method
12 % 4. Stiffness-based 2D beam-column,
13 %    flexibility-based 2D beam-column 1 and 2
14 % 5. Layer sections
15 % 6. Hardening material
16 %
17 % Section EleType
18 % EleType = 1: Stiffness-based 2D beam-column
19 % EleType = 2: Flexibility-based 2D beam-column by Spacone
20 EleType = 2;
21 %
22 % Preface
23 Unit      = {'kip', 'in'};
24 StrMode   = {2, 3};
25 %
26 % Control block
27 Iteration = {'static', {
28     {'NewtonRaphson', 100, 1.0e-8, 'ForceNorm'},
29     {'ModifiedNewtonRaphson', 1000, 1.0e-8, 'ForceNorm'},
30     {'InitialStiffness', 10000, 1.0e-8, 'ForceNorm'},
31     },
32     'element', {
33         {'NewtonRaphson', 100, 1.0e-5, 'DisplNorm'},
34         {'ModifiedNewtonRaphson', 1000, 1.0e-5, 'DisplNorm'},
35         {'InitialStiffness', 100000, 1.0e-5, 'DisplNorm'}
36     }};
37 %
38 % Geometry block
39 if (EleType == 1)
40     nodcoord = {1, 0, 0;
41                 4, 0, 100;
42                 2, 0, 200;
43                 5, 0, 300;
44                 3, 0, 400};
45 elseif (EleType == 2)
46     nodcoord = {1, 0, 0;
47                 2, 0, 200;
48                 3, 0, 400};
49 end
50 %       nodtag, x, y, z
51 constraint = {1, 1, 1, 1};
52 %
53 % Element block
54 elements = { {eletag, 'eletype', in, jn, nIp, sectag} };
55 if (EleType == 1)
56     elements = { {1, 'StiffnessBased2DBeamColumn', 1, 4, 5, 1},
57                 {2, 'StiffnessBased2DBeamColumn', 4, 2, 5, 1},
58                 {3, 'StiffnessBased2DBeamColumn', 2, 5, 5, 1},
59                 {4, 'StiffnessBased2DBeamColumn', 5, 3, 5, 1} };
60 elseif (EleType == 2)
61     elements = { {1, 'FlexibilityBased2DBeamColumn1', 1, 2, 5, 1},
62                 {2, 'FlexibilityBased2DBeamColumn1', 2, 3, 5, 1} };
63 end

```

```

63 %
64 % Section block
65 % b = 10, h = 20, number of layer = 10, hlayer = 2
66 area = 10; mtag = 1; count = 0;
67 for ydis = -9.5:1.0:9.5
68 count = count + 1; lay(count ,1:3) = [mtag, area , ydis];
69 end
70 nlay = size(lay ,1);
71 for i = 1:nlay
72 laycell{i,1}=lay(i ,1); laycell{i,2}=lay(i ,2); laycell{i,3}=lay(i ,3);
73 end
74 % sections = { sectag , 'Layer' , {mattag, A, y} }
75 sections = {1, 'Layer', laycell };
76 clear area;clear mtag;clear count;clear nlay;clear lay;
77 clear laycell;clear i;clear ydis;
78 %
79 % Material block
80 % mass density = 15.2 (slug/ft^3)
81 % = 15.2 (lb*s^2/ft^3)
82 % = 15.2*(10^-3)/(12^4) (kips*s^2/in^4)
83 materials = {1, 'Hardening', 29*10^3, 100, 290, 0, 7.3302e-007};}
84 %
85 % Force block
86 DispInput = load('cyclicwave.txt ');
87 row = size(DispInput,1);
88 for i = 1:row
89 DispCell1{i} = -30*DispInput(i);
90 DispCell2{i} = 50*DispInput(i);
91 end
92 forces = { 1, 'Static' , {'NodalForces' , {3, 1, 0} } ;
93 2, 'DispCtrl' , {2, 1, DispCell1;
94 3, 1, DispCell2 } };
95 clear DispInput; clear row; clear i; clear DispCell1; clear DispCell2;
96 %

```

```

1 --- ****
2 --- EleType = 1: Stiffness-based beam-column
3 --- EleType = 2: Flexibility-based beam-column
4 EleType = 2
5 ---
6 if (EleType == 1) then
7   nodes = {{1, 0, 0},
8             {4, 0, 100},
9             {2, 0, 200},
10            {5, 0, 300},
11            {3, 0, 400}};
12   elements = { { 1, 'StiffnessBased2DBeamColumn ', 1, 4, {1, 5} },
13               { 2, 'StiffnessBased2DBeamColumn ', 4, 2, {1, 5} },
14               { 3, 'StiffnessBased2DBeamColumn ', 2, 5, {1, 5} },
15               { 4, 'StiffnessBased2DBeamColumn ', 5, 3, {1, 5} } };
16 end
17
18 if (EleType == 2) then
19   nodes = {{1, 0, 0},
20             {2, 0, 200},
21             {3, 0, 400}};
22   flexparams = {1000, 1e-5}
23   elements = { { 1, 'FlexibilityBased2DBeamColumn ', 1, 2, {1, 5}, flexparams },
24               { 2, 'FlexibilityBased2DBeamColumn ', 2, 3, {1, 5}, flexparams } };
25 end
26 ---
27 sections = {
28 1, 'Fiber',
29 --- MatTag, Area, y-loc, z-loc
30 { 1, 10, -9.5, 0;
31 1, 10, -8.5, 0;
32 1, 10, -7.5, 0;
33 1, 10, -6.5, 0;
34 1, 10, -5.5, 0;
35 1, 10, -4.5, 0;
36 1, 10, -3.5, 0;
37 1, 10, -2.5, 0;
38 1, 10, -1.5, 0;
39 1, 10, -0.5, 0;
40 1, 10, 0.5, 0;
41 1, 10, 1.5, 0;
42 1, 10, 2.5, 0;
43 1, 10, 3.5, 0;
44 1, 10, 4.5, 0;
45 1, 10, 5.5, 0;
46 1, 10, 6.5, 0;
47 1, 10, 7.5, 0;
48 1, 10, 8.5, 0;
49 1, 10, 9.5, 0; } };
50 ---
51 materials = {1,'hardening',29000, 0, 100, 290, 0} }
52 ---
53 model = StructureModel(2,3)
54 model:addNodes(nodes)
55 model:addMaterials(materials)
56 model:addSections(sections)
57 model:addElements(elements)
58 model:constrainNode(1,1,1,1)
59 model:constrainNode(2,1,0,0)
60 model:constrainNode(3,1,0,0)
61 ---
62 --- Static analysis
63 function generateincrementalload2()
64   format:           tag          node dof
65   local loadform = {'incrementalnodaldisplacement', 2, 1}
66   local f = assert(io.open('cyclicwave.txt','r'))
67   local n = f:read('*number')
68   while (n ~= nil) do
69     table.insert(loadform, -30*n)
70     n = f:read('*number')

```

```

71     end
72     f:close()
73     return loadform
74 end
75 function generateincrementalload3()
76   -- format:           tag          node dof
77   local loadform = {'incrementalnodaldisplacement', 3 , 1}
78   local f = assert(io.open('cyclicwave.txt','r'))
79   local n = f:read('*number')
80   while (n ~= nil) do
81     table.insert(loadform, 50*n)
82     n = f:read('*number")
83   end
84   f:close()
85   return loadform
86 end
87   ****
88 staticloading = LoadDescription()
89 -- format: 'staticnodalload' <node> <dof> <amplitude>
90 l2 = generateincrementalload2()
91 l3 = generateincrementalload3()
92 staticloading:addLoad(l2)
93 staticloading:addLoad(l3)
94 ****
95 displ = {}
96 function displperstep(increment)
97   dx2,dy2,dz2 = model:nodeDisplacements(2)
98   dx3,dy3,dz3 = model:nodeDisplacements(3)
99   table.insert(displ, dx2)
100  table.insert(displ, dx3)
101 end
102 --
103 react = {}
104 function reactperstep(increment)
105   fx1,fy1,fz1 = model:nodeRestoringForces(1)
106   print("Work\n");
107   table.insert(react, fx1)
108 end
109 -- solver = NonlinearSolver("newtonraphson", { displacementdeltatolerance=1e-5, iterations=100})
110 -- solver = NonlinearSolver("initialstiffness", { displacementdeltatolerance=1e-5, iterations=10000})
111 --         multisolver <type> <disp delta> <residual> <max iterations>
112 solver = NonlinearSolver("multisolver",
113                           {"newtonraphson", 1e-5, 1e-5, 100,
114                            "initialstiffness", 1e-5, 1e-5, 1000})
115
116
117 analysis = StaticAnalysis(solver)
118 analysis:setStructureModel(model)
119 analysis:adDCALLBACK(displperstep,"increment")
120 analysis:adDCALLBACK(reactperstep,"increment")
121 analysis:solve(staticloading)
122 ****
123 -- Set output file
124 function writedata1(x, fname)
125   local f = assert(io.open(fname,'w'))
126   local writenl = 0
127   for i,v in ipairs(x) do
128     f:write(v, " ")
129     writenl = writenl + 1
130   -- length of row size: writenl
131   if (writenl > 0) then
132     writenl = 0
133     f:write("\n")
134   end
135 end
136 end
137 f:close()
138 end
139 function writedata2(x, fname)
140   local f = assert(io.open(fname,'w'))
141   local writenl = 0
142   for i,v in ipairs(x) do
143     f:write(v, " ")
144     writenl = writenl + 1
145   -- length of row size: writenl
146   if (writenl > 1) then
147     writenl = 0
148     f:write("\n")
149   end
150 end
151 f:close()
152 end
153
154 if (EleType == 1) then
155   writedata2(displ,'Ex25NodalDisp_2-3.dat')
156   writedata1(react,'Ex25React_1.dat')
157 end
158 if (EleType == 2) then
159   writedata2(displ,'Ex26NodalDisp_2-3.dat')
160   writedata1(react,'Ex26React_1.dat')
161 end

```

### 3.8 Reinforced Concrete Beam-Column, Fiber Section, Transient Analysis

This example consists of four types of beam-column element with layer section and material constitutive models for reinforced concrete, Fig. 3.9. In Ex27, material constitutive model of confined (core) or unconfined (cover) concrete using the modified Kent-Park model, whereas in Ex28, material constitutive model of confined (core) or unconfined (cover) concrete based on the anisotropic damage model with permanent strain are used. Steel is modeled with the modified Giuffre-Monegotto-Pinto model, and the shear spring in the zero-length element has a bilinear model.

At the base, a zero-length section and zero-length element are used to capture bond-slip. Fig. 3.10 succinctly describes the bar-slip zero-length fiber-section element (?) used. ? uses an empirically derived stress-deformation relation for the bar-slip fiber material between concrete and reinforcement. The material properties of the concrete are the same as those in the adjacent column element

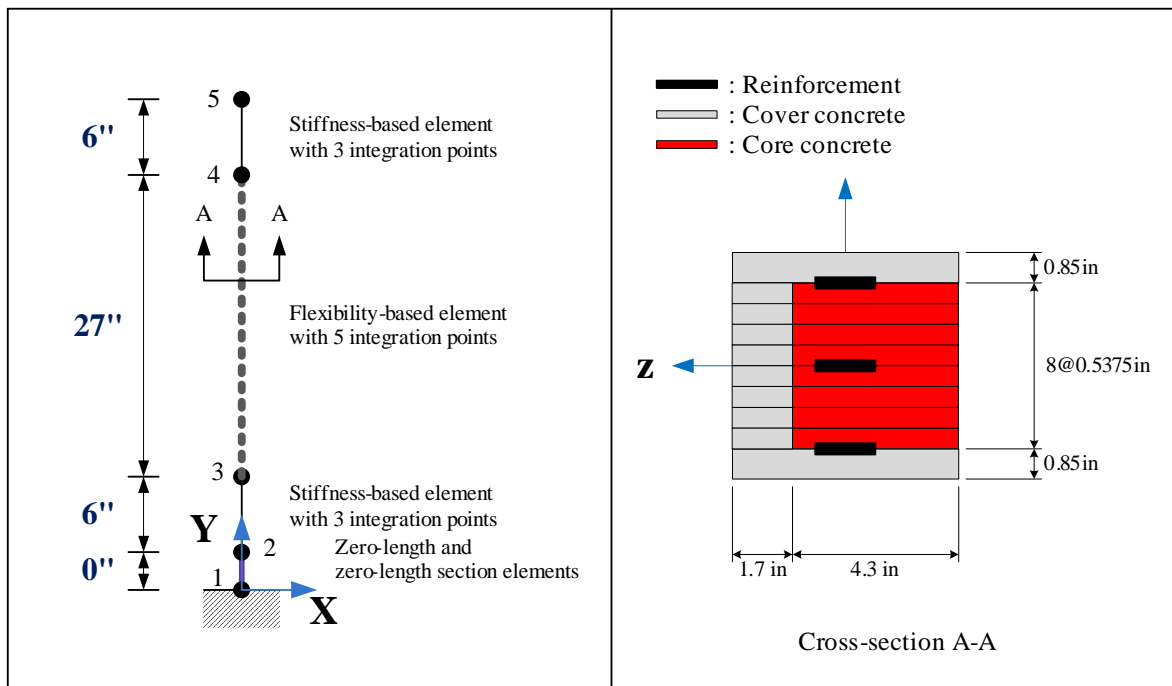


Figure 3.9: Beam-column elements for Ex27 and Ex28

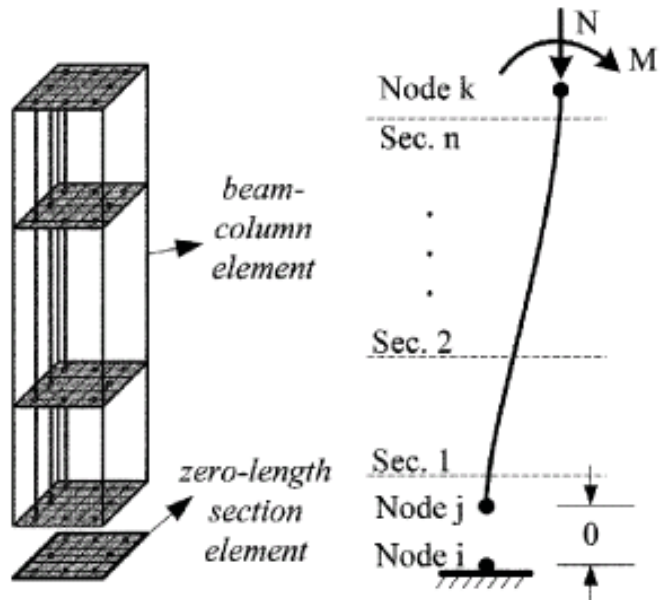


Figure 3.10: Bar slip zero-length fiber section element (?)

except the residual stress at large strains is taken as  $0.8 \cdot \sigma'_c$  (?). Zero-length elements are used to account for shear-deformations using elastic spring elements at both ends of beams and columns as well. The joints are assumed to be rigid otherwise.

Table 3.2 to 3.5 describe material properties of Ex27 and Ex28. Applied masses from node 2 to node 5 are  $2.50712E-05, 0.000137891, 0.000137891, (2.50712E-05 + 9.0/386.4)kips/in^3$  respectively. There are no rotation masses.

Table 3.2: Material properties of concrete for Ex27 (unit: kips, in)

Element	Concrete	$E_{ts}$	$\sigma_c$	$\epsilon_c$	$\sigma_{cu}$	$\epsilon_{cu}$	$\lambda$	$\sigma_t$
Beam-column	Cover	549.231	-3.57	-0.0026	-1.19	-0.0078	0.3	0.448
	Core	549.451	-7.5	-0.00546	-7.35	-0.01638	0.3	0.650
Zero-length section	Cover	105.000	-3.57	-0.0136	-1.19	-0.0408	0.3	0.448
	Core	104.167	-7.5	-0.0288	-6.75	-0.0864	0.3	0.650

Table 3.3: Material properties of concrete for Ex28 (unit: kips, in)

Element	Concrete	$E$	$\nu$	$\kappa_0$	$A$	$k_h$	$k_d$	$K_h$	$K_d$	$D_c$
Beam-column	Cover	2829	0.2	5.855E-08	1870	0.003248	0.05168	3.889E+10	22.27	1.00
	Core	1804	0.2	6.483E-06	503.6	3.125E-07	0.4054	3.159E+09	102	1.00
Zero-length section	Cover	569.3	0.2	1.689E-19	371.8	0.832	1.461	9.529E+13	100.4	1.00
	Core	396.7	0.2	0.0008326	124.8	2.084E-07	1.61	8.856E+11	62.48	1.00

Table 3.4: Material properties of reinforcement for Ex27 and Ex28 (unit: kips, in)

Element	$E$	$\sigma_y$	$b$	$R0$	$cR1$	$cR2$	$a1$	$a2$	$a3$	$a4$
Beam-column element	26500	87.5	0.01	15	0.925	0.15	0	55	0	55
Zero-length section element	6949	87.5	0.01	15	0.925	0.15	0	55	0	55

Fig. ?? describes results of Ex27 and Ex28.

```

1 %
2 % Mercury Matlab Version 1.0.1
3 % Written by Dae-Hung Kang, CU-NEES
4 % Copyright 2009, CU-NEES
5 % Written : October 2009.
6 % File name: Ex27.m (1 column)
7 %
8 % Preface
9 Unit      = {'kip', 'in'};
10 % ndim, ndofpn
11 StrMode   = {2, 3};
12 %
13 % Control block
14 Iteration = {'static', { {'NewtonRaphson', 100, 1.0e-6, 'ForceNorm'},
15                   {'InitialStiffness', 10000, 1.0e-6, 'DisplNorm'}},
16                   'element', { {'NewtonRaphson', 1000, 1.0e-6, 'DisplNorm'},
17                               {'InitialStiffness', 100000, 1.0e-6, 'DisplNorm'}},
18                   'transient', { {'NewtonRaphson', 100, 1.0e-6, 'DisplNorm'},
19                               {'InitialStiffness', 100000, 1.0e-6, 'DisplNorm'}},
20                   }];
21 %
22 %Integration = {'HHT', 0, -0.2, 0.36, 0.7, 0.6318799279194399, 0.00015503501814608252};
23 Integration = {'Shing', 0, -0.2, 0.36, 0.7, 0.6318799279194399, 0.00015503501814608252, 10};
24 addMass    = {1, 0, 0;
25               2, 2.50712E-05, 2.50712E-05, 0;
26               3, 0.000137891, 0.000137891, 0;
27               4, 0.000137891, 0.000137891, 0;
28               5, 2.50712E-05+9.0/386.4, 2.50712E-05+9.0/386.4, 0};
29 %
30 nodcoord = {1, 0, 0;
31               2, 0, 0;
32               3, 0, 6;
33               4, 0, 33;
34               5, 0, 39};
35 constraint = {1, 1, 1, 1};
36 %
37 elements = { {1, 'ZeroLength2D', 1, 2, 0, 26, 0, pi()/2};
38               {2, 'ZeroLength2DSection', 1, 2, pi()/2, 3};
39               {3, 'StiffnessBased2DBeamColumn', 2, 3, 3, 1};
40               {4, 'FlexibilityBased2DBeamColumn1', 3, 4, 5, 1};
41               {5, 'StiffnessBased2DBeamColumn', 4, 5, 3, 1}};
42 %
43 sections = {1, 'Layer', {1, 5.1, 2.575;
44                           1, 5.1, -2.575;
45                           1, 0.91375, 1.88125;
46                           1, 0.91375, 1.34375;
47                           1, 0.91375, 0.80625;
48                           1, 0.91375, 0.26875;
49                           1, 0.91375, -0.26875;
50                           1, 0.91375, -0.80625;
51                           1, 0.91375, -1.34375;
52                           1, 0.91375, -1.88125;
53                           2, 2.31125, 1.88125;
54                           2, 2.31125, 1.34375;
55                           2, 2.31125, 0.80625;
56                           2, 2.31125, 0.26875;
57                           2, 2.31125, -0.26875;
58                           2, 2.31125, -0.80625;
59                           2, 2.31125, -1.34375;
60                           2, 2.31125, -1.88125}};
```

Table 3.5: Property of shear spring in zero-length element for Ex27 and Ex28 (unit: kips, in)

Element	$E$	$\sigma_y$	$b$	$a1$	$a2$	$a3$	$a4$
Shear spring in zero-length	1690	78.2	0.173	0	55	0	55

```

61|           2, 2.31125, -0.80625;
62|           2, 2.31125, -1.34375;
63|           2, 2.31125, -1.88125;
64|           17, 0.147, 2.15;
65|           17, 0.098, 0;
66|           17, 0.147, -2.15;};
67|   3, 'Layer', {5, 5.1, 2.575;
68|     5, 5.1, -2.575;
69|     5, 0.91375, 1.88125;
70|     5, 0.91375, 1.34375;
71|     5, 0.91375, 0.80625;
72|     5, 0.91375, 0.26875;
73|     5, 0.91375, -0.26875;
74|     5, 0.91375, -0.80625;
75|     5, 0.91375, -1.34375;
76|     5, 0.91375, -1.88125;
77|     6, 2.31125, 1.88125;
78|     6, 2.31125, 1.34375;
79|     6, 2.31125, 0.80625;
80|     6, 2.31125, 0.26875;
81|     6, 2.31125, -0.26875;
82|     6, 2.31125, -0.80625;
83|     6, 2.31125, -1.34375;
84|     6, 2.31125, -1.88125;
85|     19, 0.147, 2.15;
86|     19, 0.098, 0;
87|     19, 0.147, -2.15;};

88%-----%
89 materials = { { 1 , 'ModKP' , -3.57 , -0.0026 , -1.19 , -0.0078 , 0.3 , 0.448121077 , 549.2307692 , 0
90 }; { 2 , 'ModKP' , -7.5 , -0.00546 , -7.35 , -0.01638 , 0.3 , 0.649519053 , 549.4505495
91 , 0 }; { 5 , 'ModKP' , -3.57 , -0.0136 , -1.19 , -0.0408 , 0.3 , 0.448121077 , 105 , 0
92 { 6 , 'ModKP' , -7.5 , -0.0288 , -6.75 , -0.0864 , 0.3 , 0.649519053 , 104.1666667 , 0
93 }; { 17 , 'ModGMP' , 26500 , 87.5 , 0.01 , 15 , 0.925 , 0.15 , 0 , 0 , 55 ,
94 0 , 55 }; { 19 , 'ModGMP' , 6949 , 87.5 , 0.01 , 15 , 0.925 , 0.15 , 0 , 0 , 0 , 55 ,
95 0 , 55 }; { 26 , 'Bilinear' , 1690 , 78.2 , 0.173 , 0 , 0 , 55 , 0 , 55 }};

96%-----%
97% Force block
98 ga = load('NR-g-dt-0.01-Matlab.txt');
99 nga = size(ga, 1);
100 for i = 1:nga
101 groundacceleration{i,1} = ga(i,1);
102 groundacceleration{i,2} = ga(i,2);
103 groundacceleration{i,3} = ga(i,3);
104 end
105 forces = { 1, 'Static' , {'NodalForces' , {5, 1, 0} };
106 2, 'Acceleration' , {386.4, groundacceleration} };


```

```

1-----*****
2----- 1 column
3----- *****
4----- o (39)
5----- | Stiffness-based beam-column with 2 integration points
6----- o (33)
7----- |
8----- | Flexibility-based beam-column with 5 integration points
9----- |
10----- o (6)
11----- | Stiffness-based beam-column with 2 integration points
12----- o (0)
13----- Zero-Length and zero-Length section elements(bottom bar slip and shear deformation)
14----- -o (0) (Fixed support)
15----- *****
16 elements = {}
17----- *****
18----- create ductile column node coordinates
19----- create nodes
20 nodes = {[1, 0, 0, 'mass', 0, 0,0];
21 {2, 0, 0, 'mass', 2.50712E-05, 2.50712E-05,0};
22 {3, 0, 6, 'mass', 0.000137891, 0.000137891, 0};
23 {4, 0, 33, 'mass', 0.000137891, 0.000137891, 0};
24 {5, 0, 39, 'mass', 2.50712E-05+9.0/386.4, 2.50712E-05+9.0/386.4, 0} }
25----- figure out section names
26 barslipsectionf = 'BSColDFSection'
27 barslipspringf = 'BSColDFSS'
28 columnsection = 'ColDSection'
29 columnrigidsection = 'ColRigidSection'
30 nIp_stif = 3;
31 nIp_flex = 5;
32 flexparams = {10000,1e-6}
33----- Define elements
34 barslipbottom = { 1, 'InterfaceElement2D' , 1, 2, { {barslipspringf, {1,0,0} } }, { {barslipsectionf} }, {0,1,0},{-1,0,0} }
35 plasticcolumn1 = { 2, 'StiffnessBased2DBeamColumn' , 2, 3, {columnsection, nIp_stif} }
36 flexcolumn = { 3, 'FlexibilityBased2DBeamColumn' , 3, 4, {columnsection,nIp_flex}, flexparams }
37 plasticcolumn2 = { 4, 'StiffnessBased2DBeamColumn' , 4, 5, {columnsection, nIp_stif} }
38 table.insert(elements, barslipbottom)
39 table.insert(elements, plasticcolumn1)
40 table.insert(elements, flexcolumn)
41 table.insert(elements, plasticcolumn2)
42----- *****
43----- Set section properties
44----- *****


```

```

45 ---  

46 allsections = {  

47 ---  

48 'ColDSection' , 'Fiber',  

49 --- Tag, Area, y-loc, z-loc  

50 { 'ColDCover' , 5.1 , 2.575 , 0 ,  

51 'ColDCover' , 5.1 , -2.575 , 0 ,  

52 'ColDCover' , 0.91375 , 1.88125 , 0 ,  

53 'ColDCover' , 0.91375 , 1.34375 , 0 ,  

54 'ColDCover' , 0.91375 , 0.80625 , 0 ,  

55 'ColDCover' , 0.91375 , 0.26875 , 0 ,  

56 'ColDCover' , 0.91375 , -0.26875 , 0 ,  

57 'ColDCover' , 0.91375 , -0.80625 , 0 ,  

58 'ColDCover' , 0.91375 , -1.34375 , 0 ,  

59 'ColDCover' , 0.91375 , -1.88125 , 0 ,  

60 'ColDCore' , 2.31125 , 1.88125 , 0 ,  

61 'ColDCore' , 2.31125 , 1.34375 , 0 ,  

62 'ColDCore' , 2.31125 , 0.80625 , 0 ,  

63 'ColDCore' , 2.31125 , 0.26875 , 0 ,  

64 'ColDCore' , 2.31125 , -0.26875 , 0 ,  

65 'ColDCore' , 2.31125 , -0.80625 , 0 ,  

66 'ColDCore' , 2.31125 , -1.34375 , 0 ,  

67 'ColDCore' , 2.31125 , -1.88125 , 0 ,  

68 'ColDSteel' , 0.147 , 2.15 , 0 ,  

69 'ColDSteel' , 0.098 , 0 , 0 ,  

70 'ColDSteel' , 0.147 , -2.15 , 0 } ;  

71 ---  

72 'BSCoIDFSection' , 'Fiber',  

73 { 'BSCoIDFCover' , 5.1 , 2.575 , 0 ,  

74 'BSCoIDFCover' , 5.1 , -2.575 , 0 ,  

75 'BSCoIDFCover' , 0.91375 , 1.88125 , 0 ,  

76 'BSCoIDFCover' , 0.91375 , 1.34375 , 0 ,  

77 'BSCoIDFCover' , 0.91375 , 0.80625 , 0 ,  

78 'BSCoIDFCover' , 0.91375 , 0.26875 , 0 ,  

79 'BSCoIDFCover' , 0.91375 , -0.26875 , 0 ,  

80 'BSCoIDFCover' , 0.91375 , -0.80625 , 0 ,  

81 'BSCoIDFCover' , 0.91375 , -1.34375 , 0 ,  

82 'BSCoIDFCover' , 0.91375 , -1.88125 , 0 ,  

83 'BSCoIDFCore' , 2.31125 , 1.88125 , 0 ,  

84 'BSCoIDFCore' , 2.31125 , 1.34375 , 0 ,  

85 'BSCoIDFCore' , 2.31125 , 0.80625 , 0 ,  

86 'BSCoIDFCore' , 2.31125 , 0.26875 , 0 ,  

87 'BSCoIDFCore' , 2.31125 , -0.26875 , 0 ,  

88 'BSCoIDFCore' , 2.31125 , -0.80625 , 0 ,  

89 'BSCoIDFCore' , 2.31125 , -1.34375 , 0 ,  

90 'BSCoIDFCore' , 2.31125 , -1.88125 , 0 ,  

91 'BSCoIDFSteel' , 0.147 , 2.15 , 0 ,  

92 'BSCoIDFSteel' , 0.098 , 0 , 0 ,  

93 'BSCoIDFSteel' , 0.147 , -2.15 , 0 } ;  

94 -----  

95 --- Set material properties.  

96 concretemat = 'ConcreteLinearTensionSoftening'  

97 steelmat = 'GiuffreMenegottoPinto'  

98 sspringmat = 'Bilinear'  

99 materials = {  

100 { 'ColDCover' , concretemat , 549.2307692 , 0 , -3.57 , -0.0026 , -1.19 , -0.0078 , 0.3 , 0.448121077} ,  

101 { 'ColDCore' , concretemat , 549.4505495 , 0 , -7.5 , -0.00546 , -7.35 , -0.01638 , 0.3 , 0.649519053} ,  

102 { 'BSCoIDFCover' , concretemat , 105 , 0 , -3.57 , -0.0136 , -1.19 , -0.0408 , 0.3 , 0.448121077} ,  

103 { 'BSCoIDFCore' , concretemat , 104.1666667 , 0 , -7.5 , -0.0288 , -6.75 , -0.0864 , 0.3 , 0.649519053} ,  

104 { 'ColDSteel' , steelmat , 26500 , 0 , 87.5 , 0.01 , 15 , 0.925 , 0.15 , 0 , 55 , 0 , 55 , 0} ,  

105 { 'BSCoIDFSteel' , steelmat , 6949 , 0 , 87.5 , 0.01 , 15 , 0.925 , 0.15 , 0 , 55 , 0 , 55 , 0} ,  

106 { 'BSCoIDFSS' , sspringmat , 1690 , 0 , 78.2 , 0.173 , 0 , 55 , 0 , 55} ,  

107 }  

108 -----  

109 function dumptable(x)  

110 local result = '{  

111 for i,v in ipairs(x) do  

112 if (type(v) == 'table') then  

113 result = result .. dumptable(v)  

114 else  

115 result = result .. v .. ',  

116 end  

117 end  

118 return result .. '} \n'  

119 end  

120 -----  

121 print(dumptable(nodes))  

122 print(dumptable(elements))  

123 print(dumptable(materials))  

124 print(dumptable(allsections))  

125 -----  

126 --- Preface ndim and ndofpn (ndim: dimension, ndofpn: number of degrees of freedom per node)  

127 model = StructureModel(2,3)  

128 --- Assign all input data to Mercury  

129 model:addNodes(nodes)  

130 model:addMaterials(materials)  

131 model:addSections(allsections)  

132 model:addElements(elements)  

133 -----  

134 --- constrain bottom nodes  

135 model:constrainNode(1,1,1,1)  

136 -----  

137 print(" Transient analysis started \n")  

138 earthquakeloading = LoadDescription()  

139 earthquakeloading:addLoad({'groundmotion' , 'NR-g-dt_0_01_OpneSees.txt' , dt=0.01' , 1 , 386.4})  

140 -----  

141 displ = {}  

142 function displpertime(time)  

143 dx5,dy5,dz5 = model:nodeDisplacements(5)  

144 table.insert(displ, dx5)  

145 print("Work\n");  

146 end  

147  

148 react = {}  

149 function reactpertime(time)  

150 fx1,fy1 = model:nodeRestoringForces(1)  

151 table.insert(react, fx1)

```

```

152 end
153 --- ****
154 solver = NonlinearSolver("initialstiffness", { displacementdeltatolerance=1e-6, iterations=10000})
155 transientanalysis = DynamicAnalysis("HHT", model, solver, earthquakeloading, 0.01, -0.2, 0.36, 0.7)
156 transientanalysis: addcallback(displertime, "timestep")
157 transientanalysis: addcallback(reactertime, "timestep")
158 model: setRayleighCoefficients(0.6318799279194399, 0.00015503501814608252)
159 transientanalysis: solve(7641)
160 --- ****
161 function writedata1(x, fname)
162   local f = assert(io.open(fname, 'w'))
163   local writtenl = 0
164   for i,v in ipairs(x) do
165     f:write(v, " ")
166     writtenl = writtenl + 1
167     --- length of row size: writtenl
168     if (writtenl > 0) then
169       writtenl = 0
170       f:write("\n")
171     end
172   end
173   f:close()
174 end
175 writedata1(displ, 'Ex27HHTNodalDisp-5.dat')
176 writedata1(react, 'Ex27HHTReact-1.dat')
177 print(" Transient analysis ended\n")

```

```

1 %%%%%%
2 % Mercury Matlab Version 1.0.1
3 % Written by Dae-Hung Kang, CU-NEES
4 % Copyright 2009, CU-NEES
5 % Written : October 2009.
6 % File name: Ex28.m (1 column)
7 %
8 % Preface
9 Unit      = {'kip', 'in'};
10 %        ndim, ndofpn
11 StrMode   = {2, 3};
12 %
13 % Control block
14 Iteration = {'static', { {'NewtonRaphson', 100, 1.0e-6, 'ForceNorm'},
15                   {'InitialStiffness', 10000, 1.0e-6, 'DisplNorm'}},
16                   },
17   'element', { {'NewtonRaphson', 10, 1.0e-6, 'DisplNorm'},
18               {'InitialStiffness', 100000, 1.0e-6, 'DisplNorm'}},
19             },
20   'transient', { {'NewtonRaphson', 10, 1.0e-6, 'DisplNorm'},
21                 {'InitialStiffness', 100000, 1.0e-6, 'DisplNorm'}},
22               },
23             };
24 Integration = {'HHT', 0, -0.2, 0.36, 0.7, 0.6318799279194399, 0.00015503501814608252};
25 addMass    = {1, 0, 0;
26               2, 2.50712E-05, 2.50712E-05, 0;
27               3, 0.000137891, 0.000137891, 0;
28               4, 0.000137891, 0.000137891, 0;
29               5, 2.50712E-05+9.0/386.4, 2.50712E-05+9.0/386.4, 0};
30 %
31 nodcoord = {1, 0, 0;
32               2, 0, 0;
33               3, 0, 6;
34               4, 0, 33;
35               5, 0, 39};
36 constraint = {1, 1, 1, 1};
37 %
38 elements = { {1, 'ZeroLength2D', 1, 2, 0, 26, 0, pi()/2};
39               {2, 'ZeroLength2DSection', 1, 2, pi()/2, 3};
40               {3, 'StiffnessBased2DBeamColumn', 2, 3, 3, 1};
41               {4, 'FlexibilityBased2DBeamColumn1', 3, 4, 5, 1};
42               {5, 'StiffnessBased2DBeamColumn', 4, 5, 3, 1}};

43 %
44 sections = {1, 'Layer', {1, 5.1, 2.575;
45                         1, 5.1, -2.575;
46                         1, 0.91375, 1.88125;
47                         1, 0.91375, 1.34375;
48                         1, 0.91375, 0.80625;
49                         1, 0.91375, 0.26875;
50                         1, 0.91375, -0.26875;
51                         1, 0.91375, -0.80625;
52                         1, 0.91375, -1.34375;
53                         1, 0.91375, -1.88125;
54                         2, 2.31125, 1.88125;
55                         2, 2.31125, 1.34375;
56                         2, 2.31125, 0.80625;
57                         2, 2.31125, 0.26875;
58                         2, 2.31125, -0.26875;
59                         2, 2.31125, -0.80625;
60                         2, 2.31125, -1.34375;
61                         2, 2.31125, -1.88125;
62                         2, 2.31125, -1.88125;
63                         17, 0.147, 2.15;
64                         17, 0.098, 0;
65                         17, 0.147, -2.15;};
66               3, 'Layer', {5, 5.1, 2.575;
67                         5, 5.1, -2.575;
68                         5, 0.91375, 1.88125;
69                         5, 0.91375, 1.34375;
70                         5, 0.91375, 0.80625;
71                         5, 0.91375, 0.26875;
72                         5, 0.91375, -0.26875;
73                         5, 0.91375, -0.80625;
74                         5, 0.91375, -1.34375;
75                         5, 0.91375, -1.88125;
76                         6, 2.31125, 1.88125;
77                         6, 2.31125, 1.34375;
78                         6, 2.31125, 0.80625;

```

```

79      6,  2.31125,    0.26875;
80      6,  2.31125,   -0.26875;
81      6,  2.31125,   -0.80625;
82      6,  2.31125,   -1.34375;
83      6,  2.31125,   -1.88125;
84      19,  0.147,    2.15;
85      19,  0.098,    0;
86      19,  0.147,   -2.15;});});
87 %
88 materials = { { 1 , 22.27 , 'AnisotropicDamage' , 0 , 2829 , 0.2 , 5.855E-08 , 1870 , 0.003248 , 0.05168 , 
38890000000 , { 2 , 0.9999999 , 0 } ; { 2 , 'AnisotropicDamage' , 1804 , 0.2 , 0.000006483 , 503.6 , 3.125E-07 , 0.4054 , 
31590000000 , { 5 , 'AnisotropicDamage' , 569.3 , 0.2 , 1.689E-19 , 371.8 , 0.832 , 1.461 , 
9.529E+13 , { 100.4 , 0.9999999 , 0 } ; { 6 , 'AnisotropicDamage' , 396.7 , 0.2 , 0.0008326 , 124.8 , 2.084E-07 , 1.61 , 
8.856E+11 , { 62.48 , 0.9999999 , 0 } ; { 17 , 'ModGMP' , 26500 , 87.5 , 0.01 , 15 , 0.925 , 0.15 , 0 , 0 , 55 , 
0 , 55 } ; { 19 , 'ModGMP' , 6949 , 87.5 , 0.01 , 15 , 0.925 , 0.15 , 0 , 0 , 55 , 
0 , 55 } ; { 26 , 'Bilinear' , 1690 , 78.2 , 0.173 , 0 , 0 , 55 , 0 , 55 } };};
89 %
90 % Force block
91 ga = load('NR-gdtd-0-01-Matlab.txt');
92 nga = size(ga, 1);
93 for i = 1:nga
94 groundacceleration{i,1} = ga(i,1);
95 groundacceleration{i,2} = ga(i,2);
96 groundacceleration{i,3} = ga(i,3);
97 end
98 forces = { 1, 'Static' , {'NodalForces' , {5, 1, 0} } ;
99           2, 'Acceleration' , {386.4, groundacceleration} } ;
100
101
102
103
104
105

```

```

1 --- ****
2 --- 1 column
3 --- ****
4 --- o (39) Stiffness-based beam-column with 2 integration points
5 --- o (33)
6 --- |
7 --- | Flexibility-based beam-column with 5 integration points
8 --- |
9 --- o (6) Stiffness-based beam-column with 2 integration points
10 --- o (0) Zero-Length and zero-Length section elements(bottom bar slip and shear deformation)
11 --- o (0) (Fixed support)
12
13
14
15
16
17 elements = {};
18
19 --- create ductile column node coordinates
20 --- create nodes
21 nodes = {[1, 0, 0, 'mass', 0, 0, 0];
22 [2, 0, 0, 'mass', 2.50712E-05, 2.50712E-05, 0];
23 [3, 0, 6, 'mass', 0.000137891, 0.000137891, 0];
24 [4, 0, 33, 'mass', 0.000137891, 0.000137891, 0];
25 [5, 0, 39, 'mass', 2.50712E-05+9.0/386.4, 2.50712E-05+9.0/386.4, 0] }
26 --- figure out section names
27 barslipsection = 'BSColDFSection'
28 barslipspring = 'BSColDFSS'
29 columnsection = 'ColSection'
30 columnrigidsection = 'ColRigidSection'
31 nIp_stif = 3;
32 nIp_flex = 5;
33 flexparams = {10000,1e-3}
34 --- Define elements
35 barslipbottom = { 1, 'InterfaceElement2D' , 1, 2, { {barslipspringf, {1,0,0}} } , { {barslipsectionf} } , { {0,1,0},{-1,0,0} } }
36 plasticcolumn1 = { 2, 'StiffnessBased2DBeamColumn' , 2, 3, {columnsection, nIp_stif} }
37 flexcolumn = { 3, 'FlexibilityBased2DBeamColumn' , 3, 4, {columnsection,nIp_flex}, flexparams }
38 plasticcolumn2 = { 4, 'StiffnessBased2DBeamColumn' , 4, 5, {columnsection, nIp_stif} }
39 table.insert(elements, barslipbottom)
40 table.insert(elements, plasticcolumn1)
41 table.insert(elements, flexcolumn)
42 table.insert(elements, plasticcolumn2)
43
44 --- Set section properties.
45
46 allsections = {
47
48 'ColDSection' , 'Fiber',
49 --- Tag, Area, y-loc, z-loc
50 { 'ColDCover' , 5.1 , 2.575 , 0 ,
51 'ColDCover' , 5.1 , -2.575 , 0 ,
52 'ColDCover' , 0.91375 , 1.88125 , 0 ,
53 'ColDCover' , 0.91375 , 1.34375 , 0 ,
54 'ColDCover' , 0.91375 , 0.80625 , 0 ,
55 'ColDCover' , 0.91375 , 0.26875 , 0 ,
56 'ColDCover' , 0.91375 , -0.26875 , 0 ,
57 'ColDCover' , 0.91375 , -0.80625 , 0 ,
58 'ColDCover' , 0.91375 , -1.34375 , 0 ,
59 'ColDCover' , 0.91375 , -1.88125 , 0 ,
60 'ColDCore' , 2.31125 , 1.88125 , 0 ,
61 'ColDCore' , 2.31125 , 1.34375 , 0 ,
62 'ColDCore' , 2.31125 , 0.80625 , 0 ,
63 'ColDCore' , 2.31125 , 0.26875 , 0 ,
64 'ColDCore' , 2.31125 , -0.26875 , 0 ,
65 'ColDCore' , 2.31125 , -0.80625 , 0 ,
66 'ColDCore' , 2.31125 , -1.34375 , 0 ,
67 'ColDCore' , 2.31125 , -1.88125 , 0 ,
68 'ColDSteel' , 0.147 , 2.15 , 0 ,
69 'ColDSteel' , 0.098 , 0 , 0 ,
70 'ColDSteel' , 0.147 , -2.15 , 0 };
71

```

```

72 'BSColDFSection' , 'Fiber',
73 { 'BSColDFCover' , 5.1 , 2.575 , 0 ,
74 'BSColDFCover' , 5.1 , -2.575 , 0 ,
75 'BSColDFCover' , 0.91375 , 1.88125 , 0 ,
76 'BSColDFCover' , 0.91375 , 1.34375 , 0 ,
77 'BSColDFCover' , 0.91375 , 0.80625 , 0 ,
78 'BSColDFCover' , 0.91375 , 0.26875 , 0 ,
79 'BSColDFCover' , 0.91375 , -0.26875 , 0 ,
80 'BSColDFCover' , 0.91375 , -0.80625 , 0 ,
81 'BSColDFCover' , 0.91375 , -1.34375 , 0 ,
82 'BSColDFCover' , 0.91375 , -1.88125 , 0 ,
83 'BSColDFCore' , 2.31125 , 1.88125 , 0 ,
84 'BSColDFCore' , 2.31125 , 1.34375 , 0 ,
85 'BSColDFCore' , 2.31125 , 0.80625 , 0 ,
86 'BSColDFCore' , 2.31125 , 0.26875 , 0 ,
87 'BSColDFCore' , 2.31125 , -0.26875 , 0 ,
88 'BSColDFCore' , 2.31125 , -0.80625 , 0 ,
89 'BSColDFCore' , 2.31125 , -1.34375 , 0 ,
90 'BSColDFCore' , 2.31125 , -1.88125 , 0 ,
91 'BSColDFSteel' , 0.147 , 2.15 , 0 ,
92 'BSColDFSteel' , 0.098 , 0 , 0 ,
93 'BSColDFSteel' , 0.147 , -2.15 , 0 }; }
94 -----
95 --- Set material properties.
96 concretemat = 'ConcreteLinearTensionSoftening',
97 steelmat = 'GiuffreMenegottoPinto',
98 sspringmat = 'Bilinear',
99 materials = {
100 {'ColDCover' , 'anisotropicdamage2' , 2829 , 0 , 0.2 , 5.855E-08 , 1870 , 0.003248 , 0.05168 ,
38890000000 , 22.27 , 0.9999999 },
101 {'ColDCore' , 'anisotropicdamage2' , 1804 , 0 , 0.2 , 0.000006483 , 503.6 , 3.125E-07 , 0.4054 ,
102 , 0.9999999 },
102 {'BSColDFCover' , 'anisotropicdamage2' , 569.3 , 0 , 0.2 , 1.689E-19 , 371.8 , 0.832 , 1.461 ,
103 , 0.9999999 };
103 {'BSColDFCore' , 'anisotropicdamage2' , 396.7 , 0 , 0.2 , 0.0008326 , 124.8 , 2.084E-07 , 1.61 ,
8.856E+11 , 62.48 , 0.9999999 },
104 {'ColDSteel' , steelmat , 26500 , 0 , 87.5 , 0.01 , 15 , 0.925 , 0.15 , 0 , 55 , 0 , 55 , 0 },
105 {'BSColDFSteel' , steelmat , 6949 , 0 , 87.5 , 0.01 , 15 , 0.925 , 0.15 , 0 , 55 , 0 , 55 , 0 },
106 {'BSColDFSS' , sspringmat , 1690 , 0 , 78.2 , 0.173 , 0 , 55 , 0 , 55 },
107 }
108 -----
109 function dumptable(x),
110 local result = '{',
111 for i,v in ipairs(x) do
112 if (type(v) == 'table') then
113 result = result .. dumptable(v)
114 else
115 result = result .. v .. ','
116 end
117 end
118 return result .. '}\\n'
119 end
120 -----
121 print(dumptable(nodes))
122 print(dumptable(elements))
123 print(dumptable(materials))
124 print(dumptable(allsections))
125 -----
126 --- Preface ndim and ndofpn (ndim: dimension, ndofpn: number of degrees of freedom per node)
127 model = StructureModel(2,3)
128 --- Assign all input data to Mercury
129 model:addNodes(nodes)
130 model:addMaterials(materials)
131 model:addSections(allsections)
132 model:addElements(elements)
133 -----
134 --- constrain bottom nodes
135 model:constrainNode(1,1,1,1)
136 -----
137 print(" Transient analysis started\\n")
138 earthquakeloading = LoadDescription()
139 earthquakeloading:addLoad({'groundmotion' , 'NR-g-dt-0-01-OpneSees.txt' , dt=0.01' , 1 , 386.4})
140 -----
141 displ = {}
142 function displperime(time)
143 dx5,dy5,dz5 = model:nodeDisplacements(5)
144 table.insert(displ, dx5)
145 print("Work\\n");
146 end
147 -----
148 react = {}
149 function reactperime(time)
150 fx1,fy1 = model:nodeRestoringForces(1)
151 table.insert(react, fx1)
152 end
153 -----
154 solver = NonlinearSolver("initialstiffness", { displacementdeltatotolerance=1e-3, iterations=100000})
155 transientanalysis = DynamicAnalysis("HHT", model, solver, earthquakeloading, 0.01, -0.2, 0.36, 0.7)
156 transientanalysis:adddcallback(displperime, "timestep")
157 transientanalysis:adddcallback(reactperime, "timestep")
158 model:setRayleighCoefficients(0.6318799279194399 , 0.00015503501814608252)
159 transientanalysis:solve(7641)
160 -----
161 function writedata1(x, fname)
162 local f = assert(io.open(fname, 'w'))
163 local writenl = 0
164 for i,v in ipairs(x) do
165 f:write(v, " ")
166 writenl = writenl + 1
167 --- length of row size: writenl
168 if (writenl > 0) then
169 writenl = 0
170 f:write("\\n")
171 end
172 end
173 f:close()
174 end

```

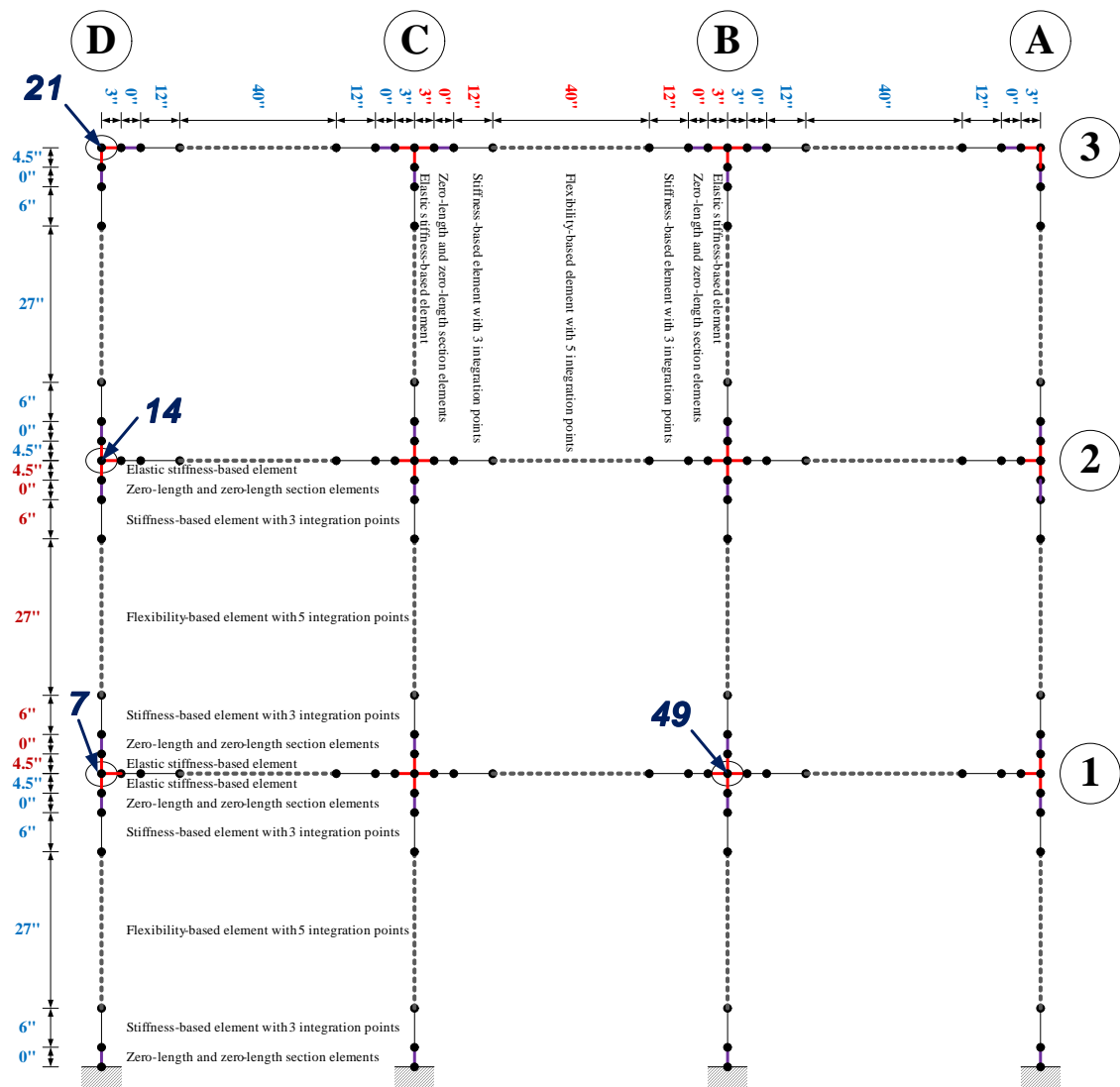


Figure 3.11: Numerical model for real-time hybrid simulation

```

175 writedata1(displ,'Ex28HHTNodalDisp_5.dat')
176 writedata1(react,'Ex28HHTReact_1.dat')
177 print(" Transient analysis ended\n")

```

## 3.9 Ex29: Full Reinforced Concrete Frame, HHT, Shing

This most complex validation example, Fig. 3.11, analyses the reinforced concrete frame tested on a shake table by ?, Fig. 3.9, and which will be later used to assess the real time hybrid simulation of Mercury, Fig. 3.9.

This example is sufficiently complex to warrant detailed description.

### 3.9.0.1 Frame discretization and properties

Beams and columns are modeled with one stiffness-based beam-columns (3 integration points) at each end, and one flexibility-based beam-column with 5 integrations.

Nodes 7, 14, 21 and 49 are monitored, in Fig. 3.11 to assess the seismic while ignoring self-weight. Columns **A** and **B** are shear critical (i.e under-reinforced), while **C** and **D** are ductile. Sectional characteristics are shown in Fig. 3.13 while Table 3.6 to 3.9 summarize those properties and constitutive model parameters used<sup>1</sup>.

Nodal masses are used in the dynamic analysis, Table 3.10 to 3.12, where each beam has an added lead bundle masses at 4<sup>th</sup> and 5<sup>th</sup> nodes. For comparison HHT integration scheme is used in OpenSees, and HHT and Shing integration scheme are used in Mercury

<sup>1</sup> Col: Column, Beam: Beam, F: Footing section, D: Ductile section, ND: Shear critical section, BS: Bar-Slip section, Rigid: Rigid section, Cover: Concrete cover fiber, Core: Concrete core fiber, SS: Shear spring of zero-length element, steel: Reinforcement fiber, ModKP: modified Kent-Park model, ModGMP: modified Giuffre-Monegotto-Pinto

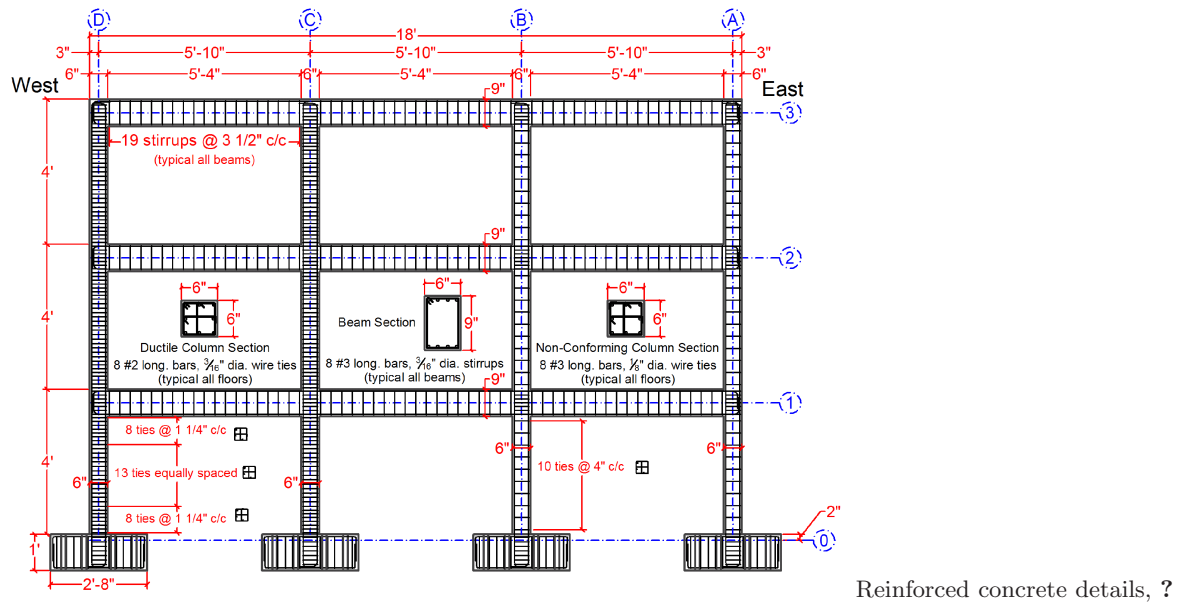


Figure 3.12: Shake table test of reinforce concrete frame, ?

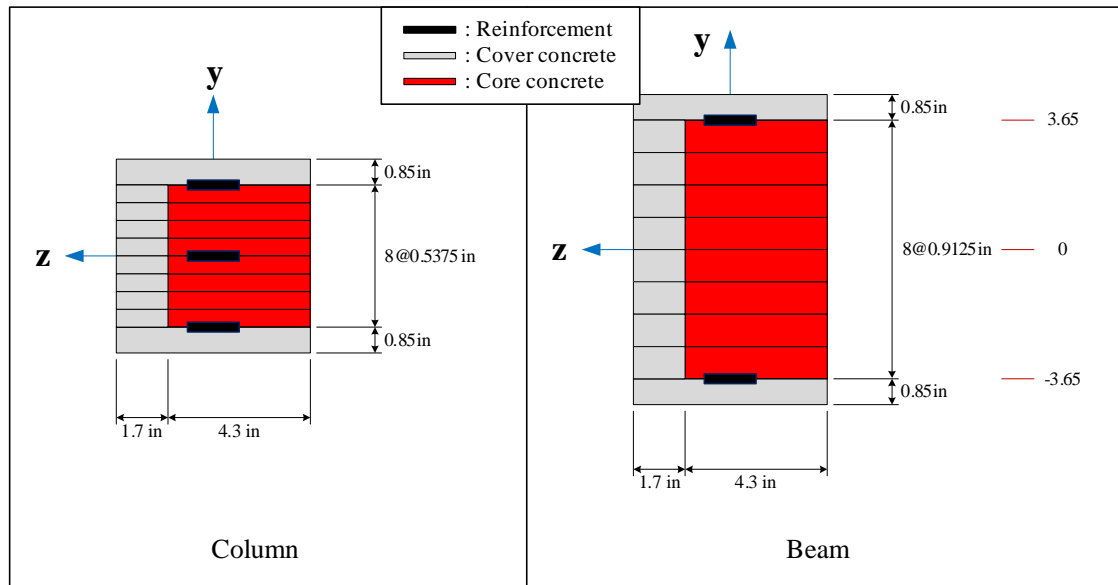


Figure 3.13: Section properties of Ex29

Table 3.6: Concrete material properties of concrete for Ex29 (unit:kips, in)

Fiber name	Material	$E_{ts}$	$\sigma_c$	$\epsilon_c$	$\sigma_{cu}$	$\epsilon_{cu}$	$\lambda$	$\sigma_t$
Col-D-Cover	ModKP	549.23	-3.57	-0.0026	-1.19	-0.0078	0.3	0.4481
Col-D-Core	ModKP	549.45	-7.5	-0.00546	-7.35	-0.01638	0.3	0.6495
BS-Col-D-Cover	ModKP	105.00	-3.57	-0.0136	-1.19	-0.0408	0.3	0.4481
BS-Col-D-Core	ModKP	104.17	-7.5	-0.0288	-7.35	-0.0864	0.3	0.6495
BS-Col-D-F-Cover	ModKP	105.00	-3.57	-0.0136	-1.19	-0.0408	0.3	0.4481
BS-Col-D-F-Core	ModKP	104.17	-7.5	-0.0288	-6.75	-0.0864	0.3	0.6495
Col-ND-Cover	ModKP	549.23	-3.57	-0.0026	-1.19	-0.0078	0.3	0.4481
Col-ND-Core	ModKP	549.30	-3.9	-0.00284	-3.51	-0.00852	0.3	0.4684
BS-Col-ND-Cover	ModKP	105.00	-3.57	-0.0136	-1.19	-0.0408	0.3	0.4481
BS-Col-ND-Core	ModKP	106.85	-3.9	-0.0146	-3.51	-0.0438	0.3	0.4684
BS-Col-ND-F-Cover	ModKP	144.24	-3.57	-0.0099	-1.19	-0.0297	0.3	0.4481
BS-Col-ND-F-Core	ModKP	106.85	-3.9	-0.0146	-3.51	-0.0438	0.3	0.4684
Beam-Cover	ModKP	549.23	-3.57	-0.0026	-1.19	-0.0078	0.3	0.4481
Beam-Core	ModKP	549.30	-3.9	-0.00284	-3.51	-0.00852	0.3	0.4684
BS-Beam-Cover	ModKP	105.00	-3.57	-0.0136	-1.19	-0.0408	0.3	0.4481
BS-Beam-Core	ModKP	106.85	-3.9	-0.0146	-3.51	-0.0438	0.3	0.4684

Table 3.7: Material properties of reinforcement for Ex29 (unit: kips, in)

Fiber name	Material	$E$	$\sigma_y$	$b$	$R0$	$cR1$	$cR2$	$a1$	$a2$	$a3$	$a4$
Col-D-Steel	ModGMP	26500	87.5	0.01	15	0.925	0.15	0	55	0	55
BS-Col-D-Steel	ModGMP	5067	87.5	0.01	15	0.925	0.15	0	55	0	55
BS-Col-D-F-Steel	ModGMP	6949	87.5	0.01	15	0.925	0.15	0	55	0	55
Col-ND-Steel	ModGMP	27300	80	0.01	15	0.925	0.15	0	55	0	55
BS-Col-ND-Steel	ModGMP	5220	80	0.01	15	0.925	0.15	0	55	0	55
BS-Col-ND-F-Steel	ModGMP	5220	80	0.01	15	0.925	0.15	0	55	0	55
Beam-Steel	ModGMP	27300	80	0.01	15	0.925	0.15	0	55	0	55
BS-Beam-Steel	ModGMP	5220	80	0.01	15	0.925	0.15	0	55	0	55

Table 3.8: Property of shear spring for Ex29 (unit: kips, in)

Fiber name	Material	$E$	$\sigma_y$	$b$	$a1$	$a2$	$a3$	$a4$
BS-Col-D-SS	Bilinear	1690	78.2	0.173	0	55	0	55
BS-Col-D-F-SS	Bilinear	1690	78.2	0.173	0	55	0	55
BS-Col-ND-SS	Bilinear	1690	78.2	0.173	0	55	0	55
BS-Col-ND-F-SS	Bilinear	1690	78.2	0.173	0	55	0	55
BS-Beam-SS	Bilinear	1545	75.8	0.396	0	55	0	55

Table 3.9: Properties of rigid elements (unit: kips, in)

Element	Model	$E$
Col-Rigid	Elasitc	1E+10
Beam-Rigid	Elastic	1E+10

c++ version with  $\alpha = -0.2$ . This last model is particularly relevant for the real-time hybrid simulation which will be conducted later. Rayleigh damping coefficients were determined to be 1.177 for mass and 0.001599 for stiffness. The reinforced concrete frame is subjected to the seismic excitation shown in Fig. 3.14 (which was measured at the base of the shake table in Ghannoum's tests).

Figure 3.14: Seismic excitation for Ex29

Table 3.10: Mass properties in first floor column nodes (unit:  $kips \cdot sec^2/in$ )

First floor node	$m_x$	$m_y$	$m_z$
7th	0.0000752	0.0000752	0.00000752
6th	0.0000188	0.0000188	0.00000188
5th	0.0000251	0.0000251	0.00000251
4th	0.0001379	0.0001379	0.00001379
3rd	0.0001379	0.0001379	0.00001379
2nd	0.0000251	0.0000251	0.00000251
1st	0.0000000	0.0000000	0.0000000

Table 3.11: Mass properties in column nodes except first floor columns (unit:  $kips \cdot sec^2/in$ )

Other floor node	$m_x$	$m_y$	$m_z$
8th	0.0000627	0.0000627	0.00000627
7th	0.0000188	0.0000188	0.00000188
6th	0.0000251	0.0000251	0.00000251
5th	0.0001379	0.0001379	0.00001379
4th	0.0001379	0.0001379	0.00001379
3rd	0.0000251	0.0000251	0.00000251
2nd	0.0000188	0.0000188	0.00000188

```

1  ****
2  earthquakefiles = {
3  'Test16AccelHHalfYield.txt',
4  'Test19AccelH1stCollapse.txt',
5  'Test30AccelH2ndCollapse.txt',
6  'Test32AccelH3rdCollapse.txt'
7 }
8 earthquakefile = earthquakefiles[2]
9 print('Excitation:', earthquakefile)
10 -----
11 alpha = -0.2
12 beta = (1-alpha)*(1-alpha)/4
13 gamma = (1-2*alpha)/2
14 --- alpha : alpha coefficient in HHT integration
15 --- beta : beta coefficient in HHT integration
16 --- gamma : gamma coefficient in HHT integration
17 -----
18 --- Multiple bay/floor building model
19 -----
20 Column : first floor
21   o (43.5)
22   | Elastic stiffness-based beam-column
23   o (39) Zero-Length and zero-Length section elements (top bar slip and shear deformation)
24   o (39) Stiffness-based beam-column with 2 integration points
25   o (33)
26   | Flexibility-based beam-column with 5 integration points
27   o (6) Stiffness-based beam-column with 2 integration points
28   o (0) Zero-Length and zero-Length section elements (bottom bar slip and shear deformation)
29   -o- (0) (Fixed support)
30 -----
31 Column : other floor
32   o (48)
33   | Elastic stiffness-based beam-column
34   o (43.5) Zero-Length and zero-Length section elements (top bar slip and shear deformation)
35   o (43.5) Stiffness-based beam-column with 2 integration points
36   o (37.5)
37   | Flexibility-based beam-column with 5 integration points
38   o (10.5)
39   | Stiffness-based beam-column with 2 integration points
40   o (4.5) Zero-Length and zero-Length section elements (bottom bar slip and shear deformation)
41   o (4.5)

```

Table 3.12: Mass properties in beam nodes (unit:  $kips \cdot sec^2/in$ )

Beam node	$m_x$	$m_y$	$m_z$
2nd	0.0000188	0.0000188	0.00000188
3rd	0.0000752	0.0000752	0.00000752
4th	0.0080899	0.0080899	0.00080899
5th	0.0080899	0.0080899	0.00080899
6th	0.0000752	0.0000752	0.00000752
7th	0.0000188	0.0000188	0.00000188

```

54 --- | Elastic stiffness-based beam-column
55 --- o (0)
56 --- **** Beam ****
57 --- o---o---o---o---o---o---o
58 --- (0) a (3) b (3) c (15) d (55)e(67) f (67) g (70)
59 --- a: Elastic stiffness-based beam-column
60 --- b: Zero-Length and zero-Length section elements(left bar slip and shear deformation)
61 --- c: Stiffness-based beam-column with 2 integration points
62 --- d: Flexibility-based beam-column with 5 integration points
63 --- e: Stiffness-based beam-column with 2 integration points
64 --- f: Zero-Length and zero-Length section elements(right bar slip and shear deformation)
65 --- g: Elastic stiffness-based beam-column
66 --- **** Basic variables for node information ****
67 --- g : gravity acceleration
68 --- nbays : Number of bays (nbays must be odd number)
69 --- nflrs : Number of floors
70 --- n1cnod: Number of nodes of the first column
71 --- nocnod: Number of nodes of other columns
72 --- nbmnod: Number of nodes of beams
73 --- cilen : Total length of the first column
74 --- colen : Total length of other columns
75 --- bmlen : Total length of beams
76 --- c1nod : Coordinate information on the first column
77 --- conod : Coordinate information on other columns
78 --- bmnod : Coordinate information on beams
79 --- cd1nodmass : Nodal mass of the first ductile column
80 --- cd1nodmass : Nodal mass of other ductile columns
81 --- cd1nodmass : Nodal mass of the first shear critical column
82 --- cd1nodmass : Nodal mass of other shear critical column
83 --- nIp-elast : Number of integration points of elastic stiffness-based beam-column
84 --- nIp-stif : Number of integration points of nonlinear stiffness-based beam-column
85 --- nIp-flex : Number of integration points of nonlinear flexibility-based beam-column
86 --- flexparams : Iteration config for flexibility elements
87 --- flexparams = {number of iterations, tolerance}
88 --- flexparams = {number of iterations, tolerance}
89 --- $$$ start of node and element information $$$
90 --- g = 386.4
91 --- nbays = 3; --- nbays must be odd number.
92 --- nflrs = 3;
93 --- n1cnod= 7;
94 --- nocnod= 8;
95 --- nbmnod= 8;
96 --- cilen = 43.5;
97 --- colen = 48;
98 --- bmlen = 70;
99 --- c1nod = {0,0,6,33,39,39,43.5};
100 --- conod = {0,4,5,4.5,10,5,37,5,43,5,43.5,48};
101 --- bmnod = {0,3,3,15,55,67,67,70};
102 --- bmaddWeight = 3
103 --- bmaddMass = bmaddWeight/g
104 --- 
105 --- c1nodmass = {0.0, 2.50712E-05, 0.000137891, 0.000137891, 2.50712E-05, 1.88034E-05, 7.52135E-05}
106 --- conodmass = {0.0, 1.88034E-05, 2.50712E-05, 0.000137891, 0.000137891, 2.50712E-05, 1.88034E-05, 6.26779E-05}
107 --- bmnodmass = {0.0, 1.88034E-05, 7.52135E-05, 0.000325925+bmaddMass, 0.000325925+bmaddMass, 7.52135E-05, 1.88034E-05, 0.0}
108 --- 
109 --- nIp-elast = 1;
110 --- nIp-stif = 3;
111 --- nIp-flex = 5;
112 --- 
113 --- 
114 --- flexparams = {1000,1e-6}
115 --- $$$ END of node and element information $$$
116 --- **** Set nodes and elements ****
117 --- Set nodes and elements.
118 --- 
119 --- 
120 --- nodes = {}
121 --- elements = {}
122 --- 
123 --- function nodename(bay,floor)
124 ---   return string.format('node%#d%#d', bay, floor)
125 --- end
126 --- 
127 --- function columnnodenname(bay,floor,subsection)
128 ---   if (subsection == 1 and floor > 1) then
129 ---     return columnnodenname(bay,floor-1,nocnod)
130 ---     if (floor == 2) then
131 ---       return columnnodenname(bay,floor-1,n1cnod)
132 ---     else
133 ---       return columnnodenname(bay,floor-1,nocnod)
134 ---     end
135 ---   else
136 ---     return string.format('colnode%#d%#d%#d', bay, floor, subsection)
137 ---   end
138 --- end
139 --- 
140 --- function beamnodename(bay,floor,subsection)
141 ---   -- section 1 nodes re-use the column nodes
142 ---   if (subsection == 1) then
143 ---     return columnnodenname(bay,floor,1)
144 ---   else

```

```

145     return string.format('beamnode-%d-%d-%d', bay, floor, subsection)
146   end
147 end
148
149 --- create ductile column node coordinates
150 ncold = (nbays+1)/2;
151 for colbay = 1,ncold do
152   for colfloor = 1,nflrs do
153     x = (colbay -1)*bmlen
154     nodeyfirst = c1nod
155     nodeyhigher = conod
156
157   --- create nodes
158   if (colfloor==1) then
159     bottomnode = columnnodenname(colbay,colfloor,1)
160     for k=1,n1cnod do
161       y = nodeyfirst[k]
162       masscd1 = c1nodmass[k]
163       curnode = { columnnodenname(colbay,colfloor,k), x,y, 'mass', masscd1, masscd1, 0.1*masscd1 }
164       table.insert(nodes,curnode)
165     end
166   else
167     bottomnode = columnnodenname(colbay,colfloor-1,no1nod)
168     for k=2,no1nod do
169       y = cilen + colen * (colfloor-2) + nodeyhigher[k]
170       masscd0 = conodmass[k]
171       curnode = { columnnodenname(colbay,colfloor,k), x,y, 'mass', masscd0, masscd0, 0.1*masscd0 }
172       table.insert(nodes,curnode)
173     end
174   end
175   --- figure out section names
176   barslipsectionf = 'BSCoLDFSection'
177   barslipspringf = 'BSCoLDFSS'
178   columnsection = 'CoLDSection'
179   barslipsection = 'BSCoLDSS'
180   barslipsection = 'BSCoLDFSection'
181   columnrigidsection = 'CoLRigidSection'
182   if (colfloor==1) then
183     node1 = columnnodenname(colbay,colfloor,1)
184     node2 = columnnodenname(colbay,colfloor,2)
185     node3 = columnnodenname(colbay,colfloor,3)
186     node4 = columnnodenname(colbay,colfloor,4)
187     node5 = columnnodenname(colbay,colfloor,5)
188     node6 = columnnodenname(colbay,colfloor,6)
189     node7 = columnnodenname(colbay,colfloor,7)
190
191   --- Define elements
192   barslipbottom = { string.format('columnnpl1-%d-%d', colbay, colfloor), 'InterfaceElement2D', node1, node2, { barslipspringf, columnsection } }
193   plasticcolumn1 = { string.format('columnnpl1-%d-%d', colbay, colfloor), 'StiffnessBased2DBeamColumn', node2, node3, { columnsection } }
194   flexcolumn = { string.format('columnnflx-%d-%d', colbay, colfloor), 'FlexibilityBased2DBeamColumn', node3, node4, { columnsection } }
195   plasticcolumn2 = { string.format('columnnpl2-%d-%d', colbay, colfloor), 'StiffnessBased2DBeamColumn', node4, node5, { columnsection } }
196   barsliptop = { string.format('columnnbs-%d-%d', colbay, colfloor), 'InterfaceElement2D', node5, node6, { barslipspringf, columnsection } }
197   rigidcolumntop = { string.format('columnnrtd-%d-%d', colbay, colfloor), 'StiffnessBased2DBeamColumn', node6, node7, { columnsection } }
198   table.insert(elements, barslipbottom)
199   table.insert(elements, plasticcolumn1)
200   table.insert(elements, flexcolumn)
201   table.insert(elements, plasticcolumn2)
202   table.insert(elements, barsliptop)
203   table.insert(elements, rigidcolumntop)
204
205   if (colfloor == 2) then
206     node1 = columnnodenname(colbay, colfloor-1, n1cnod)
207   else
208     node1 = columnnodenname(colbay, colfloor-1, no1nod)
209
210   node2 = columnnodenname(colbay, colfloor, 2)
211   node3 = columnnodenname(colbay, colfloor, 3)
212   node4 = columnnodenname(colbay, colfloor, 4)
213   node5 = columnnodenname(colbay, colfloor, 5)
214   node6 = columnnodenname(colbay, colfloor, 6)
215   node7 = columnnodenname(colbay, colfloor, 7)
216   node8 = columnnodenname(colbay, colfloor, 8)
217
218   --- Define elements
219   rigidcolumnbottom = { string.format('columnnrdb-%d-%d', colbay, colfloor), 'StiffnessBased2DBeamColumn', node1, node2, { columnsection } }
220   barslipbottom = { string.format('columnnsb-%d-%d', colbay, colfloor), 'InterfaceElement2D', node2, node3, { barslipspringf, columnsection } }
221   plasticcolumn1 = { string.format('columnnpl1-%d-%d', colbay, colfloor), 'StiffnessBased2DBeamColumn', node3, node4, { columnsection } }
222   flexcolumn = { string.format('columnnflx-%d-%d', colbay, colfloor), 'FlexibilityBased2DBeamColumn', node4, node5, { columnsection } }
223   plasticcolumn2 = { string.format('columnnpl2-%d-%d', colbay, colfloor), 'StiffnessBased2DBeamColumn', node5, node6, { columnsection } }
224   barsliptop = { string.format('columnnbs-%d-%d', colbay, colfloor), 'InterfaceElement2D', node6, node7, { barslipspringf, columnsection } }
225   rigidcolumntop = { string.format('columnnrtd-%d-%d', colbay, colfloor), 'StiffnessBased2DBeamColumn', node7, node8, { columnsection } }
226   table.insert(elements, rigidcolumnbottom)
227   table.insert(elements, plasticcolumn1)
228   table.insert(elements, flexcolumn)
229   table.insert(elements, plasticcolumn2)
230   table.insert(elements, barsliptop)
231   table.insert(elements, rigidcolumntop)
232
233 end
234
235 --- create shear critical column node coordinates
236 for colbay = ncold+1,nbays+1 do
237   for colfloor = 1,nflrs do
238     x = (colbay -1)*bmlen
239     nodeyfirst = c1nod
240     nodeyhigher = conod
241
242   --- create nodes
243   if (colfloor==1) then
244     bottomnode = columnnodenname(colbay,colfloor,1)
245     for k=1,n1cnod do
246       y = nodeyfirst[k]
247       masscd1 = c1nodmass[k]
248       curnode = { columnnodenname(colbay,colfloor,k), x,y, 'mass', masscd1, masscd1, 0.1*masscd1 }
249       table.insert(nodes,curnode)
250     end
251   else
252     bottomnode = columnnodenname(colbay,colfloor-1,no1nod)

```

```

252     for k=2,nochnod do
253         y = cilen + colen * (colfloor - 2) + nodeyhigher[k]
254         masscndo = conodmass[k]
255         curnode = { columnnodename(crbay , colfloor , k), x,y, 'mass' , masscndo, masscndo, 0.1*masscndo }
256         table.insert(nodes , curnode)
257     end
258
259     -- figure out section names
260     barslipsectionf = 'BSCoINDFSection',
261     barslipspringf = 'BSCoINDFSS',
262     columnsection = 'CoINDSection',
263     barslipsspring = 'BSCoINDSS',
264     barslipsection = 'BSCoINDSection',
265     columnrigidsection = 'CoRigidSection',
266
267     if (colfloor==1) then
268         node1 = columnnodename(crbay , colfloor , 1)
269         node2 = columnnodename(crbay , colfloor , 2)
270         node3 = columnnodename(crbay , colfloor , 3)
271         node4 = columnnodename(crbay , colfloor , 4)
272         node5 = columnnodename(crbay , colfloor , 5)
273         node6 = columnnodename(crbay , colfloor , 6)
274         node7 = columnnodename(crbay , colfloor , 7)
275
276         -- Define elements
277         barslipbottom = { string.format('columnnsb-%d-%d',crbay , colfloor), 'InterfaceElement2D' , node1 , node2 , { {barslipspring,
278             plasticcolumn1 = { string.format('columnpl1-%d-%d',crbay , colfloor), 'StiffnessBased2DBeamColumn' , node2 , node3 , {columnse
279             flexcolumn = { string.format('columnflx-%d-%d',crbay , colfloor), 'FlexibilityBased2DBeamColumn' , node3 , node4 , {column
280             plasticcolumn2 = { string.format('columnpl2-%d-%d',crbay , colfloor), 'StiffnessBased2DBeamColumn' , node4 , node5 , {column
281             barsliptop = { string.format('columnbst-%d-%d',crbay , colfloor), 'InterfaceElement2D' , node5 , node6 , { {barslipspring,
282                 rigidcolumntop = { string.format('columnrdr-%d-%d',crbay , colfloor), 'StiffnessBased2DBeamColumn' , node6 , node7 , {column
283                     table.insert(elements , barslipbottom)
284                     table.insert(elements , plasticcolumn1)
285                     table.insert(elements , flexcolumn)
286                     table.insert(elements , barsliptop)
287                     table.insert(elements , rigidcolumntop)
288
289         else if (colfloor == 2) then
290             node1 = columnnodename(crbay , colfloor -1, nlnod)
291         else
292             node1 = columnnodename(crbay , colfloor -1, nochnod)
293         end
294         node2 = columnnodename(crbay , colfloor , 2)
295         node3 = columnnodename(crbay , colfloor , 3)
296         node4 = columnnodename(crbay , colfloor , 4)
297         node5 = columnnodename(crbay , colfloor , 5)
298         node6 = columnnodename(crbay , colfloor , 6)
299         node7 = columnnodename(crbay , colfloor , 7)
300         node8 = columnnodename(crbay , colfloor , 8)
301
302         -- Define elements
303         rigidcolumnbottom = { string.format('columnrdb-%d-%d',crbay , colfloor), 'StiffnessBased2DBeamColumn' , node1 , node2 , {column
304             barslipbottom = { string.format('columnbsb-%d-%d',crbay , colfloor), 'InterfaceElement2D' , node2 , node3 , { {barslipsprin
305             plasticcolumn1 = { string.format('columnpl1-%d-%d',crbay , colfloor), 'StiffnessBased2DBeamColumn' , node3 , node4 , {column
306             flexcolumn = { string.format('columnflx-%d-%d',crbay , colfloor), 'FlexibilityBased2DBeamColumn' , node4 , node5 , {column
307             plasticcolumn2 = { string.format('columnpl2-%d-%d',crbay , colfloor), 'StiffnessBased2DBeamColumn' , node5 , node6 , {column
308             barsliptop = { string.format('columnbst-%d-%d',crbay , colfloor), 'InterfaceElement2D' , node6 , node7 , { {barslipspring,
309                 rigidcolumntop = { string.format('columnrdr-%d-%d',crbay , colfloor), 'StiffnessBased2DBeamColumn' , node7 , node8 , {column
310                     table.insert(elements , rigidcolumnbottom)
311                     table.insert(elements , barslipbottom)
312                     table.insert(elements , plasticcolumn1)
313                     table.insert(elements , barsliptop)
314                     table.insert(elements , rigidcolumntop)
315
316     end
317 end
318
319 -- create beam node coordinates
320 for beambay = 1,nbays do
321     for beamfloor = 2, nflrs+1 do
322         y=cilen+colen*(beamfloor-2)
323
324         -- create nodes
325         for k=2,nbmnod-1 do
326             x = (beambay-1)*bmlen + bmnod[k]
327             massbm= bmnodmass[k]
328             curnode = { beamnodename(beambay,beamfloor,k), x ,y, 'mass' , massbm, massbm, 0.1*massbm }
329             table.insert(nodes , curnode)
330
331         -- figure out section names
332         beamsection = 'BeamSection',
333         barslipsection = 'BSBeamSection'
334         beamrigidsection = 'BeamRigidSection'
335         barslipspring = 'BSBeamSS'
336
337         -- figure out node tag for node connectivity
338         node1 = beamnodename(beambay,beamfloor,1)
339         node2 = beamnodename(beambay,beamfloor,2)
340         node3 = beamnodename(beambay,beamfloor,3)
341         node4 = beamnodename(beambay,beamfloor,4)
342         node5 = beamnodename(beambay,beamfloor,5)
343         node6 = beamnodename(beambay,beamfloor,6)
344         node7 = beamnodename(beambay,beamfloor,7)
345         node8 = beamnodename(beambay+1, beamfloor,1)
346
347         -- Define elements
348         rigidbeamleft = { string.format('beamrdl-%d-%d',beambay,beamfloor), 'StiffnessBased2DBeamColumn' , node1 , node2 , {beamrigidsection
349             barslipleft = { string.format('beambsl-%d-%d',beambay,beamfloor), 'InterfaceElement2D' , node2 , node3 , { {barslipspring, {0,
350             plasticbeam1 = { string.format('beampl1-%d-%d',beambay,beamfloor), 'StiffnessBased2DBeamColumn' , node3 , node4 , {beamsection ,
351             flexbeam = { string.format('beamflx-%d-%d',beambay,beamfloor), 'FlexibilityBased2DBeamColumn' , node4 , node5 , {beamsection ,
352             plasticbeam2 = { string.format('beampl2-%d-%d',beambay,beamfloor), 'StiffnessBased2DBeamColumn' , node5 , node6 , {beamsection ,
353             barslipright = { string.format('beambsr-%d-%d',beambay,beamfloor), 'InterfaceElement2D' , node6 , node7 , { {barslipspring, {0,
354             rigidbeamright= { string.format('beamrdr-%d-%d',beambay,beamfloor), 'StiffnessBased2DBeamColumn' , node7 , node8 , {beamrigidsec
355                     table.insert(elements , rigidbeamleft)
356                     table.insert(elements , barslipleft)
357                     table.insert(elements , plasticbeam1)
358                     table.insert(elements , flexbeam)
359                     table.insert(elements , plasticbeam2)
360                     table.insert(elements , barslipright)
361                     table.insert(elements , rigidbeamright)

```

```

359     end
360 end
361 --- **** Set section properties ****
362 --- Set section properties.
363 ---
364 ---
365 allsections = {
366   --- ColDSection
367   'ColDSection' , 'Fiber',
368   --- Tag, Area, y-loc, z-loc
369   { 'ColDCover' , 5.1 , 2.575 , 0 ,
370     'ColDCover' , 5.1 , -2.575 , 0 ,
371     'ColDCover' , 0.91375 , 1.88125 , 0 ,
372     'ColDCover' , 0.91375 , 1.34375 , 0 ,
373     'ColDCover' , 0.91375 , 0.80625 , 0 ,
374     'ColDCover' , 0.91375 , 0.26875 , 0 ,
375     'ColDCover' , 0.91375 , -0.26875 , 0 ,
376     'ColDCover' , 0.91375 , -0.80625 , 0 ,
377     'ColDCover' , 0.91375 , -1.34375 , 0 ,
378     'ColDCover' , 0.91375 , -1.88125 , 0 ,
379     'ColDCore' , 2.31125 , 1.88125 , 0 ,
380     'ColDCore' , 2.31125 , 1.34375 , 0 ,
381     'ColDCore' , 2.31125 , 0.80625 , 0 ,
382     'ColDCore' , 2.31125 , 0.26875 , 0 ,
383     'ColDCore' , 2.31125 , -0.26875 , 0 ,
384     'ColDCore' , 2.31125 , -0.80625 , 0 ,
385     'ColDCore' , 2.31125 , -1.34375 , 0 ,
386     'ColDCore' , 2.31125 , -1.88125 , 0 ,
387     'ColDSteel' , 0.147 , 2.15 , 0 ,
388     'ColDSteel' , 0.098 , 0 , 0 ,
389     'ColDSteel' , 0.147 , -2.15 , 0 } ;
390   --- BSCoIDSection
391   'BSCoIDSection' , 'Fiber',
392   { 'BSCoIDCover' , 5.1 , 2.575 , 0 ,
393     'BSCoIDCover' , 5.1 , -2.575 , 0 ,
394     'BSCoIDCover' , 0.91375 , 1.88125 , 0 ,
395     'BSCoIDCover' , 0.91375 , 1.34375 , 0 ,
396     'BSCoIDCover' , 0.91375 , 0.80625 , 0 ,
397     'BSCoIDCover' , 0.91375 , 0.26875 , 0 ,
398     'BSCoIDCover' , 0.91375 , -0.26875 , 0 ,
399     'BSCoIDCover' , 0.91375 , -0.80625 , 0 ,
400     'BSCoIDCover' , 0.91375 , -1.34375 , 0 ,
401     'BSCoIDCover' , 0.91375 , -1.88125 , 0 ,
402     'BSCoIDCore' , 2.31125 , 1.88125 , 0 ,
403     'BSCoIDCore' , 2.31125 , 1.34375 , 0 ,
404     'BSCoIDCore' , 2.31125 , 0.80625 , 0 ,
405     'BSCoIDCore' , 2.31125 , 0.26875 , 0 ,
406     'BSCoIDCore' , 2.31125 , -0.26875 , 0 ,
407     'BSCoIDCore' , 2.31125 , -0.80625 , 0 ,
408     'BSCoIDCore' , 2.31125 , -1.34375 , 0 ,
409     'BSCoIDCore' , 2.31125 , -1.88125 , 0 ,
410     'BSCoIDSteel' , 0.147 , 2.15 , 0 ,
411     'BSCoIDSteel' , 0.098 , 0 , 0 ,
412     'BSCoIDSteel' , 0.147 , -2.15 , 0 } ;
413   --- BSCoIDFSection
414   'BSCoIDFSection' , 'Fiber',
415   { 'BSCoIDFCover' , 5.1 , 2.575 , 0 ,
416     'BSCoIDFCover' , 5.1 , -2.575 , 0 ,
417     'BSCoIDFCover' , 0.91375 , 1.88125 , 0 ,
418     'BSCoIDFCover' , 0.91375 , 1.34375 , 0 ,
419     'BSCoIDFCover' , 0.91375 , 0.80625 , 0 ,
420     'BSCoIDFCover' , 0.91375 , 0.26875 , 0 ,
421     'BSCoIDFCover' , 0.91375 , -0.26875 , 0 ,
422     'BSCoIDFCover' , 0.91375 , -0.80625 , 0 ,
423     'BSCoIDFCover' , 0.91375 , -1.34375 , 0 ,
424     'BSCoIDFCover' , 0.91375 , -1.88125 , 0 ,
425     'BSCoIDFCore' , 2.31125 , 1.88125 , 0 ,
426     'BSCoIDFCore' , 2.31125 , 1.34375 , 0 ,
427     'BSCoIDFCore' , 2.31125 , 0.80625 , 0 ,
428     'BSCoIDFCore' , 2.31125 , 0.26875 , 0 ,
429     'BSCoIDFCore' , 2.31125 , -0.26875 , 0 ,
430     'BSCoIDFCore' , 2.31125 , -0.80625 , 0 ,
431     'BSCoIDFCore' , 2.31125 , -1.34375 , 0 ,
432     'BSCoIDFCore' , 2.31125 , -1.88125 , 0 ,
433     'BSCoIDFSteel' , 0.147 , 2.15 , 0 ,
434     'BSCoIDFSteel' , 0.098 , 0 , 0 ,
435     'BSCoIDFSteel' , 0.147 , -2.15 , 0 } ;
436   --- ColNDSection
437   'ColNDSection' , 'Fiber',
438   { 'ColNDCover' , 5.1 , 2.575 , 0 ,
439     'ColNDCover' , 5.1 , -2.575 , 0 ,
440     'ColNDCover' , 0.91375 , 1.88125 , 0 ,
441     'ColNDCover' , 0.91375 , 1.34375 , 0 ,
442     'ColNDCover' , 0.91375 , 0.80625 , 0 ,
443     'ColNDCover' , 0.91375 , 0.26875 , 0 ,
444     'ColNDCover' , 0.91375 , -0.26875 , 0 ,
445     'ColNDCover' , 0.91375 , -0.80625 , 0 ,
446     'ColNDCover' , 0.91375 , -1.34375 , 0 ,
447     'ColNDCover' , 0.91375 , -1.88125 , 0 ,
448     'ColNDCore' , 2.31125 , 1.88125 , 0 ,
449     'ColNDCore' , 2.31125 , 1.34375 , 0 ,
450     'ColNDCore' , 2.31125 , 0.80625 , 0 ,
451     'ColNDCore' , 2.31125 , 0.26875 , 0 ,
452     'ColNDCore' , 2.31125 , -0.26875 , 0 ,
453     'ColNDCore' , 2.31125 , -0.80625 , 0 ,
454     'ColNDCore' , 2.31125 , -1.34375 , 0 ,
455     'ColNDCore' , 2.31125 , -1.88125 , 0 ,
456     'ColNDSteel' , 0.33 , 2.15 , 0 ,
457     'ColNDSteel' , 0.22 , 0 , 0 ,
458     'ColNDSteel' , 0.33 , -2.15 , 0 } ;
459   --- BSCoNDSection
460   'BSCoNDSection' , 'Fiber',
461   { 'BSCoNDCover' , 5.1 , 2.575 , 0 ,
462     'BSCoNDCover' , 5.1 , -2.575 , 0 ,
463     'BSCoNDCover' , 0.91375 , 1.88125 , 0 ,
464     'BSCoNDCover' , 0.91375 , 1.34375 , 0 ,
465     'BSCoNDCover' , 0.91375 , 0.80625 , 0 ,

```

```

466    'BSCoINDCover' , 0.91375 , 0.26875 , 0 , ,
467    'BSCoINDCover' , 0.91375 , -0.26875 , 0 , ,
468    'BSCoINDCover' , 0.91375 , -0.80625 , 0 , ,
469    'BSCoINDCover' , 0.91375 , -1.34375 , 0 , ,
470    'BSCoINDCover' , 0.91375 , -1.88125 , 0 , ,
471    'BSCoINDCore' , 2.31125 , 1.88125 , 0 , ,
472    'BSCoINDCore' , 2.31125 , 1.34375 , 0 , ,
473    'BSCoINDCore' , 2.31125 , 0.80625 , 0 , ,
474    'BSCoINDCore' , 2.31125 , 0.26875 , 0 , ,
475    'BSCoINDCore' , 2.31125 , -0.26875 , 0 , ,
476    'BSCoINDCore' , 2.31125 , -0.80625 , 0 , ,
477    'BSCoINDCore' , 2.31125 , -1.34375 , 0 , ,
478    'BSCoINDCore' , 2.31125 , -1.88125 , 0 , ,
479    'BSCoINDSteel' , 0.33 , 2.15 , 0 , ,
480    'BSCoINDSteel' , 0.22 , 0 , 0 , ,
481    'BSCoINDSteel' , 0.33 , -2.15 , 0 }};

482
483 'BSCoINDFSection' , 'Fiber' ,
484 { 'BSCoINDFCover' , 5.1 , 2.575 , 0 , ,
485   'BSCoINDFCover' , 5.1 , -2.575 , 0 , ,
486   'BSCoINDFCover' , 0.91375 , 1.88125 , 0 , ,
487   'BSCoINDFCover' , 0.91375 , 1.34375 , 0 , ,
488   'BSCoINDFCover' , 0.91375 , 0.80625 , 0 , ,
489   'BSCoINDFCover' , 0.91375 , 0.26875 , 0 , ,
490   'BSCoINDFCover' , 0.91375 , -0.26875 , 0 , ,
491   'BSCoINDFCover' , 0.91375 , -0.80625 , 0 , ,
492   'BSCoINDFCover' , 0.91375 , -1.34375 , 0 , ,
493   'BSCoINDFCover' , 0.91375 , -1.88125 , 0 , ,
494   'BSCoINDFCore' , 2.31125 , 1.88125 , 0 , ,
495   'BSCoINDFCore' , 2.31125 , 1.34375 , 0 , ,
496   'BSCoINDFCore' , 2.31125 , 0.80625 , 0 , ,
497   'BSCoINDFCore' , 2.31125 , 0.26875 , 0 , ,
498   'BSCoINDFCore' , 2.31125 , -0.26875 , 0 , ,
499   'BSCoINDFCore' , 2.31125 , -0.80625 , 0 , ,
500   'BSCoINDFCore' , 2.31125 , -1.34375 , 0 , ,
501   'BSCoINDFCore' , 2.31125 , -1.88125 , 0 , ,
502   'BSCoINDFSteel' , 0.33 , 2.15 , 0 , ,
503   'BSCoINDFSteel' , 0.22 , 0 , 0 , ,
504   'BSCoINDFSteel' , 0.33 , -2.15 , 0 }};

505
506 'BeamSection' , 'Fiber' ,
507 { 'BeamCover' , 5.1 , 4.075 , 0 , ,
508   'BeamCover' , 5.1 , -4.075 , 0 , ,
509   'BeamCover' , 1.55125 , 3.19375 , 0 , ,
510   'BeamCover' , 1.55125 , 2.28125 , 0 , ,
511   'BeamCover' , 1.55125 , 1.36875 , 0 , ,
512   'BeamCover' , 1.55125 , 0.45625 , 0 , ,
513   'BeamCover' , 1.55125 , -0.45625 , 0 , ,
514   'BeamCover' , 1.55125 , -1.36875 , 0 , ,
515   'BeamCover' , 1.55125 , -2.28125 , 0 , ,
516   'BeamCover' , 1.55125 , -3.19375 , 0 , ,
517   'BeamCore' , 3.92375 , 3.19375 , 0 , ,
518   'BeamCore' , 3.92375 , 2.28125 , 0 , ,
519   'BeamCore' , 3.92375 , 1.36875 , 0 , ,
520   'BeamCore' , 3.92375 , 0.45625 , 0 , ,
521   'BeamCore' , 3.92375 , -0.45625 , 0 , ,
522   'BeamCore' , 3.92375 , -1.36875 , 0 , ,
523   'BeamCore' , 3.92375 , -2.28125 , 0 , ,
524   'BeamCore' , 3.92375 , -3.19375 , 0 , ,
525   'BeamSteel' , 0.44 , 3.65 , 0 , ,
526   'BeamSteel' , 0.44 , -3.65 , 0 }};

527
528 'BSBeamSection' , 'Fiber' ,
529 { 'BSBeamCover' , 5.1 , 4.075 , 0 , ,
530   'BSBeamCover' , 5.1 , -4.075 , 0 , ,
531   'BSBeamCover' , 1.55125 , 3.19375 , 0 , ,
532   'BSBeamCover' , 1.55125 , 2.28125 , 0 , ,
533   'BSBeamCover' , 1.55125 , 1.36875 , 0 , ,
534   'BSBeamCover' , 1.55125 , 0.45625 , 0 , ,
535   'BSBeamCover' , 1.55125 , -0.45625 , 0 , ,
536   'BSBeamCover' , 1.55125 , -1.36875 , 0 , ,
537   'BSBeamCover' , 1.55125 , -2.28125 , 0 , ,
538   'BSBeamCover' , 1.55125 , -3.19375 , 0 , ,
539   'BSBeamCore' , 3.92375 , 3.19375 , 0 , ,
540   'BSBeamCore' , 3.92375 , 2.28125 , 0 , ,
541   'BSBeamCore' , 3.92375 , 1.36875 , 0 , ,
542   'BSBeamCore' , 3.92375 , 0.45625 , 0 , ,
543   'BSBeamCore' , 3.92375 , -0.45625 , 0 , ,
544   'BSBeamCore' , 3.92375 , -1.36875 , 0 , ,
545   'BSBeamCore' , 3.92375 , -2.28125 , 0 , ,
546   'BSBeamCore' , 3.92375 , -3.19375 , 0 , ,
547   'BSBeamSteel' , 0.44 , 3.65 , 0 , ,
548   'BSBeamSteel' , 0.44 , -3.65 , 0 }};

549
550 'ColRigidSection' , 'general' ,
551 { 'ColRigid' , 36 , 108 };

552
553 'BeamRigidSection' , 'general' ,
554 { 'BeamRigid' , 54 , 364.5 };

555
556 ----- Set material properties .
557
558
559
560 concretemat = 'ConcreteLinearTensionSoftening'
561 steelmat = 'GiuffreMenegottoPinto'
562 sspringmat = 'Bilinear'
563 materials =
564 --- Concrete (ConcreteLinearTensionSoftening)
565   Tag, mat_type, Ets, density, sc, ec, scu, ecu, lam, st
566 { 'ColDCover' , concretemat , 549.2307692 , 0 , -3.57 , -0.0026 , -1.19 , -0.0078 , 0.3 , 0.448121077} ,
567 { 'ColCore' , concretemat , 549.4505495 , 0 , -7.5 , -0.00546 , -7.35 , -0.01638 , 0.3 , 0.649519053} ,
568 { 'BSCoIDCover' , concretemat , 105 , 0 , -3.57 , -0.0136 , -1.19 , -0.0408 , 0.3 , 0.448121077} ,
569 { 'BSCoIDCore' , concretemat , 104.1666667 , 0 , -7.5 , -0.0288 , -7.35 , -0.0864 , 0.3 , 0.649519053} ,
570 { 'BSCoIDFCover' , concretemat , 105 , 0 , -3.57 , -0.0136 , -1.19 , -0.0408 , 0.3 , 0.448121077} ,
571 { 'BSCoIDFCore' , concretemat , 104.1666667 , 0 , -7.5 , -0.0288 , -6.75 , -0.0864 , 0.3 , 0.649519053} ,
572 { 'ColNDCover' , concretemat , 549.2307692 , 0 , -3.57 , -0.0026 , -1.19 , -0.0078 , 0.3 , 0.448121077} ,

```

```

573 {'ColINDCore' , concretemat , 549.2957746 , 0 , -3.9 , -0.00284 , -3.51 , -0.00852 , 0.3 , 0.46837485 } ,
574 {'BSColINDCover' , concretemat , 105 , 0 , -3.57 , -0.0136 , -1.19 , -0.0408 , 0.3 , 0.448121077} ,
575 {'BSColINDCore' , concretemat , 106.8493151 , 0 , -3.9 , -0.0146 , -3.51 , -0.0438 , 0.3 , 0.46837485 } ,
576 {'BSColNDFCover' , concretemat , 144.2424242 , 0 , -3.57 , -0.0099 , -1.19 , -0.0297 , 0.3 , 0.448121077} ,
577 {'BSColNDFCore' , concretemat , 106.8493151 , 0 , -3.9 , -0.0146 , -3.51 , -0.0438 , 0.3 , 0.46837485 } ,
578 {'BeamCover' , concretemat , 549.2307692 , 0 , -3.57 , -0.0026 , -1.19 , -0.0078 , 0.3 , 0.448121077} ,
579 {'BeamCore' , concretemat , 549.2957746 , 0 , -3.9 , -0.00284 , -3.51 , -0.00852 , 0.3 , 0.46837485 } ,
580 {'BSBeamCover' , concretemat , 105 , 0 , -3.57 , -0.0136 , -1.19 , -0.0408 , 0.3 , 0.448121077} ,
581 {'BSBeamCore' , concretemat , 106.8493151 , 0 , -3.9 , -0.0146 , -3.51 , -0.0438 , 0.3 , 0.46837485 } ,
582 -- Steel (GiuffreMenegottoPinto)
583 -- Tag, mat_type, E, density, sy, b, R0, cR1, cR2, a1, a2, a3, a4, s_init
584 {'ColdSteel' , steelmat , 26500 , 0 , 87.5 , 0.01 , 15 , 0.925 , 0.15 , 0 , 55 , 0 , 55 , 0} ,
585 {'BSCoIDSteel' , steelmat , 5067 , 0 , 87.5 , 0.01 , 15 , 0.925 , 0.15 , 0 , 55 , 0 , 55 , 0} ,
586 {'BSCoIDFSteel' , steelmat , 6949 , 0 , 87.5 , 0.01 , 15 , 0.925 , 0.15 , 0 , 55 , 0 , 55 , 0} ,
587 {'CoINDSteel' , steelmat , 27300 , 0 , 80 , 0.01 , 15 , 0.925 , 0.15 , 0 , 55 , 0 , 55 , 0} ,
588 {'BSCoINDSteel' , steelmat , 5220 , 0 , 80 , 0.01 , 15 , 0.925 , 0.15 , 0 , 55 , 0 , 55 , 0} ,
589 {'BSCoINDFSteel' , steelmat , 5220 , 0 , 80 , 0.01 , 15 , 0.925 , 0.15 , 0 , 55 , 0 , 55 , 0} ,
590 {'BeamSteel' , steelmat , 27300 , 0 , 80 , 0.01 , 15 , 0.925 , 0.15 , 0 , 55 , 0 , 55 , 0} ,
591 {'BSBeamSteel' , steelmat , 5220 , 0 , 80 , 0.01 , 15 , 0.925 , 0.15 , 0 , 55 , 0 , 55 , 0} ,
592 -- Shear spring (Bilinear)
593 -- Tag, mat_type, E, density, sy, b, a1, a2, a3, a4
594 {'BSCoIDSS' , sspringmat , 1690 , 0 , 78.2 , 0.173 , 0 , 55 , 0 , 55 , 0} ,
595 {'BSCoIDFSS' , sspringmat , 1690 , 0 , 78.2 , 0.173 , 0 , 55 , 0 , 55 , 0} ,
596 {'BSCoINDSS' , sspringmat , 1690 , 0 , 78.2 , 0.173 , 0 , 55 , 0 , 55 , 0} ,
597 {'BSCoINDFSS' , sspringmat , 1690 , 0 , 78.2 , 0.173 , 0 , 55 , 0 , 55 , 0} ,
598 {'BSBeamSS' , sspringmat , 1545 , 0 , 75.8 , 0.396 , 0 , 55 , 0 , 55 , 0} ,
599 -- Rigid element (Elastic)
600 -- Tag, mat_type, E, density
601 {'ColRigid' , 'Elastic' , 100000000000 , 0} ,
602 {'BeamRigid' , 'Elastic' , 100000000000 , 0} ,
603 }
604 ****
605 function dumpable(x)
606   local result = '{'
607   for i,v in ipairs(x) do
608     if (type(v) == 'table') then
609       result = result .. dumpable(v)
610     else
611       result = result .. v .. ','
612     end
613   end
614   return result .. '}\\n'
615 end
616 ****
617 -- print(dumpable(nodes))
618 -- print(dumpable(elements))
619 -- print(dumpable(materials))
620 -- print(dumpable(allsections))
621 ****
622 -- Preface ndim and ndofpn (ndim: dimension, ndofpn: number of degrees of freedom per node)
623 model = StructureModel(2,3)
624 -- Assign all input data to Mercury
625 model:addNodes(nodes)
626 model:addMaterials(materials)
627 model:addSections(allsections)
628 model:addElements(elements)
629 ****
630 -- constrain bottom nodes
631 for bay=1,nbays+1 do
632   model:constrainNode(columnnnodenname(bay,1,1),1,1,1)
633 end
634 ****
635 solver = NonlinearSolver("initialstiffness", { displacementdeltatolerance=le-5, iterations=100000})
636 ****
637 -- Monitoring node number
638 node06 = columnnnodenname(1,1,6);
639 node13 = columnnnodenname(1,2,7);
640 node20 = columnnnodenname(1,3,7);
641 node07 = columnnnodenname(1,1,7);
642 node14 = columnnnodenname(1,2,8);
643 node21 = columnnnodenname(1,3,8);
644 node48 = columnnnodenname(3,1,6);
645 node49 = columnnnodenname(3,1,7);
646 node01 = columnnnodenname(1,1,1);
647 node22 = columnnnodenname(2,1,1);
648 node43 = columnnnodenname(3,1,1);
649 node64 = columnnnodenname(4,1,1);
650 ****
651 disp_06_13_20 = {}
652 function disp1perime(timestep)
653   dx06,dy06,dz06 = model:nodeDisplacements(node06)
654   dx13,dy13,dz13 = model:nodeDisplacements(node13)
655   dx20,dy20,dz20 = model:nodeDisplacements(node20)
656   table.insert(disp_06_13_20,dx06)
657   table.insert(disp_06_13_20,dy06)
658   table.insert(disp_06_13_20,dz06)
659   table.insert(disp_06_13_20,dx13)
660   table.insert(disp_06_13_20,dy13)
661   table.insert(disp_06_13_20,dz13)
662   table.insert(disp_06_13_20,dx20)
663   table.insert(disp_06_13_20,dy20)
664   table.insert(disp_06_13_20,dz20)
665 end
666 disp_07_14_21 = {}
667 function disp2perime(timestep)
668   dx07,dy07,dz07 = model:nodeDisplacements(node07)
669   dx14,dy14,dz14 = model:nodeDisplacements(node14)
670   dx21,dy21,dz21 = model:nodeDisplacements(node21)
671   table.insert(disp_07_14_21,dx07)
672   table.insert(disp_07_14_21,dy07)
673   table.insert(disp_07_14_21,dz07)
674   table.insert(disp_07_14_21,dx14)
675   table.insert(disp_07_14_21,dy14)
676   table.insert(disp_07_14_21,dz14)
677   table.insert(disp_07_14_21,dx21)
678   table.insert(disp_07_14_21,dy21)
679   table.insert(disp_07_14_21,dz21)

```

```

680 end
681 disp_48_49 = {}
682 function disp3pertime(timestep)
683 dx48,dy48,dz48 = model:nodeDisplacements(node48)
684 dx49,dy49,dz49 = model:nodeDisplacements(node49)
685 table.insert(disp_48_49,dx48)
686 table.insert(disp_48_49,dy48)
687 table.insert(disp_48_49,dz48)
688 table.insert(disp_48_49,dx49)
689 table.insert(disp_48_49,dy49)
690 table.insert(disp_48_49,dz49)
691 end
692 --
693 react = {}
694 function reactpertime(timestep)
695 fx01,fy01,fz01 = model:nodeRestoringForces(node01)
696 fx22,fy22,fz22 = model:nodeRestoringForces(node22)
697 fx43,fy43,fz43 = model:nodeRestoringForces(node43)
698 fx64,fy64,fz64 = model:nodeRestoringForces(node64)
699 table.insert(react,fx01)
700 table.insert(react,fy01)
701 table.insert(react,fz01)
702 table.insert(react,fx22)
703 table.insert(react,fy22)
704 table.insert(react,fz22)
705 table.insert(react,fx43)
706 table.insert(react,fy43)
707 table.insert(react,fz43)
708 table.insert(react,fx64)
709 table.insert(react,fy64)
710 table.insert(react,fz64)
711 print(timestep);
712 end
713 --
714 ****
715 earthquakeloading = LoadDescription()
716 accelamp = 1.0*g
717 earthquakeloading:addLoad({'groundmotion',earthquakefile .. ',dt=0.005', 1,accelamp})
718 --
719 transientanalysis = DynamicAnalysis("hht", model, solver, earthquakeloading, {[ dt, alpha, beta, gamma]} 0.005, alpha, beta, gamma)
720 transientanalysis = DynamicAnalysis("hybridhht", model, solver, earthquakeloading, {[ dt, alpha, beta, gamma, iteration]} 0.005, alpha, beta, gamma, iteration)
721 model:setRayleighCoefficients(1.1770500887303603,0.0015992014979696392)
722 --
723 transientanalysis:adcallback(disp1pertime, "timestep")
724 transientanalysis:adcallback(disp2pertime, "timestep")
725 transientanalysis:adcallback(disp3pertime, "timestep")
726 transientanalysis:adcallback(reactpertime, "timestep")
727 --
728 transientanalysis:solve(15281)
729 transientanalysis:solve(152810)
730 --
731 -- Set output file
732 function writedata6(x, fname)
733 local f = assert(io.open(fname,'w'))
734 local writenl = 0
735 for i,v in ipairs(x) do
736 f:write(v, " ")
737 writenl = writenl + 1
738 -- length of row size: writenl
739 if (writenl > 5) then
740 writenl = 0
741 f:write("\n")
742 end
743 end
744 f:close()
745 end
746 --
747 function writedata9(x, fname)
748 local f = assert(io.open(fname,'w'))
749 local writenl = 0
750 for i,v in ipairs(x) do
751 f:write(v, " ")
752 writenl = writenl + 1
753 -- length of row size: writenl
754 if (writenl > 8) then
755 writenl = 0
756 f:write("\n")
757 end
758 end
759 f:close()
760 end
761 --
762 function writedata12(x, fname)
763 local f = assert(io.open(fname,'w'))
764 local writenl = 0
765 for i,v in ipairs(x) do
766 f:write(v, " ")
767 writenl = writenl + 1
768 -- length of row size: writenl
769 if (writenl > 11) then
770 writenl = 0
771 f:write("\n")
772 end
773 end
774 f:close()
775 end
776 --
777 writedata9(disp_06_13_20,'Ex29HHT_06_13_20_displ.dat')
778 writedata9(disp_07_14_21,'Ex29HHT_07_14_21_displ.dat')
779 writedata6(disp_48_49,'Ex29HHT_48_49_displ.dat')
780 writedata12(react,'Ex29HHT_01_22_43_64.react.dat')
781 
782 writedata9(disp_06_13_20,'Ex29Shing_06_13_20_displ.dat')
783 writedata9(disp_07_14_21,'Ex29Shing_07_14_21_displ.dat')
784 writedata6(disp_48_49,'Ex29Shing_48_49_displ.dat')
785 writedata12(react,'Ex29Shing_01_22_43_64.react.dat')
786 --

```



## Chapter 4

# NONLINEAR PUSHOVER ANALYSIS

first part requires some major editing

### 4.1 pushover

A pushover analysis is a nonlinear static procedure wherein monotonically increasing lateral loads are applied to the structure till a target displacement is achieved or the structure is unable to resist further loads.

A pushover analysis is associated with a load pattern. In this case, use the same later load pattern that was used for the seismic design. It is necessary to apply dead and live loads before doing a pushover analysis. Since the pushover procedure is nonlinear, it is necessary to setup a new load case for dead and live which is also nonlinear. The recent advent of performance based design has brought the static nonlinear analysis, also known as sequential yield analysis, or simply “push-over” analysis has gained significant popularity during the past few years. It is a static, nonlinear procedure in which the magnitude of the structural loading is incrementally increased in accordance with a certain predefined pattern. Typically, a predefined lateral load pattern is distributed along the building height. The lateral forces are then monotonically increased in constant proportion with a displacement control at the top of the building until a certain level of deformation is reached. The target top displacement may be the deformation expected in the design earthquake in case of designing a new structure, or the drift corresponding to structural collapse for assessment purposes. The method allows tracing the sequence of yielding and failure on the member and the structure levels as well as the progress of the overall capacity curve of the structure, (?).

With the increase in the magnitude of the loading, weak links and failure modes of the structure are found. The loading is monotonic with the effects of the cyclic behavior and load reversals being estimated by using a modified monotonic force-deformation criteria and with damping approximations. Static pushover analysis is an attempt by the structural engineering profession to evaluate the real strength of the structure and it promises to be a useful and effective tool for performance based design. The ATC-40 and FEMA-273 documents have developed modeling procedures, acceptance criteria and analysis procedures for pushover analysis. These documents define force-deformation criteria for hinges used in pushover analysis.

The design of structures based on plastic approach is called **limit design** and is at the core of most modern design codes (ACI, AISC).

### 4.2 Shakedown

A structure subjected to a general variable load can collapse even if the loads remain inside the elastic plastic domain of the load space. Thus the elasto plastic domain represents a safe domain only for monotonic loads. Under general, non-monotonic loading, a structure can nevertheless fail by incremental collapse or plastic fatigue. The behavior of a structure is termed **shakedown**.

### 4.3 Control Method

In pushover analysis it is highly desirable to first subject the structure to an initial force without constrained degrees of freedom for imposed pushover displacements. This would allow the structure to properly deform, be subjected to the correct state of initial stress prior to the application of the actual imposed pushover displacements. This section presents a simple method to perform such an analysis in one step. Traditional method in Sec. 4.4 would require two separate analysis shown in Fig. ???. Sec. 4.5 describes pushover analysis with imposed displacement on unconstrained degrees of freedom.

### 4.4 Classical Pushover

A nonlinear pushover analysis entails two parts, Fig. 4.3:

**Vertical Load** is the first step where the structure is subjected to the vertical load (such as gravity and possibly a fraction of the live load).

**Lateral Loads** is the application of increasing lateral force or displacement up to failure. Imposed displacement is preferred as it enables us to capture the post-peak response.

A nonlinear pushover analysis can not separate the vertical loads from the lateral loads. Application of the vertical loads will results in an initial state of stress to which those induced by the lateral loads must be added.

Traditional methods entail performing the first analysis under load control, and then results are either used as part of the restart (correct), or they are added to the results of the displacement control when this one is complete (erroneous).

Since only imposed displacements can enable us to capture the post-peak response, the question is how should those displacements be applied.

With reference to Fig. 4.2, one could apply a single imposed displacement at the top of the discretized building. However, the resulting displacements may not be compatible with the dynamic response of the structure.

A better approach consists in first evaluating the first mode shape, determine the normalized displacements (with respect to the one of the top floor) of each floor  $\alpha_i$ , and then use this  $\alpha_i$  distribution for the imposed lateral displacements in the subsequent nonlinear pushover analysis.

### 4.5 Improved Pushover Analysis Procedure

With reference to Fig. 4.3, we shall examine the two steps of the pushover analysis.

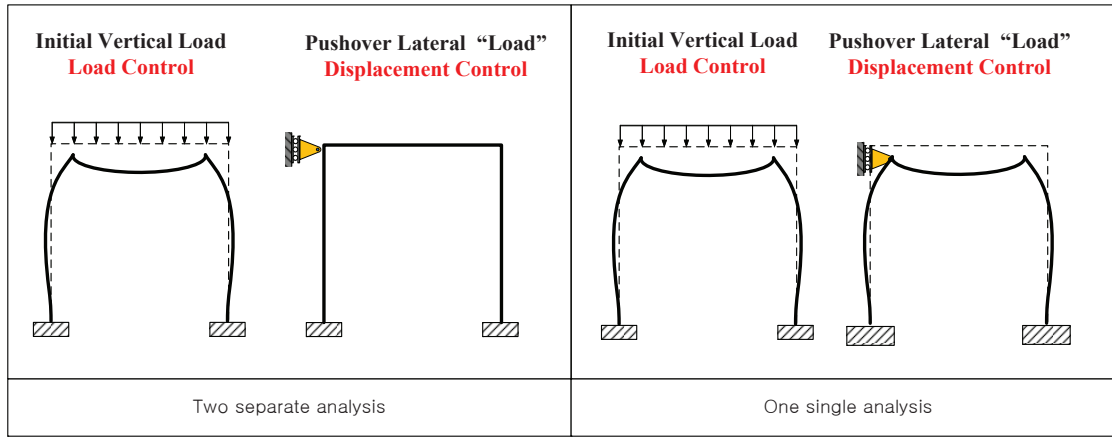


Figure 4.1: Pushover analysis

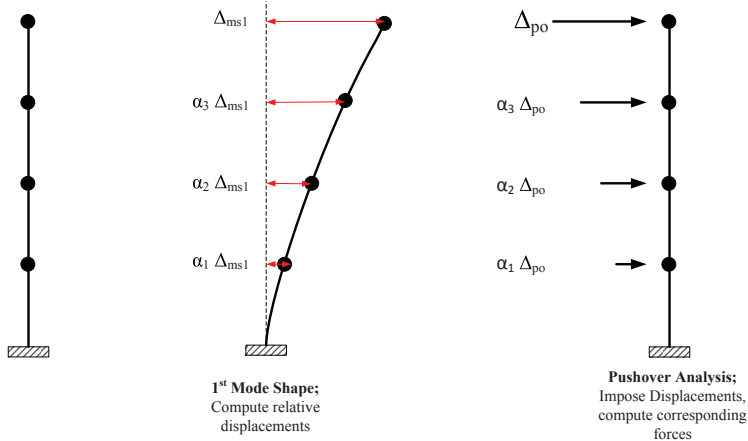


Figure 4.2: Determination of pushover displacements magnitudes

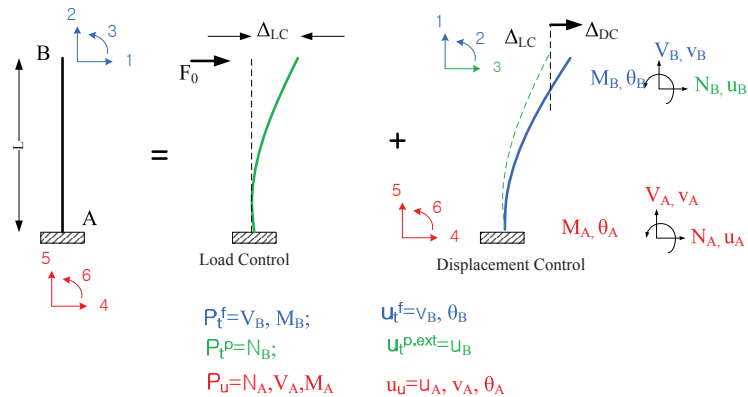


Figure 4.3: Pushover Analysis of a Frame

### 4.5.1 Load Control

This first part is consistent with classical methods where the governing equilibrium equation of a nonlinear system can be expressed as

$$\underbrace{\begin{Bmatrix} \mathbf{P}_t^{ext} \\ \mathbf{P}_u \end{Bmatrix}}_{\mathbf{P}} = \underbrace{\begin{bmatrix} \mathbf{K}_{tt} & \mathbf{K}_{tu} \\ \mathbf{K}_{ut} & \mathbf{K}_{uu} \end{bmatrix}}_{\mathbf{K}} \underbrace{\begin{Bmatrix} \mathbf{u}_t \\ \mathbf{u}_u \end{Bmatrix}}_{\mathbf{u}} \quad (4.1)$$

where  $\mathbf{P}$ ,  $\mathbf{u}$  and  $\mathbf{K}$  are the nodal force, nodal displacement and stiffness terms expressed in the structural level, and the subscript  $u$  and  $t$  are associated with  $\Gamma_u$  and  $\Gamma_t$  where the essential and natural boundary conditions are defined.

Equilibrium is satisfied when external nodal forces are equal to the internal ones,

$$\mathbf{P}^{ext} - \mathbf{P}^{int} = 0 \quad (4.2)$$

and  $\mathbf{P}^{int}$  is determined from state determination in Ch. 1.

In nonlinear system, the incremental displacement vector is defined by

$$\Delta \mathbf{u}_n = \mathbf{u}_n - \mathbf{u}_{n-1}$$

and the corresponding nodal displacement vector at the  $k^{th}$  iteration is given by:

$$\mathbf{u}_n^k = \mathbf{u}_n^{k-1} + \delta \mathbf{u}_n^k$$

where  $\delta \mathbf{u}_n^k = \mathbf{u}_n^k - \mathbf{u}_n^{k-1}$ .

We can rewrite Eq. 4.1 in incremental form at the  $k^{th}$  iteration of the  $n^{th}$  increment as:

$$\underbrace{\begin{Bmatrix} \mathbf{P}_{t,n}^{R,k} = \mathbf{P}_{t,n}^{ext\checkmark} - \mathbf{P}_{t,n}^{int,k\checkmark} \\ \mathbf{P}_{u,n}^{R,k} = \mathbf{P}_{u,n}^{k\checkmark} - \mathbf{P}_{u,n}^{int,k\checkmark} \end{Bmatrix}}_{\mathbf{P}_n^{R,k} = \delta \mathbf{P}_n^k} = \underbrace{\begin{bmatrix} \mathbf{K}_{tt,n}^{k-1} & \mathbf{K}_{tu,n}^{k-1} \\ \mathbf{K}_{ut,n}^{k-1} & \mathbf{K}_{uu,n}^{k-1} \end{bmatrix}}_{\mathbf{K}_n^{k-1}} \underbrace{\begin{Bmatrix} \delta \mathbf{u}_{t,n}^k ? \\ \Delta \mathbf{u}_{u,n}^{ext\checkmark} \end{Bmatrix}}_{\delta \mathbf{u}_n^k} \quad (4.3)$$

where, superscript ' $\checkmark$ ' and '?' refer to known and unknown quantities. It should be noted that the known imposed displacement  $\Delta \mathbf{u}_{u,n}^{ext\checkmark}$  is applied in the first iteration only, and then it is set to  $\mathbf{0}$ .

The incremental displacements can now be expressed as:

$$\begin{aligned} \delta \mathbf{u}_{t,n}^k ? &= \mathbf{u}_{t,n}^k ? - \mathbf{u}_{t,n}^{k-1\checkmark} \\ \Delta \mathbf{u}_{u,n}^{ext\checkmark} &= \mathbf{u}_{u,n}^{ext\checkmark} - \mathbf{u}_{u,n-1}^{ext\checkmark} \end{aligned}$$

and the essence of the finite element analysis is to first determine the displacement  $\delta \mathbf{u}_{t,n}^k ?$ , and then  $\mathbf{P}_{u,n}^{k\checkmark}$  from Eq. 4.3.

In this preliminary analysis, the structure is subjected to its original load, the (yet to be constrained dofs in the pushover analysis) are left as free. At the end of this analysis, we keep track of the nodal displacement

### 4.5.2 Displacement Control

Following the load control part, we now move to displacement control for the pushover analysis.

Rewriting Eq. 4.1 with prescribed external nodal displacements

$$\underbrace{\begin{Bmatrix} \mathbf{P}_t^{f\checkmark} \\ \mathbf{P}_t^{p?} \\ \mathbf{P}_u ? \end{Bmatrix}}_{\delta \mathbf{P}_{t,n}^{p,k-1?}} = \left[ \begin{array}{c|c} \mathbf{K}_{ff}^{ff} & \mathbf{K}_{ff}^{fp} \\ \mathbf{K}_{ff}^{pf} & \mathbf{K}_{ff}^{pp} \\ \hline \mathbf{K}_{ut} & \mathbf{K}_{uu} \end{array} \right] \begin{Bmatrix} \mathbf{u}_t^f ? \\ \mathbf{u}_t^{p,ext\checkmark} \\ \mathbf{u}_u ? \end{Bmatrix} \quad (4.4)$$

where, superscript 'f' and 'p' refer to unknown and prescribed displacement. With reference to Fig. ??, we would have

$$\begin{aligned} \mathbf{P}_t^{f\checkmark} &= [V_B, M_B]^T \\ \mathbf{P}_t^{p?} &= [N_B]^T \\ \mathbf{P}_u ? &= [N_A, V_A, M_A]^T \\ \mathbf{u}_t^f ? &= [v_B, \theta_B]^T \\ \mathbf{u}_t^{p,ext\checkmark} &= [u_B]^T \\ \mathbf{u}_u ? &= [u_A, v_A, \theta_A]^T \end{aligned}$$

Again, in the context of a nonlinear pushover analysis, we rewrite the  $\mathbf{K}_{tt}$  submatrix in incremental form for the  $k^{th}$  iteration of the  $n^{th}$  increment, and since we are now in displacement control, there are no more applied forces. Thus:

$$\underbrace{\begin{Bmatrix} \mathbf{0} \\ \delta \mathbf{P}_{t,n}^{p,k-1?} \end{Bmatrix}}_{\delta \mathbf{P}_{t,n}^{p,k-1?}} = \left[ \begin{array}{cc} \mathbf{K}_{tt,n}^{ff,k-1} & \mathbf{K}_{tt,n}^{fp,k-1} \\ \mathbf{K}_{tt,n}^{pf,k-1} & \mathbf{K}_{tt,n}^{pp,k-1} \end{array} \right] \begin{Bmatrix} \delta \mathbf{u}_t^{f,k-1?} \\ \Delta \mathbf{u}_t^{p,ext\checkmark} \end{Bmatrix} \quad (4.5)$$

We should keep in mind that we are primarily interested in  $\delta \mathbf{P}_{t,n}^{p,k-1?}$  which is the vector of force(s) corresponding to the imposed displacement(s) in the pushover analysis. Also, it should be noted that  $\Delta \mathbf{u}_t^{p,ext\checkmark}$  is only applied in the first iteration, and in subsequent ones, it is  $\mathbf{0}$ .

We first solve for the unknown displacements corresponding to the free degrees of freedom  $\delta \mathbf{u}_t^{f,k-1?}$ .

$$\begin{aligned} \mathbf{0} &= \mathbf{K}_{tt,n}^{ff,k-1} \cdot \delta \mathbf{u}_t^{f,k-1?} + \mathbf{K}_{tt,n}^{fp,k-1} \cdot \delta \mathbf{u}_t^{p,ext\checkmark} \\ \delta \mathbf{u}_t^{f,k-1?} &= -[\mathbf{K}_{tt,n}^{ff,k-1}]^{-1} \cdot \mathbf{K}_{tt,n}^{fp,k-1} \cdot \Delta \mathbf{u}_t^{p,ext\checkmark} \end{aligned} \quad (4.6)$$

Then we address the second row of Eq. to solve for the forces corresponding to the imposed displacements in the pushover analysis,  $\delta \mathbf{P}_{t,n}^{p,k-1?}$ .

It should be noted that the original ID matrix which refers to the global degrees of freedom has to be readjusted into a new one `dispID`.

Also, the internal forces computed from the load control part are transferred to the displacement control part. Thus the entire nonlinear pushover analysis can be performed in a single analysis in Mercury without the need for a restart.

The algorithm for this procedure is shown in Fig. 4.4.

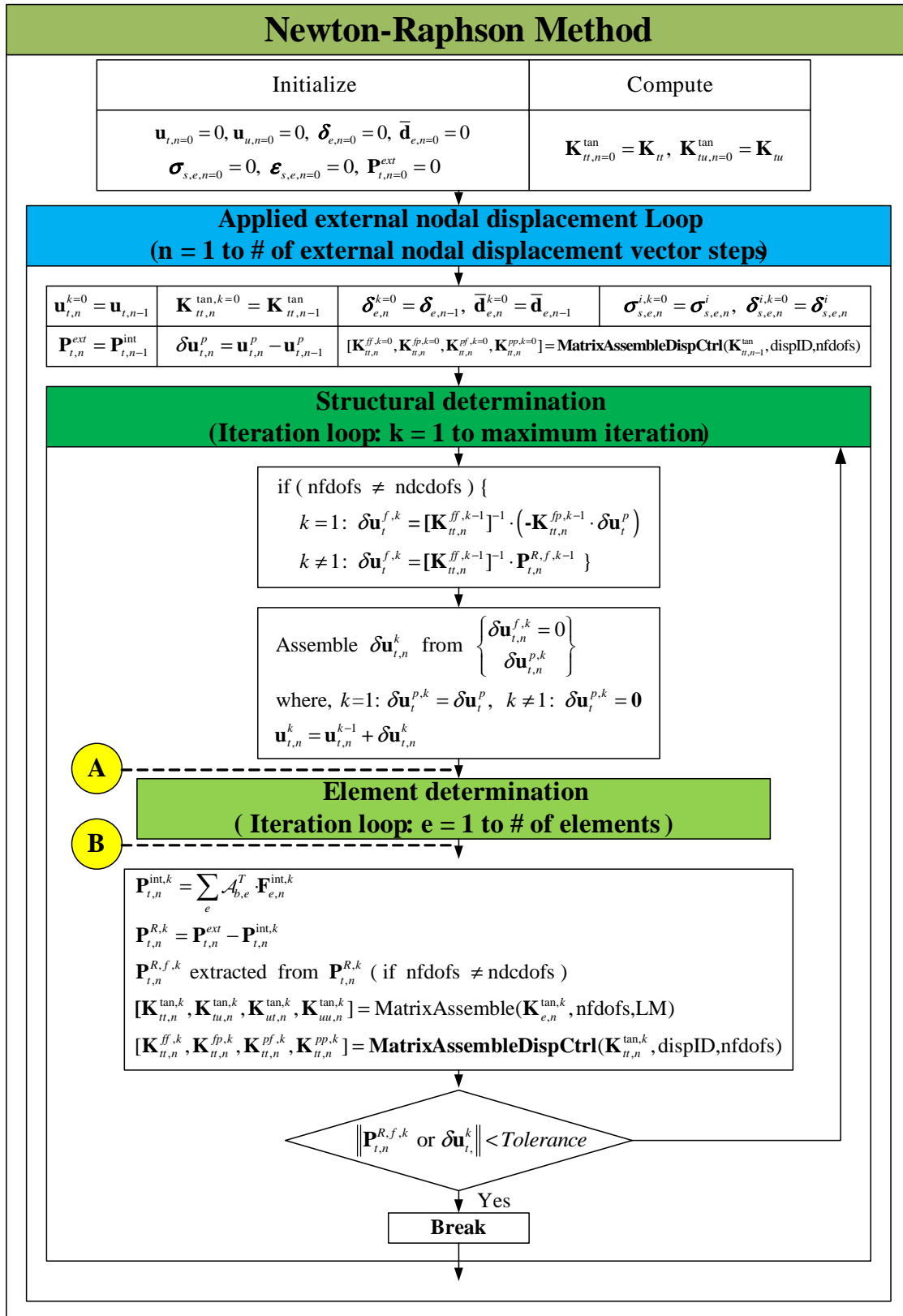


Figure 4.4: Implementation for displacement control



## Chapter 5

### DYNAMIC ANALYSIS

#### 5.1 Preliminaries

1 When the frequency of excitation of a structure is less than about a third of its lowest natural frequency of vibration, then we can neglect inertia effects and treat the problem as a quasi-static one.

2 If the structure is subjected to an impact load, than one must be primarily concerned with (stress) wave propagation. In such a problem, we often have high frequencies and the duration of the dynamic analysis is about the time it takes for the wave to travel across the structure.

3 If inertia forces are present, then we are confronted with a dynamic problem and can analyse it through any one of the following solution procedures:

1. Natural frequencies and mode shapes (only linear elastic systems)
2. Time history analysis through modal analysis (again linear elastic), or direct integration.

4 Methods of structural dynamics are essentially independent of finite element analysis as these methods presume that we already have the stiffness, mass, and damping matrices. Those matrices may be obtained from a single degree of freedom system, from an idealization/simplification of a frame structure, or from a very complex finite element mesh. The time history analysis procedure remains the same.

#### 5.1.1 Variational Formulation

5 In a general three-dimensional continuum, the equations of motion of an elementary volume  $\Omega$  without damping is

$$\mathbf{L}^T \boldsymbol{\sigma} + \mathbf{b} = \mathbf{m}\ddot{\mathbf{u}} \quad (5.1)$$

where  $\mathbf{m}$  is the mass density matrix equal to  $\rho\mathbf{I}$ , and  $\mathbf{b}$  is the vector of body forces. The Differential operator  $\mathbf{L}$  is

$$\mathbf{L} = \begin{bmatrix} \frac{\partial}{\partial x} & 0 & 0 \\ 0 & \frac{\partial}{\partial y} & 0 \\ 0 & 0 & \frac{\partial}{\partial z} \\ \frac{\partial}{\partial y} & \frac{\partial}{\partial x} & 0 \\ \frac{\partial}{\partial z} & 0 & \frac{\partial}{\partial x} \\ 0 & \frac{\partial}{\partial z} & \frac{\partial}{\partial y} \end{bmatrix} \quad (5.2)$$

6 For linear elastic material

$$\boldsymbol{\sigma} = \mathbf{D}_e \boldsymbol{\varepsilon} \quad (5.3)$$

for nonlinear material, the constitutive equations can be written as

$$\dot{\boldsymbol{\sigma}} = \mathbf{D}_i \dot{\boldsymbol{\varepsilon}} \quad (5.4)$$

where  $\mathbf{D}_i$  is the tangent stiffness matrix.

7 Whereas Eq. 5.1 describes the body motion in a strong sense, a weak formulation is obtained by the principle of minimum complementary virtual work (or Weighted Residual/Galerkin)

$$\int_{\Omega} \delta \mathbf{u}^T [\mathbf{L}^T \boldsymbol{\sigma} + \mathbf{b} - \mathbf{m}\ddot{\mathbf{u}}] d\Omega = 0 \quad (5.5)$$

Applying Gauss divergence theorem, Eq. ??:

$$\int \int_A \phi \operatorname{div} \mathbf{q} dA = \oint_s \phi \mathbf{q}^T \mathbf{n} ds - \int \int_A (\nabla \phi)^T \mathbf{q} dA \quad (5.6)$$

and recalling that  $\mathbf{L}\mathbf{u} = \boldsymbol{\varepsilon}$ ,

$$\int_{\Omega} \delta \mathbf{u}^T \mathbf{L}^T \boldsymbol{\sigma} d\Omega = - \int_{\Omega} \delta \boldsymbol{\varepsilon}^T \boldsymbol{\sigma} d\Omega + \int_{\Gamma} \delta \mathbf{u}^T \boldsymbol{\sigma} \mathbf{n} d\Gamma \quad (5.7)$$

thus, Eq. 5.5 transforms into

$$\int_{\Omega} [\delta \mathbf{u}^T (\mathbf{m}\ddot{\mathbf{u}} - \mathbf{b}) + \delta \boldsymbol{\varepsilon}^T \boldsymbol{\sigma}] d\Omega - \int_{\Gamma} \delta \mathbf{u}^T \mathbf{t} d\Gamma = 0 \quad (5.8)$$

so far no assumption has been made with regard to material behavior.

8 Next we will seek the spatial discretization of the virtual work equation (Eq. 5.8). From the previous chapters, we have the following relations

$$\begin{aligned} \mathbf{u} &= \mathbf{N}\bar{\mathbf{u}}; & \delta \mathbf{u}^T &= \delta \bar{\mathbf{u}}^T \mathbf{N}^T; & \ddot{\mathbf{u}} &= \mathbf{N}\ddot{\bar{\mathbf{u}}} \\ \mathbf{B} &= \mathbf{L}\mathbf{N}; & \boldsymbol{\varepsilon} &= \mathbf{B}\bar{\mathbf{u}}; & \delta \boldsymbol{\varepsilon}^T &= \delta \bar{\mathbf{u}}^T \mathbf{B}^T \\ \dot{\boldsymbol{\varepsilon}} &= \mathbf{B}\dot{\bar{\mathbf{u}}} \end{aligned} \quad (5.9)$$

<sup>9</sup> For implicit time integration, equilibrium was reached at time step  $n - 1$ , and we write the equation of equilibrium for time step  $n$ . thus Eq. 5.8 transforms into

$$\int_{\Omega} \delta \mathbf{u}^T \mathbf{m} d\Omega \ddot{\mathbf{u}}^{t+\Delta t} + \int_{\Omega} \delta \boldsymbol{\varepsilon}^T \boldsymbol{\sigma}_{t,n} d\Omega = \int_{\Gamma} \delta \mathbf{u}^T \mathbf{t}_{t,n} d\Gamma + \int_{\Omega} \delta \mathbf{u}^T \mathbf{b}_{t,n} d\Omega \quad (5.10)$$

<sup>10</sup> For linear problems

$$\boldsymbol{\sigma}_{t,n} = \mathbf{D}_e \mathbf{B} \bar{\mathbf{u}}_{t,n} \quad (5.11)$$

<sup>11</sup> Again, upon proper substitution, this would yield

$$\delta \bar{\mathbf{u}}^T \left[ \underbrace{\int_{\Omega} \mathbf{N}^T \mathbf{m} \mathbf{N} d\Omega \bar{\mathbf{u}}_{t,n}}_{\mathbf{M}_{tt}} + \underbrace{\int_{\Omega} \mathbf{B}^T \mathbf{D}_e \mathbf{B} d\Omega \bar{\mathbf{u}}_{t,n}}_{\mathbf{K}} - \underbrace{\left( \int_{\Omega} \mathbf{N}^T \mathbf{P}_{t,n}^{ext} d\Omega + \int_{\Gamma} \mathbf{N}^T \mathbf{t}_{t,n} d\Gamma \right)}_{\mathbf{P}_{t,n}^{ext}} \right] = 0 \quad (5.12)$$

or

$$\boxed{\mathbf{M} \ddot{\mathbf{u}}_{t,n} + \mathbf{K} \bar{\mathbf{u}}_{t,n} = \mathbf{P}_{t,n}^{ext}} \quad (5.13)$$

Which represents the semi-discrete linear equation of motion in the implicit time integration.

Generalizing the previous equation to include the effect of damping, and replacing  $\bar{\mathbf{u}}$  by  $\mathbf{u}$  we have

$$\mathbf{M}_{tt} \cdot \ddot{\mathbf{u}}_t + \mathbf{C}_{tt} \cdot \dot{\mathbf{u}}_t + \mathbf{P}_t^{int} = \mathbf{P}_t^{ext} \quad (5.14)$$

where  $\mathbf{M}_{tt}$  and  $\mathbf{C}_{tt}$  are the mass and viscous damping matrices for the idealization of the structure;  $\ddot{\mathbf{u}}_t$  is the nodal acceleration vector,  $\dot{\mathbf{u}}_t$  is the nodal velocity vector,  $\mathbf{P}_t^{int}$  is the static restoring or internal nodal force vector resulting from the nodal displacement vector  $\mathbf{u}_t$ , and  $\mathbf{P}_t^{ext}$  is the vector of applied nodal forces due to a seismic loading. Numerical methods for solving Eq. 5.14 are divided into two major categories; explicit and implicit methods. This chapter will limit its coverage to implicit schemes and in particular: 1) Newmark  $\beta$  method, 2) the Hilber-Hughes-Taylor(HHT) method.

## 5.1.2 Mass Representation

There are two possible representation of the mass matrix: lumped and consistent.

Nodal lumped masses contribute only to the diagonal terms of the mass matrix and the terms associated with the rotational degrees of freedom are often taken as zero. However, in some cases the rotational inertias can be accounted for. The  $x$ ,  $y$  and  $z$  inertia quantities may be different in a structure particularly in a two-dimensional analysis where the frame being analyzed is flanked by adjoining frames which carry vertical loads but have relatively insignificant lateral stiffness. In this case the vertical inertia is associated only with that of the frame being analyzed while the horizontal inertia has to represent the sum of the inertia contributions of all frames being supported, in the lateral direction, by the frame being analyzed.

The mass matrix may take one of two forms.

1. In this formulation it is assumed that all the masses are concentrated at the end nodes. Though not exactly correct, the advantage of this model is that we will have a diagonal matrix which can be easily inverted. The term associated with rotation is often neglected.
2. The consistent mass model uses a kinematically equivalent mass matrix where inertia forces are associated with all degrees of freedom. This will result in a mass matrix for the structures with the same skyline form as that of the stiffness matrix. The consistent mass model requires a greater computational cost in the multiplication by the nodal accelerations to get the inertia forces at each time-step in the analysis. It also includes all natural frequencies and consequently gives a slight bias to the frequency content of the structure.

### 5.1.2.1 Lumped mass

In prismatic 2D framed structure, the lumped mass matrix in the global reference is simply given by

$$\mathbf{M}_e = \rho \cdot A \cdot L_e \begin{bmatrix} 1/2 & 0 & 0 & 0 & 0 & 0 \\ 0 & 1/2 & 0 & 0 & 0 & 0 \\ 0 & 0 & \alpha_r \cdot L_e^2 & 0 & 0 & 0 \\ 0 & 0 & 0 & 1/2 & 0 & 0 \\ 0 & 0 & 0 & 0 & 1/2 & 0 \\ 0 & 0 & 0 & 0 & 0 & \alpha_r \cdot L_e^2 \end{bmatrix} \quad (5.15)$$

Here  $\alpha_r$  is a nonnegative coefficient for rotation.  $\alpha_r$  zero will result in a singular mass matrix which is undesirable if we have to invert the mass matrix. An *ad hoc* solution to define  $\alpha_r$  is to imagine that a uniform slender bar of length  $L_e/2$  and mass  $m/2$  is attached to each node and rotates with it. The associated mass moment of inertia would  $I_z = (m/2)(L_e/2)^2/3$ , and consequently  $\alpha_r = 1/24$ , (?). It should be noted that models based on lumped mass can run substantially faster than those based on consistent mass.

### 5.1.2.2 Consistent mass

The consistent mass matrix is defined in the local reference frame as

$$\mathbf{m}_e = \int_0^{L_e} \rho \cdot A(x) \cdot \mathbf{N}_d(x)^T \cdot \mathbf{N}_d(x) dx$$

where,

$$\mathbf{N}_d(x) = \begin{bmatrix} 1 - \frac{x}{L_e} & 0 & 0 & \frac{x}{L_e} & 0 & 0 \\ 0 & 1 + 2(\frac{x}{L_e})^3 - 3(\frac{x}{L_e})^2 & x(1 - \frac{x}{L_e})^2 & 0 & -2(\frac{x}{L_e})^3 + 3(\frac{x}{L_e})^2 & x((\frac{x}{L_e})^2 - \frac{x}{L_e}) \end{bmatrix}$$

Hence,

$$\mathbf{m}_e = \frac{\rho \cdot A \cdot L_e}{420} \begin{bmatrix} 140 & 0 & 0 & 70 & 0 & 0 \\ 0 & 156 & 22 \cdot L_e & 0 & 54 & -13 \cdot L_e \\ 0 & 22 \cdot L_e & 4 \cdot L_e^2 & 0 & 13 \cdot L_e & -3 \cdot L_e^2 \\ 70 & 0 & 0 & 140 & 0 & 0 \\ 0 & 54 & 13 \cdot L_e & 0 & 156 & -22 \cdot L_e \\ 0 & -13 \cdot L_e & -3 \cdot L_e^2 & 0 & -22 \cdot L_e & 4 \cdot L_e^2 \end{bmatrix} \quad (5.16)$$

The mass matrix is then transformed into the global reference by rewriting Eq. 5.16 in terms of the rotation matrix,  $\mathbf{\Gamma}_e$ .

$$\mathbf{M}_e = \mathbf{\Gamma}_e^T \cdot \mathbf{m}_e \cdot \mathbf{\Gamma}_e$$

### 5.1.3 Damping Representation

All structures are damped, otherwise their oscillations will never stop. Damping can be viewed as a frictional force which dissipates energy, and can take different form.

The most commonly used form of damping is the so-called viscous or Rayleigh damping which, when inserted in the equation of motion, has the following form

$$\mathbf{M}_{tt} \cdot \ddot{\mathbf{u}}_{t,n} + \mathbf{C}_{tt} \cdot \dot{\mathbf{u}}_{t,n} + \mathbf{P}_{t,n}^{int} = \mathbf{P}_{t,n}^{ext}$$

where,  $\ddot{\mathbf{u}}_{t,n}$ ,  $\dot{\mathbf{u}}_{t,n}$  and  $\mathbf{u}_{t,n}$  are the nodal acceleration, velocity, and displacement vectors at the current time step, respectively;  $\mathbf{P}_{t,n}^{int}$  is the static restoring or internal nodal force vector at the current time step.

Damping is supposed to model the dissipation of energy. In a nonlinear analysis, this is accounted for by some constitutive models which include hysteresis damping, such as the Modified Kent and Park model for concrete (Sect. 2.2.1.1). In linear elastic analysis, the most common form of damping is the so-called viscous damping (better known as Rayleigh damping). In this simplification, we assume the presence of a viscous damper (which by definition is sensitive to velocity) between the structure and an external fixed point (mass proportional), and another set of dampers inside the structure connecting all the degrees of freedom (stiffness proportional damper). Hence, we assume that

$$\mathbf{C}_{tt} = a_m \cdot \mathbf{M}_{tt} + b_k \cdot \mathbf{K}_{tt} \quad (5.17)$$

where,  $a_m$  and  $b_k$  are coefficients which pre-multiply the mass and stiffness terms respectively. Eq. 5.17 is known as proportional Rayleigh damping, Fig. 5.1.

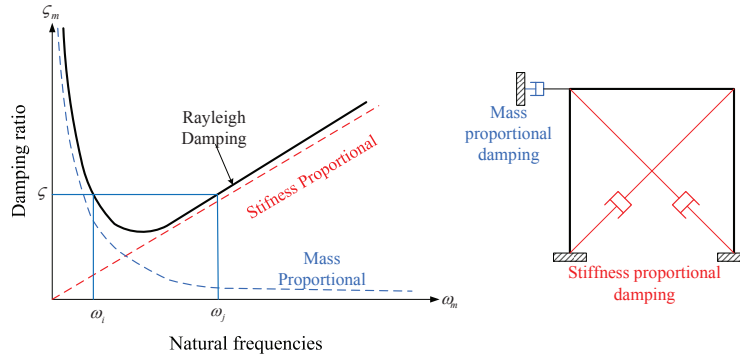


Figure 5.1: Rayleigh damping

Rayleigh damping is the most widely used (but not only) model for damping. The coefficients  $a_m$  and  $b_k$  in Eq. 5.17 are calculated based upon two circular frequencies ( $\omega_1$  and  $\omega_2$ , radians/sec.) to be damped at  $\xi_1$  and  $\xi_2$  respectively. Where  $\omega_m$  and  $\xi_m$  are the circular frequency and the damping ratio of the  $m^{th}$  mode.

We recall that the damping ratio for a single degree of freedom (SDF) for mode  $m$  is given by

$$\zeta_m = \frac{C_{tt,m}}{2 \cdot M_{tt,m} \cdot \omega_m} \quad (5.18)$$

Thus for mass proportional damping of multi degree of freedom (MDF) system, with  $\mathbf{C}_{tt,m} = a_m \cdot \mathbf{M}_{tt,m}$ , this would lead to

$$\zeta_m = \frac{a_m}{2} \cdot \frac{1}{\omega_m}$$

The damping ratio is thus inversely proportional to the natural frequency and  $a_m$  can be selected to obtain a specified damping ratio in any one mode  $i$  or

$$a_m = 2 \cdot \zeta_i \cdot \omega_i \quad (5.19)$$

Similarly, and recalling that  $\mathbf{K}_{tt} \cdot \phi_m = \omega_m^2 \cdot \mathbf{M}_{tt} \cdot \phi_m$ , a stiffness proportional damping  $\mathbf{C}_{tt,m} = b_k \cdot \mathbf{K}_{tt,m}$  combined with Eq. 5.18 will lead to

$$\zeta_m = \frac{b_k}{2} \cdot \omega_m \quad (5.20)$$

In this case the damping ratio is proportional to the natural frequency and  $b_k$  can be selected to obtain a specified damping ratio in any one mode  $j$  or

$$b_k = \frac{2 \cdot \zeta_j}{\omega_j} \quad (5.21)$$

Combining Eq. 5.19 and 5.21 leads to the following linear equations

$$\frac{1}{2} \begin{bmatrix} \frac{1}{\omega_i} & \omega_i \\ \frac{1}{\omega_j} & \omega_j \end{bmatrix} \begin{Bmatrix} a_m \\ b_k \end{Bmatrix} = \begin{Bmatrix} \zeta_i \\ \zeta_j \end{Bmatrix} \quad (5.22)$$

If one assumes the same damping ratio  $\zeta$  for both modes (reasonable practical assumption), then

$$a_m = \zeta \frac{2\omega_i \cdot \omega_j}{\omega_i + \omega_j}$$

$$b_k = \zeta \frac{2}{\omega_i + \omega_j}$$

Again, it should be emphasized that different damping coefficients should be used in linear and in nonlinear analysis (specially if the nonlinear constitutive model accounts for hysteresis damping). Furthermore, if Rayleigh damping is used in a nonlinear analysis, then coefficients  $a_m$  and  $b_k$  may have to be updated at each time increment to reflect the change in the tangential stiffness matrix  $\mathbf{K}_t$ .

### 5.1.4 Euler Methods

Euler method is a numerical procedure to solve initial values ordinary differential equations (as in structural dynamics). In other words, given a solution  $y$  at time  $t_n$ , how do we get the solution at time  $t_{n+1}$ .

In our case, we discretize space by the finite element, and discretize time by the finite difference. Spatial discretization is by now well understood, the question is how do we discretize time, or in its most elementary form a derivative.

As with Newton's method, it all starts with the Taylor's series. We begin with the forward version

$$y(t_n + h) \equiv y_{n+1} = y(t_n) + h \left. \frac{dy}{dt} \right|_{t_n} + O(h^2) \quad (5.23-a)$$

$$\Rightarrow y_{n+1} \simeq y_n + hf(y_n, t_n) \quad (5.23-b)$$

This forward Euler method is also referred to as *explicit* since  $y_{n+1}$  is given explicitly in terms of known quantities such as  $y_n$  and  $f(y_n, t_n)$  and there is no equation to solve. Explicit methods are easy to implement but are conditionally stable (i.e.  $h$  should be smaller than a critical value).

An alternative formulation is one based on the *backward Euler* method which starts with the following Taylor series expansion

$$y(t_n) \equiv y_n = y(t_{n+1} - h) = y(t_{n+1}) - h \left. \frac{dy}{dt} \right|_{t_{n+1}} + O(h^2) \quad (5.24-a)$$

$$\Rightarrow y_{n+1} \simeq y_n + hf(y_{n+1}, t_{n+1}) \quad (5.24-b)$$

This is an *implicit* method since  $f(y_{n+1}, t_{n+1})$  is not known and a (usually) nonlinear equation must be solved at every time step (possibly by the Newton-Raphson method). Evidently, this is more computationally expensive than the explicit method, however the method is *unconditionally stable*.

The geometric interpretation of Euler's method is shown in Fig. 5.2. We note that the implicit method (at the cost of a Newton-Raphson solution) always provides an "exact" solution. In the context of structural dynamics, we can say that equilibrium is satisfied. This is not the case in the explicit method.

#### Example 5.1. Euler Method

Solve the following ordinary linear first order differential equation:

$$\frac{dy}{dt} = 1 + (t - y)^2; \quad 2 \leq t \leq 3; \quad y(2) = 1 \quad (5.25)$$

Solution:

Forward Euler with  $h=0.1$

$$y_{n+1} = y_n + hf(y_n, t_n) \quad (5.26-a)$$

$$y_1 = 1 + 0.1 [1 + (2.1 - 1)^2] = 1.2 \quad (5.26-b)$$

The Backward Euler will give

$$y_{n+1} = y_n + hf(y_{n+1}, t_{n+1}) \quad (5.27-a)$$

$$y_1 = 1 + 0.1 [1 + (2.1 - y_1)^2] \quad (5.27-b)$$

$$0 = 0.1y_1^2 - 1.42y_1 + 1.541 \quad (5.27-c)$$

$$y_1 = 1.1839 \quad (5.27-d)$$

In this case we had a quadratic equation to solve, however in general we may have to use Newton's method to solve for  $y_n$ . ■

## 5.2 Time Integration Methods

Time integration is performed through a finite difference solution of the time discretization. We will (have to) assume that equilibrium was reached in the previous time step  $n-1$

$$\mathbf{M}_{tt} \cdot \ddot{\mathbf{u}}_{t,n-1} + \mathbf{C}_{tt} \cdot \dot{\mathbf{u}}_{t,n-1} + \mathbf{P}_{t,n-1}^{int} = \mathbf{P}_{t,n-1}^{ext}$$

At the current time step  $n$ , the equation of motion will be given by

$$\mathbf{M}_{tt} \cdot \ddot{\mathbf{u}}_{t,n} + \mathbf{C}_{tt} \cdot \dot{\mathbf{u}}_{t,n} + \mathbf{P}_{t,n}^{int} = \mathbf{P}_{t,n}^{ext} \quad (5.28)$$

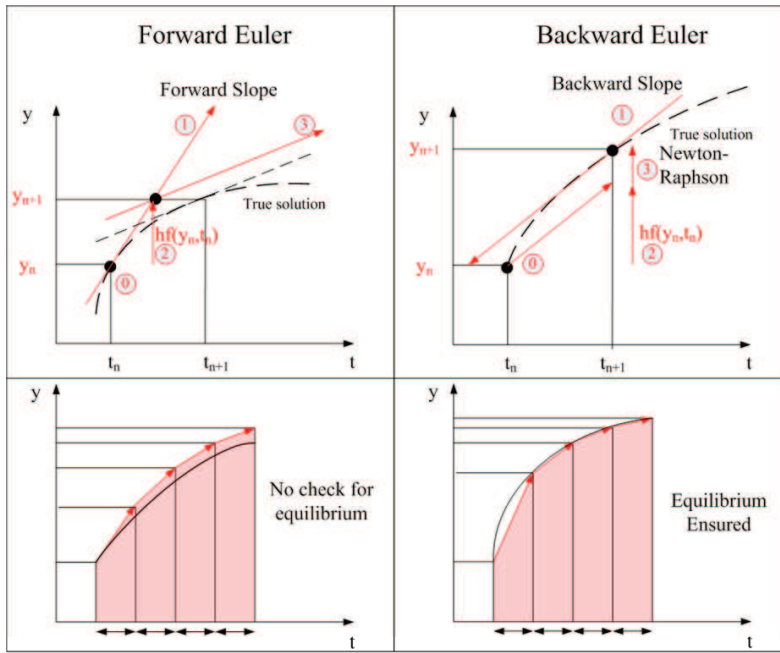


Figure 5.2: Geometric interpretation of Euler's method

There are two broad classes of solution to solve this equation

1. Explicit methods

The nodal displacement vector  $\mathbf{u}_{t,n}$  at the current time step can be calculated from a function of structural response solutions at the previous time step  $n - 1$ . The effective stiffness matrix for solving the equation of motion consists of mass matrix and/or damping matrix. This indicates that it is not necessary to invert the structural stiffness matrix.

2. Implicit methods

The nodal displacement vector  $\mathbf{u}_{t,n}$  at the current time step is often represented as a function of structural response quantities with both the previous time step  $n - 1$  and the current time step  $n$ . For this reason, iteration procedure such as Newton-Raphson iterative method has to be applied so as to solve equations and to achieve convergence if the response is nonlinear.

Advantages of using explicit methods for transient analysis include the simplicity of the algorithm, easy implementation and their fast and efficient computation without the demand for iterations. In addition, there are no need for the knowledge of the tangent stiffness during the test. However, explicit methods are only conditionally stable. This means that the computed response may grow without bound when the product of the time step and the highest natural frequency of the structure  $\Delta t \cdot \omega$  exceeds a limitation. In analyzing a structure with a very high natural frequency  $\omega$ , a small time interval needs to be used and it can be too small to be practical. On the other hand, most implicit methods are unconditionally stable. This means that it is possible to analyze a multi-degree-of-freedom system with high frequency modes using a reasonably large time step without stability problems. Furthermore, implicit methods can be customized to provide favorable numerical energy dissipation properties. In addition to the prescribed viscous damping matrix  $\mathbf{C}_{tt}$ , implicit methods provide numerical damping which can be controlled by certain parameters. The value of these parameters can be selected in order to suppress the spurious higher-mode responses, excited by experimental errors during the test. However, an iterative solution procedure for a nonlinear system is computationally more demanding. It introduces the possibility of inducing undesirable loading and unloading hysteresis in a structure whose behavior can be highly sensitive to prior inelastic deformation history. Last but not least implicit methods are ideal candidates for real time hybrid simulation.

### 5.2.1 Newmark $\beta$ method

Euler's method is now generalized for second order differential equations (equation of motion)

$$\begin{aligned} \begin{pmatrix} \mathbf{u} \\ \dot{\mathbf{u}} \end{pmatrix}^n &= \begin{pmatrix} \mathbf{u} \\ \dot{\mathbf{u}} \end{pmatrix}^{n-1} + \Delta t \begin{pmatrix} \dot{\mathbf{u}} \\ \ddot{\mathbf{u}} \end{pmatrix}^{n-1} && \text{Forward Euler} \\ \begin{pmatrix} \mathbf{u} \\ \dot{\mathbf{u}} \end{pmatrix}^n &= \begin{pmatrix} \mathbf{u} \\ \dot{\mathbf{u}} \end{pmatrix}^{n-1} + \Delta t \begin{pmatrix} \dot{\mathbf{u}} \\ \ddot{\mathbf{u}} \end{pmatrix}^n && \text{Backward Euler} \end{aligned} \quad (5.29)$$

Newmark's method is a variation of Euler's method, where higher order derivatives (Eq. 5.28) are computed with lower accuracy for the sake of efficiency.

Again, we first consider the Taylor series expansions of the nodal displacement and velocity vector terms about the values at the previous time  $n - 1$ .

$$\begin{aligned} \mathbf{u}_{t,n} &\approx \mathbf{u}_{t,n-1} + \frac{\partial \mathbf{u}_{t,n-1}}{\partial t} \Delta t + \frac{\partial^2 \mathbf{u}_{t,n-1}}{\partial t^2} \frac{\Delta t^2}{2!} + \frac{\partial^3 \mathbf{u}_{t,n}}{\partial t^3} \frac{\Delta t^3}{3!} + \dots \\ \dot{\mathbf{u}}_{t,n} &\approx \dot{\mathbf{u}}_{t,n-1} + \frac{\partial^2 \mathbf{u}_{t,n-1}}{\partial t^2} \Delta t + \frac{\partial^3 \mathbf{u}_{t,n}}{\partial t^3} \frac{\Delta t^2}{2!} + \dots \end{aligned} \quad (5.30)$$

The above two equations represent the approximate displacement and velocity vectors ( $\mathbf{u}_{t,n}$  and  $\dot{\mathbf{u}}_{t,n}$ ) except for high order terms

Table 5.1: Properties of the Newmark  $\beta$  method

Method	Type	$\beta$	$\gamma$	Stability condition	Order of accuracy
Constant acceleration	Implicit	1/4	1/2	Unconditional	2
Linear acceleration	implicit	1/6	1/2	$\Delta t \leq 2\sqrt{3}/\omega$	2
Central difference	Explicit	0	1/2	$\Delta t \leq 2/\omega$	2

of Taylor series. We represent the last terms of the above two equations as follow:

$$\frac{\partial^3 \mathbf{u}_{t,n}}{\partial^3 t} \frac{\Delta t^3}{3!} \approx \frac{\frac{\partial^2 \mathbf{u}_{t,n}}{\partial^2 t} - \frac{\partial^2 \mathbf{u}_{t,n-1}}{\partial^2 t}}{\Delta t} \frac{\Delta t^3}{3!} \approx (\ddot{\mathbf{u}}_{t,n} - \ddot{\mathbf{u}}_{t,n-1}) \frac{\Delta t^2}{3!} \\ \approx \beta (\ddot{\mathbf{u}}_{t,n} - \ddot{\mathbf{u}}_{t,n-1}) \Delta t^2 \quad (5.31)$$

$$\frac{\partial^3 \mathbf{u}_{t,n}}{\partial^3 t} \frac{\Delta t^2}{2!} \approx \frac{\frac{\partial^2 \mathbf{u}_{t,n}}{\partial^2 t} - \frac{\partial^2 \mathbf{u}_{t,n-1}}{\partial^2 t}}{\Delta t} \frac{\Delta t^2}{2!} \approx (\ddot{\mathbf{u}}_{t,n} - \ddot{\mathbf{u}}_{t,n-1}) \frac{\Delta t}{2!} \\ \approx \gamma (\ddot{\mathbf{u}}_{t,n} - \ddot{\mathbf{u}}_{t,n-1}) \Delta t \quad (5.32)$$

where  $\beta$  and  $\gamma$  are parameters which depict numerical approximations. These parameters will account for Eq. 5.31 and Eq. 5.32 including additional terms which were dropped from Taylor series approximation. Substituting Eq. 5.31 and Eq. 5.32 into Eq. ?? and Eq. 5.30, respectively, we obtain the two equations as follow:

$$\mathbf{u}_{t,n} = \mathbf{u}_{t,n-1} + \Delta t \cdot \dot{\mathbf{u}}_{t,n-1} + \frac{\Delta t^2}{2} \cdot \ddot{\mathbf{u}}_{t,n-1} + \Delta t^2 \cdot \beta \cdot (\ddot{\mathbf{u}}_{t,n} - \ddot{\mathbf{u}}_{t,n-1}) \quad (5.33)$$

$$\dot{\mathbf{u}}_{t,n} = \dot{\mathbf{u}}_{t,n-1} + \Delta t \cdot \ddot{\mathbf{u}}_{t,n-1} + \Delta t \cdot \gamma \cdot (\ddot{\mathbf{u}}_{t,n} - \ddot{\mathbf{u}}_{t,n-1})$$

Hence, we obtain the Newmark  $\beta$  method, which consists of the following equations:

$$\mathbf{P}_{t,n}^{ext} = \mathbf{M}_{tt} \cdot \ddot{\mathbf{u}}_{t,n} + \mathbf{C}_{tt} \cdot \dot{\mathbf{u}}_{t,n} + \mathbf{P}_{t,n}^{int} \quad (5.34)$$

$$\mathbf{u}_{t,n} = \mathbf{u}_{t,n-1} + \Delta t \cdot \dot{\mathbf{u}}_{t,n-1} + \frac{\Delta t^2}{2} [(1 - 2\beta) \ddot{\mathbf{u}}_{t,n-1} + 2\beta \cdot \ddot{\mathbf{u}}_{t,n}] \quad (5.35)$$

$$\dot{\mathbf{u}}_{t,n} = \dot{\mathbf{u}}_{t,n-1} + \Delta t [(1 - \gamma) \ddot{\mathbf{u}}_{t,n-1} + \gamma \cdot \ddot{\mathbf{u}}_{t,n}] \quad (5.36)$$

where, Eq. 5.34 is the equation of equilibrium expressed at time  $n+1$ , and Eq. 5.35 and Eq. 5.36 are finite difference formulas describing the evolution of the approximation solution.  $\beta$  and  $\gamma$  are parameters that determine the stability and accuracy characteristics. Stability conditions for the Newmark  $\beta$  method follows:

1. unconditionally stable if

$$\begin{aligned} \gamma &\geq \frac{1}{2} \\ \beta &\geq \frac{\gamma}{2} \end{aligned}$$

2. conditionally stable if

$$\begin{aligned} \gamma &\geq \frac{1}{2} \\ \beta &< \frac{\gamma}{2} \end{aligned}$$

with the following stability limit:

$$\omega \cdot \Delta t \leq \Omega_{crit} = \frac{\xi(\gamma - 1/2) + [\gamma/2 - \beta + \xi^2(\gamma - 1/2)^2]^{1/2}}{\gamma/2 - \beta} \quad (5.37)$$

where  $\omega$  is maximum natural frequency,  $\Omega_{crit}$  is critical sampling frequency, and  $\xi$  is the damping ratio.

The constant acceleration (trapezoidal rule) method is implicit and unconditionally stable. The linear acceleration method is implicit and conditionally stable. The central difference method is conditionally stable. Note that if  $\gamma = 1/2$  has no effect on stability. In practice it is more convenient to express Eq. 5.37 in terms of the period of vibration,  $T = 2\pi/\omega$ , in which case Eq. 5.37 becomes  $\Delta t/T \leq \Omega_{crit}/(2\pi)$ . In the case of the linear acceleration,  $\Delta t/T$  is calculated as follows:

$$\frac{\Delta t}{T} \leq \frac{1}{2\pi} \frac{1}{\sqrt{\gamma - 2\beta}} = 0.551$$

A summary for the Newmark  $\beta$  method is shown in Table. 5.1.

### 5.2.1.1 Newmark $\beta$ implicit method

The Newmark  $\beta$  implicit method can be expressed with Eq. 5.34, 5.35, and 5.36. Rewriting Eq. 5.35 and 5.36:

$$\mathbf{u}_{t,n} = \tilde{\mathbf{u}}_{t,n} + \Delta t^2 \cdot \beta \cdot \ddot{\mathbf{u}}_{t,n} \quad (5.38)$$

$$\dot{\mathbf{u}}_{t,n} = \tilde{\mathbf{u}}_{t,n} + \Delta t \cdot \gamma \cdot \ddot{\mathbf{u}}_{t,n} \quad (5.39)$$

where we have labeled the known quantities at time step  $n-1$  as  $(\tilde{\cdot})$

$$\tilde{\mathbf{u}}_{t,n} = \mathbf{u}_{t,n-1} + \Delta t \cdot \dot{\mathbf{u}}_{t,n-1} + \frac{\Delta t^2}{2} (1 - 2\beta) \ddot{\mathbf{u}}_{t,n-1}$$

$$\tilde{\mathbf{u}}_{t,n} = \dot{\mathbf{u}}_{t,n-1} + \Delta t (1 - \gamma) \ddot{\mathbf{u}}_{t,n-1}$$

Rewriting Eq. 5.38, we can solve for  $\ddot{\mathbf{u}}_{t,n}$ :

$$\ddot{\mathbf{u}}_{t,n} = \frac{\mathbf{u}_{t,n} - \tilde{\mathbf{u}}_{t,n}}{\Delta t^2 \cdot \beta} \quad (5.40)$$

Substituting Eq. 5.40 into Eq. 5.39, we can rewrite  $\dot{\mathbf{u}}_{t,n}$ :

$$\dot{\mathbf{u}}_{t,n} = \tilde{\mathbf{u}}_{t,n} + \frac{\gamma}{\Delta t \cdot \beta} (\mathbf{u}_{t,n} - \tilde{\mathbf{u}}_{t,n}) \quad (5.41)$$

Substituting Eq. 5.40 and Eq. 5.41 into Eq. 5.34, we have:

$$\mathbf{M}_{tt} \left[ \frac{\mathbf{u}_{t,n} - \tilde{\mathbf{u}}_{t,n}}{\Delta t^2 \cdot \beta} \right] + \mathbf{C}_{tt} \left[ \tilde{\mathbf{u}}_{t,n} + \frac{\gamma}{\Delta t \cdot \beta} (\mathbf{u}_{t,n} - \tilde{\mathbf{u}}_{t,n}) \right] + \mathbf{P}_{t,n}^{int} = \mathbf{P}_{t,n}^{ext} \quad (5.42)$$

Rewriting Eq. 5.42,

$$\begin{aligned} & \frac{1}{\Delta t^2 \cdot \beta} \mathbf{M}_{tt} \cdot \mathbf{u}_{t,n} + \frac{\gamma}{\Delta t \cdot \beta} \mathbf{C}_{tt} \cdot \mathbf{u}_{t,n} + \mathbf{P}_{t,n}^{int} \\ &= \mathbf{P}_{t,n}^{ext} + \frac{1}{\Delta t^2 \cdot \beta} \mathbf{M}_{tt} \cdot \tilde{\mathbf{u}}_{t,n} + \frac{\gamma}{\Delta t \cdot \beta} \mathbf{C}_{tt} \cdot \tilde{\mathbf{u}}_{t,n} - \mathbf{C}_{tt} \cdot \tilde{\mathbf{u}}_{t,n} \end{aligned} \quad (5.43)$$

If the trial solutions in given iteration step  $k$  are  $\mathbf{u}_{t,n}^k$ , and  $\mathbf{P}_{t,n}^{int,k}$ , then it does not satisfy the equations of motion. Hence, we can write for this particular step with residual force vector  $\mathbf{P}_{t,n}^{R,k}$ :

$$\mathbf{P}_{t,n}^{R,k} = \mathbf{P}_{t,n}^{ext} + \overline{\mathbf{M}}_{tt} (\tilde{\mathbf{u}}_{t,n} - \mathbf{u}_{t,n}^k) - \mathbf{C}_{tt} \cdot \tilde{\mathbf{u}}_{t,n} - \mathbf{P}_{t,n}^{int,k}$$

where,

$$\overline{\mathbf{M}}_{tt} = \frac{\mathbf{M}_{tt} + \Delta t \cdot \gamma \cdot \mathbf{C}}{\Delta t^2 \cdot \beta}$$

Using initial stiffness iterative method, we can solve for  $\Delta \mathbf{u}_{t,n}^k$ :

$$\mathbf{P}_{t,n}^{R,k} = \mathbf{K}_{eff} \cdot \Delta \mathbf{u}_{t,n}^k \quad (5.44)$$

where,  $\mathbf{K}_{eff}$  is the effective stiffness matrix, and  $\Delta \mathbf{u}_{t,n}^k$  is:

$$\Delta \mathbf{u}_{t,n}^k = \mathbf{u}_{t,n} - \mathbf{u}_{t,n}^k$$

In elastic section, we can rewrite  $\mathbf{P}_{t,n}^{int}$  to compute the effective stiffness matrix with initial stiffness matrix  $\mathbf{K}_{tt}$ :

$$\mathbf{P}_{t,n}^{int} = \mathbf{K}_{tt} \cdot \mathbf{u}_{t,n} \quad (5.45)$$

Substituting Eq. 5.45 into Eq. 5.43, we can solve for  $\mathbf{u}_{t,n}$ :

$$\mathbf{K}_{eff} \cdot \mathbf{u}_{t,n} = \mathbf{P}_{t,n}^{ext} + \overline{\mathbf{M}}_{tt} \cdot \tilde{\mathbf{u}}_{t,n} - \mathbf{C}_{tt} \cdot \tilde{\mathbf{u}}_{t,n}$$

where,

$$\mathbf{K}_{eff} = \overline{\mathbf{M}}_{tt} + \mathbf{K}_{tt}$$

From Eq. 5.44, we can solve for  $\delta \mathbf{u}_{t,n}^k$  and the updated displacement vector  $\mathbf{u}_{t,n}^{k+1}$  at the next iteration step  $k+1$ :

$$\delta \mathbf{u}_{t,n}^k = [\mathbf{K}_{eff}]^{-1} \cdot \mathbf{P}_{t,n}^{R,k}$$

$$\mathbf{u}_{t,n}^{k+1} = \mathbf{u}_{t,n}^k + \delta \mathbf{u}_{t,n}^k$$

Fig. 5.3 and 5.4 explain the implementation of transient analysis using the Newmark  $\beta$  implicit method with flexibility-based 2D beam-column elements.

## 5.2.2 Hilber-Hughes-Taylor Method

### 5.2.2.1 General Formulation

A major drawback of Newmark  $\beta$  method is the tendency for high frequency noise to persist in the solution. On the other hand, when linear damping or artificial viscosity is added via the parameter  $\gamma$ , the accuracy is markedly degraded. The  $\alpha$  method, (?) improves numerical dissipation for high frequency without degrading the accuracy as much.

Equation of motion in HHT method is written at current time step  $n$  (forward difference) as:

$$\mathbf{M}_{tt} \cdot \ddot{\mathbf{u}}_{t,n} + \mathbf{P}_{t,n}^{int} = \mathbf{P}_{t,n}^{ext}$$

Seeking an approximate solution of this equation by one-step difference, we write,

$$\mathbf{M}_{tt} \cdot \ddot{\mathbf{u}}_{t,n} + (1 + \alpha) \mathbf{P}_{t,n}^{int} - \alpha \cdot \mathbf{P}_{t,n-1}^{int} = \mathbf{P}_{t,n}^{ext}$$

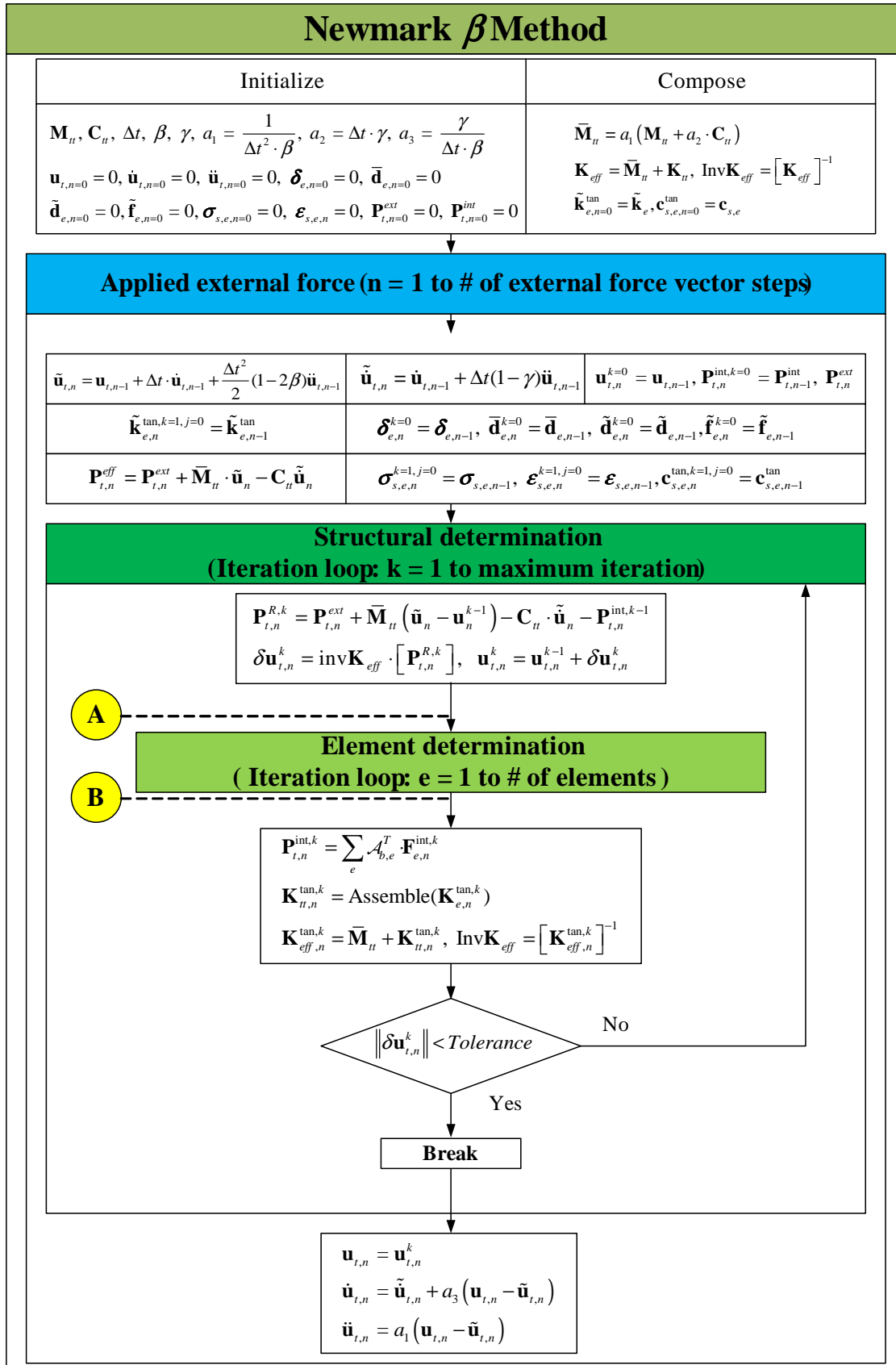
with Eq. 5.33.

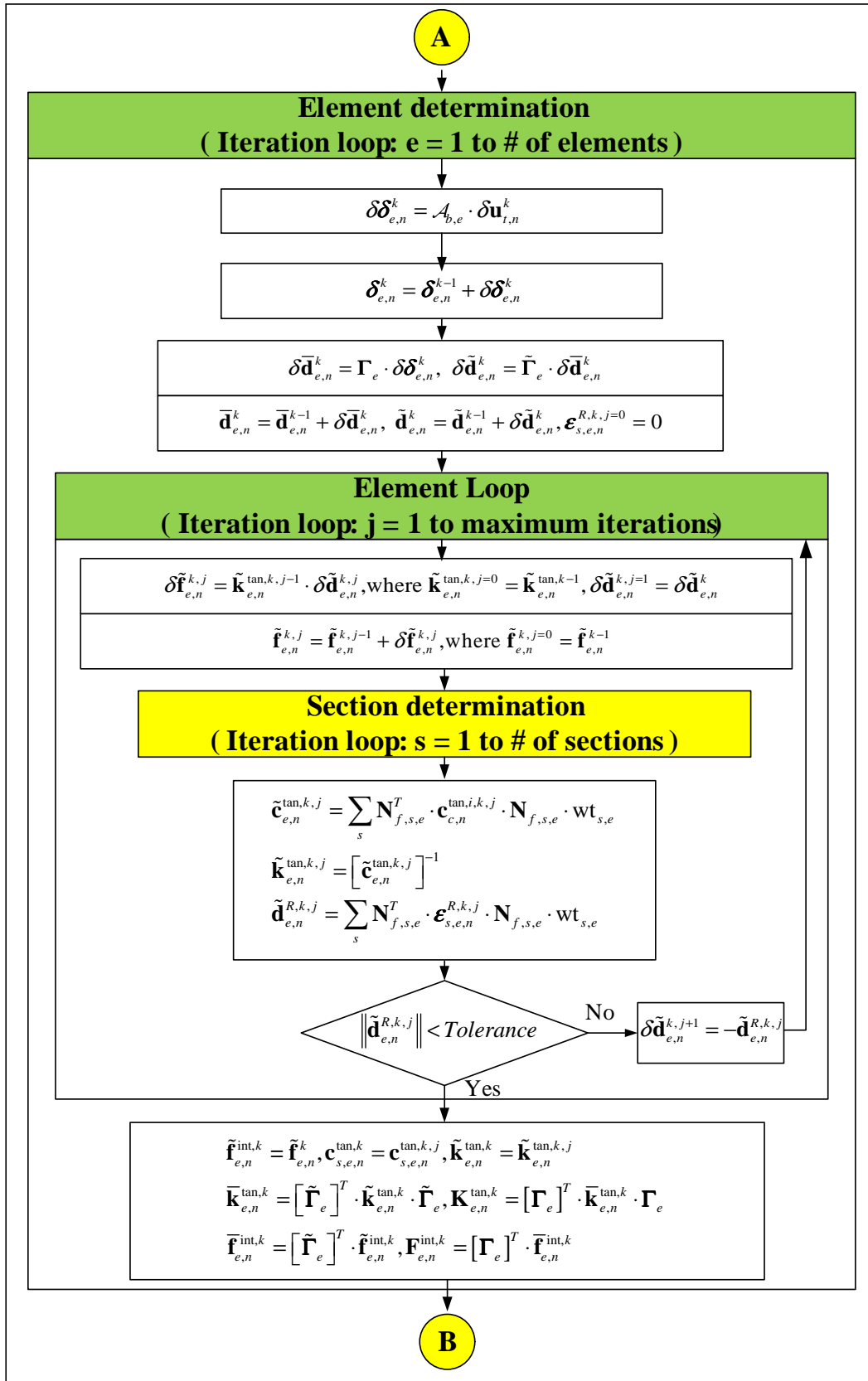
We note that the HHT method introduces  $\alpha(\mathbf{P}_{t,n}^{int} - \mathbf{P}_{t,n-1}^{int})$  which is akin of stiffness proportional damping (indeed it is commonly said that the  $\alpha$  method provides numerical damping). If the above equation is expanded, effect of damping introduced, and possible material nonlinearity introduced, we obtain:

$$(1 + \alpha) \mathbf{P}_{t,n}^{ext} - \alpha \mathbf{P}_{t,n-1}^{ext} = \mathbf{M}_{tt} \cdot \ddot{\mathbf{u}}_{t,n} + (1 + \alpha) \mathbf{C}_{tt} \cdot \dot{\mathbf{u}}_{t,n} - \alpha \cdot \mathbf{C}_{tt} \cdot \dot{\mathbf{u}}_{t,n-1} + (1 + \alpha) \mathbf{P}_{t,n}^{int} - \alpha \cdot \mathbf{P}_{t,n-1}^{int} \quad (5.46)$$

If  $-1/3 \leq \alpha \leq 0$ ,  $\beta = (1 - \alpha)^2/4$ , and  $\gamma = (1 - 2\alpha)/2$ , then the  $\alpha$  method is unconditionally stable and has a second-order accuracy. Hence, Eq. 5.33 and 5.46 must all be simultaneously satisfied through an iterative method.

Assuming that we have obtained the response at the previous time step  $n-1$ , i.e.  $\mathbf{u}_{t,n-1}$ ,  $\dot{\mathbf{u}}_{t,n-1}$  and  $\ddot{\mathbf{u}}_{t,n-1}$  which satisfy the equation of motion, we now seek to determine the solution at the current time step  $n$  by iteration. First of all, we need to determine

Figure 5.3: Flow chart (1) of transient analysis using the Newmark  $\beta$  implicit method

Figure 5.4: Flow chart (2) of transient analysis using the Newmark  $\beta$  implicit method

effective external force and effective stiffness. These are calculated from Eq. 5.40, 5.41 and 5.46.

$$\begin{aligned} & \frac{1}{\Delta t^2 \cdot \beta} \mathbf{M}_{tt} \cdot \mathbf{u}_{t,n} + \frac{\gamma}{\Delta t \cdot \beta} (1+\alpha) \mathbf{C}_{tt} \cdot \mathbf{u}_{t,n} + (1+\alpha) \mathbf{P}_{t,n}^{int} \\ &= (1+\alpha) \mathbf{P}_{t,n}^{ext} - \alpha \cdot \mathbf{P}_{t,n-1}^{ext} + \frac{1}{\Delta t^2 \cdot \beta} \mathbf{M}_{tt} \cdot \tilde{\mathbf{u}}_{t,n} + \frac{\gamma}{\Delta t \cdot \beta} (1+\alpha) \mathbf{C}_{tt} \cdot \tilde{\mathbf{u}}_{t,n} \\ &\quad - (1+\alpha) \mathbf{C}_{tt} \cdot \tilde{\mathbf{u}}_{t,n} + \alpha \cdot \mathbf{C}_{tt} \cdot \dot{\mathbf{u}}_{t,n-1} + \alpha \cdot \mathbf{P}_{t,n}^{int} \end{aligned} \quad (5.47)$$

The trial solutions in iteration step  $k$  are  $\mathbf{u}_{t,n}^k$ , and  $\mathbf{P}_{t,n}^{int,k}$ , does not necessarily satisfy the equations of motion. Hence, we can write for this particular step:

$$\begin{aligned} \mathbf{P}_{t,n}^{R,k} &= (1+\alpha) \mathbf{P}_{t,n}^{ext} - \alpha \cdot \mathbf{P}_{t,n-1}^{ext} + \bar{\mathbf{M}}_{tt} (\tilde{\mathbf{u}}_{t,n} - \mathbf{u}_{t,n}^k) - (1+\alpha) \mathbf{C}_{tt} \cdot \tilde{\mathbf{u}}_{t,n} + \alpha \cdot \mathbf{C}_{tt} \cdot \dot{\mathbf{u}}_{t,n-1} \\ &\quad - (1+\alpha) \mathbf{P}_{t,n}^{int,k} + \alpha \cdot \mathbf{P}_{t,n-1}^{int} \end{aligned}$$

where,

$$\bar{\mathbf{M}}_{tt} = \frac{\mathbf{M}_{tt} + \Delta t \cdot \gamma (1+\alpha) \mathbf{C}_{tt}}{\Delta t^2 \cdot \beta}$$

and  $\mathbf{P}_{t,n}^{R,k}$  is the residual force vector.

Using the initial stiffness iterative method, we can solve for  $\Delta \mathbf{u}_{t,n}^k$ :

$$\mathbf{P}_{t,n}^{R,k} = \mathbf{K}_{eff} \cdot \Delta \mathbf{u}_{t,n}^k \quad (5.48)$$

where,  $\mathbf{K}_{eff}$  is the effective stiffness matrix, and  $\Delta \mathbf{u}_{t,n}^k$  is:

$$\Delta \mathbf{u}_{t,n}^k = \mathbf{u}_{t,n} - \mathbf{u}_{t,n}^k$$

In elastic section, we can express  $\mathbf{P}_{t,n}^{int}$  to compute the effective stiffness matrix with initial stiffness matrix  $\mathbf{K}_{tt}$  as:

$$\mathbf{P}_{t,n}^{int} = \mathbf{K}_{tt} \cdot \mathbf{u}_{t,n} \quad (5.49)$$

Substituting Eq. 5.49 into Eq. 5.47, we solve for  $\mathbf{u}_{t,n}$ :

$$\begin{aligned} \mathbf{K}_{eff} \cdot \mathbf{u}_{t,n} &= (1+\alpha) \mathbf{P}_{t,n}^{ext} - \alpha \cdot \mathbf{P}_{t,n-1}^{ext} + \bar{\mathbf{M}}_{tt} \cdot \tilde{\mathbf{u}}_{t,n} \\ &\quad - (1+\alpha) \cdot \mathbf{C}_{tt} \cdot \tilde{\mathbf{u}}_{t,n} + \alpha \cdot \mathbf{C}_{tt} \cdot \dot{\mathbf{u}}_{t,n-1} + \alpha \cdot \mathbf{P}_{t,n-1}^{int} \end{aligned}$$

where,

$$\mathbf{K}_{eff} = \bar{\mathbf{M}}_{tt} + (1+\alpha) \mathbf{K}_{tt}$$

From Eq. 5.48, we solve for  $\delta \mathbf{u}_{t,n}^k$  and the updated displacement vector  $\mathbf{u}_{t,n}^{k+1}$  at the next iteration step  $k+1$ :

$$\begin{aligned} \delta \mathbf{u}_{t,n}^k &= [\mathbf{K}_{eff}]^{-1} \cdot \mathbf{P}_{t,n}^{R,k} \\ \mathbf{u}_{t,n}^{k+1} &= \mathbf{u}_{t,n}^k + \delta \mathbf{u}_{t,n}^k \end{aligned}$$

Finally, we note that:

1.  $\alpha$  introduces a damping that grows with the ratio of time increment to the period of vibration of a node.
2. Negative values of  $\alpha$  provide damping
3. If  $\alpha = 0$ , we have no artificial damping (energy preseving) and is exactly the constant acceleration (trapezoidal rule) - Newmark's  $\beta$  method if  $\beta = 1/4$  and  $\gamma = 1/2$ .
4. Maximum value is  $\alpha = -1/3$  which provides the maximum artificial damping. This results in a damping ratio of about 6% when the time increment is 40% of the period of oscillation of the mode being studied and smaller if the oscillation period increases.
5. This artificial damping is not very substantial for realistic time increment and low frequencies, but is non-negligible for high frequencies.
6. A default value of -0.05 is recommended.

Fig. 5.5 explains the implementation of transient analysis using the HHT implicit method in structural level. Element state determination is identical to Fig. 5.4.

### 5.3 Free Vibration

<sup>12</sup> The governing equation for the free (undamped) vibration of a structure is

$$\mathbf{M}\ddot{\mathbf{u}} + \mathbf{K}\mathbf{u} = 0 \quad (5.50)$$

where the motion is referred to being free, since there are no applied loads.

<sup>13</sup> By assuming a *harmonic motion*

$$\mathbf{u} = \phi \sin \omega t \quad (5.51)$$

the *natural frequencies*  $\omega$  and the corresponding *mode shapes*  $\phi$  can be determined from the *generalized eigenvalue problem*

$$\omega^2 \mathbf{M}\phi = \mathbf{K}\phi \quad (5.52)$$

or

$$(\mathbf{K} - \omega^2 \mathbf{M})\phi = 0 \quad (5.53)$$

Since  $\phi$  is nontrivial

$$|\mathbf{K} - \omega^2 \mathbf{M}| = 0 \quad (5.54)$$

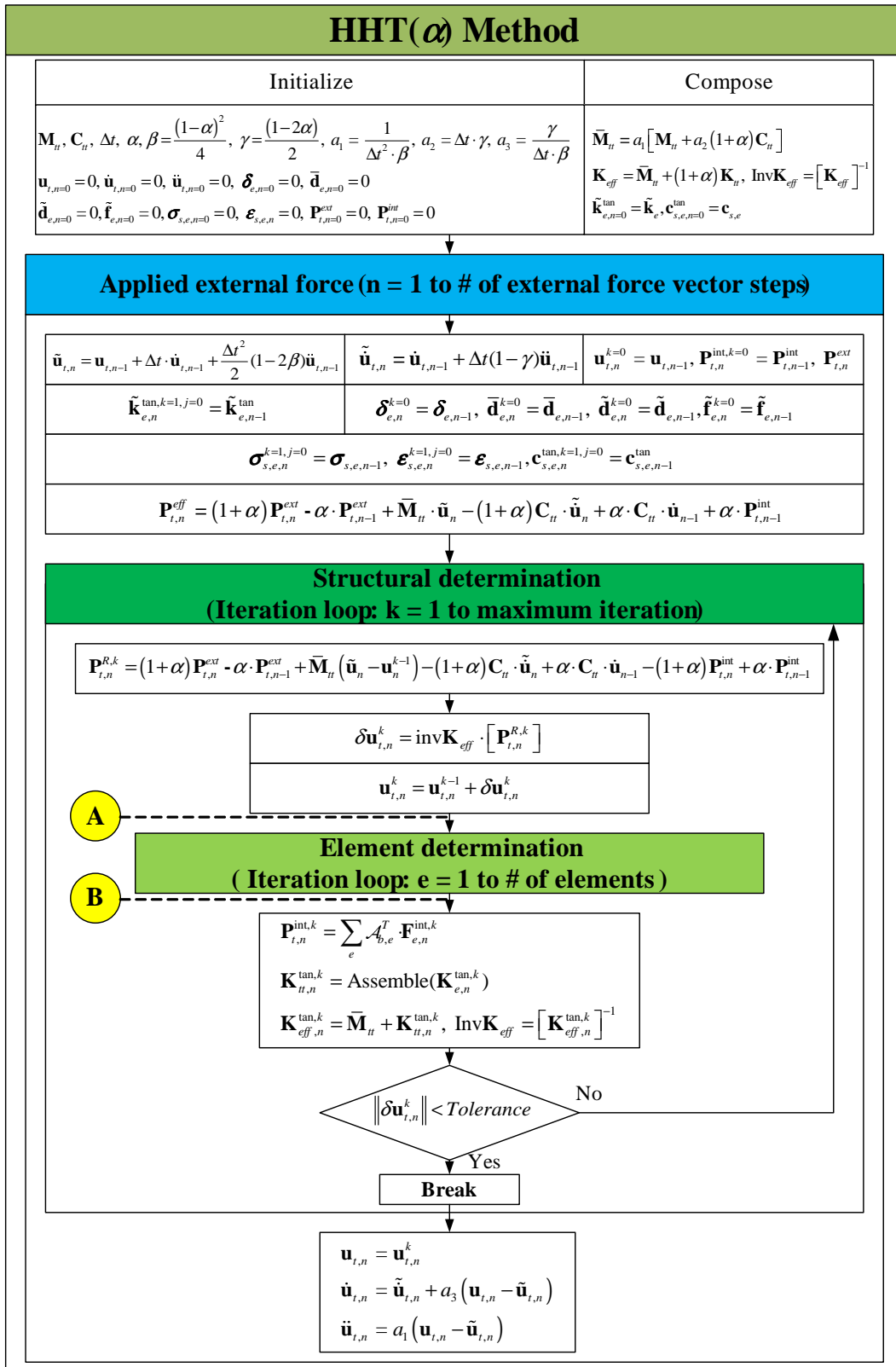


Figure 5.5: Flow chart of transient analysis using the HHT implicit method

or with  $\omega^2 = \lambda$

$$|\mathbf{K} - \lambda\mathbf{M}| = 0$$

(5.55)

which is the *characteristic equation*, and  $\lambda$  is called the *eigenvalue* of the equation, and the structure is said to respond in the *mode* corresponding to a particular frequency.

14 For computational purposes, if we premultiply each side of the preceding equation by  $\mathbf{M}^{-1}$ , then

$$(\mathbf{M}^{-1}\mathbf{K} - \lambda\mathbf{I})\phi = 0$$

(5.56)

It should be noted that a zero eigenvalue is obtained for each possible rigid body motion of a structure that is not completely supported.

15 Depending on which mass matrix is adopted, slightly different results are obtained. In general, lumped mass matrices approach the exact value (consistent mass matrix) from below.

16 The mode shapes  $\phi$  are “shapes”, and give a relative magnitude of the DOF, not the absolute values (since they are the solution to a set of homogeneous equations).

17 The natural frequencies and mode shapes provide a fundamental description of the vibrating structure.

## Chapter 6

### Notation

$\mathbf{P}_S^{int}$	:	Internal nodal force vector
$\mathbf{P}_t^{ext}$	:	External nodal force vector at free degrees of freedom at structural level
$\mathbf{P}_t^{int}$	:	Internal nodal force vector at free degrees of freedom at structural level
$\mathbf{P}_t^{con}$	:	Internal nodal force vector at constraint degrees of freedom at structural level
$\mathbf{P}_t^R$	:	Residual nodal force vector at free degrees of freedom at structural level
$\mathbf{u}_t$	:	Nodal displacement vector at free degrees of freedom at structural level
$\mathbf{F}_e$	:	Element nodal force vector in global reference
$\mathbf{F}_e^{int}$	=	$[N_{X1}, V_{Y1}, M_{Z1}, N_{X2}, V_{Y2}, M_{Z2}]^T$
$\mathbf{F}_e^R$	:	Internal element nodal force vector in global reference
$\delta_e$	:	Element nodal displacement vector in global reference
$\dot{\delta}_e$	=	$[u_{X1}, v_{Y1}, \theta_{Z1}, u_{X2}, v_{Y2}, \theta_{Z2}]^T$
$\tilde{\mathbf{f}}_e$	:	Element nodal force vector in local reference with rigid body modes
$\tilde{\mathbf{f}}_e^{int}$	=	$[\bar{N}_{x1}, \bar{V}_{y1}, \bar{M}_{z1}, \bar{N}_{x2}, \bar{V}_{y2}, \bar{M}_{z2}]^T$
$\tilde{\mathbf{f}}_e^R$	:	Internal element nodal force vector in local reference with rigid body modes
$\tilde{\mathbf{d}}_e$	:	Element nodal displacement vector in local reference with rigid body modes
$\tilde{\mathbf{d}}_e$	=	$[\bar{u}_{x1}, \bar{v}_{y1}, \bar{\theta}_{z1}, \bar{u}_{x2}, \bar{v}_{y2}, \bar{\theta}_{z2}]^T$
$\tilde{\mathbf{f}}_e^R$	:	Element nodal force vector in local reference without rigid body modes
$\tilde{\mathbf{f}}_e^{int}$	=	$[\bar{M}_{z1}, \bar{M}_{z2}, \bar{N}_{x2}]^T$
$\tilde{\mathbf{r}}_e^R$	:	Internal element nodal force vector in local reference without rigid body modes
$\tilde{\mathbf{d}}_e$	:	Residual element nodal force vector in local reference without rigid body modes
$\tilde{\mathbf{d}}_e$	:	Element nodal displacement vector in local reference without rigid body modes
$\tilde{\mathbf{d}}_e$	=	$[\bar{\theta}_{z1}, \bar{\theta}_{z2}, \bar{u}_{x2}]^T$
$\tilde{\mathbf{d}}_e^R$	:	Residual element nodal displacement vector in local reference without rigid body modes
$\mathbf{d}_s(x)$	:	Section displacement vector
$\mathbf{d}_s(x)$	=	$[u(x), v(x)]^T$
$\sigma_s(x)$	:	Section force vector
$\kappa$	:	Plastic stress

$\sigma_s(x)$	=	$[N(x), M(x)]^T$
$\sigma_{int}(x)$	:	Internal section force vector
$\sigma_s^R(x)$	:	Residual section force vector
$\epsilon_s(x)$	:	Section deformation vector
$\epsilon_s(x)$	=	$[\varepsilon_x(x), \phi_z(x)]^T$
$\epsilon_s^{int}(x)$	:	Residual section deformation vector
$\sigma$	:	Uniaxial stress
$\varepsilon$	:	Uniaxial strain
$\sigma_r$	:	Uniaxial stress of layer/fiber
$\varepsilon_r$	:	Uniaxial strain of layer/fiber
$N_d(x)$	:	Shape function on displacement field
$B_d(x)$	:	The matrix derived from the derivatives of $N_d(x)$
$N_f(x)$	:	Shape function on force field
$K_S$	:	Augmented stiffness matrix at structural level
$K_{tt}$	:	Stiffness matrix associated natural boundary conditions
$K_{tu}$	:	Stiffness matrix associated natural and essential boundary conditions
$K_{ut}$	:	Stiffness matrix associated essential and natural boundary conditions
$K_{uu}$	:	Stiffness matrix associated essential boundary conditions
$K_e$	:	Element stiffness matrix in global reference
$\bar{K}_e$	:	Element stiffness matrix in local reference with rigid body modes
$\bar{K}_e^{tan}$	:	Element tangent stiffness matrix in local reference with rigid body modes
$k_e$	:	Element stiffness matrix in local reference without rigid body modes
$\bar{c}_e$	:	Element flexibility matrix in local reference without rigid body modes
$k_s(x)$	:	Section stiffness matrix
$k_s^{tan}(x)$	:	Section tangent stiffness matrix
$c_s(x)$	:	Section flexibility matrix
$E(x)$	:	Elastic modulus
$A(x)$	:	Section area
$I_z(x)$	:	Moment of inertia on section area
$\delta\bar{d}_e$	:	Virtual element nodal displacement vector in local reference
$\delta\epsilon_s(x)$	:	Virtual section deformation vector
$L_e$	:	Element length
$\Gamma_e$	:	Transformation matrix between local and global coordinate system
$\tilde{\Gamma}_e$	:	Transformation matrix between rigid body modes and no rigid body modes

**Subscript**

$t$  : Known traction  
 $u$  : Known displacement  
 $S$  : Structural level  
 $e$  : Element level or  $e^{th}$  element at element state determination  
 $r$  : Layer/fiber level or  $r^{th}$  layer/fiber at layer/fiber state determination  
 $s$  : Section level or  $s^{th}$  section at section state determination  
 $d$  : Displacement field  
 $f$  : Force field  
 $n$  : Current step of External force/displacement vector

**Superscript**

$int$  : Internal  
 $ext$  : External  
 $R$  : Residual  
 $k$  :  $k^{th}$  iteration at structural level  
 $j$  :  $j^{th}$  iteration at element level

## NOTATION; Old Matrix Lecture Notes

<b>a</b>	Vector of coefficients in assumed displacement field
<b>A</b>	Area
<b>A</b>	Kinematics Matrix
<b>b</b>	Body force vector
<b>B</b>	Statics Matrix, relating external nodal forces to internal forces
$[B']$	Statics Matrix relating nodal load to internal forces $\mathbf{p} = [B']\mathbf{P}$
$[B]$	Matrix relating assumed displacement fields parameters to joint displacements
<b>C</b>	Cosine
$[C1 C2]$	Matrices derived from the statics matrix
$\{\mathbf{d}\}$	Element flexibility matrix (lc)
$\{d_c\}$	
$[D]$	Structure flexibility matrix (GC)
<b>E</b>	Elastic Modulus
$[E]$	Matrix of elastic constants (Constitutive Matrix)
$\{F\}$	Unknown element forces and unknown support reactions
$\{F_0\}$	Nonredundant element forces (lc)
$\{F_x\}$	Redundant element forces (lc)
$\{F_e\}$	Element forces (lc)
$\{\bar{F}^0\}$	Nodal initial forces
$\{\bar{F}^e\}$	Nodal energy equivalent forces
$\{\bar{F}\}$	Externally applied nodal forces
FEA	Fixed end actions of a restrained member
<b>G</b>	Shear modulus
<b>I</b>	Moment of inertia
$[\mathcal{L}]$	Matrix relating the assumed displacement field parameters to joint displacements
$[I]$	Identity matrix
$[ID]$	Matrix relating nodal dof to structure dof
<b>J</b>	St Venant's torsional constant
$[k]$	Element stiffness matrix (lc)
$[p]$	Matrix of coefficients of a polynomial series
$[k_g]$	Geometric element stiffness matrix (lc)
$[k_r]$	Rotational stiffness matrix ( $[d]$ inverse )
$[K]$	Structure stiffness matrix (GC)
$[K_g]$	Structure's geometric stiffness matrix (GC)
<b>L</b>	Length
<b>L</b>	Linear differential operator relating displacement to strains
$l_{ij}$	Direction cosine of rotated axis i with respect to original axis j
$\{LM\}$	structure dof of nodes connected to a given element
$\{N\}$	Shape functions
$\{p\}$	Element nodal forces = F (lc)
$\{P\}$	Structure nodal forces (GC)
$P, V, M, T$	Internal forces acting on a beam column (axial, shear, moment, torsion)
<b>R</b>	Structure reactions (GC)
<b>S</b>	Sine
<b>t</b>	Traction vector
$\hat{t}$	Specified tractions along $\Gamma_t$
<b>u</b>	Displacement vector
$\hat{u}$	Neighbour function to $u(x)$
$\hat{u}(x)$	Specified displacements along $\Gamma_u$
$u, v, w$	Translational displacements along the x, y, and z directions
<b>U</b>	Strain energy
$U^*$	Complementary strain energy
$x, y$	local coordinate system (lc)
$X, Y$	Global coordinate system (GC)
<b>W</b>	Work
$\alpha$	Coefficient of thermal expansion
$[\Gamma]$	Transformation matrix
$\{\delta\}$	Element nodal displacements (lc)
$\{\Delta\}$	Nodal displacements in a continuous system
$\{\Delta\}$	Structure nodal displacements (GC)
$\epsilon$	Strain vector
$\epsilon_0$	Initial strain vector
$\{\Upsilon\}$	Element relative displacement (lc)
$\{\Upsilon_0\}$	Nonredundant element relative displacement (lc)
$\{\Upsilon_x\}$	Redundant element relative displacement (lc)
$\theta$	rotational displacement with respect to z direction (for 2D structures)
$\delta$	Variational operator
$\delta M$	Virtual moment
$\delta P$	Virtual force
$\delta \theta$	Virtual rotation
$\delta u$	Virtual displacement
$\delta \phi$	Virtual curvature
$\delta U$	Virtual internal strain energy
$\delta W$	Virtual external work
$\delta \epsilon$	Virtual strain vector
$\delta \sigma$	Virtual stress vector
$\Gamma$	Surface

$\Gamma_t$	Surface subjected to surface tractions
$\Gamma_u$	Surface associated with known displacements
$\sigma$	Stress vector
$\sigma_0$	Initial stress vector
$\Omega$	Volume of body

lc: Local Coordinate system

GC: Global Coordinate System

